UNIVERSITY OF CALIFORNIA

Los Angeles

Economic Model Predictive Control Theory: Computational Efficiency and Application to Smart Manufacturing

A dissertation submitted in partial satisfaction of the

requirements for the degree Doctor of Philosophy

in Chemical Engineering

by

Matthew Ellis

2015

ABSTRACT OF THE DISSERTATION

Economic Model Predictive Control Theory: Computational Efficiency and Application to Smart Manufacturing

by

Matthew Ellis

Doctor of Philosophy in Chemical Engineering

University of California, Los Angeles, 2015

Professor Panagiotis D. Christofides, Chair

The chemical industry is a vital sector of the US economy. Maintaining optimal chemical process operation is critical to the future success of the US chemical industry on a global market. Traditionally, economic optimization of chemical processes has been addressed in a two-layer hierarchical architecture. In the upper layer, real-time optimization carries out economic process optimization by computing optimal process operation set-points using detailed nonlinear steady-state process models. These set-points are used by the lower layer feedback control systems to force the process to operate on these set-points. While this paradigm has been successful, we are witnessing an increasing need for dynamic market and demand-driven operations for more efficient process operation, increasing response capability to changing customer demand, and achieving real-time energy management. To enable next-generation market-driven operation, economic model predictive control (EMPC), which is an model predictive control scheme formulated with a stage cost that represents the process economics, has been proposed to integrate dynamic

economic optimization of processes with feedback control.

Motivated by these considerations, novel theory and methods needed for the design of computationally tractable economic model predictive control systems for nonlinear processes are developed in this dissertation. Specifically, the following considerations are addressed: a) EMPC structures for nonlinear systems which address: infinite-time and finite-time closed-loop economic performance and time-varying economic considerations such as changing energy pricing; b) two-layer (hierarchical) dynamic economic process optimization and feedback control frameworks that incorporate EMPC with other control strategies allowing for computational efficiency; and c) EMPC schemes that account for real-time computation requirements. The EMPC schemes and methodologies are applied to chemical process applications. The application studies demonstrate the effectiveness of the EMPC schemes to maintain process stability and improve economic performance under dynamic operation as well as to increase efficiency, reliability and profitability of processes, thereby contributing to the vision of Smart Manufacturing.

The dissertation of Matthew Ellis is approved.

Lieven Vandenberghe

Dante Simonetti

James F. Davis

Panagiotis D. Christofides, Committee Chair

University of California, Los Angeles

2015

Contents

List of Figures viii

List of Tables xiii

1 Introduction 1
- 1.1 Motivation . . . 1
- 1.2 Objectives and Organization of the Dissertation . . . 6
- 1.3 Chemical Process Examples . . . 9
  - 1.3.1 Catalytic Oxidation of Ethylene . . . 10
  - 1.3.2 Continuously-Stirred Tank Reactor with Second-order Reaction . . . 14

2 Brief Overview of EMPC Methods and Some Preliminary Results 19
- 2.1 Background on EMPC Methods . . . 19
  - 2.1.1 Notation . . . 20
  - 2.1.2 Class of Nonlinear Systems . . . 21
  - 2.1.3 EMPC Methods . . . 22
- 2.2 Application of EMPC to a Chemical Process Example . . . 34
- 2.3 A Few Preliminary Results on Sampled-data Systems and Lyapunov-based MPC . . . 39
  - 2.3.1 Stabilization of Nonlinear Sampled-data Systems . . . 39
  - 2.3.2 Tracking Lyapunov-based MPC . . . 46

3 Lyapunov-based EMPC 49
- 3.1 Introduction . . . 49
- 3.2 Lyapunov-based EMPC Design and Implementation . . . 51
  - 3.2.1 Class of Nonlinear Systems . . . 51
  - 3.2.2 Stabilizability Assumption . . . 51
  - 3.2.3 LEMPC Formulation . . . 52
  - 3.2.4 Implementation Strategy . . . 56
  - 3.2.5 Satisfying State Constraints . . . 58
  - 3.2.6 Extensions and Variants of LEMPC . . . 61
- 3.3 Closed-loop Stability and Robustness under LEMPC . . . 63
  - 3.3.1 Synchronous Measurement Sampling . . . 64

3.3.2 Application to a Chemical Process Example . . . 73
3.4 Closed-loop Performance under LEMPC . . . 83
3.4.1 Stabilizability Assumption . . . 84
3.4.2 Formulation and Implementation of the LEMPC with a Terminal Equality Constraint . . . 86
3.4.3 Closed-loop Performance and Stability Analysis . . . 88
3.5 LEMPC with a Time-varying Stage Cost . . . 95
3.5.1 Class of Economic Costs and Stabilizability Assumption . . . 96
3.5.2 The Union of the Stability Regions . . . 98
3.5.3 Formulation of LEMPC with Time-Varying Economic Cost . . . 101
3.5.4 Implementation Strategy . . . 105
3.5.5 Stability Analysis . . . 106
3.5.6 Application to a Chemical Process Example . . . 109
3.6 Conclusions . . . 124

4 Two-layer EMPC Implementation 126
4.1 Introduction . . . 126
4.1.1 Notation . . . 128
4.2 Two-Layer Control and Optimization Framework . . . 131
4.2.1 Class of Systems . . . 131
4.2.2 Formulation and Implementation . . . 133
4.2.3 Application to a Chemical Process . . . 148
4.3 Unifying Optimization with Time-Varying Economics and Control . . . 156
4.3.1 Stabilizability Assumption . . . 158
4.3.2 Two-layer EMPC Scheme Addressing Time-Varying Economics . . . 160
4.3.3 Application to a Chemical Process Example . . . 172
4.4 Addressing Closed-loop Performance and Computational Efficiency . . . 182
4.4.1 Class of Systems . . . 183
4.4.2 Existence of a Stabilizing Controller . . . 184
4.4.3 Two-layer EMPC Structure . . . 185
4.4.4 Application to Chemical Process Example . . . 200
4.5 Conclusions . . . 214

5 Real-Time Economic Model Predictive Control of Nonlinear Process Systems 215
5.1 Introduction . . . 215
5.2 Real-time Economic Model Predictive Control . . . 218
5.2.1 Class of Systems . . . 219
5.2.2 Real-time LEMPC Formulation . . . 220
5.2.3 Implementation Strategy . . . 223
5.2.4 Stability Analysis . . . 227
5.3 Application to a Chemical Process Network . . . 235
5.4 Conclusions . . . 254

6 EMPC of Time-Delay Systems: Closed-loop Stability and Delay Compensation 255
6.1 Introduction . . . 255
6.2 Preliminaries . . . 258
6.2.1 Notation and Preliminary Results . . . 258
6.2.2 Class of Nonlinear Time-Delay Systems . . . 260
6.2.3 Controller Emulation Design . . . 262
6.3 Robustness of LEMPC to Small Time-Delays . . . 266
6.3.1 Formulation and Implementation . . . 266
6.3.2 Closed-loop Stability Analysis . . . 270
6.3.3 Application to a Chemical Process Example . . . 277
6.4 Time-delay Compensation for Improved Closed-loop Performance . . . 286
6.4.1 Predictor Feedback LEMPC Methodology and Implementation . . . 286
6.4.2 Application to a Chemical Process Example . . . 290
6.5 Conclusion . . . 293

7 Selection of Control Configurations for Economic Model Predictive Control Systems 294
7.1 Introduction . . . 294
7.1.1 Notation . . . 297
7.1.2 Class of Nonlinear Systems . . . 297
7.2 Input Selection for Economic Model Predictive Control . . . 298
7.2.1 Relative Degree of Cost to Inputs . . . 299
7.2.2 Dynamic Sensitivity of the Economic Cost . . . 304
7.2.3 Steady-state Sensitivities of the Economic Cost . . . 309
7.2.4 Stabilizability of Control Configurations . . . 310
7.2.5 Input Selection Methodology . . . 314
7.3 EMPC Input Selection for a Chemical Process Example . . . 317
7.4 Conclusions . . . 329

8 Conclusions 331

Bibliography 335

List of Figures

1.1 The traditional hierarchical paradigm employed in the chemical process industries for planning/scheduling, optimization, and control of chemical plants (adapted from [165]). 3
1.2 Average economic performance $\bar{J}_e$ as a function of the period length τ. . . . 17
1.3 State, input, and $\lambda_1 + \lambda_3/\tau$ trajectories of the CSTR under the bang-bang input policy with period $\tau = 1.20$. 17

2.1 An illustration of possible open-loop predicted trajectories under EMPC formulated with a terminal constraint (dotted), under EMPC formulated with a terminal region constraint (dashed), and under LEMPC (solid). . . . 33
2.2 Design of the open-loop periodic operation strategy over one period τ. . . . 35
2.3 The open-loop CSTR (a) state trajectories and (b) input trajectories with the periodic operating strategy shown in Fig. 2.2. 37
2.4 The closed-loop CSTR (a) state trajectories and (b) input trajectories with EMPC of Eq. 2.22. 37
2.5 State-space evolution in the $x_2 - x_3$ phase plane of the reactor system given with the EMPC of Eq. 2.22 and with the periodic control strategy shown in Fig. 2.2. 38

3.1 An illustration of the state-space evolution of a system under LEMPC. The red trajectory represents the state trajectory under mode 1 operation of the LEMPC, and the blue trajectory represents the state trajectory under mode 2 operation. 58
3.2 An illustration of the various state-space sets described for enforcing state constraints with LEMPC. The case when $\mathbb{X} \subset \Phi_u$ is depicted in this illustration. 59
3.3 Two closed-loop state trajectories under the LEMPC in state-space. 80
3.4 The closed-loop state and input trajectories of the CSTR under the LEMPC of Eq. 3.44 for two initial conditions (solid and dashed trajectories) and the steady-state is the dashed-dotted line. 82
3.5 An illustration of the construction of the stability region $\mathscr{X}$. The shaded region corresponds to the set $\mathscr{X}$. 99
3.6 This illustration gives the state evolution over two sampling periods. 104

3.7 The construction of the set $\mathscr{X}$ for the CSTR of Eq. 3.79. 111
3.8 The states and inputs of the nominally operated CSTR under LEMPC-1 (mode 1 operation only) initialized at $C_A(0) = 2.0\,\text{kmol}\,\text{m}^{-3}$ and $T(0) = 410.0\,\text{K}$. 116
3.9 The states and inputs of the nominally operated CSTR under LEMPC-2 (mode 1 operation only) initialized at $C_A(0) = 2.0\,\text{kmol}\,\text{m}^{-3}$ and $T(0) = 410.0\,\text{K}$. 116
3.10 The states and inputs of the CSTR under the LEMPC of Eq. 3.86 (mode 1 operation only) when the economic cost weights are constant with time (solid line) with the economically optimal steady-state (dashed line). 117
3.11 The states and inputs of the CSTR under the LMPC of Eq. 3.89 used to track the economically optimal steady-state (dashed line). 120
3.12 The states and inputs of the nominally operated CSTR under LEMPC-1 initialized at $C_A(0) = 4.0\,\text{kmol}\,\text{m}^{-3}$ and $T(0) = 370.0\,\text{K}$. 121
3.13 The states and inputs of the nominally operated CSTR under LEMPC-2 initialized at $C_A(0) = 4.0\,\text{kmol}\,\text{m}^{-3}$ and $T(0) = 370.0\,\text{K}$. 122
3.14 The states and inputs of the CSTR under the two-mode LEMPC with added process noise; evolution with respect to time. 123
3.15 The states and inputs of the CSTR under the two-mode LEMPC with added process noise; state-space plot. 123

4.1 A block diagram of the two-layer integrated framework for dynamic economic optimization and control with EMPC in the upper layer and tracking MPC in the lower layer. Both the upper and lower layers compute control actions that are applied to the system. 133
4.2 The closed-loop state trajectories of the reactor under the two-layer dynamic economic optimization and control framework (the two trajectories are overlapping). 151
4.3 The closed-loop input trajectories computed by two-layer dynamic economic optimization and control framework (the two trajectories are overlapping). 152
4.4 The computational time reduction of the two-layer optimization and control framework relative to the one-layer implementation of LEMPC. 153
4.5 The closed-loop state trajectories of the catalytic reactor under the two-layer dynamic economic optimization and control framework and with process noise added to the states. 154
4.6 The closed-loop input trajectories computed by two-layer dynamic economic optimization and control framework and with process noise added to the states (the two trajectories are nearly overlapping). 155
4.7 A block diagram of the dynamic economic optimization and control framework for handling time-varying economics. 161

4.8 The closed-loop state and input trajectories of Eq. 4.58a-4.58b under the two-layer optimization and control framework with the feed disturbances and starting from 400 K and 0.1 kmol m^{-3}. 177
4.9 The closed-loop state trajectory of Eq. 4.58a-4.58b under the two-layer optimization and control framework with the feed disturbances and starting from 400 K and 0.1 kmol m^{-3} shown in deviation state-space. 177
4.10 The closed-loop system states and inputs of Eq. 4.58a-4.58b without the feed disturbances and starting from 400 K and 3.0 kmol m^{-3}. 178
4.11 The closed-loop system states and inputs of Eq. 4.58a-4.58b without the feed disturbances and starting from 320 K and 3.0 kmol m^{-3}. 179
4.12 Block diagram of the two-layer EMPC structure addressing closed-loop performance and computational efficiency. 186
4.13 A state-space illustration of the evolution of the closed-loop system (solid line) in the stability region Ω_ρ over two operating periods. The open-loop predicted state trajectory under the auxiliary controller is also given (dashed line). At the beginning of each operating window, the closed-loop state converges to the open-loop state under the auxiliary controller. 189
4.14 Process flow diagram of the reactor and separator process network. 200
4.15 The closed-loop economic performance (J_E) with the length of prediction horizon (N_E) for the reactor-separator process under the upper layer LEMPC with a terminal constraint computed from an auxiliary LMPC. . . . 205
4.16 Closed-loop state trajectories of the reactor-separator process network with the upper layer LEMPC formulated with a terminal constraint computed by the auxiliary LMPC. 206
4.17 Input trajectories of the reactor-separator process network computed by the upper layer LEMPC formulated with a terminal constraint computed by the auxiliary LMPC. 207
4.18 Closed-loop state trajectories of the reactor-separator process network with an LEMPC formulated without terminal constraints. 208
4.19 Input trajectories of the reactor-separator process network computed by an LEMPC formulated without terminal constraints. 209
4.20 Closed-loop state trajectories of the reactor-separator process network with the two-layer LEMPC structure. 209
4.21 Input trajectories of the reactor-separator process network computed by the two-layer LEMPC structure. 210
4.22 Closed-loop state trajectories of the reactor-separator process network with process noise added with the two-layer LEMPC structure. 213
4.23 Input trajectories of the reactor-separator process network with process noise added computed by the two-layer LEMPC structure. 213

5.1 Implementation strategy for determining the control action at each sampling period. 223

5.2 Computation strategy for the real-time LEMPC scheme. 225
5.3 An illustration of an example input trajectory resulting under the real-time LEMPC scheme. 227
5.4 Process flow diagram of the reactor and separator process network. 236
5.5 The total economic cost J_e over one operating window length of operation (2.4 h) of the process network under LEMPC with the prediction horizon length. 245
5.6 The closed-loop (a) state and (b) input trajectories of the nominally operated process network under the real-time LEMPC scheme. 247
5.7 The number of times the LEMPC problem was solved (Comp.) as dictated by the real-time implementation strategy compared to the sampling period (Δ) over the first 0.5 h of operation. 248
5.8 The closed-loop (a) state and (b) input trajectories of process network under the real-time LEMPC scheme where the computational delay is modeled as a bounded random number. 250
5.9 The closed-loop (a) state and (b) input trajectories of process network under LEMPC subject to computational delay where the computational delay is modeled as a bounded random number. 250
5.10 A discrete trajectory depicting when the control action applied to the process network over each sampling period was from a precomputed LEMPC solution or from the back-up controller for the closed-loop simulation of Fig. 5.8. 251
5.11 The closed-loop (a) state and (b) input trajectories of process network under the real-time LEMPC scheme with bounded process noise. 252
5.12 The closed-loop (a) state and (b) input trajectories of process network under LEMPC subject to computational delay with bounded process noise. 253

6.1 Process flow diagram of the CSTR with recycle. 278
6.2 The closed-loop trajectories of the CSTR under the LEMPC without time-delays ($d_1 = d_2 = 0$). 282
6.3 The state-space evolution of the closed-loop CSTR states under LEMPC with (a) $d = 0.05$ h and (b) $d = 0.10$ h. 283
6.4 A comparison of the closed-loop performance with the tuning parameter $\hat{\rho}$ and magnitude of the time-delay. 285
6.5 Flow diagram of the predictor feedback LEMPC scheme. 286
6.6 An illustration of the phases of the predictor feedback LEMPC scheme. . . 288
6.7 The closed-loop trajectories of the CSTR under the LEMPC with time-delay of $d = 0.10$ h. The input trajectories shown in the plots correspond to the input values applied to the system at each time. 291
6.8 The state-space evolution of the closed-loop CSTR states under LEMPC with (a) $d = 0.05$ h and (b) $d = 0.10$ h. 291

7.1 Directed graph representing the system of Eq. 7.8. 304

7.2 A flowchart of the input selection for EMPC methodology. Solid lines are used to represent necessary steps and dashed lines are used to represent optional steps. 313
7.3 The closed-loop state trajectories under the EMPC of Eq. 7.33. 321
7.4 The manipulated input trajectories under the EMPC of Eq. 7.33. 321
7.5 A directed graph constructed for the chemical process example for the economic cost function of Eq. 7.31 to compute the relative degree of various input variables using the methodology of [35]. The candidate manipulated inputs are dark gray and the economic cost is light gray. 323
7.6 The dynamic sensitivities for inputs with relative degree 2 which are computed with the closed-loop state trajectory under the EMPC with all inputs on EMPC. 324
7.7 The dynamic sensitivities for inputs with relative degree 3 which are computed with the closed-loop state trajectory under the EMPC with all inputs on EMPC. 324
7.8 The closed-loop state trajectories of the chemical process under EMPC with added process noise. 327
7.9 The manipulated input trajectories of the chemical process under EMPC with added process noise. 328

List of Tables

1.1 Dimensionless process model parameters of the ethylene oxidation reactor model. The parameters are from [144]. 10
1.2 Process parameters of the CSTR. 14

3.1 CSTR parameter values. 73
3.2 Average economic cost over several simulations under the LEMPC, the Lyapunov-based controller applied in a sample-and-hold fashion, and the constant input equal to u_s. For the case denoted with a "*", the system under the constant input u_s settled at a different steady-state, i.e., not x_s. . . 81
3.3 CSTR process parameters. 109
3.4 The optimal steady-state variation with respect to the time-varying economic weights. 118
3.5 The total economic cost of the closed-loop reactor over several simulations with different initial states. The performance improvement is relative to the economic performance under LMPC. 120

4.1 A summary of the notation used to describe the two-layer EMPC structure. 129
4.2 Process parameters of the CSTR of Eq. 4.58. 172
4.3 Comparison of the total economic cost, given by Eq. 4.63, of the closed-loop system with and without the feed disturbances for four hours of operation. 180
4.4 Process parameters of the reactor and separator process network. 201
4.5 Total economic cost and average computational time in seconds per sampling period for several 4.0 h simulations with: (a) the auxiliary LMPC, (b) the one-layer LEMPC and (c) the two-layer LEMPC structure. 210

5.1 Process parameters of the reactor and separator process network. 237
5.2 The performance indices of the process network under the back-up explicit controller, under the LEMPC subject to computational delay, and under the real-time LEMPC for several simulations. 249

6.1 Notation and parameter values of the CSTR with recycle. 277

6.2 Closed-loop performance relative to the performance at the steady-state and closed-loop stability properties of the CSTR under LEMPC. 284
6.3 Closed-loop performance of the CSTR of Eq. 6.32 under the predictor feedback LEMPC relative to the performance at the steady-state. 292

7.1 Process parameters of the reactor-reactor process. 317

ACKNOWLEDGEMENTS

I would like to express my deepest gratitude to my advisor, Panagiotis D. Christofides, for the tremendous amount of guidance and support he has given me throughout my graduate studies. Professor Christofides has mentored me through learning about the intricacies of control theory, process/systems engineering, and life in general. I am also grateful for my family and friends and for their encouragement, support, patience, and guidance throughout my graduate career and throughout my life. In particular, I am grateful for my parents, Jeff and Barb, my brother, Chad, my sister, Carissa, and my long-time friend and loving roommate and partner, Ashli.

In addition, I would like to acknowledge several other mentors that have had significant influence on my life, including my grandfather, Earl "Buzz" Keesler, my uncle, Tim Pack, and Kevin Beauchamp and Rocco Vanden Wyngaard of Galloway Company. My journey in process/systems engineering began at Galloway Company, and I am sincerely appreciative of the people I have met and the knowledge I have gained there.

Moreover, I want to acknowledge the many researchers I have had the privilege to collaborate with along my journey, including: Liangfeng Lao, Jinfeng Liu, Mohsen Heidarinejad, Iasson Karafyllis, Mirko Messori, and TungSheng Tu, and also, Helen Durand for her valuable comments in proofreading my papers. Further, to my lab mates, in particular: Grant Crose, Larry Gao, Joseph Sangil Kwon, Michael Nayhouse, and Anh Tran for the many valuable and insightful conversations about research, programming, careers, and life.

I would also like to thank Professor James F. Davis, Professor Dante Simonetti, and Professor Lieven Vandenberghe for serving on my doctoral committee.

Finally, financial support from the National Science Foundation (NSF), the Department of Energy (DOE), and Dissertation Year Fellowship is gratefully acknowledged.

Chapter 2 contains versions of: M. Ellis and P. D. Christofides. Economic model pre-

dictive control: Elucidation of the role of constraints. In *Proceedings of 5th IFAC Conference on Nonlinear Model Predictive Control*, Seville, Spain, in press (EMPC Methods); M. Ellis and P. D. Christofides. Optimal time-varying operation of nonlinear process systems with economic model predictive control. *Industrial & Engineering Chemistry Research*, 53:4991–5001, 2014 (chemical process example); and M. Ellis, I. Karafyllis, and P. D. Christofides. Stabilization of nonlinear sampled-data systems and economic model predictive control application. In *Proceedings of the American Control Conference*, pages 5594–5601, Portland, OR, 2014 (results on stabilization of sampled-data systems).

Chapter 3 provides a review of Lyapunov-based economic model predictive control, which was introduced in: M. Heidarinejad, J. Liu, and P. D. Christofides. Economic model predictive control of nonlinear process systems using Lyapunov techniques. *AIChE Journal*, 58:855–870, 2012. It also contains a version of M. Ellis and P. D. Christofides. Economic model predictive control with time-varying objective function for nonlinear process systems. *AIChE Journal*, 60:507–519, 2014.

Chapter 4 contains versions of: M. Ellis and P. D. Christofides. Optimal time-varying operation of nonlinear process systems with economic model predictive control. *Industrial & Engineering Chemistry Research*, 53:4991–5001, 2014; M. Ellis and P. D. Christofides. Integrating dynamic economic optimization and model predictive control for optimal operation of nonlinear process systems. *Control Engineering Practice*, 22:242–251, 2014; and M. Ellis and P. D. Christofides. On finite-time and infinite-time cost improvement of economic model predictive control for nonlinear systems. *Automatica*, 50:2561–2569, 2014.

Chapter 5 is a version of: M. Ellis and P. D. Christofides. Real-time economic model predictive control of nonlinear process systems. *AIChE Journal*, 61:555–571, 2015.

Chapter 6 is a version of: M. Ellis and P. D. Christofides. Economic model predictive control of nonlinear time-delay systems: Closed-loop stability and delay compensation.

AIChE Journal, in press, DOI: 10.1002/aic.14964.

Chapter 7 is a version of: M. Ellis and P. D. Christofides. Selection of control configurations for economic model predictive control systems. *AIChE Journal*, 60:3230–3242, 2014.

VITA

2006–2010 Bachelor of Science, Chemical and Biological Engineering
Department of Chemical and Biological Engineering
University of Wisconsin – Madison

2011–2015 Graduate Student
Department of Chemical and Biomolecular Engineering
University of California, Los Angeles

2012–2014 Teaching Assistant/Associate
Department of Chemical and Biomolecular Engineering
University of California, Los Angeles

PUBLICATIONS AND PRESENTATIONS

1. M. Ellis and P. D. Christofides. Economic model predictive control of nonlinear time-delay systems: Closed-loop stability and delay compensation. *AIChE Journal*, in press, DOI: 10.1002/aic.14964.

2. L. Lao, M. Ellis, and P. D. Christofides. Handling state constraints and economics in feedback control of transport-reaction processes. *Journal of Process Control*, 32:98–108, 2015.

3. L. Lao, M. Ellis, H. Durand, and P. D. Christofides. Real-time preventive sensor maintenance using robust moving horizon estimation and economic model predictive control. *AIChE Journal*, in press, DOI: 10.1002/aic.14960.

4. A. Alanqar, M. Ellis, and P. D. Christofides. Economic model predictive control of nonlinear process systems using empirical models. *AIChE Journal*, 61:816–830, 2015.

5. M. Ellis and P. D. Christofides. Real-time economic model predictive control of nonlinear process systems. *AIChE Journal*, 61:555–571, 2015.

6. M. Ellis and P. D. Christofides. Economic model predictive control: Elucidation of the role of constraints. In *Proceedings of 5th IFAC Conference on Nonlinear Model Predictive Control*, Seville, Spain, in press.

7. M. Ellis and P. D. Christofides. Handling computational delay in economic model predictive control of nonlinear process systems. In *Proceedings of the American Control Conference*, pages 2962–2967, Chicago, IL, 2015.

8. M. Messori, M. Ellis, C. Cobelli, P. D. Christofides, and L. Magni. Improved postprandial glucose control with a customized model predictive controller. In *Proceedings of the American Control Conference*, pages 5108–5115, Chicago, IL, 2015.

9. H. Durand, M. Ellis, and P. D. Christofides. Accounting for the control actuator layer in economic model predictive control of nonlinear processes. In *Proceedings of the American Control Conference*, pages 2968–2973, Chicago, IL, 2015.

10. A. Alanqar, M. Ellis, and P. D. Christofides. Economic model predictive control of nonlinear process systems using multiple empirical models. In *Proceedings of the American Control Conference*, pages 4953–4958, Chicago, IL, 2015.

11. T. Anderson, M. Ellis and P. D. Christofides. Distributed economic model predictive control of a catalytic reactor: Evaluation of sequential and iterative architectures. In *Proceedings of the IFAC International Symposium on Advanced Control of Chemical Processes*, pages 278–283, 2015.

12. H. Durand, M. Ellis, and P. D. Christofides. Integrated design of control actuator layer and economic model predictive control for nonlinear processes. *Industrial & Engineering Chemistry Research*, 53:20000–20012, 2014.

13. M. Ellis and P. D. Christofides. On finite-time and infinite-time cost improvement of

economic model predictive control for nonlinear systems. *Automatica*, 50:2561–2569, 2014.

14. M. Ellis and P. D. Christofides. Performance monitoring of economic model predictive control systems. *Industrial & Engineering Chemistry Research*, 53:15406–15413, 2014.

15. L. Lao, M. Ellis, and P. D. Christofides. Economic model predictive control of parabolic PDE systems: Addressing state estimation and computational efficiency. *Journal of Process Control*, 24:448–462, 2014.

16. M. Ellis and P. D. Christofides. Selection of control configurations for economic model predictive control systems. *AIChE Journal*, 60:3230–3242, 2014.

17. M. Ellis, H. Durand, and P. D. Christofides. A tutorial review of economic model predictive control methods. *Journal of Process Control*, 24:1156–1178, 2014.

18. L. Lao, M. Ellis, and P. D. Christofides. Economic model predictive control of transport-reaction processes. *Industrial & Engineering Chemistry Research*, 53:7382–7396, 2014.

19. L. Lao, M. Ellis, and P. D. Christofides. Smart manufacturing: Handling preventive actuator maintenance and economics using model predictive control. *AIChE Journal*, 60:2179–2196, 2014.

20. M. Ellis, J. Zhang, J. Liu, and P. D. Christofides. Robust moving horizon estimation based output feedback economic model predictive control. *Systems & Control Letters*, 68:101–109, 2014.

21. M. Ellis and P. D. Christofides. Optimal time-varying operation of nonlinear process systems with economic model predictive control. *Industrial & Engineering Chemistry*

Research, 53:4991–5001, 2014.

22. M. Ellis and P. D. Christofides. Economic model predictive control with time-varying objective function for nonlinear process systems. *AIChE Journal*, 60:507–519, 2014.

23. M. Ellis and P. D. Christofides. Integrating dynamic economic optimization and model predictive control for optimal operation of nonlinear process systems. *Control Engineering Practice*, 22:242–251, 2014.

24. M. Ellis and P. D. Christofides. Control configuration selection for economic model predictive control. In *Proceedings of the 53rd IEEE Conference on Decision and Control*, pages 789–796, 2014.

25. L. Lao, M. Ellis, and P. D. Christofides. Economic model predictive control of a first-order hyperbolic PDE system. In *Proceedings of the 53rd IEEE Conference on Decision and Control*, pages 563–570, Los Angeles, CA, 2014.

26. L. Lao, M. Ellis, A. Armaou, and P.D. Christofides. Economic model predictive control of parabolic PDE systems: Handling state constraints by adaptive proper orthogonal decomposition. In *Proceedings of the 53rd IEEE Conference on Decision and Control*, pages 2758–2763, Los Angeles, CA, 2014.

27. L. Lao, M. Ellis, A. Armaou, and P. D. Christofides. Economic model predictive control of parabolic PDE systems using empirical eigenfunctions. In *Proceedings of the American Control Conference*, pages 3375–3380, 2014.

28. L. Lao, M. Ellis, and P. D. Christofides. Output feedback economic model predictive control of parabolic PDE systems. In *Proceedings of the American Control Conference*, pages 1655–1660, 2014.

29. M. Ellis, I. Karafyllis, and P. D. Christofides. Stabilization of nonlinear sampled-data systems and economic model predictive control application. In *Proceedings of the American Control Conference*, pages 5594–5601, Portland, OR, 2014.

30. M. Ellis and P. D. Christofides. Economic model predictive control of nonlinear time-delay systems: Closed-loop stability and delay compensation. AIChE Annual Meeting, paper 148c, Atlanta, GA, 2014.

31. M. Ellis and P. D. Christofides. Real-time economic model predictive control of nonlinear systems. AIChE Annual Meeting, paper 148h, Atlanta, GA, 2014.

32. M. Ellis and P. D. Christofides. Selection of control configurations for economic model predictive control systems. AIChE Annual Meeting, paper 721e, Atlanta, GA, 2014.

33. Alanqar A., M. Ellis, and P. D. Christofides. Economic model predictive control using empirical models. AIChE Annual Meeting, paper 699a, Atlanta, GA, 2014.

34. A. Alanqar, L. Lao, M. Ellis, and P. D. Christofides. Safe economic model predictive control. AIChE Annual Meeting, paper 721g, Atlanta, GA, 2014.

35. T. Anderson, M. Ellis, and P. D. Christofides. On distributed economic model predictive control of nonlinear process systems. AIChE Annual Meeting, paper 555b, Atlanta, GA, 2014.

36. H. Durand, M. Ellis, and P. D. Christofides. Accounting for the regulatory control layer in economic model predictive control of nonlinear chemical processes. AIChE Annual Meeting, paper 610e, Atlanta, GA, 2014.

37. L. Lao, M. Ellis, and P. D. Christofides. Handling state constraints and economics in feedback control of transport-reaction processes. AIChE Annual Meeting, paper 610e, Atlanta, GA, 2014.

38. L. Lao, M. Ellis, and P. D. Christofides. Handling preventive sensor maintenance in economic model predictive control of nonlinear chemical processes. AIChE Annual Meeting, paper 721a, Atlanta, GA, 2014.

39. T. S. Tu, M. Ellis, and P. D. Christofides. Model predictive control of a nonlinear large-scale process network used in the production of vinyl acetate. *Industrial & Engineering Chemistry Research*, 52:12463–12481, 2013.

40. L. Lao, M. Ellis, and P. D. Christofides. Proactive fault-tolerant model predictive control. *AIChE Journal*, 59:2810–2820, 2013.

41. M. Ellis, M. Heidarinejad, and P. D. Christofides. Economic model predictive control of nonlinear singularly perturbed systems. *Journal of Process Control*, 23:743–754, 2013.

42. M. Ellis, M. Heidarinejad, and P. D. Christofides. Economic model predictive control of nonlinear two-time-scale systems. In *Proceedings of the 21st IEEE Mediterranean Conference on Control and Automation*, pages 323–328, Platanias-Chania, Crete, Greece, 2013.

43. L. Lao, M. Ellis, and P. D. Christofides. Economic model predictive control of a transport-reaction process. In *Proceedings of the 21st IEEE Mediterranean Conference on Control and Automation*, pages 329–334, Platanias-Chania, Crete, Greece, 2013.

44. L. Lao, M. Ellis, and P. D. Christofides. Proactive fault-tolerant model predictive control: Concept and application. In *Proceedings of the American Control Conference*, pages 5140–5145, Washington, D.C., 2013.

45. M. Ellis and P. D. Christofides. Unifying dynamic economic optimization and model predictive control for optimal process operation. In *Proceedings of the American Control Conference*, pages 3135–3140, Washington, D.C., 2013.

46. M. Ellis and P. D. Christofides. Optimal time-varying operation of nonlinear process systems with a two-layer economic model predictive control scheme. AIChE Annual Meeting, paper 137a, San Francisco, CA, 2013.

47. M. Ellis, J. Zhang, J. Liu, and P. D. Christofides. Robust moving horizon estimation based output-feedback economic model predictive control. AIChE Annual Meeting, paper 139d, San Francisco, CA, 2013.

48. M. Ellis and P. D. Christofides. Economic model predictive control with time-varying objective function: Handling dynamic energy pricing and demand changes in process systems. AIChE Annual Meeting, paper 231c, San Francisco, CA, 2013.

49. M. Ellis and P. D. Christofides. Performance monitoring of economic model predictive control systems. AIChE Annual Meeting, paper 325b, San Francisco, CA, 2013.

50. L. Lao, M. Ellis, J. F. Davis, and P. D. Christofides. Economic model predictive control with switching objective function and constraints: Merging actuator preventive maintenance and economically-optimal operation. AIChE Annual Meeting, paper 139a, San Francisco, CA, 2013.

51. L. Lao, M. Ellis, and P. D. Christofides. Economic model predictive control of transport-reaction processes. AIChE Annual Meeting, paper 613b, San Francisco, CA, 2013.

52. T. Tu, M. Ellis, and P. D. Christofides. Model predictive control of a large-scale process network used in the production of vinyl acetate. AIChE Annual Meeting, paper 325b, San Francisco, CA, 2013.

53. M. Ellis. Economic model predictive control: Computational efficiency and chemical process applications. 24th Southern California Nonlinear Control Workshop, California Institute of Technology, Pasadena, CA, May 2013.

54. M. Ellis and P. D. Christofides. Integrating dynamic economic optimization and model predictive control for optimal operation of nonlinear process systems. UCLA Electrical Engineering Annual Research Review, University of California, Los Angeles, December 2012.

55. M. Ellis and P. D. Christofides. Integrating dynamic economic optimization and model predictive control for optimal operation of nonlinear process systems. AIChE Annual Meeting, AIChE Annual Meeting, paper 551e, Pittsburgh, PA, 2012.

56. L. Lao, M. Ellis, and P. D. Christofides. Proactive fault-tolerant model predictive control. AIChE Annual Meeting, paper 461a, Pittsburgh, PA, 2012.

Chapter 1

Introduction

1.1 Motivation

Optimal operation and control of dynamic systems and processes has been a subject of significant research for many years. Important early results on optimal control of dynamic systems include optimal control based on the Hamilton-Jacobi-Bellman equation and dynamic programming [18], Pontryagin's maximum principle [150], and the linear quadratic regulator [95]. Within the context of the chemical process industries, room for performance improvement in process operations will always exist because operating a process at the theoretical, globally optimal operating conditions for any substantial length of time is almost certainly impossible. One methodology for improving process performance is to employ the solution of optimal control problems (OCPs) on-line. In other words, control actions for the manipulated inputs of a process are computed by formulating and solving a dynamic optimization problem on-line that takes advantage of a dynamic process model while accounting for process constraints. With the available computing power of modern computers, solving complex dynamic optimization problems (e.g., large-scale, nonlinear, and non-convex optimization problems) on-line is becoming an increasingly viable option

to use as a control scheme to improve the steady-state and dynamic performance of process operations.

The process performance of a chemical process refers to the process operating economics and encapsulates many objectives: profitability, efficiency, variability, capacity, sustainability, etc. As a result of continuously changing process economics, e.g., variable feedstock, changing energy prices, variable customer demand, process operation objectives and strategies need to be frequently updated to account for these changes. Traditionally, a hierarchical strategy for planning/scheduling, optimization, and control has been employed in the chemical process industries. A block diagram of the hierarchical strategy is shown in Fig. 1.1 (adapted from [165]). Although the block diagram provides an overview of the main components, it is a simplified view of modern planning/scheduling, optimization, and control systems employed in the chemical process industry in the sense that each layer may be comprised of many distributed and hierarchical computing units. The underlying design principle of the hierarchical strategy invokes time-scale separation arguments between the execution/evolution of each layer (Fig. 1.1). In the highest level of the hierarchy, enterprise-wide and/or plant-wide planning and scheduling decisions are made on the order of days-months. These decisions are made on the basis of multiple operating processes even multiple operating plants, and are out-of-scope of the current monograph.

In the next layers of the hierarchy, economic optimization and control of chemical processes is addressed in the multi-layer hierarchical architecture, e.g., [121, 36] (Fig. 1.1). The upper-layer, called real-time optimization (RTO), is responsible for process optimization. Within the RTO layer, a metric, usually defining the operating profit or operating cost, is optimized with respect to an up-to-date and rigorous steady-state process model to compute optimal process steady-state. The computed steady-state is sent to the lower-layer feedback process control systems, which consists of the supervisory control and regulatory control layers. The process control system steers the process to operate at the steady-state

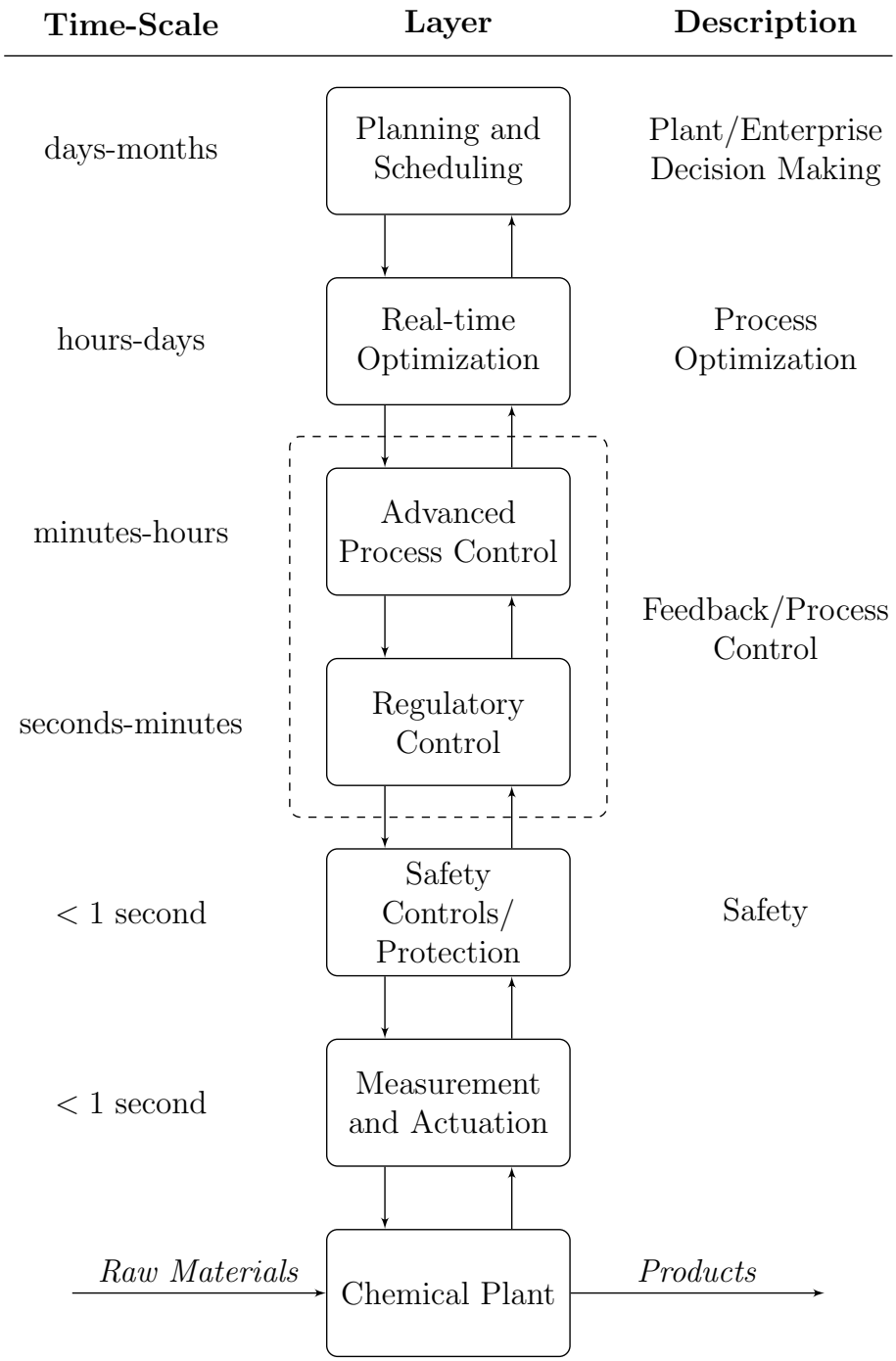

Figure 1.1: The traditional hierarchical paradigm employed in the chemical process industries for planning/scheduling, optimization, and control of chemical plants (adapted from [165]).

using the manipulated inputs to the process. Also, the process control system also must work to reject disturbances and ideally guide the trajectory of the process dynamics along an optimal path to the steady-state.

The advanced or supervisory process control layer of Fig. 1.1 consists of control algorithms that are used to account for process constraints, coupling of process variables, and processing units. In the advanced process control layer, model predictive control (MPC), a control strategy based on optimal control concepts, has been widely implemented in the chemical process industry, e.g., [125, 81, 132, 124, 155, 152]; see, also, the books [3, 27, 118, 159, 34, 69]. MPC uses a dynamic model of the process in an optimization problem to predict the future evolution of the process over a finite-time horizon and to determine the optimal input trajectory with respect to a specified performance index. Furthermore, MPC can account for the process constraints and multi-variable interactions in the optimization problem. Thus, it has the ability to optimally control constrained multiple-input multiple-output nonlinear systems. The conventional or tracking formulations of MPC use a quadratic performance index, which is a measure of the predicted squared weighted error of the states and inputs from their corresponding steady-state values, to force the process to the (economically) optimal steady-state. The regulatory control layer is composed of mostly single-input single-output control loops like proportional-integral-derivative (PID) control loops that work to implement the computed control actions by the supervisory control layer, i.e., it ensures that the control actuators achieve the control action requested by the MPC layer.

As previously mentioned, the overall control architecture of Fig. 1.1 invokes intuitive time-scale separation arguments between the various layers. For instance, RTO is executed at a rate of hours-days, while the feedback control layers compute control actions for the process at a rate of seconds-minutes-hours [165]. Though this paradigm has been successful, we are witnessing the growing need for dynamic market-driven operations which

include more efficient and nimble process operation [9, 92, 167, 38]. To enable next-generation or "Smart" operations/manufacturing, novel control methodologies capable of handling dynamic optimization of process operations should be designed and investigated. More specifically, there is a need to develop theory, algorithms, and implementation strategies to tightly integrate the layers of Fig. 1.1. The benefits of such work may be to transform process operations and usher in a new era of dynamic (off steady-state and demand and market-driven) process operations.

In an attempt to integrate economic process optimization and process control as well as realize the possible process performance improvement achieved by consistently dynamic, transient, or time-varying operation, i.e., not forcing the process to operate at a pre-specified steady-state, economic MPC (EMPC) has been proposed which incorporates a general cost function or performance index in its formulation [80, 61, 156, 86, 6, 76]. The cost function may be a direct or indirect reflection of the process economics. However, a by-product of this modification is that EMPC may operate a system in a possibly time-varying fashion to optimize the process economics and may not operate the system at a specified steady-state or target. The rigorous design of EMPC systems that operate large-scale processes in a dynamically optimal fashion while maintaining safe and stable operation of the closed-loop process system is challenging as traditional notions of stability, e.g., asymptotic stability of a steady-state, may not apply to the closed-loop system under EMPC. It is important to point out that the use of OCPs with an economic cost function is not a new concept. In fact, MPC with an economic cost is not new either (e.g., one such EMPC framework was presented in [80]). However, closed-loop stability, performance, and computational efficiency under EMPC has only recently been considered and proved for various EMPC formulations.

1.2 Objectives and Organization of the Dissertation

This dissertation considers issues related to computational efficiency of EMPC, theoretical analysis of closed-loop stability and performance under EMPC, and chemical process applications controlled by EMPC. Specifically, the objectives of this dissertation are summarized as follows:

1. To develop economic model predictive control methods that address infinite-time and finite-time closed-loop economic performance and time-varying economic considerations.

2. To develop two-layer (hierarchical) dynamic economic process optimization and feedback control frameworks that incorporate EMPC with other control strategies allowing for computational efficiency.

3. To address real-time computation of EMPC requirements.

4. To develop EMPC schemes for nonlinear time-delay systems that address closed-loop stability and performance.

5. To develop control configuration techniques for EMPC.

The dissertation is organized as follows. In the subsequent section of this chapter, a few chemical process examples that will be used to study the closed-loop properties of EMPC are presented to motivate the need for unsteady-state process operation to improve economic performance.

In Chapter 2, a brief overview of EMPC methods is provided. In particular, the role of constraints imposed in the optimization problem of EMPC for feasibility, closed-loop stability, and closed-loop performance is explained. Three main types of constraints are

considered including terminal equality constraints, terminal region constraints, and constraints designed via Lyapunov-based techniques. EMPC is applied to a benchmark chemical process example to illustrate the effectiveness of time-varying operation to improve closed-loop economic performance compared to steady-state operation and to an open-loop periodic operating policy. A few preliminary results on stabilization of sampled-data systems and on Lyapunov-based MPC is presented.

In Chapter 3, a review of Lyapunov-based EMPC (LEMPC), presented in [76], is given including closed-loop stability and robustness properties. The LEMPC designs that address closed-loop performance and time-varying economic stage cost function are also addressed in this chapter. The methods are applied to two chemical process examples.

In Chapter 4, several two-layer approaches to dynamic economic optimization and control are developed and discussed. The upper layer, utilizing an EMPC, is used to compute economically optimal policies and potentially, also, control actions that are applied to the closed-loop system. The economically optimal policies are sent down to a lower layer MPC scheme which may be a tracking MPC or an EMPC. The lower layer MPC scheme forces the closed-loop state to closely follow the economically optimal policy computed in the upper layer EMPC. The methodologies are applied to several chemical process examples to demonstrate their effectiveness.

In Chapter 5, closed-loop stability of nonlinear systems under real-time Lyapunov-based economic model predictive control (LEMPC) with potentially unknown and time-varying computational delay is considered. To address guaranteed closed-loop stability (in the sense of boundedness of the closed-loop state in a compact state-space set), an implementation strategy is developed which features a triggered evaluation of the LEMPC optimization problem to compute an input trajectory over a finite-time prediction horizon in advance. At each sampling period, stability conditions must be satisfied for the pre-computed LEMPC control action to be applied to the closed-loop system. If the stability

conditions are not satisfied, a backup explicit stabilizing controller is applied over the sampling period. Closed-loop stability under the real-time LEMPC strategy is analyzed and specific stability conditions are derived. The real-time LEMPC scheme is applied to a chemical process network example to demonstrate closed-loop stability and closed-loop economic performance improvement over that achieved for operation at the economically optimal steady-state.

In Chapter 6, closed-loop stability of nonlinear time-delay systems under LEMPC is considered. LEMPC is initially formulated with an ordinary differential equation model and is designed on the basis of an explicit stabilizing control law. To address closed-loop stability under LEMPC, first, we consider the stability properties of the sampled-data system resulting from the nonlinear continuous-time delay system with state and input delay under a sample-and-hold implementation of the explicit controller. The steady-state of the resulting closed-loop system is shown to be practically stable. Second, conditions such that closed-loop stability, in the sense of boundedness of the closed-loop state, under LEMPC are derived. A chemical process example is used to demonstrate that indeed closed-loop stability is maintained under LEMPC for sufficiently small time-delays. To cope with performance degradation owing to the effect of input delay, a predictor feedback LEMPC methodology is also discussed. The predictor feedback LEMPC design employs a predictor to compute a prediction of the state after the input delay period and an LEMPC scheme that is formulated with a differential difference model (DDE) model, which describes the time-delay system, initialized with the predicted state. The predictor feedback LEMPC is also applied to the chemical process example and yields improved closed-loop stability and economic performance properties.

In Chapter 7, an input selection methodology for EMPC is developed. The methodology utilizes the relative degree and the sensitivity of the economic cost with respect to an input to identify and select stabilizing manipulated inputs with the most dynamic and

steady-state influence on the economic cost function to be assigned to EMPC. Other considerations for input selection for EMPC are also discussed and integrated into an input selection methodology for EMPC. The control configuration selection method for EMPC is demonstrated using a chemical process example.

Chapter 8 summarizes the main results of the dissertation.

1.3 Chemical Process Examples

As discussed in the introduction, steady-state operation is typically adopted in chemical process industries, i.e., the control system is used to force a chemical process to a pre-specified steady-state and maintain operation at this steady-state thereafter. However, steady-state operation may not necessarily be the best operation strategy with respect to the process economics. In fact, the chemical process control literature is rich with chemical process examples that demonstrate performance improvement with respect to specific cost metrics with dynamic process operation, e.g., [42, 110, 171, 189, 188, 14, 168, 166, 179, 180, 144, 146, 145, 170, 24, 114, 139, 25, 120, 169], and the numerous references therein. To help identify systems that achieve a performance benefit from periodic operation, several techniques have been proposed including frequency response techniques and the application of the maximum principle [42, 11, 22, 10, 72, 179]. Periodic control strategies have also been developed for several applications, for instance, [114, 139, 24, 166, 146].

While the periodic operating strategies listed above do demonstrate economic performance improvement, in the case of forced periodic operation, i.e., periodic operation induced by periodic switching of manipulated inputs, the periodic operating policy is identified through a low-order control parameterization, e.g., a bang-bang input profile. Owing to recent advances in dynamic optimization (numerical solution strategies or direct methods), it is possible that these chemical process examples previously considered in the context of

Table 1.1: Dimensionless process model parameters of the ethylene oxidation reactor model. The parameters are from [144].

Parameter	Value	Parameter	Value
A_1	92.80	B_3	2170.57
A_2	12.66	B_4	7.02
A_3	2412.71	γ_1	-8.13
B_1	7.32	γ_2	-7.12
B_2	10.39	γ_3	-11.07

periodic operation may achieve further economic performance improvement under EMPC (two such example are given below). Moreover, the main advantage of EMPC is that it systematically determines, in real-time, the optimal operating strategy based on the economic measure while accounting for operating constraints. Two chemical process examples that benefit from time-varying operation are provided below.

1.3.1 Catalytic Oxidation of Ethylene

Consider a benchmark chemical reactor example previously studied in the context of forced periodic operation [144, 146]. Within the reactor, ethylene oxide (C_2H_4O) is produced from the catalytic oxidation of ethylene with air. Ethylene oxide is an important raw material within the chemical industry because it is used for the synthesis of ethylene glycol which is subsequently used to produce many materials. The reactor is modeled as a non-isothermal continuous stirred-tank reactor (CSTR) with a coolant jacket to remove heat from the reactor. Two combustion reactions occur that consume both the reactant and the

product, i.e., ethylene and ethylene oxide, respectively. The reactions are given by

$$\mathrm{C_2H_4} + \frac{1}{2}\mathrm{O_2} \xrightarrow{r_1} \mathrm{C_2H_4O}$$
$$\mathrm{C_2H_4} + 3\mathrm{O_2} \xrightarrow{r_2} 2\mathrm{CO_2} + 2\mathrm{H_2O}$$
$$\mathrm{C_2H_4O} + \frac{5}{2}\mathrm{O_2} \xrightarrow{r_3} 2\mathrm{CO_2} + 2\mathrm{H_2O}$$

where r_i, $i = 1,2,3$ is the reaction rate of the ith reaction, and the reaction rate expressions are

$$r_1 = k_1 \exp\left(\frac{-E_1}{RT}\right) P_E^{0.5} \tag{1.1}$$
$$r_2 = k_2 \exp\left(\frac{-E_2}{RT}\right) P_E^{0.25} \tag{1.2}$$
$$r_3 = k_3 \exp\left(\frac{-E_3}{RT}\right) P_{EO}^{0.5} \tag{1.3}$$

where k_i and E_i, $i = 1,2,3$ are the reaction rate constant and activation energy for the ith reaction, respectively, T is the temperature, R is the ideal gas constant, and P_j is the partial pressure of the jth component in the reactor ($j = E, EO$ denotes ethylene and ethylene oxide, respectively). The reaction rate expressions are from [2] where catalytic oxidation of ethylene using an unmodified, commercial catalyst was studied over the temperature range 523-573 K. To model the gaseous mixture within the reactor, ideal gas is assumed and the concentration of the jth component within the reactor, denoted by C_j, is

$$C_j = \frac{P_j}{RT} \ . \tag{1.4}$$

A model describing the dynamic behavior of the reactor is derived through first principles under standard modeling assumptions, e.g., ideal gas and constant heat capacity. The

dimensionless states are

$$x_1 = \rho/\rho_{\text{ref}}, \quad x_2 = C_E/C_{\text{ref}}, \quad x_3 = C_{EO}/C_{\text{ref}}, \quad x_4 = T/T_{\text{ref}}$$

where ρ/ρ_{ref} is the dimensionless vapor density in the reactor, C_E/C_{ref} is the dimensionless ethylene concentration in the reactor, C_{EO}/C_{ref} is the dimensionless ethylene oxide concentration in the reactor, and T/T_{ref} is the dimensionless reactor temperature. The manipulated inputs are

$$u_1 = Q_f/Q_{\text{ref}}, \quad u_2 = C_{E,f}/C_{\text{ref}}, \quad u_3 = T_c/T_{\text{ref}}$$

where Q_f/Q_{ref} is the dimensionless volumetric flow rate of the reactor feed, $C_{E,f}/C_{\text{ref}}$ is the dimensionless ethylene concentration of the reactor feed, and T_c/T_{ref} is the dimensionless coolant temperature. The model of the reactor is given by the following set of nonlinear ordinary differential equations:

$$\frac{dx_1}{dt} = u_1(1 - x_1x_4) \tag{1.5}$$

$$\frac{dx_2}{dt} = u_1(u_2 - x_2x_4) - A_1\bar{r}_1(x_2,x_4) - A_2\bar{r}_2(x_2,x_4) \tag{1.6}$$

$$\frac{dx_3}{dt} = -u_1x_3x_4 + A_1\bar{r}_1(x_2,x_4) - A_3\bar{r}_3(x_3,x_4) \tag{1.7}$$

$$\frac{dx_4}{dt} = \frac{u_1}{x_1}(1 - x_4) + \frac{B_1}{x_1}\bar{r}_1(x_2,x_4) + \frac{B_2}{x_1}\bar{r}_2(x_2,x_4) + \frac{B_3}{x_1}\bar{r}_3(x_3,x_4) - \frac{B_4}{x_1}(x_4 - u_3) \tag{1.8}$$

where

$$\bar{r}_1(x_2,x_4) = \exp(\gamma_1/x_4)(x_2x_4)^{1/2} \tag{1.9}$$

$$\bar{r}_2(x_2,x_4) = \exp(\gamma_2/x_4)(x_2x_4)^{1/4} \tag{1.10}$$

$$\bar{r}_3(x_3,x_4) = \exp(\gamma_3/x_4)(x_3x_4)^{1/2} \tag{1.11}$$

and the parameters are given in Table 1.1 from [144, 146]. The maximum available control energy is considered to be bounded in the following set:

$$u_1 \in [0.0704, 0.7042],$$
$$u_2 \in [0.2465, 2.4648],$$
$$u_3 \in [0.6, 1.1] \ .$$

The profitability of the reactor scales with the yield of ethylene oxide. Therefore, to optimize the profitability or economics of the reactor, one seeks to maximize the time-averaged yield of ethylene oxide. The time-averaged yield of ethylene oxide over an operating time t_f is given by

$$Y = \frac{\frac{1}{t_f}\int_0^{t_f} x_3(\tau)x_4(\tau)u_1(\tau)\,d\tau}{\frac{1}{t_f}\int_0^{t_f} u_1(\tau)u_2(\tau)\,d\tau} \tag{1.12}$$

which is a measure of the amount of ethylene oxide leaving the reactor relative to the amount of ethylene fed into the reactor. For practical reasons, one may want to optimize the yield while also ensuring that the time-averaged amount of ethylene that is fed to the reactor be fixed, i.e., determine the method to distribute ethylene to the reactor that maximizes the yield. Limiting the time-averaged amount of ethylene that may be fed to the reactor is described by the following constraint:

$$\frac{1}{t_f}\int_0^{t_f} u_1(\tau)u_2(\tau)\,d\tau = \dot{M}_E \tag{1.13}$$

where $\dot{M}_E$ is the time-averaged dimensionless molar flow rate of ethylene that may be fed to the reactor. If $u_{1,\min}u_{2,\min} < \dot{M}_E < u_{1,\max}u_{2,\max}$, the constraint of Eq. 1.13 prevents one from simply considering feeding in the minimum or maximum flow rate of ethylene

Table 1.2: Process parameters of the CSTR.

k_0	8.46×10^6	A_1	1.69×10^6
x_{20}	0.050	A_2	1.41×10^4

to the reactor over time. Within the context of EMPC, the constraint of Eq. 1.13 gives rise to a class of economically motivated constraints which take the form of integral or average constraints. In stark contrast to traditional or conventional control methodologies (e.g., proportional-integral-derivative control or tracking MPC), economically motivated constraints may be directly incorporated into EMPC.

1.3.2 Continuously-Stirred Tank Reactor with Second-order Reaction

A well-known chemical engineering example that demonstrates performance improvement through time-varying operation is a CSTR where a second-order reaction occurs. Specifically, consider the system described by the following dynamic equations given in dimensionless form:

$$\dot{x}_1 = -x_1 - A_1 e^{-1/x_2} x_1^2 + u \tag{1.14a}$$

$$\dot{x}_2 = -x_2 + A_2 e^{-1/x_2} x_1^2 + x_{20} \tag{1.14b}$$

where x_1 is the dimensionless reactant concentration, x_2 is the dimensionless temperature, and A_1, A_2 and x_{20} are constant parameters. The values of the parameters are given in Table 1.2. The input is bounded: $u \in [u_{\min}, u_{max}] = [0.5, 7.5]$. The system of Eq. 1.14 describes a non-isothermal CSTR where a second-order reaction occurs and the inlet concentration of the reactant material is the manipulated input. The economic stage cost is

$$l_e(x,u) = k_0 e^{-1/x_2} x_1^2 \tag{1.15}$$

which is the production rate of the desired product (k_0 is a parameter). The system has an input average constraint (dynamic constraint) given by:

$$\frac{1}{t_f}\int_0^{t_f} u(t)\ dt = u_{avg} = 4.0 \tag{1.16}$$

where t_f is the length of operation. The practical motivation of the average constraint of Eq. 1.16 is that the average amount of material that may be distributed to the reactor over time is fixed, i.e., the constraint is economically motivated. The CSTR has an optimal steady-state $x_s^T = [1.182 \quad 0.073]$ which corresponds to the steady-state input that satisfies the average input constraint ($u_s = u_{avg}$) with a production rate of 14.03.

An analysis is completed to determine if the economic performance, i.e., the average production rate of the product, can be improved by using a time-varying operating strategy compared to operating at the optimal steady-state. An auxiliary state is defined for the average constraint:

$$x_3(t) := \frac{1}{t_f}\int_0^t \left(u(t) - u_{avg}\right)\ dt \tag{1.17}$$

which has dynamics:

$$\dot{x}_3(t) = \frac{1}{t_f}(u(t) - u_{avg})\ . \tag{1.18}$$

The non-isothermal CSTR with the objective function of Eq. 1.15 is a member of a special class of nonlinear systems:

$$\dot{x} = \bar{f}(x) + Bu \tag{1.19}$$

where $B \in \mathbb{R}^n \times \mathbb{R}^m$ is a constant matrix and $\bar{f} : \mathbb{R}^n \to \mathbb{R}^n$ is a differentiable vector function. Additionally, the stage cost only depends on the states:

$$l_e(x,u) = \bar{l}_e(x) \tag{1.20}$$

where $\bar{l}_e : \mathbb{R}^n \to \mathbb{R}$ is a differentiable function. The Hamiltonian function of the system of Eq. 1.19 and cost of Eq. 1.20 is

$$H(x,u,\lambda) = \bar{l}_e(x) + \lambda^T \bar{f}(x) + \lambda^T B u \tag{1.21}$$

where λ is the adjoint variable vector that satisfies

$$\dot{\lambda}(t) = -H_x(x(t),u(t),\lambda(t)) \tag{1.22}$$

where H_x denotes the partial derivative of H with respect to x. From Pontryagin's maximum principle [150], a necessary condition can be derived for the optimal control, i.e., the control that maximizes the Hamiltonian:

$$u_i^*(t) = \begin{cases} u_{i,\max}, & \text{if } b_i^T \lambda(t) > 0 \\ u_{i,\min}, & \text{if } b_i^T \lambda(t) < 0 \end{cases} \tag{1.23}$$

where b_i is the i-th column of B. For this class of systems and stage costs, if some time-varying operating policy is the optimal operating strategy, then the operating policy is a bang-bang input policy of Eq. 1.23.

Although the analysis above significantly reduces the space of possible optimal input trajectories, it still yields an infinite space of input trajectories. Thus, consider the following periodic bang-bang input trajectory over one period:

$$u(t) = \begin{cases} u_{\max} & \text{if } t < \tau/2 \\ u_{\min} & \text{else} \end{cases} \tag{1.24}$$

where τ is the period and $t \in [0,\tau)$. The input trajectory of Eq. 1.24 satisfies the average

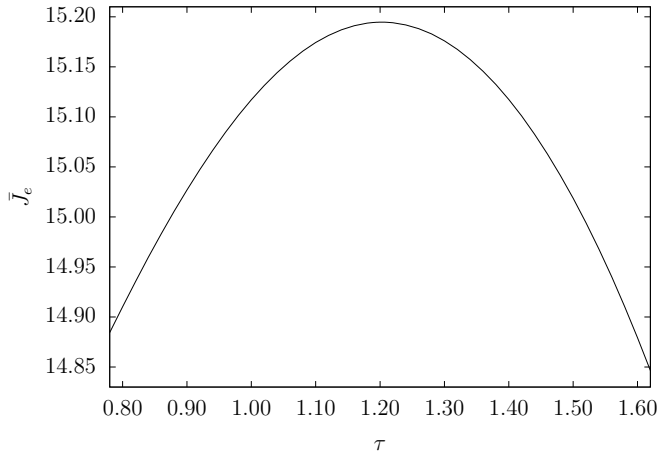

Figure 1.2: Average economic performance $\bar{J}_e$ as a function of the period length τ.

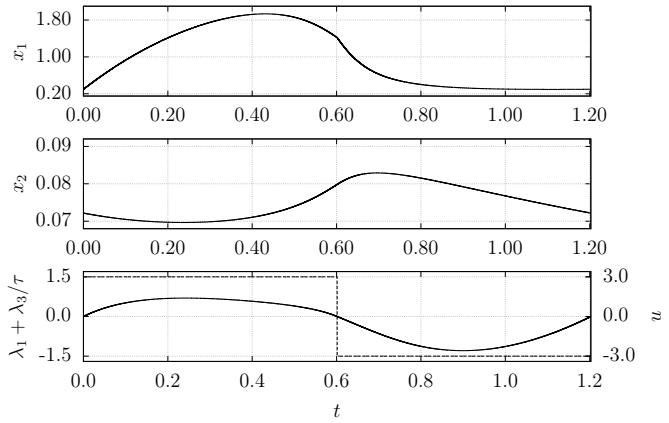

Figure 1.3: State, input, and $\lambda_1 + \lambda_3/\tau$ trajectories of the CSTR under the bang-bang input policy with period $\tau = 1.20$.

constraint of Eq. 1.16 over each period. For the system of Eq. 1.14 with the input trajectory of Eq. 1.24, there exists a periodic state trajectory for some $\tau > 0$, i.e., it has the property $x(t) = x(t+\tau)$ for all t.

Indeed, the periodic solution of the system of Eq. 1.14 with the input of Eq. 1.24 achieves better economic performance compared to the economic performance at steady-state for some τ. Moreover, the economic performance depends on the period which is shown in Fig. 1.2. Over the range of periods considered (0.5 to 2.4), the period $\tau = 1.20$

yields the best performance (Fig. 1.2). The periodic solution with the input period of $\tau = 1.20$ has an average cost of $\bar{J}_e = 15.20$ which is 8.30 percent better than the performance at the optimal steady-state. Periods greater than 1.96 achieve worse performance compared to that at steady-state. The state, input, and $B^T\lambda = b_1^T\lambda = \lambda_1 + \lambda_3/\tau$ trajectories are given in Fig. 1.3 over one period. From Fig. 1.3, the input trajectory satisfies the necessary condition of Eq. 1.23. From these results, time-varying operation is better than steady-state operation from an economical point of view for this example. If the average constraint of Eq. 1.16 was not imposed, the optimal operating strategy would be steady-state operation at the steady-state corresponding to the input $u_{\max}$. The average constraint plays a crucial role for this particular example.

As pointed out, the above analysis only considers economic performance. If the periodic solution depicted in Fig. 1.3 is indeed optimal or some other bang-bang policy is the best operating strategy, feedback control is needed to force the system state from an initial state to the optimal time-varying solution. Moreover, the control problem becomes more complex when one considers disturbances, plant-model mismatch and other forms of uncertainty, implementability of the computed input trajectory, i.e., bang-bang control may not be implementable in practice, and time-varying economic objectives and constraints. The example further motivates the inquiry and theoretical developments in the context of EMPC systems that dictate time-varying operating policies.

Chapter 2

Brief Overview of EMPC Methods and Some Preliminary Results

This chapter contains a brief background on EMPC methods and some preliminary results on sampled-data systems and Lyapunov-based MPC (LMPC). The background on EMPC methods is meant to provide context to the EMPC design methodologies of the subsequent chapters. However, it is not meant to be comprehensive and rigorous. For a more comprehensive and rigorous treatment, please refer to the reviews [157, 57] as well as the relevant literature. The preliminary results are used in subsequent chapters.

2.1 Background on EMPC Methods

A brief overview of EMPC methods is provided in this section. The review of EMPC methods is a version of [55]. First, the notation used throughout this dissertation is presented.

2.1.1 Notation

The set of real numbers is denoted by $\mathbb{R}$, while the set of integers is denoted by $\mathbb{I}$. The symbol $\mathbb{R}_{\geq 0}$ ($\mathbb{I}_{\geq 0}$) is used to denote positive reals (integers), and $\mathbb{R}^n$ is an n-dimensional real (Euclidean) space. The notation $x(t) \in \mathbb{R}^n$ represents a time-dependent vector. The symbol $|\cdot|$ denotes the Euclidean norm of a vector, i.e., $|x| = \sqrt{x^T x}$ where $x \in \mathbb{R}^n$ and x^T denotes the transpose of x, and $|\cdot|_Q^2$ denotes the square of a weighted Euclidean norm of a vector, i.e., $|x|_Q^2 = x^T Q x$ where Q is a positive definite matrix. A square diagonal matrix with diagonal elements equal to the elements of a vector v is written as $\text{diag}(v)$. An infinite sequence is denoted by $\{t_k\}_{k\geq 0}$, while a finite sequence is written as $\{t_i\}_{i=0}^N$ which describes the sequence: $t_0, t_1, \ldots, t_{N-1}, t_N$.

With regard to functions, a function, $V : \mathbb{R}^n \to \mathbb{R}$, is said to be positive definite with respect to $\bar{x}$ if $V(x) > 0$ for all $x \in \mathbb{R}^n$ except for $\bar{x}$ when $V(\bar{x}) = 0$. When a function is positive definite with respect to the origin ($\bar{x} = 0$), the function is simply called positive definite and the distinction that it is positive definite with respect to the origin is omitted. A function, $V : \mathbb{R}^n \to \mathbb{R}$, is negative definite if $-V$ is positive definite. A continuous function $\alpha : [0, a) \to \mathbb{R}_{\geq 0}$ is said to be of class $\mathcal{K}$ if it is strictly increasing and $\alpha(0) = 0$, and it is of class $\mathcal{K}_\infty$ if it is of class $\mathcal{K}$, $a = \infty$, and $\alpha(r)$ as $r \to \infty$, i.e., it is radially unbounded. A function $\beta : [0, a) \times \mathbb{R}_{\geq 0} \to \mathbb{R}_{\geq 0}$ is said to be of class-$\mathcal{KL}$ if $\beta(\cdot, t)$ is of class-$\mathcal{K}$ for each $t \geq 0$ and $\beta(s, \cdot)$ is monotonically decreasing to zero for each $s \geq 0$. The family of piecewise constant, right-continuous functions with period Δ is denoted as $S(\Delta)$, and with a slight abuse of notation, we will say $u(\cdot) \in S(\Delta)$ (or simply, $u \in S(\Delta)$) when the vector-valued function $u : [0, N\Delta) \to \mathbb{R}^m$, $u : t \mapsto u(t)$, may be described by

$$u(t) = \bar{u}_i, \text{ for } t \in [i\Delta, (i+1)\Delta)$$

for $i = 0, 1, \ldots, N-1$ where $\Delta > 0$ is the period and $\bar{u}_i \in \mathbb{R}^m$ (note that the appropriate

domain of the function u will be implied by the context). The floor and ceiling functions, denoted as $\lfloor a \rfloor$ and $\lceil a \rceil$ ($a \in \mathbb{R}$), respectively, are the largest integer not greater than a and the smallest integer not less than a, respectively.

The set Ω_r is a level set, also referred to as a level surface or sublevel set, of a scalar-valued positive definite function: $\Omega_r := \{x \in \mathbb{R}^n : V(x) \leq r\}$ where $r > 0$. A ball of radius $\nu > 0$ is given by $B_\nu := \{x \in \mathbb{R}^n : |x| \leq \nu\}$. The notation $B \setminus A$ denotes the relative complement of the set A in B, i.e., $B \setminus A = \{x \in B : x \notin A\}$. Finally, for algorithms, the notation $j \leftarrow j + 1$ is used to denote that at the next time step or the next iteration of the loop, the index j is incremented by one.

2.1.2 Class of Nonlinear Systems

The class of systems considered is described by the system of nonlinear ordinary differential equations (ODEs):

$$\dot{x} = f(x, u, w) \tag{2.1}$$

where $x \in \mathbb{X} \subset \mathbb{R}^n$ denotes the state vector, $u(t) \in \mathbb{U} \subset \mathbb{R}^m$ denotes the manipulated (control) input vector, and $w \in \mathbb{W} \subset \mathbb{R}^l$ denotes the disturbance vector. The set of admissible input values $\mathbb{U}$ is assumed to be compact, and the disturbance vector is bounded in the set $\mathbb{W} := \{w \in \mathbb{R}^l : |w| \leq \theta\}$ where $\theta > 0$ bounds the norm of the disturbance vector. The vector function $f : \mathbb{X} \times \mathbb{U} \times \mathbb{W} \to \mathbb{X}$ is locally Lipschitz on $\mathbb{X} \times \mathbb{U} \times \mathbb{W}$. A state measurement is synchronously sampled at sampling instances denoted by the sequence $\{t_k\}_{k \geq 0}$ where $t_k := k\Delta$, $k \in \mathbb{I}_{\geq 0}$, and $\Delta > 0$ is the sampling period (the initial time is taken to be zero). The assumption of state feedback is standard owing to the fact that the separation principle does not generally hold for nonlinear systems. Nevertheless, some rigorous output feedback implementations of EMPC exist, e.g., [77, 60, 201].

The system of Eq. 2.1 is assumed to be equipped with a continuous function $l_e : \mathbb{X} \times$

$\mathbb{U} \to \mathbb{R}$, which reflects the instantaneous process/system economics. The function $l_e(\cdot,\cdot)$ will be used as a stage cost in a model predictive control (MPC) framework and will be referred to as the economic stage cost. The system of Eq. 2.1 may have additional constraints other than the input and state constraints. Collecting all the constraints including the input, state, and additional constraints, the constraints may be written generally as static constraints:

$$g_s(x,u) \leq 0 \tag{2.2}$$

where $g_s : \mathbb{X} \times \mathbb{U} \to \mathbb{R}^{n_s}$ and as dynamic constraints, e.g., average constraints like that of Eq. 1.13 and Eq. 1.16 of the two examples of Chapter 1:

$$\int_0^{t_d} g_d(x(t),u(t))\, dt \leq 0 \tag{2.3}$$

where $g_d : \mathbb{X} \times \mathbb{U} \to \mathbb{R}^{n_d}$ and t_d is the time horizon that the constraint is imposed. The dynamic constraints are often motivated by economic considerations. The economically optimal steady-state and steady-state input pair is:

$$(x_s^*, u_s^*) = \underset{(x_s,u_s)}{\arg\min} \{ l_e(x_s,u_s) : f(x_s,u_s,0) = 0,\ g_s(x_s,u_s) \leq 0,\ g_d(x_s,u_s) \leq 0 \}. \tag{2.4}$$

With the notation above, the optimal (minimizing) steady-state pair (x_s^*, u_s^*) is assumed to exist and to be unique. If the minimizing pair is not unique, let (x_s^*, u_s^*) denote one of the minimizing steady-state pairs. Without loss of generality, the optimal steady-state is taken to be the origin of the unforced system ($f(0,0,0) = 0$) in what follows.

2.1.3 EMPC Methods

Economic model predictive control is an MPC method that uses the economic stage cost in its formulation. The EMPC problem, with a finite-time prediction horizon, may be broadly

characterized by the following optimal control problem (OCP):

$$\min_{u \in S(\Delta)} \int_{t_k}^{t_{k+N}} l_e(\tilde{x}(t), u(t))\, dt + V_f(\tilde{x}(t_{k+N})) \tag{2.5a}$$

$$\text{s.t. } \dot{\tilde{x}}(t) = f(\tilde{x}(t), u(t), 0) \tag{2.5b}$$

$$\tilde{x}(t_k) = x(t_k) \tag{2.5c}$$

$$g_s(\tilde{x}(t), u(t)) \leq 0,\ \forall\, t \in [t_k, t_{k+N}) \tag{2.5d}$$

$$\int_{t_k}^{t_{k+N}} \tilde{g}_d(\tilde{x}(t), u(t), t_k)\, dt \leq 0 \tag{2.5e}$$

where the decision variable of the optimization problem is the piecewise constant input trajectory over the prediction horizon, i.e., the time interval $[t_k, t_{k+N})$, and $\tilde{x}$ denotes the predicted state trajectory over the prediction horizon. Higher-order control parameterizations may also be considered. Nevertheless, sample-and-hold, i.e., zeroth-order hold, implementation of controls is one of the most commonly employed control parameterizations. Since the input trajectory of Eq. 2.5 may be parameterized by N, m-dimensional vectors, the optimization problem is finite dimensional.

The cost functional of Eq. 2.5a consists of the economic stage cost with a terminal cost/penalty $V_f : \mathbb{X} \to \mathbb{R}$. The nominal dynamic model of Eq. 2.5b is used to predict the future evolution of the system and is initialized with a state measurement of Eq. 2.5c. When available, disturbance estimates or predictions may be incorporated in the model of Eq. 2.5b. The constraints of Eqs. 2.5d-2.5e represent the system constraints which may include, input, state, mixed state and input, economic, and stability constraints. The constraint of Eq. 2.5e may be time-varying, i.e., formulated for the sampling time t_k, so that the constraint of Eq. 2.3 is satisfied over the desired operating interval, and hence, the notation of Eq. 2.5e is used to denote that the constraint is formulated for the sampling time t_k. For the remainder of this section, the dynamic constraints are dropped and only

EMPC schemes of the form of Eqs. 2.5a-2.5d are considered. Thus, the constraint set is $\mathbb{Z} := \{(x,u) : x \in \mathbb{X},\ u \in \mathbb{U},\ g_s(x,u) \leq 0\} \subseteq \mathbb{X} \times \mathbb{U}$ and $\mathbb{Z}$ is assumed to be compact.

EMPC is typically implemented with a receding horizon implementation to better approximate the infinite-horizon solution and to ensure robustness of the control solution to disturbances and open-loop instabilities. At a sampling time t_k, the EMPC receives a state measurement, which is used to initialize the model of Eq. 2.5b. The OCP of Eq. 2.5 is solved on-line for a (local) optimal piecewise input trajectory, denoted by $u^*(t|t_k)$ for $t \in [t_k, t_{k+N})$. The control action computed for the first sampling period of the prediction horizon, denoted as $u^*(t_k|t_k)$, is sent to the control actuators to be implemented over the sampling period from t_k to t_{k+1}, i.e., sample-and-hold implementation. At the next sampling time, the OCP of Eq. 2.5 is re-solved after receiving a new state measurement and by shifting the prediction horizon into the future by one sampling period.

EMPC, which consists of the on-line solution of the OCP of Eq. 2.5 along with a receding horizon implementation, results in an implicit state feedback law $u(t) = \kappa(x(t_k))$ for $t \in [t_k, t_{k+1})$. From a theoretical perspective, three fundamental issues are considered and addressed with respect to EMPC. The first consideration is the feasibility of the optimization problem (both initial and recursive feasibility are considered). Second, if Eq. 2.5 is recursively feasible, it is important to consider the stability properties of the closed-loop system under EMPC. In general, one may not expect that EMPC will force the state to a desired steady-state. The last theoretical consideration is closed-loop economic performance under EMPC. Within the context of EMPC, closed-loop performance typically means the average closed-loop economic performance. Over a finite-time operating interval of length t_f, the average performance is defined by the following index:

$$\bar{J}_e := \frac{1}{t_f} \int_0^{t_f} l_e(x(t), u(t))\, dt \tag{2.6}$$

where x and u are the closed-loop state and input trajectories, respectively, and over an infinite-time operating interval, the infinite-time (asymptotic) average economic performance is given by:

$$\bar{J}_{e,\infty} := \limsup_{t_f \to \infty} \frac{1}{t_f} \int_0^{t_f} l_e(x(t), u(t))\, dt \ . \tag{2.7}$$

Within the context of EMPC, the average economic performance is of interest because EMPC may dictate a time-varying operating strategy to optimize the process/system economics. Thus, it may not enforce convergence to the economically optimal steady-state. While the instantaneous stage cost under EMPC at any time may be better or worse than the stage cost at the economically optimal steady-state and steady-state input pair, the average economic performance under the time-varying operating policy dictated by EMPC over the length of operation may be better than that achieved by operation at the economically optimal steady-state.

Without additional assumptions and conditions, one may easily construct examples of systems and stage costs of the form described above where the closed-loop under EMPC (without additional stability constraints) is unstable. Clearly, additional conditions and/or constraints enforced in the EMPC problem may be needed to guarantee closed-loop stability. Some theoretical investigations on EMPC that do not incorporate additional stability constraints exist including the work of [68, 70] which require that the resulting EMPC has a sufficiently long horizon as well as certain controllability assumptions and turnpike conditions be satisfied to guarantee closed-loop stability and performance properties. Moreover, even though EMPC optimizes the process/system economics, it does so over a finite-time prediction horizon. Over long periods of operation, no conclusion, in general, may be made on closed-loop performance under EMPC (without additional constraints). For provable results on feasibility, closed-loop stability, and closed-loop performance under EMPC, typically, additional stability and/or performance constraints are added to the formulation

of EMPC. These formulations are discussed in the subsequent sections.

To address closed-loop stability, one may consider employing an infinite-horizon in the EMPC. This may be a more appropriate prediction horizon because many chemical processes are continuously operated over long periods of time (practically infinite time). At least intuitively, the resulting control law will provide some form of closed-loop stability assuming the existence of a solution to the infinite-horizon EMPC as well as the ability to solve for a solution on-line. However, it is practically impossible to solve an OCP with an infinite-horizon. To overcome this problem, two approaches include: (1) approximating the infinite-horizon with a sufficiently long finite-time horizon and (2) dividing the infinite-horizon into a finite-time horizon and estimating the infinite-horizon tail through an auxiliary control law or with modeling-based techniques, e.g., [195, 86, 39, 85, 126, 127, 143, 196, 194]. Although some of these EMPC schemes may be computationally tractable, the use of constraints typically enables shorter prediction horizons, which may reduce the on-line computation relative to those that require sufficiently long horizons. Thus, infinite-horizon EMPC and EMPC without stability constraints are not discussed, but rather, EMPC systems formulated with constraints to provide guaranteed closed-loop properties are considered.

EMPC with an Equality Terminal Constraint

Much of the recent theoretical work on EMPC investigates the extension of stabilizing elements used in tracking MPC to EMPC such as adding a terminal constraint and/or terminal cost (see, for instance, [124] for more details on the use of terminal constraints and/or a terminal cost within the context of tracking MPC). Numerous EMPC formulations and theoretical developments which include a terminal constraint and/or terminal cost have been proposed and studied, e.g., [158, 156, 63, 4, 39, 86, 111, 6, 134, 44, 112, 157, 5, 62, 67, 83, 135, 136, 13, 137, 191, 199]. There are two main types of EMPC with terminal constraints:

(1) EMPC with an equality terminal constraint, and (2) EMPC with a terminal region constraint. In this subsection, the former type of EMPC is considered which is an EMPC that is described by the optimization problem:

$$\min_{u\in S(\Delta)} \int_{t_k}^{t_{k+N}} l_e(\tilde{x}(t), u(t))\, dt \tag{2.8a}$$

$$\text{s.t. } \dot{\tilde{x}}(t) = f(\tilde{x}(t), u(t), 0) \tag{2.8b}$$

$$\tilde{x}(t_k) = x(t_k) \tag{2.8c}$$

$$\tilde{x}(t_N) = x_s^* \tag{2.8d}$$

$$g_s(\tilde{x}(t), u(t)) \leq 0,\ \forall\ t \in [t_k, t_{k+N}) \tag{2.8e}$$

where the constraint of Eq. 2.8d forces that the predicted state trajectory to converge to the optimal steady-state at the end of the finite-time horizon. For EMPC with an equality terminal constraint, the terminal cost is often omitted as it is not required for stability and performance guarantees.

Feasibility. EMPC with a terminal equality constraint is (initially) feasible for any initial state in $\mathbb{X}_N \in \mathbb{R}^n$ which denotes the feasibility region of EMPC of Eq. 2.8. The feasible region depends on the prediction horizon, and an explicit characterization of $\mathbb{X}_N$ is difficult in general. Recursive feasibility, i.e., feasibility at each subsequent sampling time, of EMPC with an equality terminal constraint is guaranteed for the nominally operated system for any initial state $x(0) \in \mathbb{X}_N$. This follows from the fact that a feasible solution to the EMPC may be constructed from the solution from the previous sampling time. Namely, $u(t) = u^*(t|t_{k-1})$ for $t \in [t_k, t_{k+N-1})$ and $u(t) = u_s^*$ for $t \in [t_{k+N-1}, t_{k+N})$ is a feasible solution for the EMPC at t_k because it satisfies the constraints and the terminal constraint of Eq. 2.8d. However, recursive feasibility is harder to show, in general, when $w(\cdot) \not\equiv 0$.

Closed-loop Stability. With respect to closed-loop stability, a weak notion of stability

follows from the EMPC with terminal constraint formulation. If the initial state is in the feasible set, the closed-loop state trajectory remains contained in the feasible set for nominal operation. For stronger stability properties, e.g., asymptotic stability of x_s^*, additional assumptions on the closed-loop system must be satisfied. To discuss this issue, nonlinear discrete-time systems are considered that have the form:

$$x(k+1) = f_d(x(k), u(k)) \tag{2.9}$$

where $f_d : \mathbb{X} \times \mathbb{U} \to \mathbb{X}$ is the discrete-time state transition map and $k \in \mathbb{I}_{\geq 0}$ is the time index. As before, the system of Eq. 2.9 is subject to mixed state and input constraints $(x,u) \in \mathbb{Z} \subseteq \mathbb{X} \times \mathbb{U}$ where $\mathbb{Z}$ is a compact set and the origin is assumed to be the optimal steady-state ($f_d(0,0) = 0$). Discrete-time systems are considered here to maintain consistency with the literature on the topic. Nonetheless, some of these conditions and results have been extended to continuous-time systems, e.g., [1]. One condition that leads to stronger stability properties is the notion of dissipativity which has been extended to EMPC. Dissipativity was originally presented in [190] for continuous-time systems and then, extended to discrete-time systems [26].

Definition 2.1 ([6])**.** The system of Eq. 2.9 is *strictly dissipative* with respect to a supply rate $s : \mathbb{X} \times \mathbb{U} \to \mathbb{R}$ if there exist a function $\lambda : \mathbb{X} \to \mathbb{R}$ and a positive definite function $\beta : \mathbb{X} \to \mathbb{R}_{\geq 0}$ such that

$$\lambda(f_d(x,u)) - \lambda(x) \leq -\beta(x) + s(x,u) \tag{2.10}$$

for all $(x,u) \in \mathbb{Z}$.

If the system of Eq. 2.9 is strictly dissipative with a supply rate:

$$s(x,u) = l_e(x,u) - l_e(x_s^*, u_s^*) \tag{2.11}$$

then, the optimal steady-state is asymptotically stable for the closed-loop system under EMPC with an equality terminal constraint [6]. Moreover, a Lyapunov function for the closed-loop system was derived using the cost functional of the so-called rotated cost function [6]:

$$L(x,u) := l_e(x,u) + \lambda(x) - \lambda(f_d(x,u)) \ . \tag{2.12}$$

The idea of using the rotated cost function to construct a Lyapunov function for the closed-loop system was originally proposed in [39]. However, it relied on strong duality of the steady-state optimization problem, which is a stronger assumption than strict dissipativity.

Closed-loop Performance. Utilizing the optimal input trajectory at t_k (or time step k in discrete-time) as a feasible solution to the EMPC at the next sampling period, one may upper bound the difference between the cost functional value at the next sampling time and at the current sampling time under nominal operation. The optimal input trajectory in discrete-time is denoted $u^*(j|k)$ for $j = k,\ k+1,\ \ldots,\ k+N-1$, and the optimal cost functional value at time step k is denoted:

$$L_e^*(x(k)) = \sum_{j=k}^{k+N-1} l_e(x^*(j|k), u^*(j|k)) \ , \tag{2.13}$$

where $u^*(\cdot|k)$ is the optimal input sequence (trajectory), $x^*(\cdot|k)$ is the corresponding state sequence starting at $x(k)$, and $x(k)$ denotes the closed-loop state at time step k. Using the bound on the difference between the two consecutive cost functional values, the closed-

loop average economic performance may be bounded:

$$\frac{1}{T+1}\sum_{k=0}^{T} l_e(x(k),u^*(k|k)) \leq l_e(x_s^*,u_s^*) + \frac{L_e^*(x(0)) - L_e^*(x(T+1))}{T+1} \tag{2.14}$$

where $x(k)$ is the closed-loop state at time step k, and $T < \infty$ is the length of operation. From Eq. 2.14, the effect of the second term of the right-hand side dissipates with longer (but finite) operation. For infinite-time, the average economic performance is bounded by:

$$\limsup_{T\to\infty} \frac{1}{T+1}\sum_{k=0}^{T} l_e(x(k),u^*(k|k)) \leq l_e(x_s^*,u_s^*)\ , \tag{2.15}$$

that is, the asymptotic average performance is no worse than that at the steady-state pair (x_s^*,u_s^*) [6].

Remark 2.1. If the dynamic constraints of Eq. 2.3 take the form of average constraints, [6] and [137] provide methodologies for EMPC with an equality terminal constraint to ensure that the average constraint is satisfied asymptotically and over finite-time operating horizons, respectively.

EMPC with a Terminal Region Constraint

EMPC of Eq. 2.8 requires that the initial state be sufficiently close to the steady-state such that it is possible to reach the steady-state in N sampling times. This type of constraint may limit the feasible region [4]. Numerically computing a solution that satisfies such a constraint exactly may also be challenging. Therefore, terminal region constraints may be employed in EMPC.

One such method is a terminal region constraint designed via an auxiliary local control law. The terminal region is designed to be a forward invariant set for the nonlinear system under the local control law. The local control law can, for instance, be designed on the basis

of the linearization of the system around the optimal steady-state. The terminal region is denoted as $\mathbb{X}_f$ and the resulting EMPC is given by the following problem:

$$\min_{u \in S(\Delta)} \int_{t_k}^{t_{k+N}} l_e(\tilde{x}(t), u(t))\, dt + V_f(\tilde{x}(t_{k+N})) \tag{2.16a}$$

$$\text{s.t. } \dot{\tilde{x}}(t) = f(\tilde{x}(t), u(t), 0) \tag{2.16b}$$

$$\tilde{x}(t_k) = x(t_k) \tag{2.16c}$$

$$\tilde{x}(t_N) \mathbb{X}_f \tag{2.16d}$$

$$g_s(\tilde{x}(t), u(t)) \leq 0,\ \forall\, t \in [t_k, t_{k+N}) \tag{2.16e}$$

where Eq. 2.16d is the terminal region constraint. In general, for closed-loop stability and performance, the terminal cost is such that $V_f(\cdot) \not\equiv 0$.

In [4], a procedure to design a local control law, a terminal region constraint, and a terminal cost for EMPC satisfying the assumption below was proposed:

Assumption 2.1. *There exist a compact terminal region $\mathbb{X}_f \subset \mathbb{R}^n$, containing the point x_s^* in its interior, and control law $h_L : \mathbb{X}_f \to \mathbb{U}$, such that (for the discrete-time system of Eq. 2.9):*

$$V_f(f_d(x, h_L(x))) \leq V_f(x) - l_e(x, h_L(x)) + l_e(x_s^*, u_s^*) \tag{2.17}$$

for all $x \in \mathbb{X}_f$.

Feasibility. For nominal operation, if the EMPC with a terminal region is initially feasible, the EMPC will be recursively feasible. This may be shown by using similar recursive arguments as those used in showing the feasibility of the EMPC with the equality terminal constraint. If $u^*(t|t_{k-1})$ for $t \in [t_{k-1}, t_{k+N-1})$ is the optimal input trajectory at t_{k-1}, then at t_k, a feasible solution is $u(t) = u^*(t|t_{k-1})$ for $t \in [t_k, t_{k+N-1})$ and $u(t) = h_L(\tilde{x}(t_{k+N-1}))$ for $t \in [t_{k+N-1}, t_{k+N})$ where $\tilde{x}(t_{k+N-1})$ is the predicted state at t_{k+N-1}. For recursive feasibility

when $w(\cdot) \not\equiv 0$, one EMPC methodology designed with a terminal region constraint was presented in [15].

Closed-loop Stability. The closed-loop stability properties of EMPC with a terminal constraint designed to satisfy Assumption 2.1 is similar to those of EMPC with an equality terminal constraint. For nominal operation, the closed-loop state trajectory will stay in the feasible region. If the system of Eq. 2.9 is strictly dissipative with supply rate of Eq. 2.11, the steady-state is asymptotically stable under EMPC with a terminal region constraint [4]; see, also, [1] which extends these results to continuous-time systems.

Closed-loop Performance. If the local control law, terminal cost, and terminal region are designed such that Assumption 2.1 is satisfied, the bound on asymptotic average performance of Eq. 2.15 holds [4]. For finite-time, a similar bound to the bound of Eq. 2.14 may be derived for the closed-loop system under EMPC with a terminal cost and a terminal region constraint.

EMPC designed with Lyapunov-based Techniques

The feasible region of EMPC with a terminal region constraint, while larger than the feasible region of EMPC with an equality terminal constraint, depends on the prediction horizon length. Moreover, the feasible region of both EMPC formulations is difficult to characterize. As an alternative to overcome these challenges, one may consider designing an explicit nonlinear control law for the nonlinear system of Eq. 2.1 and constructing a Lyapunov function for the resulting closed-loop system consisting of the system of Eq. 2.1 under the explicit control law. With the control law and Lyapunov function, a region constraint may be designed to be imposed within EMPC. Because the control law and Lyapunov function are derived for the nonlinear system of Eq. 2.1, they can be used to provide an estimate of the region of attraction of the nonlinear system. The resulting EMPC is the so-called Lyapunov-based EMPC (LEMPC) [76, 32, 77, 78, 79, 58, 48]. LEMPC is discussed in-

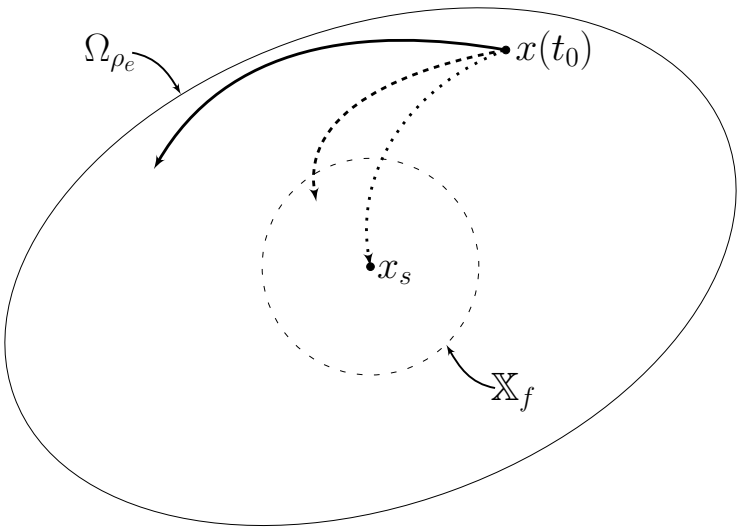

Figure 2.1: An illustration of possible open-loop predicted trajectories under EMPC formulated with a terminal constraint (dotted), under EMPC formulated with a terminal region constraint (dashed), and under LEMPC (solid).

depth in Chapter 3. However, it is important to point out that LEMPC is a dual-mode control strategy. Under the first mode of operation, the LEMPC may dictate a time-varying operating policy to optimize the economics within the region derived using the nonlinear control law. If steady-state operation is desired, the second mode of operation, defined by a contractive constraint, is used to ensure that the closed-loop state trajectory converges to a small neighborhood of the steady-state. In contrast to the aforementioned EMPC methods, no dissipativity requirement is needed to accomplish steady-state operation.

Comparison of the Open-loop Predicted State Trajectory

The EMPC formulations of Eq. 2.8, Eq. 2.16, and the LEMPC (described in detail in the next chapter) may result in different open-loop predicted state trajectories which are illustrated in Fig. 2.1 (Ω_{ρ_e} denotes the region constraint in LEMPC). Nonetheless, if the prediction horizon is sufficiently long, the closed-loop behavior of the system under the

various EMPC formulations would (intuitively) be expected to be similar because for a long prediction horizon, the EMPC solution starts to closely approximate the infinite horizon solution and the effect on the closed-loop behavior of the terminal conditions of the open-loop predicted trajectory is less significant than the corresponding effect for shorter prediction horizons.

2.2 Application of EMPC to a Chemical Process Example

To motivate the use of EMPC over conventional control methods that enforce steady-state operation as well as periodic operation, EMPC is applied to the benchmark example of Section 1.3.1 (these results first appeared in [51]). The reactor has an asymptotically stable steady-state:

$$x_s^T = [0.998\ 0.424\ 0.032\ 1.002] \tag{2.18}$$

which corresponds to the steady-state input:

$$u_{s,1} = 0.35,\ u_{s,2} = 0.5 \tag{2.19}$$

where throughout this study the coolant temperature is fixed to its nominal value of $u_{s,3} = 1.0$. The control objective considered here is to optimize the time-averaged yield of ethylene oxide by operating the reactor in a time-varying fashion around the stable steady-state. Owing to practical considerations, the average amount of ethylene that may be fed into the reactor over the length of operation is constrained to be equal to that when uniformly distributing the reactant material to the reactor which is given by the following integral constraint:

$$\frac{1}{t_f}\int_0^{t_f} u_1(t)u_2(t)dt = u_{s,1}u_{s,2} = 0.175 \tag{2.20}$$

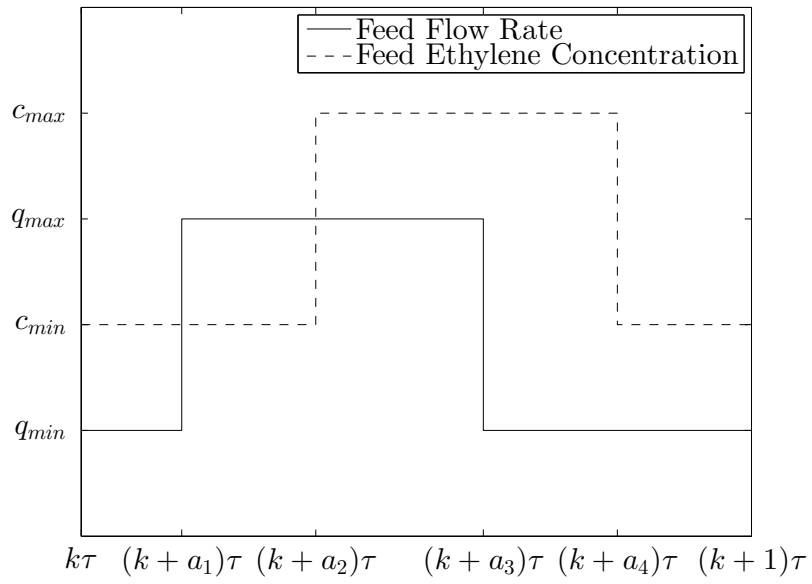

Figure 2.2: Design of the open-loop periodic operation strategy over one period τ.

where $u_{s,1}$ and $u_{s,2}$ are the steady-state inlet volumetric flow rate and ethylene concentration, respectively. Since the average ethylene fed to the reactor is fixed, which fixes the denominator of the yield, the economic stage cost used in the formulation of the upper layer LEMPC is given by:

$$l_e(x,u) = -x_3 x_4 u_1 \ . \tag{2.21}$$

For the periodic operating policy, a similar periodic control strategy as that proposed in [144] which varies the inlet feed flow rate and feed concentration in an open-loop periodic fashion as shown in Fig. 2.2. The parameters used for the periodic control strategy are $\tau = 46.8$, $a_1 = 0.073$, $a_2 = 0.500$, $a_3 = 0.514$, and $a_4 = 0.941$, which are similar parameters to the ones used in [144]. It is important to note that the periodic control strategy of Fig. 2.2 with the aforementioned parameters satisfies the integral constraint of Eq. 2.20.

To compare steady-state operation and periodic operating strategy with the operating policy achieved under EMPC, an EMPC is designed for the reactor system with a sampling period of $\Delta = 0.1$. To enforce that the integral constraint of Eq. 2.20 be satisfied over each

operating window of length $\tau = 46.8$, the EMPC is formulated with a shrinking horizon, i.e., at $t = 0$, the horizon is set to $N_0 = 468$. At the next sampling time ($t = 0.1$), the horizon is decreased by one ($N_1 = 467$). At subsequent sampling times, the prediction horizon is similarly decreased by one sampling period. At $t = 46.8$, the horizon is reset to $N_{468} = 468$. For simplicity of notation, let j be the number of operating windows of length $\tau = 46.8$ that have elapsed and the EMPC considered in this example is given by the following formulation:

$$\min_{u \in S(\Delta)} -\int_{t_k}^{(j+1)\tau} \tilde{x}_3(t)\tilde{x}_4(t)u_1(t)\,dt \tag{2.22a}$$

$$\text{s.t. } \dot{\tilde{x}}(t) = f(\tilde{x}(t), u(t), 0) \tag{2.22b}$$

$$\tilde{x}(t_k) = x(t_k) \tag{2.22c}$$

$$u_1(t) \in [0.0704, 0.7042],\ \forall\ [t_k, (j+1)\tau) \tag{2.22d}$$

$$u_2(t) \in [0.2465, 2.4648],\ \forall\ [t_k, (j+1)\tau) \tag{2.22e}$$

$$\frac{1}{\tau}\int_{t_k}^{(j+1)\tau} u_1(t)u_2(t)\,dt += 0.175 - \frac{1}{\tau}\int_{j\tau}^{t_k} u_1^*(t)u_2^*(t)\,dt \tag{2.22f}$$

where $u_1^*(t)$ and $u_2^*(t)$ denotes the inputs applied to the system over the time $j\tau$ to t_k and $(j+1)\tau$ denotes the end of the operating window.

The catalytic reactor system is initialized at

$$x_0^T = [0.997\ 1.264\ 0.209\ 1.004] \tag{2.23}$$

which corresponds to an initial state on the stable limit cycle that the process with the periodic strategy follows. Simulations are carried out with the periodic control strategy and the EMPC of Eq. 2.22 over 10 operating windows. The evolution of the CSTR for both cases is given in Fig. 2.3 with the open-loop periodic operation and Fig. 2.4 under

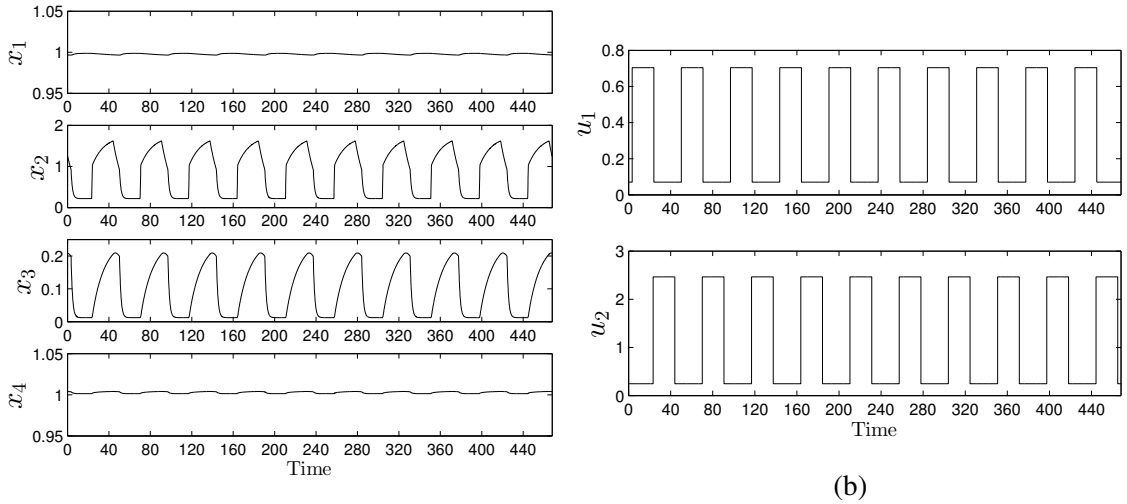

(a) (b)

Figure 2.3: The open-loop CSTR (a) state trajectories and (b) input trajectories with the periodic operating strategy shown in Fig. 2.2.

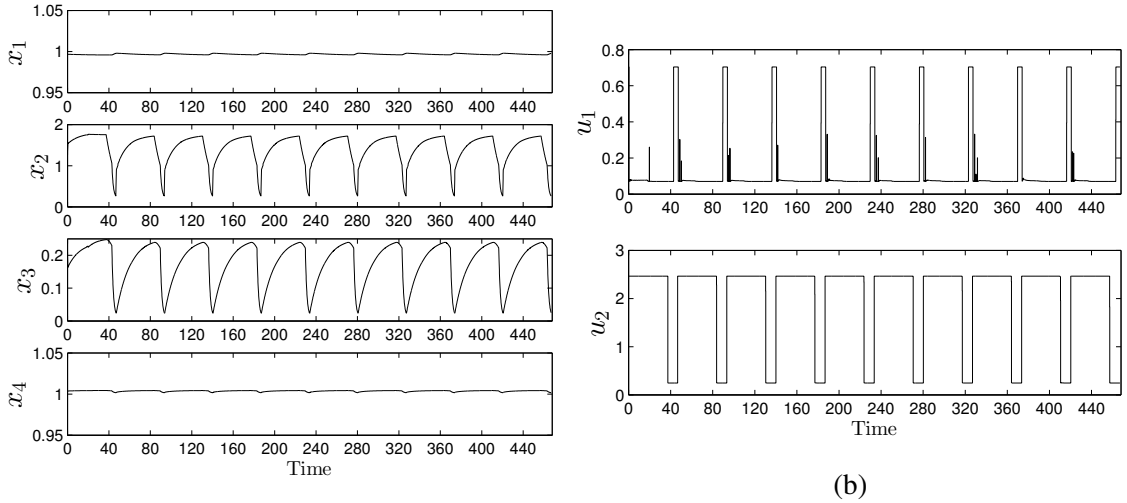

(a) (b)

Figure 2.4: The closed-loop CSTR (a) state trajectories and (b) input trajectories with EMPC of Eq. 2.22.

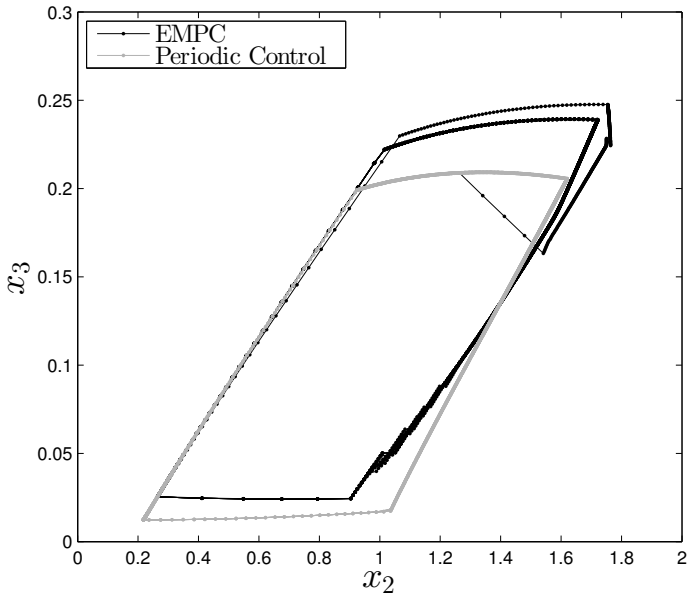

Figure 2.5: State-space evolution in the $x_2 - x_3$ phase plane of the reactor system given with the EMPC of Eq. 2.22 and with the periodic control strategy shown in Fig. 2.2.

EMPC. The state-space evolution of the two strategies are shown in the $x_2 - x_3$ phase plane in Fig. 2.5. From these figures, the system with the two operating strategies approaches different limit cycles. Under EMPC, the time-averaged yield over the entire time-interval of the simulation is 9.97% compared to 7.93% with the periodic operation. If the reactor is initialized with the same initial point and the material is instead distributed uniformly over the length of operation, the average yield is 6.63%. On the other hand, initializing the system at the steady-state and maintain the system at steady-state thereafter achieves a yield of 6.41%. Therefore, operation under EMPC has a clear performance benefit compared to steady-state operation and the open-loop periodic operating strategy.

2.3 A Few Preliminary Results on Sampled-data Systems and Lyapunov-based MPC

In this section, some preliminary results on nonlinear sampled-data systems and tracking Lyapunov-based MPC is provided. This material will be used in the subsequent chapters. Some of these results were originally presented in [59].

2.3.1 Stabilization of Nonlinear Sampled-data Systems

In the subsequent chapters, LEMPC methods are considered. LEMPC is designed with an explicit controller that satisfies the following assumption.

Assumption 2.2. *There exists a feedback controller $h(x) \in \mathbb{U}$ with $h(0) = 0$ that renders the origin of the closed-loop system of Eq. 2.1 with $u = h(x)$ and $w \equiv 0$ asymptotically stable for all $x \in D_0$ where D_0 is an open neighborhood of the origin.*

Applying converse theorems [123, 100], Assumption 2.2 implies that there exists a continuously differentiable Lyapunov function, $V : D \to \mathbb{R}^n$, for the closed-loop system of Eq. 2.1 with $u = h(x) \in \mathbb{U}$ and $w \equiv 0$ such that the following inequalities hold:

$$\alpha_1(|x|) \leq V(x) \leq \alpha_2(|x|), \tag{2.24a}$$

$$\frac{\partial V(x)}{\partial x} f(x, h(x), 0) \leq -\alpha_3(|x|), \tag{2.24b}$$

$$\left| \frac{\partial V(x)}{\partial x} \right| \leq \alpha_4(|x|) \tag{2.24c}$$

for all $x \in D$ where D is an open neighborhood of the origin and α_i, $i = 1, 2, 3, 4$ are functions of class $\mathscr{K}$. A level set of the Lyapunov function Ω_ρ, which defines a subset of D (ideally the largest subset contained in D), is taken to be the stability region of the

closed-loop system under the controller $h(x)$. Standard techniques exist for designing a stabilizing control law for various classes of continuous-time nonlinear systems (see, for instance, [87, 105, 88, 101, 100, 33] as well as the references contained therein).

Currently, there are no general methods for constructing Lyapunov functions for broad classes of nonlinear systems with constraints. However, for certain classes of systems, there exists some general methods for constructing Lyapunov functions, e.g., Zubov's method [45] and the sum of squares decomposition [147]. Within the context of chemical process control, quadratic Lyapunov functions have been widely used and have been demonstrated to be effective for estimating the region of attraction of a given equilibrium point of a system (see, for example, the numerous examples in [33] as well as the examples of the subsequent chapters).

The explicit controller poses a degree of robustness to disturbances/uncertainty in the sense that when $w \not\equiv 0$, the controller will force the closed-loop state to a small neighborhood of the origin if the bound on the disturbance, θ, is sufficiently small. Moreover, since EMPC implements control actions in a sample-and-hold fashion, we must also consider the closed-loop stability properties of the controller $h(x)$ applied in a sample-and-hold fashion. When the feedback controller $h(x)$ is applied in a sample-and-hold fashion, the resulting closed-loop system is a nonlinear sampled-data system given by:

$$\dot{x}(t) = f(x(t), h(x(t_k)), w(t)) \tag{2.25}$$

for $t \in [t_k, t_{k+1})$, $t_k = k\Delta$, $k = 0, 1, \ldots$, and $\Delta > 0$ is the sampling period. Applying standard results on sampled-data systems, e.g., [183, 133, 108, 140, 141], it can be shown that when the bound on the disturbances and the sampling period are sufficient small the origin is practically stable for all initial conditions in Ω_ρ. More specifically, the state trajectory of Eq. 2.25 starting in Ω_ρ will remain bounded in Ω_ρ and converge to a small compact

set containing the origin where it will be maintained thereafter when the bound on the disturbance and the sampling period are sufficiently small. It is important to emphasize that asymptotic stability of the origin of Eq. 2.25 is not achieved.

To achieve asymptotic stability of the origin of sampled-data system of Eq. 2.25, a stronger assumption is required. In the following assumption and result, no restrictions are placed on the state and input.

Assumption 2.3. *There exists a locally Lipschitz feedback controller $u = h(x)$ with $h(0) = 0$ such that the vector field of the closed-loop system $f(x,h(x),0)$ is continuously differentiable on $\mathbb{R}^n$. Furthermore, the origin of the nominal closed-loop system of Eq. 2.1 ($w \equiv 0$) under the controller $h(x)$ implemented continuously is locally exponentially stable and globally asymptotically stable.*

The following theorem characterizes the type of stability achieved when the controller $h(x)$ is applied in a sample-and-hold fashion with a sufficiently small hold period.

Theorem 2.1. *If Assumption 2.3 holds, then given $R > 0$, there exist $\Delta^* > 0$ and $M, \sigma > 0$ such that for $\Delta \in (0, \Delta^*)$ the nominal closed-loop sampled-data system of Eq. 2.25 with arbitrary initial condition $x(0) = x_0 \in B_R$ satisfies the estimate:*

$$|x(t)| \leq M \exp(-\sigma t)|x_0| \tag{2.26}$$

for all $t \geq 0$.

Proof. By virtue of Proposition 4.4 of [97], there exists a C^1 positive definite and radially unbounded function $V : \mathbb{R}^n \to \mathbb{R}_{\geq 0}$, constants $\mu,\ \varepsilon > 0$ and a symmetric, positive definite matrix $P \in \mathbb{R}^{n \times n}$ for the nominal closed-loop system of Eq. 2.1 under the controller $h(x)$

implemented continuously such that

$$\frac{\partial V(x)}{\partial x} f(x,h(x),0) \leq -\mu |x|^2, \quad \text{for all } x \in \mathbb{R}^n, \tag{2.27}$$

$$V(x) = x^T P x, \quad \text{for all } x \in \mathbb{R}^n \text{ with } |x| \leq \varepsilon\,. \tag{2.28}$$

Let $R > 0$ and define $\hat{\rho} := \max\{V(x) : x \in B_R\}$. By virtue of Eq. 2.28 and the compactness of $\Omega_{\hat{\rho}}$, there exist constants $c_1, c_2 > 0$ and $c_4 > 0$ such that:

$$c_1 |x|^2 \leq V(x) \leq c_2 |x|^2, \tag{2.29}$$

$$\left| \frac{\partial V(x)}{\partial x} \right| \leq c_4 |x| \tag{2.30}$$

for all $x \in \Omega_{\hat{\rho}}$. Since f and h are locally Lipschitz mappings with $f(0,0,0) = 0$ and $h(0) = 0$, there exist constants $L, M > 0$ such that:

$$|f(x,h(z),0) - f(x,h(x),0)| \leq L|x-z|, \tag{2.31}$$

$$|f(x,h(z),0)| \leq M|x| + M|z| \tag{2.32}$$

for all $x, z \in \Omega_{\hat{\rho}}$. Let $\Delta^* > 0$ be sufficiently small so that the following inequality holds:

$$c_4 L \frac{2M\Delta^* \exp(M\Delta^*)}{1 - 2M\Delta^* \exp(M\Delta^*)} < \mu \tag{2.33}$$

In order to prove of estimate of Eq. 2.26, it suffices to show that for every initial condition $x(0) \in \Omega_{\hat{\rho}}$ and for every integer $k \geq 0$ it holds that:

$$\frac{\partial V(x(t))}{\partial x} f(x(t), h(x(t_k)), 0) \leq -\frac{q}{2} |x(t)|^2, \tag{2.34}$$

for all $t \in [t_k, t_{k+1})$ where

$$q := \mu - c_4 L \frac{2M\Delta^* \exp(M\Delta^*)}{1 - 2M\Delta^* \exp(M\Delta^*)} > 0\,. \tag{2.35}$$

Using Eq. 2.29 and Eq. 2.34, local exponential stability can be established. The proof of Eq. 2.34 is given below for $k = 0$ and $t \in [0, t_1)$. For every other interval, the proof is similar.

If $x(0) = 0$, then Eq. 2.34 trivially holds (since $x(t) = 0$ for $t \in [0, t_1)$). Therefore, consider the case when $x(0) \neq 0$. The proof is made by contradiction. Suppose that there exists $t \in [0, t_1)$ with

$$\frac{\partial V(x(t))}{\partial x} f(x(t), h(x(0)), 0) > -\frac{q}{2}|x(t)|^2\,.$$

The case that $x(t)$ is not defined for some $t \in [0, t_1)$ is also covered by this assumption. Define

$$a := \inf\left\{ t \in [0, t_1) : \frac{\partial V(x(t))}{\partial x} f(x(t), h(x(0)), 0) > -\frac{q}{2}|x(t)|^2 \right\}\,.$$

A standard continuity argument in conjunction with the fact that

$$\frac{\partial V(x(0))}{\partial x} f(x(0), h(x(0)), 0) \leq -\mu|x(0)|^2 < -\frac{q}{2}|x(0)|^2$$

shows that $a \in (0, t_1)$ and that

$$\frac{\partial V(x(t))}{\partial x} f(x(t), h(x(0)), 0) \leq -\frac{q}{2}|x(t)|^2$$

for all $t \in [0, a]$ with $(\partial V(x(a))/\partial x) f(x(a), h(x(0)), 0) = -\frac{q}{2}|x(a)|^2$. Moreover, for all $t \in [0, a]$ the inequality of Eq. 2.34 implies that $V(x(t)) \leq V(x(0)) \leq \hat{\rho}$. Therefore, $x(t) \in \Omega_{\hat{\rho}}$

for all $t \in [0,a]$. Using inequalities Eqs. 2.27, 2.30, 2.31, we obtain:

$$\frac{\partial V(x(t))}{\partial x} f(x(t),h(x(0)),0) \leq -\mu |x(t)|^2 + c_4 L |x(t)||x(t)-x(0)| \tag{2.36}$$

for all $t \in [0,a]$. Using Eq. 2.32 and since $a \leq t_1 \leq \Delta^*$, a bound on the difference between $x(t)$ and $x(0)$ is obtained:

$$|x(t)-x(0)| \leq 2M\Delta^* |x(0)| + M \int_0^t |x(\tau)-x(0)| \, d\tau \tag{2.37}$$

for all $t \in [0,a]$. Applying the Gronwall-Bellman lemma to Eq. 2.37, we obtain:

$$|x(t)-x(0)| \leq 2M\Delta^* \exp(M\Delta^*) |x(0)| \tag{2.38}$$

for all $t \in [0,a]$. Using Eq. 2.38, the triangle inequality and the fact that $2M\Delta^* \exp(M\Delta^*) < 1$ (implied by Eq. 2.33), we get for all $t \in [0,a]$:

$$|x(t)-x(0)| \leq \frac{2M\Delta^* \exp(M\Delta^*)}{1-2M\Delta^* \exp(M\Delta^*)} |x(t)| \, . \tag{2.39}$$

Thus, using Eq. 2.36, Eq. 2.39 and the fact that $q := \mu - c_4 L \frac{2M\Delta^* \exp(M\Delta^*)}{1-2M\Delta^* \exp(M\Delta^*)} > 0$ we get for all $t \in [0,a]$:

$$\frac{\partial V(x(t))}{\partial x} f(x(t),h(x(0)),0) \leq -q|x(t)|^2 \, . \tag{2.40}$$

Consequently, we must have:

$$\frac{\partial V(x(a))}{\partial x} f(x(a),h(x(0)),0) \leq -q|x(a)|^2 \leq -\frac{q}{2}|x(a)|^2 \, . \tag{2.41}$$

Since $(\partial V(x(a))/\partial x) f(x(a),h(x(0)),0) = -\frac{q}{2}|x(a)|^2$, we get $x(a) = 0$. However, this contradicts Eq. 2.38 (since Eq. 2.38 in conjunction with the fact that $2M\Delta^* \exp(M\Delta^*) < 1$

implies that $|x(a) - x(0)| < |x(0)|$), which completes the proof. □

Explicit feedback controllers that may be designed to satisfy Assumption 2.3 include, for example, feedback linearizing controller and some Lyapunov-based controllers [100, 101]. Owing to the input constraints, it may not be possible to design a controller $h(x)$ that achieves global asymptotic stability of the origin. In which case, we must modify the assumption which is considered in the following corollary.

Corollary 2.1. *Suppose there exists a locally Lipschitz feedback controller $u = h(x)$ with $h(0) = 0$ for the system of Eq. 2.1 that renders the origin of the nominal closed-loop system under continuous implementation of the controller $h(x)$ locally exponentially stable. More specifically, there exist constants $\rho > 0$, $c_i > 0$, $i = 1,2,3,4$ and a continuously differentiable Lyapunov function $V : \mathbb{R}^n \to \mathbb{R}_+$ such that the following inequalities hold:*

$$c_1 |x|^2 \leq V(x) \leq c_2 |x|^2, \tag{2.42a}$$

$$\frac{\partial V(x)}{\partial x} f(x, h(x), 0) \leq -c_3 |x|^2, \tag{2.42b}$$

$$\left| \frac{\partial V(x)}{\partial x} \right| \leq c_4 |x|, \tag{2.42c}$$

for all $x \in \Omega_\rho$. There exists $\Delta^* > 0$ and $M, \sigma > 0$ such that for all $\Delta \in (0, \Delta^*)$ the estimate of Eq. 2.26 holds for the nominal closed-loop sampled-data system of Eq. 2.25 with arbitrary initial condition $x(0) \in \Omega_\rho$.

Proof. The proof follows along the same lines of Theorem 2.1 and shows that V is a Lyapunov function for the closed-loop sampled-data system and takes advantage of the compactness of the set Ω_ρ to establish an exponentially decaying estimate for the state trajectory of the closed-loop sample-data system for any initial condition $x(0) \in \Omega_\rho$. □

Remark 2.2. Sufficient conditions such that there exists a function V satisfying the inequalities of Eq. 2.42 are when $x = 0$ is a locally exponentially stable (LES) equilibrium point for the closed-loop system $\dot{x} = f(x, h(x), 0)$ and the mapping $f(x, h(x), 0)$ is continuously differentiable on $\mathbb{R}^n$. Indeed, by Lemma 8.1 in [100] the region of attraction A of $x = 0$ is an open, connected, invariant set. Let $r > 0$ be such that the set $S = \{x \in \mathbb{R}^n : |x| \leq r\}$ is contained in the region of attraction A. Then LES and compactness of S imply that an exponential bound holds for the solutions of the closed-loop system $\dot{x} = f(x, h(x), 0)$ with initial conditions $x(0) \in S$. It follows from Theorem 4.14 in [100] that there exists a Lyapunov function V for the closed-loop system $\dot{x} = f(x, h(x), 0)$ that satisfies inequalities of Eq. 2.42 for certain constants c_1, c_2, c_3, $c_4 > 0$ and for all $x \in \text{int}(S)$ ($\text{int}(S)$ denotes the interior of S). Let $R < r$ be an arbitrary positive number and define $V(x) = V(\text{Proj}(x))$ for all $x \in \mathbb{R}^n$, where $\text{Proj}(x)$ denotes the projection on the closed ball of radius R centered at $x = 0$. Then all inequalities of Eq. 2.42 hold with arbitrary $\rho < c_1 R^2$.

2.3.2 Tracking Lyapunov-based MPC

To address stability of the closed-loop system with model predictive control (MPC) and recursive feasibility, one tracking MPC technique unites the stability and robustness properties of the Lyapunov-based controller with the optimal control properties of model predictive control (MPC) [128, 129, 133, 34]. The resulting tracking MPC is called Lyapunov-

based MPC (LMPC) and is characterized by the following optimization problem:

$$\min_{u \in S(\Delta)} \int_{t_k}^{t_{k+N}} l_T(\tilde{x}(\tau), u(\tau))\, d\tau \tag{2.43a}$$

$$\text{s.t.} \quad \dot{\tilde{x}}(t) = f(\tilde{x}(t), u(t), 0) \tag{2.43b}$$

$$\tilde{x}(t_k) = x(t_k) \tag{2.43c}$$

$$u_1(t) \in \mathbb{U},\ \forall\ t \in [t_k, t_{k+N}) \tag{2.43d}$$

$$\frac{\partial V(x(t_k))}{\partial x} f(x(t_k), u(t_k), 0) \leq \frac{\partial V(x(t_k))}{\partial x} f(x(t_k), h(x(t_k)), 0) \tag{2.43e}$$

with

$$l_T(x,u) = |x|_Q^2 + |u|_R^2 \tag{2.44}$$

where Q and R are positive definite weighting matrix, $\tilde{x}$ is the predicted state trajectory over the prediction horizon with the computed input trajectory by the LMPC, and $N > 0$ is the number of sampling periods in the finite prediction horizon. Given that the cost function is positive definite with respect to the origin, which is the steady-state of the system of Eq. 2.1, the global minimum of the cost function occurs at the optimal steady-state.

In the optimization problem of Eq. 2.43, Eq. 2.43b is the nominal system of Eq. 2.1 used to predict the future evolution of the system, which is initialized with a measurement of the state at the current sampling time (Eq. 2.43c). To ensure that the computed input trajectory takes values within the admissible set, the input constraints are included in the optimization problem (Eq. 2.43d).

The constraint of Eq. 2.43e ensures that the LMPC computes a control action for the first sampling period that decreases the Lyapunov function by at least the rate achieved by the Lyapunov-based controller at t_k. The Lyapunov-based constraint of Eq. 2.43e is a contractive constraint and ensures that Lyapunov function decays until the closed-loop state converges to a small neighborhood of steady-state. Moreover, from the Lyapunov-

based constraint, the LMPC inherits the closed-loop stability and robustness properties and the stability region Ω_ρ of the Lyapunov-based controller in the sense that for any initial condition $x(0) \in \Omega_\rho$, the closed-loop system state is guaranteed to converge to a small neighborhood of the origin and the optimization problem of Eq. 2.43 is guaranteed to be feasible.

Chapter 3

Lyapunov-based EMPC: Closed-loop Stability, Robustness, and Performance

3.1 Introduction

Within chemical process industries, many chemical processes are safety critical, and maintaining safe and stable operation is the highest priority of a control system. Given that EMPC may operate a process/system in a consistently dynamic fashion to optimize the economics, maintaining the closed-loop state trajectory in a well-defined state-space region, where a degree of robustness to uncertainty is achieved, is one method to achieve safe and stable operation under EMPC. This objective is the main motivating factor in designing Lyapunov-based EMPC (LEMPC). LEMPC is a dual-mode control strategy that allows for time-varying operation while maintaining the closed-loop state in a compact state-space set. If it is desirable to force the closed-loop state to a steady-state at any point over the length of operation, the second mode of operation of the LEMPC may be used and will steer the closed-loop state to a small neighborhood of the steady-state.

In this chapter, several LEMPC designs are developed. The LEMPC designs, which

are capable of optimizing closed-loop performance with respect to general economic considerations for nonlinear systems, address recursive feasibility of the optimization problem at each sampling time, closed-loop stability, and closed-loop performance. The fundamental design concept employed in the LEMPC designs is based on uniting receding horizon control with explicit Lyapunov-based nonlinear controller design techniques. These techniques allow for an explicit characterization of the stability region of the closed-loop system. Time-varying economic stage cost functions are also addressed in this chapter. The results on LEMPC with time-varying economic stage cost functions were originally presented in [48].

In all cases considered, sufficient conditions are derived such that the closed-loop nonlinear system under the LEMPC designs possess a specific form of closed-loop stability and robustness to be made precise in what follows. A critical property of the sufficient conditions derived for closed-loop stability is that they do not rely on solving the LEMPC problem to optimality at each sampling time, i.e., suboptimal solutions also stabilize the closed-loop system. In other words, feasibility of the solution returned by the LEMPC and not optimality implies closed-loop stability under LEMPC (this is a property initially investigated within the context of tracking MPC [164]). Owing to the LEMPC design methodology, a feasible solution to the LEMPC may always be readily computed. Terminal constraint design for LEMPC is also addressed. The terminal constraint imposed in the LEMPC problem allows for guaranteed finite-time and infinite-time closed-loop economic performance improvement over a stabilizing controller. The LEMPC methodologies are applied to chemical process examples to demonstrate, evaluate, and analyze the closed-loop properties of the systems controlled by LEMPC. Also, the closed-loop properties are compared to traditional/conventional approaches to optimization and control, i.e., steady-state optimization and tracking MPC.

3.2 Lyapunov-based EMPC Design and Implementation

3.2.1 Class of Nonlinear Systems

The class of nonlinear systems, described by the following state-space model, considered is given by:

$$\dot{x} = f(x,u,w) \tag{3.1}$$

where $x \in \mathbb{X} \subset \mathbb{R}^n$ denotes the state vector, $u \in \mathbb{U} \subset \mathbb{R}^m$ denotes the control (manipulated) input vector, and $w \in \mathbb{W} \subset \mathbb{R}^l$ denotes the disturbance vector. The control inputs are restricted to a nonempty compact set $\mathbb{U}$. The disturbance is bounded, i.e., $\mathbb{W} := \{w \in \mathbb{R}^l : |w| \leq \theta\}$ where $\theta > 0$ bounds the norm of the disturbance vector. The vector field f is assumed to be a locally Lipschitz vector function on $\mathbb{X} \times \mathbb{U} \times \mathbb{W}$. Without loss of generality, the origin is an equilibrium point of the unforced nominal system ($f(0,0,0) = 0$). State measurements of the system are assumed to be available synchronously at sampling times denoted by the time sequence $\{t_k\}_{k\geq 0}$ where $t_k = k\Delta$, $k = 0,1,\ldots$ and $\Delta > 0$ is the sampling period. To describe the system economics, e.g., operating profit or operating cost, the system of Eq. 3.1 is equipped with a time-invariant cost function $l_e : \mathbb{X} \times \mathbb{U} \to \mathbb{R}$ which is a measure of the instantaneous system economics. The function l_e is referred to as the economic cost function and is continuous over $\mathbb{X} \times \mathbb{U}$.

3.2.2 Stabilizability Assumption

The existence of an explicit controller $h : \mathbb{X} \to \mathbb{U}$, which renders the origin of the nominal closed-loop system asymptotically, is assumed. This assumption is a stabilizability assumption for the nonlinear system of Eq. 3.1 and is similar to the assumption that the pair (A,B) is stabilizable in the case of linear systems. Throughout the dissertation, the explicit controller may be referred to as the stabilizing controller or the Lyapunov-based

controller. When convenient, the notation $h(x)$ may be used when referring to the explicit controller. However, this notation refers to the controller itself, which is a function, and not the value of the function h at x. Even though the explicit controller is referred to as the Lyapunov-based controller, it may be designed using any controller design techniques and not just Lyapunov-based techniques.

Applying converse Lyapunov theorems, e.g., [123, 103, 73, 100, 115, 184], the stabilizability assumption implies that there exists a continuously differentiable Lyapunov function $V : D \to \mathbb{R}$ for the nominal closed-loop system ($\dot{x} = f(x, h(x), 0)$) that satisfies the inequalities:

$$\alpha_1(|x|) \leq V(x) \leq \alpha_2(|x|) \tag{3.2a}$$

$$\frac{\partial V(x)}{\partial x} f(x, h(x), 0) \leq -\alpha_3(|x|) \tag{3.2b}$$

$$\left| \frac{\partial V(x)}{\partial x} \right| \leq \alpha_4(|x|) \tag{3.2c}$$

for all $x \in D \subset \mathbb{R}^n$ where $\alpha_i \in \mathcal{K}$ for $i = 1, 2, 3, 4$ and D is an open neighborhood of the origin. The region $\Omega_\rho \subset D$ such that also $\Omega_\rho \subseteq \mathbb{X}$ is called the stability region of the closed-loop system under the Lyapunov-based controller, and is an estimate of the region of attraction of the nonlinear system of Eq. 3.1. Since the stability region depends on the explicit controller, the choice and design of the controller plays a significant role in the estimated region of attraction. The case that the set $\mathbb{X}$ represents explicit hard state constraints is discussed further in Section 3.2.5.

3.2.3 LEMPC Formulation

In the LEMPC design, the LEMPC optimizes the economic cost function, which is used as the stage cost in the EMPC. Lyapunov-based MPC techniques, e.g., [129, 133, 34], are employed in the EMPC design to take advantage of the stability properties of the Lyapunov-

based controller. The LEMPC is equipped with two operation modes. Under the first operation mode, the LEMPC optimizes the economic cost function while maintaining the system state within the stability region Ω_ρ. The LEMPC may dictate a general time-varying operating policy under the first operation mode. Under the second operation mode, the LEMPC optimizes the economic cost function while ensuring that the computed control action for the closed-loop system forces the state along a path that causes the Lyapunov function value to decay. The first and second operation mode of the LEMPC will be referred to as mode 1 and mode 2 operation of the LEMPC, respectively, and are defined by specific Lyapunov-based constraints imposed in the LEMPC optimization problem.

To enforce convergence of the closed-loop state to the steady-state (if desirable), the LEMPC is formulated with a switching time t_s. From the initial time ($t_0 = 0$) to time t_s, the LEMPC may dictate a time-varying operating policy to optimize the economics while maintaining the closed-loop state in Ω_ρ. After the time t_s, the LEMPC operates exclusively in the second operation mode and calculates the inputs in a way that the state of the closed-loop system is steered to a neighborhood of the steady-state. For the sake of simplicity, the switching time t_s is an integer multiple of the sampling period (Δ) of the LEMPC. This assumption poses little practical restrictions.

LEMPC is an EMPC scheme that uses the Lyapunov-based controller to design two regions of operation where closed-loop stability of the system of Eq. 3.1 under the LEMPC and recursive feasibility of the optimization problem are guaranteed for operation in the

presence of bounded disturbances. The formulation of the LEMPC optimization is:

$$\min_{u\in S(\Delta)} \int_{t_k}^{t_{k+N}} l_e(\tilde{x}(\tau), u(\tau))\, d\tau \tag{3.3a}$$

$$\text{s.t.} \quad \dot{\tilde{x}}(t) = f(\tilde{x}(t), u(t), 0) \tag{3.3b}$$

$$\tilde{x}(t_k) = x(t_k) \tag{3.3c}$$

$$u(t) \in \mathbb{U},\ \forall\, t \in [t_k, t_{k+N}) \tag{3.3d}$$

$$V(\tilde{x}(t)) \leq \rho_e,\ \forall\, t \in [t_k, t_{k+N})$$

$$\text{if } V(x(t_k)) \leq \rho_e \text{ and } t_k < t_s \tag{3.3e}$$

$$\frac{\partial V(x(t_k))}{\partial x} f(x(t_k), u(t_k), 0) \leq \frac{\partial V(x(t_k))}{\partial x} f(x(t_k), h(x(t_k)), 0)$$

$$\text{if } V(x(t_k)) > \rho_e \text{ or } t_k \geq t_s \tag{3.3f}$$

where the decision variable of the optimization problem is the piecewise constant input trajectory over the prediction horizon and $N < \infty$ denotes the number of sampling periods in the prediction horizon. The notation $\tilde{x}$ is used to denote the predicted (open-loop) state trajectory. Owing to the control vector parameterization, i.e., zeroth-order hold control parameterization is used, the optimization problem of Eq. 3.3 is finite-dimensional, i.e., the input trajectory is parameterized by a finite number of variables. While zeroth-order hold is assumed, higher-order control vector parameterization may also be employed. Moreover, the theoretical analysis may also apply to the case that a higher-order parameterization is used because zeroth-order hold may, for some methods, be considered to be a special case of the higher-order control vector parameterization method.

The LEMPC dynamic optimization problem of Eq. 3.3 minimizes a cost functional (Eq. 3.3a) consisting of the economic cost function, i.e., l_e is used as the stage cost in the LEMPC. The nominal system model is the constraint of Eq. 3.3b and is used to predict the evolution of the system under the computed input trajectory over the prediction horizon.

The dynamic model is initialized with a state measurement obtained at the current sampling period (Eq. 3.3c). The constraint of Eq. 3.3d limits the computed control actions to be in the set of the available control actions.

Mode 1 operation of the LEMPC is defined by the constraint of Eq. 3.3e and is active when the current state is inside a predefined subset of the stability region $\Omega_{\rho_e} \subset \Omega_\rho$ and $t_k < t_s$. Since an economic performance benefit may be realized when operating the system of Eq. 3.1 in a consistently dynamic fashion compared to operating the system at the economically optimal steady-state, i.e., a steady-state that minimizes the economic stage cost amongst all of the admissible steady-states, mode 1 is used to allow the LEMPC to enforce a potentially dynamic or transient operating policy. The set Ω_{ρ_e} is designed such that if the current state $x(t_k) \in \Omega_{\rho_e}$ and the predicted state at the next sampling time $\tilde{x}(t_{k+1}) \in \Omega_{\rho_e}$, then the actual (closed-loop) state at the next sampling time, which may be forced away from Ω_{ρ_e} by a bounded disturbance/uncertainty, will be in Ω_ρ. The maximum size of Ω_{ρ_e} depends on the bound on the disturbance and sampling period size; please refer to Eq. 3.21 of Section 3.3.1.

To maintain boundedness of the closed-loop state within a well-defined state-space set (in this case, boundedness of the state trajectory in Ω_ρ), the second mode is used, which is defined by the constraint of Eq. 3.3f. This constraint forces the computed control action by the LEMPC to decrease the Lyapunov function by at least the decay rate achieved by the Lyapunov-based controller. Owing to the properties of the Lyapunov-based controller implemented in a sample-and-hold fashion with a sufficiently small sampling period, the Lyapunov function value under the LEMPC operating in mode 2 will decrease over the sampling period when the constraint of Eq. 3.3f is active and when the state at t_k is outside a small compact set containing the steady-state (this set is defined as Ω_{ρ_s} in Theorem 3.1). If steady-state operation is desired, i.e., enforcing the closed-loop state to a neighborhood of the steady-state, selecting the switching time to be finite will guarantee that LEMPC

forces the state to converge to a small forward invariant set containing the steady-state.

The two tuning parameters of LEMPC, besides the user-defined economic cost function, are the switching time t_s and the set Ω_{ρ_e}. If $t_s = 0$, the LEMPC will always operate in mode 2. This may be desirable if steady-state operation is expected and/or if it is the best operating strategy. If $t_s \to \infty$, the LEMPC may dictate a time-varying operating policy over the entire length of operation. An intermediate choice for the switching time ($t_s \in (0, \infty)$) may be used to balance the trade-off between achieving better economic performance through time-varying operation and excessive control actuator wear required to enforce the time-varying operating policy. The other tuning parameter of LEMPC is ρ_e which does not need to be chosen so that Ω_{ρ_e} is the largest subset of Ω_ρ such that the state at the next sampling time is guaranteed to be in Ω_ρ under mode 1 operation of the LEMPC. A larger set Ω_{ρ_e} may allow for better closed-loop economic performance. On the other hand, a smaller set Ω_{ρ_e} may allow for more robustness to uncertainty.

3.2.4 Implementation Strategy

The LEMPC is implemented in a receding horizon fashion. At each sampling time, the LEMPC receives a state measurement $x(t_k)$, solves the optimization problem of Eq. 3.3, and sends the control action for the first sampling period of the prediction horizon to be implemented by the control actuators from t_k to t_{k+1}. At the next sampling time, the LEMPC receives a state measurement $x(t_{k+1})$ and solves the optimization problem again by rolling the horizon one sampling period into the future. The optimal input trajectory computed by the LEMPC at a given sampling time t_k is denoted as $u^*(t|t_k)$ and is defined for $t \in [t_k, t_{k+N})$. The control action that is sent at time t_k to the control actuators to be applied over the sampling period from t_k to t_{k+1} is denoted as $u^*(t_k|t_k)$. The receding horizon fashion implementation of the dual-mode LEMPC is stated formally in the following algorithm:

1. At a sampling time t_k, the controller receives the state measurement $x(t_k)$. Go to Step 2.

2. If $t_k < t_s$, go to Step 3. Else, go to Step 3.2.

3. If $x(t_k) \in \Omega_{\rho_e}$, go to Step 3.1. Else, go to Step 3.2.

    3.1. Mode 1 operation of the LEMPC is active, i.e., Eq. 3.3e is imposed in the optimization problem and Eq. 3.3f is inactive. Go to Step 4.

    3.2. Mode 2 operation of the LEMPC is active, i.e., Eq. 3.3f is imposed in the optimization problem and Eq. 3.3e is inactive. Go to Step 4.

4. The LEMPC of Eq. 3.3 is solved to compute an optimal input trajectory $u^*(t|t_k)$ for $t \in [t_k, t_{k+N})$ and sends the control action $u^*(t_k|t_k)$ computed for the first sampling period of the prediction horizon to be applied to the closed-loop system over the sampling period (from t_k to t_{k+1}). Go to Step 5.

5. Go to Step 1 ($k \leftarrow k+1$).

The notation $k \leftarrow k+1$ used in Step 5 of the algorithm means that k is set to $k+1$ for the next time through the algorithm loop. In other words, k is set to $k+1$ before going to Step 1.

An illustration of the possible evolution of a system under LEMPC is shown in Fig. 3.1. At the initial time, t_0, the state is outside Ω_{ρ_e}. The contractive constraint of Eq. 3.3f is active to steer the state to Ω_{ρ_e}. Once the state is in Ω_{ρ_e}, the LEMPC computes control actions using mode 1 operation, i.e., the constraint of Eq. 3.3e is active. Under this mode of operation, the LEMPC dictates a time-varying operating policy. After some point, a disturbance forces the state trajectory outside of Ω_{ρ_e}. Owing to the properties of the set Ω_{ρ_e}, the state remains in Ω_{ρ}. The mode 2 constraint is active to force the state back into

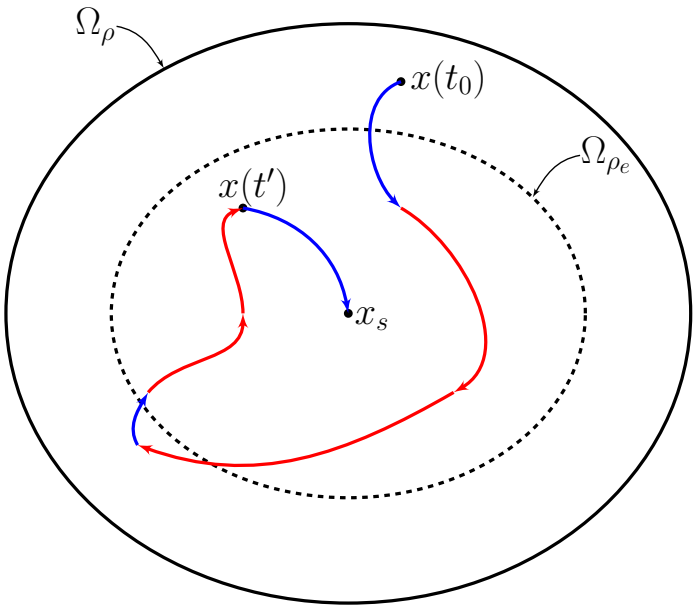

Figure 3.1: An illustration of the state-space evolution of a system under LEMPC. The red trajectory represents the state trajectory under mode 1 operation of the LEMPC, and the blue trajectory represents the state trajectory under mode 2 operation.

Ω_{ρ_e} where the LEMPC operates under mode 1 operation. Finally, at t', the contractive constraint (Eq. 3.3f) is imposed at all subsequent sampling times to ensure that the closed-loop state trajectory converges to a small neighborhood of the steady-state.

3.2.5 Satisfying State Constraints

While it may not appear that hard state constraints are included in the LEMPC problem of Eq. 3.3, hard constraints may be accounted for through the design of Ω_ρ, which extends the ideas of imposing state constraints from Lyapunov-based MPC [129]. Specifically, define the set Φ_u as the set in state-space that includes all the states where $\dot{V} < 0$ under the Lyapunov-based controller $h(x)$. Since the Lyapunov-based controller accounts for the input constraints, the set Φ_u also accounts for the inputs constraints. Consider the case where $\Phi_u \subseteq \mathbb{X}$. This means that any initial state starting in the region $\mathbb{X} \setminus \Phi_u$ will satisfy the

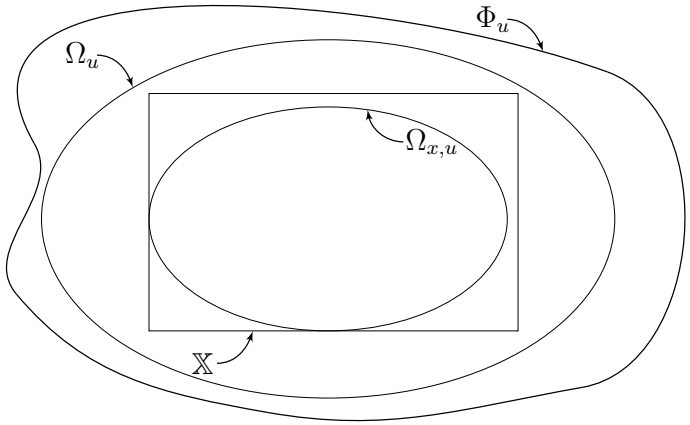

Figure 3.2: An illustration of the various state-space sets described for enforcing state constraints with LEMPC. The case when $\mathbb{X} \subset \Phi_u$ is depicted in this illustration.

state constraint. However, the time-derivative of the Lyapunov function may be positive and thus, it may not be possible to stabilize the closed-loop system under the Lyapunov-based controller starting from such initial conditions. Therefore, the stability region used in the formulation of the LEMPC for this case is $\Omega_\rho = \Omega_{x,u} = \{x \in \mathbb{R}^n : V(x) \leq \rho_{x,u}\}$ where $\rho_{x,u}$ is chosen such that $\Omega_{x,u} \subseteq \Phi_u$ because there exists a feasible input trajectory that maintains the state in $\Omega_{x,u}$ for all initial conditions in $\Omega_{x,u}$ while satisfying both the state and input constraints. The notation $\rho_{x,u}$ denotes that both state and input constraints are accounted for in the design of the region $\Omega_{x,u}$.

Now, consider the case where $\mathbb{X} \subset \Phi_u$. This case is depicted in Fig. 3.2. For any initial state starting outside $\mathbb{X}$, the state constraint will be violated from the onset. Also, for any initial state in the set $\mathbb{X}$, it is not possible, in general, to guarantee that the set $\mathbb{X}$ is forward invariant because there may exist a stabilizing state trajectory, i.e., a trajectory where $\dot{V} < 0$ along this trajectory, that goes outside of the set $\mathbb{X}$ before it enters back into the set $\mathbb{X}$ to converge to the origin. For the case with hard constraints, define the set Ω_ρ as $\Omega_\rho = \Omega_{x,u} = \{x \in \mathbb{R}^n : V(x) \leq \rho_{x,u}\}$ where $\rho_{x,u}$ is such that $\Omega_{x,u} \subseteq \mathbb{X}$. Since Φ_u cannot

be computed in practice, the set $\Omega_u := \{x \in \mathbb{R}^n : V(x) \leq \rho_u\}$ where ρ_u is such that $\dot{V} < 0$ for all states in Ω_u under the Lyapunov-based controller $h(x)$ which accounts for the input constraint only may be used. An illustration of the set definitions is provided in Fig. 3.2.

On the other hand, consider the case that it is desirable to impose the state constraints as soft constraints. This may potentially allow for a larger region (Ω_ρ) at the expense that the state constraints may not be satisfied for all time. If $\mathbb{X} \subset \Phi_u$, Ω_ρ is constructed such that $\Omega_\rho \subset \mathbb{X}$, and the state constraint is always satisfied for any initial conditions in Ω_ρ. From a closed-loop stability stand-point, it is not desirable to increase the size of the set Ω_ρ because there may be states outside of Ω_ρ where $\dot{V} > 0$. Therefore, consider the more interesting case that $\mathbb{X} \subset \Phi_u$. If the state constraints are imposed as soft constraints, then one could take $\Omega_\rho = \Omega_u \subseteq \Phi_u$. For any initial state in Ω_ρ, the amount of time that the state constraint (imposed as a soft constraint) will be violated is finite. This statement holds because for any state in $\Omega_\rho \notin \mathbb{X}$, $\dot{V} < 0$ and therefore, the state trajectory evolves along a path where the Lyapunov function value decays over time. Eventually, the state trajectory will converge to a level set $\Omega_{\rho'}$ in finite-time that is contained in $\mathbb{X}$.

The following example illustrates the above methodology to satisfy (hard) state constraints.

Example 3.1. Consider the scalar system:

$$\dot{x} = x + u \tag{3.4}$$

which has an open-loop unstable steady-state at the origin. If the system was subject to the following constraints on the state and input: $x \in \mathbb{X} = [-2, 2]$ and $u \in \mathbb{U} = [-1, 1]$. For any initial state $x_0 \notin [-1, 1]$, the state will diverge to positive/negative infinity, i.e., some initial states that initially satisfy the state constraint will not continue satisfying the state constraints over the length of operation. Following the approach detailed above, the

nonlinear control law $u = -\text{sat}(Kx)$ where $\text{sat}(\cdot)$ is the saturation function and $K > 1$ is a tuning parameter renders the origin of Eq. 3.4 locally exponentially stable while satisfying the input constraints. The quadratic function:

$$V(x) = x^2 \tag{3.5}$$

is a Lyapunov function for the closed-loop system. Moreover, the stability region, i.e., region where $\dot{V} < 0$, is $\Omega_u = \{x \in \mathbb{R} : V(x) \leq \rho_u\}$ where ρ_u is chosen such that $\rho_u < 1$. Since $\Omega_u \subset \mathbb{X}$, Ω_ρ may be taken to be Ω_u. If, instead, $\mathbb{X} = [-0.9, 0.9]$, then $\mathbb{X} \subset \Omega_u$ and Ω_ρ may be taken to be $\{x \in \mathbb{R} : V(x) \leq 0.81\}$, i.e., $\Omega_\rho = \mathbb{X}$. In either situation, one may verify that for any initial state in Ω_ρ, the closed-loop state trajectory will remain bounded in Ω_ρ and converge exponentially to the origin without violating the state constraints. If one were to apply the LEMPC of Eq. 3.3 to the system of Eq. 3.4 designed based on the nonlinear control law, the Lyapunov function of Eq. 3.5, and the region Ω_ρ, the closed-loop state trajectory for all initial conditions in Ω_ρ is guaranteed to satisfy the state constraint for all times.

3.2.6 Extensions and Variants of LEMPC

A few extensions and variants of the LEMPC formulation of Eq. 3.3 and implementations are discussed below.

- For closed-loop economic performance reasons, terminal conditions, e.g., a terminal constraint or a terminal cost, may be added to the problem of Eq. 3.3 which is discussed in Section 3.4.

- For all $t < t_s$, the LEMPC may dictate a time-varying operating policy. If the LEMPC enforces that the closed-loop state trajectory evolves along a path close to the bound-

ary of Ω_{ρ_e}, it is possible that the LEMPC continuously switches between mode 1 and mode 2 operation. The successive switching between mode 1 and mode 2 could lead to closed-loop performance deterioration. For these cases, various modifications could be made to LEMPC to avoid this behavior. First, owing to the fact that the economic cost is user-defined, one could add penalization terms to the stage cost of the LEMPC that penalize the closeness of the predicted state to the boundary of Ω_{ρ_e}. Then, the LEMPC will ideally maintain the closed-loop state in the interior of Ω_{ρ_e} preventing the state from coming out of Ω_{ρ_e}.

- For closed-loop stability, the constraint $\tilde{x}(t) \in \Omega_{\rho_e}$ (Eq. 3.3e) only needs to hold for all $t \in [t_k, t_{k+1})$ under mode 1 operation, i.e., the predicted state at the next sampling time must be contained in Ω_{ρ_e}. However, the constraint of Eq. 3.3e is written for all $t \in [t_k, t_{k+N})$ owing to two reasons. First, it ensures that the predicted state trajectory remains in a compact set. Second, it allows the LEMPC to optimize the input trajectory with respect to (ideally) a better prediction of the closed-loop behavior (recall that the closed-loop state must remain in Ω_ρ and under mode 1 operation, it is desirable to maintain the closed-loop state in the interior of Ω_{ρ_e} to avoid continuous switching between mode 1 and mode 2 operation). Nonetheless, for practical implementation, one may consider imposing the constraint at a few time instances along the prediction horizon, which will decrease the number of constraints relative to imposing the constraint at every sampling time instance, for example.

- For mode 2 operation, one may need to enforce a similar constraint as the mode 1 constraint to maintain the predicted state in Ω_ρ, i.e., enforce $\tilde{x}(t) \in \Omega_\rho$ for $t \in [t_k, t_{k+N})$. This ensures that the predicted state trajectory is maintained in a compact set, which guarantees existence and uniqueness of the solution as well as prevents numerical problems when large (in a norm sense) state trajectories are computed.

This issue is particularly relevant when the prediction horizon is long.

- The LEMPC may be modified to handle potentially asynchronous and delayed measurements; see [76].

- For certain applications, one may consider driving some of the states of the system to certain set-points and allowing the other states to evolve in a time-varying manner to optimize the economics. For the LEMPC design of Eq. 3.3, this means that part of the system is operated in the first operation mode and part of the system in the second operation mode simultaneously. This is considered in the example of Section 3.3.2.

- With the formulated constraints of the LEMPC of Eq. 3.3, the optimization problem is always feasible in the sense that there exists an input trajectory that satisfies the constraints for all $x(t_k) \in \mathbb{R}^n$. To force the closed-loop state to converge to Ω_ρ when $x(t_k) \notin \Omega_\rho$, one could employ the contractive constraint of Eq. 3.3f in an attempt to enforce that the Lyapunov function value decays (for states outside of Ω_ρ, it is not guaranteed that the Lyapunov function value will decay even with such a constraint) or use a constraint, e.g., a terminal constraint, to enforce that the predicted state converges to Ω_ρ (feasibility of the resulting problem is not guaranteed). However, no guarantee may be made that the predicted state exists or remains bounded as well as no guarantee may be made that the state will converge to Ω_ρ starting from outside Ω_ρ in general.

3.3 Closed-loop Stability and Robustness under LEMPC

Closed-loop stability robustness of the closed-loop system of Eq. 3.1 under the LEMPC of Eq. 3.3. LEMPC is applied to a chemical process example to demonstrate the closed-loop stability and robustness properties.

To complete the closed-loop stability analysis, a few properties of the system of Eq. 3.1 are needed in the analysis. Owing to the fact that f is locally Lipschitz on $\mathbb{X} \times \mathbb{U} \times \mathbb{W}$ and the sets Ω_ρ, $\mathbb{U}$, and $\mathbb{W}$ are compact, there exists a positive constant M such that

$$|f(x,u,w)| \leq M \tag{3.6}$$

for all $x \in \Omega_\rho$, $u \in \mathbb{U}$ and $w \in \mathbb{W}$. By the continuous differentiable property of the Lyapunov function V and the Lipschitz property assumed for the vector field f, there exist positive constants L_x, L_w, L'_x and L'_w such that

$$|f(x,u,w) - f(x',u,0)| \leq L_x|x-x'| + L_w|w|, \tag{3.7}$$

$$\left| \frac{\partial V(x)}{\partial x} f(x,u,w) - \frac{\partial V(x')}{\partial x} f(x',u,0) \right| \leq L'_x|x-x'| + L'_w|w| \tag{3.8}$$

for all x, $x' \in \Omega_\rho$, $u \in \mathbb{U}$, and $w \in \mathbb{W}$.

3.3.1 Synchronous Measurement Sampling

The stability properties of the LEMPC of Eq. 3.3 for the system of Eq. 3.1 is analyzed under ideal sampling. In order to proceed, preliminary results are presented. First, for a bounded disturbance, the difference between the state of Eq. 3.1 and the nominal state of Eq. 3.1 (the system of Eq. 3.1 with $w \equiv 0$) may be bounded, which is stated in the following proposition.

Proposition 3.1. *Consider the systems*

$$\dot{x}(t) = f(x(t),u(t),w(t)) \,, \tag{3.9}$$

$$\dot{\hat{x}}(t) = f(\hat{x}(t),u(t),0) \,. \tag{3.10}$$

Let $x(t)$ and $\hat{x}(t)$ be the solutions of Eqs. 3.9-3.10, respectively, for $t \in [t_0, t_f]$ ($t_f > t_0$) with initial states $x(t_0) = \hat{x}(t_0) \in \Omega_\rho$ and input trajectory $u(t) \in \mathbb{U}$ for all $t \in [t_0, t_f]$ where $u(\cdot)$ is piecewise constant in t. The system of Eq. 3.9 is also forced by some disturbance $w(t) \in \mathbb{W}$ for all $t \in [t_0, t_f]$. If $x(t) \in \Omega_\rho$ and $\hat{x}(t) \in \Omega_\rho$ for all $t \in [t_0, t_f]$, then there exists a function $f_w \in \mathscr{K}$ such that

$$|x(t) - \hat{x}(t)| \leq f_w(t - t_0) \tag{3.11}$$

for all $t \in [t_0, t_f]$.

Proof. Consider the difference between the solutions of Eqs. 3.9-3.10, which are denoted as $x(t)$ and $\hat{x}(t)$, respectively, and let $e := x - \hat{x}$. From Eq. 3.7 and the fact that $w(t) \in \mathbb{W}$ for all $t \in [t_0, t_f]$, the time-derivative of e may be bounded as follows:

$$|\dot{e}(t)| = |f(x(t), u(t), w(t)) - f(\hat{x}(t), u(t), 0)| \tag{3.12}$$

$$\leq L_x |x(t) - \hat{x}(t)| + L_w |w(t)| \tag{3.13}$$

$$\leq L_x |e(t)| + L_w \theta \tag{3.14}$$

for $t \in [t_0, t_f]$. Integrating the above bound with respect to time and noting that $e(0) = x(0) - \hat{x}(0) = 0$, the following bound on the error is obtained:

$$|e(t)| \leq f_w(t - t_0) := \frac{L_w \theta}{L_x} (e^{L_x (t - t_0)} - 1). \tag{3.15}$$

for all $t \in [t_0, t_f]$ when $x(t)$, $\hat{x}(t) \in \Omega_\rho$, $u(t) \in \mathbb{U}$, and $w(t) \in \mathbb{W}$ for all $t \in [t_0, t_f]$. It is straightforward to show that $f_w \in \mathscr{K}$ which completes the proof. □

Proposition 3.2 bounds the difference between the Lyapunov function values evaluated at two points in Ω_ρ.

Proposition 3.2. *Consider the Lyapunov function $V(\cdot)$ that satisfies Eq. 3.2. There exists a quadratic function $f_V(\cdot)$ such that*

$$V(x_2) - V(x_1) \leq f_V(|x_2 - x_1|) \tag{3.16}$$

for all x_1, $x_2 \in \Omega_\rho$.

Proof. Since the Lyapunov function is continuously differentiable and bounded on compact sets, there exists a positive constant $M_V > 0$ such that:

$$V(x_2) \leq V(x_1) + \left| \frac{\partial V(x_1)}{\partial x} \right| |x_2 - x_1| + M_V |x_2 - x_1|^2 \tag{3.17}$$

for all x_1, $x_2 \in \Omega_\rho$. From Eq. 3.2, the partial derivative of V may be bounded as follows:

$$\left| \frac{\partial V(x_1)}{\partial x} \right| \leq \alpha_4(\alpha_1^{-1}(\rho)) \tag{3.18}$$

for all $x_1 \in \Omega_\rho$. From Eqs. 3.17-3.18, the existence of a quadratic function $f_V(\cdot)$ that bounds the Lyapunov function values for any two points in Ω_ρ follows:

$$V(x_2) \leq V(x_1) + f_V(|x_2 - x_1|) \tag{3.19}$$

where

$$f_V(s) := \alpha_4(\alpha_1^{-1}(\rho))s + M_V s^2 \,. \tag{3.20}$$

□

Theorem 3.1 below provides sufficient conditions that guarantee that the state of the closed-loop system of Eq. 3.1 under the LEMPC of Eq. 3.3 is always bounded in Ω_ρ and is ultimately bounded in a small region containing the origin.

Theorem 3.1. *Consider the system of Eq. 3.1 in closed-loop under the LEMPC design of Eq. 3.3 based on the Lyapunov-based controller that satisfies the conditions of Eq. 3.2. Let* $\Delta > 0$, $N \geq 1$, $\varepsilon_w > 0$, *and* $\rho > \rho_e \geq \rho_{\min} > \rho_s > 0$ *satisfy*

$$\rho_e < \rho - f_V(f_w(\Delta)), \tag{3.21}$$

$$-\alpha_3(\alpha_2^{-1}(\rho_s)) + L_x' M\Delta + L_w'\theta \leq -\varepsilon_w/\Delta, \tag{3.22}$$

and

$$\rho_{\min} = \max_{s\in[0,\Delta]} \{V(x(s)) : V(x(0)) \leq \rho_s\}, \tag{3.23}$$

If $x(0) \in \Omega_\rho$, *then the state* $x(t)$ *of the closed-loop system of Eq. 3.1 is always bounded in* Ω_ρ *for all* $t \geq 0$ *and is ultimately bounded in* $\Omega_{\rho_{\min}}$ *if* t_s *is finite.*

Proof. The proof is organized into three parts. In Part 1, feasibility of the LEMPC optimization problem of Eq. 3.3 is proved when the state measurement at a specific sampling time is in Ω_ρ. In Part 2, boundedness of the closed-loop state in Ω_ρ is established. In Part 3, ultimate boundedness of the closed-loop state in a small state-space set containing the origin is proved when the switching time is finite.

Part 1: The sample-and-hold input trajectory obtained from the Lyapunov-based controller is a feasible solution to the LEMPC optimization problem of Eq. 3.3 when $x(t_k) \in \Omega_\rho$. Let $\hat{x}(t)$ denote the solution at time t to the nominal sampled-data system:

$$\dot{\hat{x}}(t) = f(\hat{x}(t), h(\hat{x}(\tau_i)), 0) \tag{3.24}$$

for $t \in [\tau_i, \tau_{i+1})$ ($\tau_i := t_k + i\Delta$), $i = 0, 1, \ldots, N-1$ with initial condition $\hat{x}(t_k) = x(t_k) \in \Omega_\rho$. Define $\hat{u}$ as the resulting input trajectory of Eq. 3.24 defined over the interval $[t_k, t_{k+N})$. The input trajectory $\hat{u}$ is a feasible solution to the LEMPC problem. The input trajectory

meets the input constraints by the formulation of the Lyapunov-based controller. For mode 2 operation, the mode 2 contractive constraint of Eq. 3.3f is trivially satisfied with this feasible input trajectory. For mode 1 operation, the region Ω_{ρ_e} is forward invariant under the Lyapunov-based controller applied in a sample-and-hold fashion when $\Omega_{\rho_{\min}} \subseteq \Omega_{\rho_e} \subset \Omega_\rho$ where $\Omega_{\rho_{\min}}$ will be explained further in Part 3.

Part 2: To show that the state is maintained in Ω_ρ when $x(0) \in \Omega_\rho$, mode 1 and mode 2 operation of the LEMPC must be each considered. To show the desired result, it is sufficient to show that if the state at any arbitrary sampling time is such that $x(t_k) \in \Omega_\rho$, then the state at the next sampling time is in Ω_ρ, i.e., $x(t_{k+1}) \in \Omega_\rho$ and the closed-loop state does not come out of Ω_ρ over the sampling period. Recursive application of this result, proves that the closed-loop state is always bounded in Ω_ρ for all $t \geq 0$ when $x(0) \in \Omega_\rho$.

Case 1: If $x(t_k) \in \Omega_{\rho_e}$ and $t_k < t_s$, the LEMPC operates under mode 1 operation. From Part 1, the LEMPC is feasible. Moreover, from the formulation of the LEMPC, the LEMPC computes a control action such that $\tilde{x}(t) \in \Omega_{\rho_e}$ for all $t \in [t_k, t_{k+1})$. Owing to the effect of the bounded disturbances, the closed-loop state does not evolve according to the model of Eq. 3.3b. Nevertheless, if Eq. 3.21 is satisfied, the state at the next sampling time will be contained in Ω_ρ.

To show this result, let ρ_e satisfy Eq. 3.21. The proof proceeds by contradiction. Assume there exists a time $\tau^* \in [t_k, t_{k+1})$ such that $V(x(\tau^*)) > \rho$. The case that $x(t)$ is not defined for some $t \in [t_k, t_{k+1})$ is also covered by this assumption. Define $\tau_1 := \inf\{\tau \in [t_k, t_{k+1}) : V(x(\tau)) > \rho\}$. A standard continuity argument in conjunction with the fact that $V(x(t_k)) \leq \rho_e < \rho$ shows that $\tau_1 \in (t_k, t_{k+1})$, $V(x(t)) \leq \rho$ for all $t \in [t_k, \tau_1]$ with

$V(x(\tau_1)) = \rho$, and $V(x(t)) > \rho$ for some $t \in (\tau_1, t_{k+1})$. If ρ_e satisfies Eq. 3.21, then

$$\begin{aligned} \rho = V(x(\tau_1)) &\leq V(\tilde{x}(\tau_1)) + f_V(f_w(\tau_1)) \\ &\leq \rho_e + f_V(f_w(\Delta)) < \rho \end{aligned} \tag{3.25}$$

where the first inequality follows from Propositions 3.1-3.2 and the second inequality follows from the fact that $f_V \circ f_w \in \mathscr{K}$ and $\tau_1 \leq \Delta$. Eq. 3.25 is a contradiction. Thus, $x(t) \in \Omega_\rho$ for all $t \in [t_k, t_{k+1})$ if Eq. 3.21 is satisfied.

Case 2: Now, consider that the LEMPC under mode 2 operation at an arbitrary sampling time t_k. If $x(t_k) \in \Omega_\rho$, the LEMPC is feasible (Part 1). The LEMPC computes a control action that satisfies

$$\begin{aligned} \frac{\partial V(x(t_k))}{\partial x} f(x(t_k), u^*(t_k|t_k), 0) &\leq \frac{\partial V(x(t_k))}{\partial x} f(x(t_k), h(x(t_k)), 0) \\ &\leq -\alpha_3(|x(t_k)|) \end{aligned} \tag{3.26}$$

for all $x(t_k) \in \Omega_\rho$ where the inequality follows from Eq. 3.2b. Consider the time-derivate of the Lyapunov function for $\tau \in [t_k, t_{k+1})$

$$\begin{aligned} \dot{V}(x(\tau)) &= \frac{\partial V(x(\tau))}{\partial x} f(x(\tau), u^*(t_k|t_k), w(\tau)) \\ &\leq -\alpha_3(|x(t_k)|) + \frac{\partial V(x(\tau))}{\partial x} f(x(\tau), u^*(t_k|t_k), w(\tau)) \\ &\quad - \frac{\partial V(x(t_k))}{\partial x} f(x(t_k), u^*(t_k|t_k), 0) \end{aligned} \tag{3.27}$$

for $\tau \in [t_k, t_{k+1})$ where the inequality follows by adding and subtracting the left-hand side of Eq. 3.26 and accounting for the bound of Eq. 3.26. Owing to the Lipschitz bound of

Eq. 3.8, Eq. 3.27 may be upper bounded by:

$$\begin{aligned}\dot{V}(x(\tau)) &\leq -\alpha_3(|x(t_k)|) + L'_x|x(\tau) - x(t_k)| + L'_w|w(\tau)| \\ &\leq -\alpha_3(|x(t_k)|) + L'_x|x(\tau) - x(t_k)| + L'_w\theta \end{aligned} \tag{3.28}$$

for $\tau \in [t_k, t_{k+1})$ where the second inequality follows from the fact that $w(t) \in \mathbb{W} = \{\bar{w} \in \mathbb{R}^l : |\bar{w}| \leq \theta\}$ for all $t \geq 0$. Taking into account Eq. 3.6, the continuity of x and the fact that $u^*(t_k|t_k) \in \mathbb{U}$ and $w(\tau) \in \mathbb{W}$, the norm of the difference between the state at $\tau \in [t_k, t_{k+1})$ and the state at t_k scales with Δ. More specifically, the bound of:

$$|x(\tau) - x(t_k)| \leq M\Delta \tag{3.29}$$

for $\tau \in [t_k, t_{k+1})$ follows from Eq. 3.6. From Eqs. 3.28-3.29, the inequality follows:

$$\dot{V}(x(\tau)) \leq -\alpha_3(|x(t_k)|) + L'_x M\Delta + L'_w\theta \tag{3.30}$$

for $\tau \in [t_k, t_{k+1})$.

If $\Delta > 0$ and $\theta > 0$ are sufficiently small such that there exists a $\rho_s > 0$ and $\varepsilon_w > 0$ satisfying Eq. 3.22, then, for any $x(t_k) \in \Omega_\rho \setminus \Omega_{\rho_s}$, the bound of

$$\dot{V}(x(\tau)) \leq -\alpha_3(\alpha_2^{-1}(\rho_s)) + L'_x M\Delta + L'_w\theta. \tag{3.31}$$

for $\tau \in [t_k, t_{k+1})$ follows from Eq. 3.30 and Eq. 3.2a. If the condition of Eq. 3.22 is satisfied, then there exists $\varepsilon_w > 0$ such that the following inequality holds for any $x(t_k) \in \Omega_\rho \setminus \Omega_{\rho_s}$:

$$\dot{V}(x(\tau)) \leq -\varepsilon_w/\Delta \tag{3.32}$$

for $\tau \in [t_k, t_{k+1})$. Integrating the bound of Eq. 3.33 for $\tau \in [t_k, t_{k+1})$, one obtains that the following is satisfied:

$$\begin{aligned} V(x(t_{k+1})) &\leq V(x(t_k)) - \varepsilon_w \\ V(x(t)) &\leq V(x(t_k)) \; \forall \; t \in [t_k, t_{k+1}) \end{aligned} \tag{3.33}$$

for all $x(t_k) \in \Omega_\rho \setminus \Omega_{\rho_s}$.

If $x(t_k) \in \Omega_\rho \setminus \Omega_{\rho_e}$ where $\Omega_{\rho_e} \supseteq \Omega_{\rho_{\min}}$ (where $\rho_{\min}$ is defined in Eq. 3.23), then using Eq. 3.33 recursively, it follows that the state converges to Ω_{ρ_e} in a finite number of sampling times without coming out of Ω_ρ. If $x(t_k) \in \Omega_\rho \setminus \Omega_{\rho_s}$ and $t_k \geq t_s$, then again, by recursive application of Eq. 3.33, $x(t) \in \Omega_\rho$ for all $t \in [t_k, t_{k+1})$. If $x(t_k) \in \Omega_{\rho_s}$, the state at the next sampling time will be bounded in $\Omega_{\rho_{\min}}$ if $\rho_{\min}$ is defined according to Eq. 3.23. Thus, if $x(t_k) \in \Omega_\rho$, then $x(\tau) \in \Omega_\rho$ for all $\tau \in [t_k, t_{k+1})$ under the LEMPC when the conditions of Eq. 3.21-3.23 are satisfied. Using this result recursively, $x(t) \in \Omega_\rho$ for all $t \geq 0$ when $x(0) \in \Omega_\rho$.

Part 3: If t_s is finite and Eq. 3.23 is satisfied with $\rho > \rho_{\min} > \rho_s > 0$, the closed-loop state is ultimately bounded in $\Omega_{\rho_{\min}}$ owing to the definition of $\rho_{\min}$. In detail, from Part 2, if $x(t_k) \in \Omega_\rho \setminus \Omega_{\rho_s}$ and $t_k \geq t_s$, then $V(x(t_{k+1})) < V(x(t_k))$ and the state converges to Ω_{ρ_s} in finite time. Once the closed-loop state converges to $\Omega_{\rho_s} \subset \Omega_{\rho_{\min}}$, it remains inside $\Omega_{\rho_{\min}} \subset \Omega_\rho$ for all times, which follows from the definition of $\rho_{\min}$. This proves that the closed-loop system under the LEMPC of Eq. 3.3 is ultimately bounded in $\Omega_{\rho_{\min}}$ when t_s is finite. □

A few notes and remarks on the results on closed-loop stability and robustness under LEMPC are in order:

- The set Ω_ρ is an invariant set for the nominal closed-loop system and is also an invariant set for the closed-loop system subject to bounded disturbances w, i.e., $|w| \leq \theta$, under piecewise constant control action implementation when the conditions stated

in Theorem 3.1 are satisfied. This may be interpreted as follows: $\dot{V}$ is negative everywhere in Ω_ρ but the origin when there are no disturbances and the control actions are updated continuously. For sufficiently small disturbances and sampling period, i.e., θ and Δ are sufficiently small, $\dot{V}$ of the closed-loop system will continue to be negative for all $x \in \Omega_\rho \setminus \Omega_{\rho_s}$ where Ω_{ρ_s} is a small set containing the origin.

- Solving the dynamic model of Eq. 3.3b requires a numerical integration method. Therefore, numerical and discretization error will result. Owing to the fact that the error of many numerical integration methods may be bounded by a bound that depends on the integration step size, one may consider the numerical error as a source of bounded disturbance. The integration step size may be selected to be small. i.e., much smaller than the sampling period, to decrease the discretization error. Thus, the stability results remain valid when the discretization error is sufficiently small.

- For any state $x(t_k) \in \Omega_\rho$, the LEMPC is feasible where a feasible solution may be readily computed from the Lyapunov-based controller. Moreover, feasibility of the LEMPC, and not optimality of the LEMPC solution, implies closed-loop stability. Both of these issues are important owing to practical computational considerations. When solving the LEMPC to optimality results in significant computational time, one could force early termination of the optimization problem solver and closed-loop stability is still guaranteed (assuming the returned solution is feasible). If the returned solution is infeasible or at sampling times where the computation time required to solve the LEMPC is significant relative to the sampling period, the control action computed from the Lyapunov-based controller may be applied to the system.

Table 3.1: CSTR parameter values.

T_0	$300\,\mathrm{K}$	F	$5.0\,\mathrm{m^3\,h^{-1}}$
V_R	$1.0\,\mathrm{m^3}$	E	$5.0\times10^4\,\mathrm{kJ\,kmol^{-1}}$
k_0	$8.46\times10^6\,\mathrm{m^3\,kmol^{-1}\,h^{-1}}$	ΔH	$-1.15\times10^4\,\mathrm{kJ\,kmol^{-1}}$
C_p	$0.231\,\mathrm{kJ\,kg^{-1}\,K^{-1}}$	R	$8.314\,\mathrm{kJ\,kmol^{-1}\,K^{-1}}$
ρ_L	$1000\,\mathrm{kg\,m^{-3}}$		

3.3.2 Application to a Chemical Process Example

Consider a well-mixed, non-isothermal continuous stirred-tank reactor (CSTR) where an irreversible second-order exothermic reaction $A \rightarrow B$ takes place (A is the reactant and B is the desired product). The feed to the reactor consists of A in an inert solvent at flow rate F, temperature T_0 and molar concentration C_{A0}. A jacket is used to provide/remove heat to the reactor. The dynamic equations describing the behavior of the system, obtained through material and energy balances under standard modeling assumptions, are given below:

$$\frac{dC_A}{dt} = \frac{F}{V_R}(C_{A0} - C_A) - k_0 e^{-E/RT} C_A^2 \tag{3.34a}$$

$$\frac{dT}{dt} = \frac{F}{V_R}(T_0 - T) - \frac{\Delta H}{\rho_L C_p} k_0 e^{-E/RT} C_A^2 + \frac{Q}{\rho_L C_p V_R} \tag{3.34b}$$

where C_A denotes the concentration of the reactant A, T denotes the temperature of the reactor, Q denotes the rate of heat input/removal, V_R represents the volume of the reactor, ΔH, k_0, and E denote the enthalpy, pre-exponential constant and activation energy of the reaction, respectively and C_p and ρ_L denote the heat capacity and the density of the fluid in the reactor, respectively. The values of the process parameters used in the simulations are given in Table 3.1. The process model of Eq. 3.34 is numerically simulated using an explicit Euler integration method with integration step $h_c = 1.0\times10^{-3}\,\mathrm{h}$.

The CSTR has two manipulated inputs. One of the inputs is the concentration of A in the inlet to the reactor, C_{A0}, and the other manipulated input is the external heat input/removal,

Q. The input vector is given by $u^T = [C_{A0}\ Q]$, and the admissible input values are as follows: $u_1 = C_{A0} \in [0.5, 7.5]$ kmol m^{-3} and $u_2 = Q \in [-50.0, 50.0]$ MJ h^{-1}. The CSTR, described by the equations of Eq. 3.34, has an open-loop asymptotically stable steady-state within the operating range of interest given by $C_{As} = 1.18\,\text{kmol m}^{-3}$ and $T_s^* = 440.9\,\text{K}$ with corresponding steady-state input values of $C_{A0} = 4.0\,\text{kmol m}^{-3}$ and $Q_s = 0\,\text{MJ h}^{-1}$. The steady-state and the steady-state input are denoted by $x_s^T = [C_{As}\ T_s]$ and $u_s^T = [C_{A0s}\ Q_s]$, respectively. The control objective is to regulate the process in a region around the steady-state to maximize the production rate of B. To accomplish the desired objective, the economic cost function considered in this example is:

$$l_e(x,u) = -k_0 e^{-E/RT} C_A^2 \tag{3.35}$$

which is equal to the negative of the instantaneous production rate of B, i.e., the production rate should be maximized. Also, there is limitation on the amount of reactant material which may be used over the length of operation t_f. Specifically, the input trajectory of u_1 should satisfy the following time-averaged constraint:

$$\frac{1}{t_f}\int_0^{t_f} u_1(t)\,dt = C_{A0,avg} = C_{A0s} \tag{3.36}$$

where t_f denotes the length of operation.

One method to ensure that the average constraint of Eq. 3.36 is satisfied over the entire length of operation is to divide the length of operation into equal-sized operating periods and to construct constraints that are imposed in the EMPC problem to ensure that the average constraint is satisfied over each consecutive operating period. This may be accomplished by using an inventory balance that accounts for the total amount of input energy available over each operating period compared to the total amount of input energy already

used in the operating period. The main advantages of enforcing the average constraint in this fashion are that (1) only a limited number of constraints are required to be added to the EMPC, and (2) it ensures that the average constraint is satisfied over the length of operation.

To explain this type of input average constraint implementation, consider a general input average constraint given by:

$$\frac{1}{\tau_M}\int_0^{\tau_M} u(t)\,dt = u_{\text{avg}} \tag{3.37}$$

where τ_M is the operating period length that the average input constraint is imposed, i.e., $M = \tau_M/\Delta$ is the number of sampling periods in the operating period, and u_{avg} is the average input constraint value. Let τ_j denote the jth sampling time of the current operating period where τ_0 and τ_M denote the beginning and ending (time) of the current operating period, respectively. The constraint of Eq. 3.37 is enforced as follows: if the prediction horizon covers the entire operating period, then the average constraint may be enforced directly by imposing the following constraint in the EMPC problem:

$$\sum_{i=j}^{M-1} u(\tau_i) = Mu_{\text{avg}} - \sum_{i=0}^{j-1} u^*(\tau_i|\tau_i)\ . \tag{3.38}$$

where $u^*(\tau_i|\tau_i)$ denotes the input computed and applied at sampling time $\tau_i \in [\tau_0, \tau_j)$. The integral of Eq. 3.37 may be converted to a sum in Eq. 3.38 because the input trajectory is piecewise constant.

If the prediction horizon does not cover the entire operating period, then the remaining part of the operating period not covered in the prediction horizon from τ_{j+N} to τ_M should be accounted for in the constraints to ensure feasibility at subsequent sampling times. Namely,

at a sampling period $\tau_j \in [\tau_0, \tau_M)$, the following must be satisfied:

$$Mu_{\text{avg}} - \sum_{i=j}^{j+N} u(\tau_i) - \sum_{i=0}^{j-1} u^*(\tau_i|\tau_i) \leq \max\{M-N-j,0\}u_{\max} \ , \tag{3.39a}$$

$$Mu_{\text{avg}} - \sum_{i=j}^{j+N} u(\tau_i) - \sum_{i=0}^{j-1} u^*(\tau_i|\tau_i) \geq \max\{M-N-j,0\}u_{\min} \tag{3.39b}$$

where $u_{\min}$ and $u_{\max}$ denote the minimum and maximum admissible input value. Eq. 3.39 means that the difference between the total available input energy (Mu_{avg}) and the total input energy used from the beginning of the operating period through the end of the prediction horizon must be less/greater than or equal to the total input energy if the maximum/minimum allowable input was applied over the remaining part of the operating period from τ_{k+N} to τ_M, which is the part of the operating period not covered in the prediction horizon.

If the prediction horizon extends over multiple consecutive operating periods, a combination of the constraints of Eq. 3.38 and Eq. 3.39 may be employed. Let $N_{op} = \lceil (j+N)/M \rceil$ denote the number of operating periods covered in the prediction horizon. For the first operating period in the horizon, the constraint is given by:

$$\sum_{i=j}^{M-1} u(\tau_i) + \sum_{i=0}^{j-1} u^*(\tau_i|\tau_i) = Mu_{\text{avg}} \ . \tag{3.40}$$

If $N_{op} > 2$, then, the following set of constraints is imposed:

$$\sum_{i=lM}^{(l+1)M-1} u(\tau_i) = Mu_{\text{avg}}, \ \forall \ l \in \{1,2,\ldots,N_{op}-2\} \ . \tag{3.41}$$

For the last operating period covered in the horizon, the following constraint is used:

$$Mu_{\text{avg}} - \sum_{j=(N_{op}-1)M}^{(j+N)-(N_{op}-1)M} u(\tau_j) \leq \max\{N_{op}M - N - j, 0\} u_{\max} \ , \tag{3.42a}$$

$$Mu_{\text{avg}} - \sum_{j=(N_{op}-1)M}^{(j+N)-(N_{op}-1)M} u(\tau_j) \geq \max\{N_{op}M - N - j, 0\} u_{\min} \ . \tag{3.42b}$$

The index j is reset to zero at the beginning of each operating period. In the implementation of input average constraints, it may be sufficient, in terms of acceptable closed-loop behavior, to impose the input average constraint over one or two operating periods if the horizon covers multiple operating periods.

An LEMPC is designed and applied to the CSTR model of Eq. 3.34. Since the economic cost does not penalize the use of control energy, the optimal operating strategy with respect to the economic cost of Eq. 3.35 is to operate with the maximum allowable heat rate supplied to the reactor for all time. However, this may lead to a large temperature operating range which may be impractical or undesirable. Therefore, a modified control objective is considered for more practical closed-loop operation of the CSTR under EMPC. The modified control objective is to maximize the reaction rate while feeding a fixed time-averaged amount of the reactant A to the process and while forcing and maintaining operation to/at a set-point temperature of T_s. Additionally, the temperature of the reactor contents must be maintained below the maximum allowable temperature $T \leq T_{\max} = 470.0\,\text{K}$, which is treated as a hard constraint and thus, $\mathbb{X} = \{x \in \mathbb{R}^2 : x_2 \leq 470.0\}$.

A stabilizing state feedback controller, i.e., Lyapunov-based controller, is designed for the CSTR. The first input C_{A0} in the stabilizing controller is fixed to the average inlet concentration to satisfy the average input constraint of Eq. 3.36. The second input Q is designed via feedback linearization techniques while accounting for the input constraint. The

gain of the feedback linearizing controller is $\gamma = 1.4$ (see [76] for more details regarding the controller design). A quadratic Lyapunov function is considered of the form $V(x) = \bar{x}^T P \bar{x}$ where $\bar{x}$ is the deviation of the states from their corresponding steady-state values and P is the following positive definite matrix:

$$P = \begin{bmatrix} 250 & 5 \\ 5 & 0.2 \end{bmatrix}. \tag{3.43}$$

The stability region of the CSTR under the Lyapunov-based controller is characterized by taking it to be a level set of the Lyapunov function where the time-derivative of the Lyapunov function along the closed-loop state trajectories is negative and is denoted as $\Omega_u = \{x \in \mathbb{R}^2 : V(x) \leq \rho_u\}$ where $\rho_u = 138$. However, $\mathbb{X} \subset \Omega_u$ which is shown in Fig. 3.3. Thus, the set Ω_ρ where $\rho = 84.76$ is defined to account for the state constraint. Bounded Gaussian process noise is added to the CSTR with a standard deviation of $\sigma = [0.3\,5.0]^T$ and bound $\theta = [1.0\,20.0]^T$. A random noise vector is generated and applied additively to the right-hand side of the ODEs of Eq. 3.34 over the sampling period ($\Delta = 0.01$ h) and the bounds are given for each element of the noise vector ($|w_i| \leq \theta_i$ for $i = 1, 2$). Through extensive closed-loop simulations of the CSTR under the Lyapunov-based controller and under the LEMPC (described below) and with many realizations of the process noise, the set Ω_{ρ_e} was determined to be $\rho_e = 59.325$.

The first differential equation of Eq. 3.34 (C_A) is input-to-state-stable (ISS) with respect to T. Therefore, a contractive Lyapunov-based constraint may be applied to the LEMPC to ensure that the temperature converges to a neighborhood of the optimal steady-state temperature value. Namely, a Lyapunov function for the temperature ordinary differential equation (ODE) of Eq. 3.34b is defined and is given by: $V_T(T) := (T - T_s)^2$. The LEMPC

formulation is given by:

$$\min_{u\in S(\Delta)} \quad -\int_{t_k}^{t_{k+N}} k_0 e^{-E/R\tilde{T}(\tau)}\tilde{C}_A^2(\tau)\, d\tau \tag{3.44a}$$

$$\text{s.t.} \quad \dot{\tilde{C}}_A(t) = \frac{F}{V}(u_1(t)-\tilde{C}_A(t)) - k_0 e^{-E/R\tilde{T}(t)}\tilde{C}_A^2(t) \tag{3.44b}$$

$$\dot{\tilde{T}}(t) = \frac{F}{V}(T_0-\tilde{T}(t)) - \frac{\Delta H k_0}{\rho_L C_p} e^{-E/R\tilde{T}(t)}\tilde{C}_A^2(t) + \frac{u_2(t)}{\rho_L C_p V_R} \tag{3.44c}$$

$$\tilde{C}_A(t_k) = C_A(t_k),\ \tilde{T}(t_k) = T(t_k) \tag{3.44d}$$

$$u_1(t) \in [0.5, 7.5]\ \text{kmol}\,\text{m}^{-3},\ \forall\, t \in [t_k, t_{k+N}) \tag{3.44e}$$

$$u_2(t) \in [-50.0, 50.0]\ \text{MJ}\,\text{h}^{-1},\ \forall\, t \in [t_k, t_{k+N}) \tag{3.44f}$$

$$\sum_{i=j}^{M-1} u_1(\tau_i) + \sum_{i=0}^{j-1} u_1^*(\tau_i|\tau_i) = MC_{A0s} \tag{3.44g}$$

$$MC_{A0s} - \sum_{j=M}^{j+N-M} u_1(\tau_j) \leq \max\{2M-N-j, 0\} u_{1,\max}\ , \tag{3.44h}$$

$$MC_{A0s} - \sum_{j=M}^{j+N-M} u_1(\tau_j) \geq \max\{2M-N-j, 0\} u_{1,\min}\ . \tag{3.44i}$$

$$\tilde{T}(t) \leq T_{\max} \tag{3.44j}$$

$$V(\tilde{x}(t)) \leq \rho_e,\ \forall\, t \in [t_k, t_{k+N}) \tag{3.44k}$$

$$\frac{\partial V_T(T(t_k))}{\partial T} f_2(\tilde{x}(t_k), u(t_k), 0) \leq \frac{\partial V_T(T(t_k))}{\partial T} f_2(\tilde{x}(t_k), h(\tilde{x}(t_k)), 0) \tag{3.44l}$$

where $f_2(\cdot)$ is the right-hand side of the ODE of Eq. 3.34b. The CSTR was initialized at many states distributed throughout state-space including some cases where the initial state is outside Ω_u. The LEMPC described above was applied to the CSTR with an operating period over which to enforce the average input constraint of $M = 20$ ($\tau_M = 0.2\,\text{h}$) and a prediction horizon of $N = 20$.

Several simulations of 50.0 h length of operation were completed. In all cases, the LEMPC was able to force the system to Ω_ρ and maintain operation inside Ω_ρ without

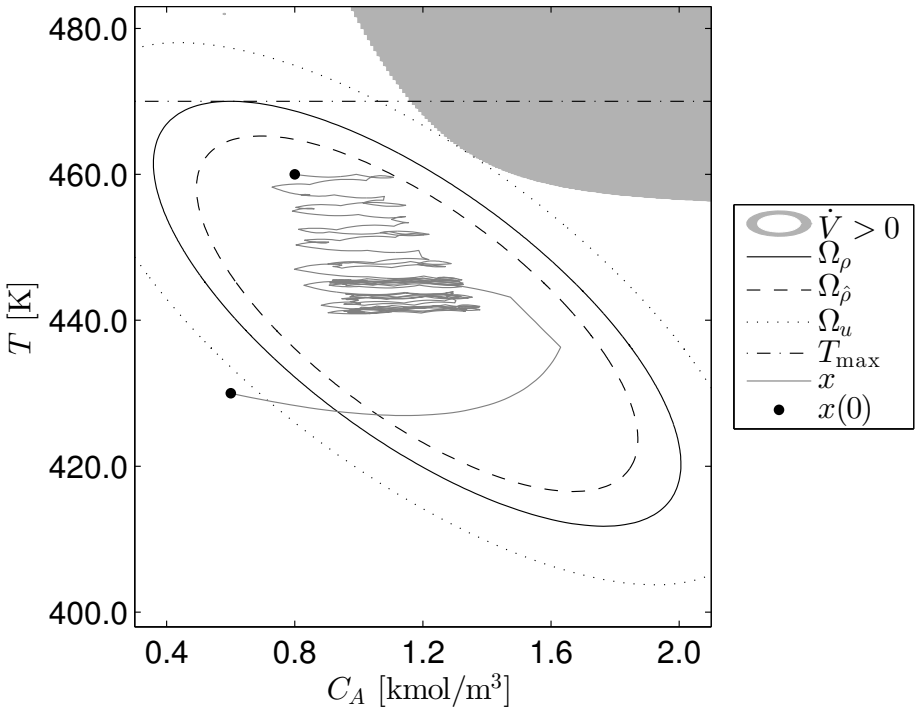

Figure 3.3: Two closed-loop state trajectories under the LEMPC in state-space.

violating the state constraint. The closed-loop state trajectories over the first 1.0 h are shown in Fig. 3.3 for one initial condition starting inside Ω_ρ and one starting outside Ω_u. From Fig. 3.3, the LEMPC forces the temperature to a neighborhood of the temperature set-point where it maintains the temperature thereafter. The reactant concentration trajectory varies with time and never settles at a steady-state owing to a periodic-like forcing of the inlet concentration.

The CSTR was simulated with the same realization of the process noise and same initial condition under the Lyapunov-based controller applied in a sample-and-hold fashion and under a constant input equal to the steady-state input. To evaluate the average economic cost under LEMPC and under the other two control strategies, the following index is defined:

$$\bar{J}_e := \frac{1}{t_f} \int_0^{t_f} l_e(x(t), u(t))\, dt \tag{3.45}$$

Table 3.2: Average economic cost over several simulations under the LEMPC, the Lyapunov-based controller applied in a sample-and-hold fashion, and the constant input equal to u_s. For the case denoted with a "*", the system under the constant input u_s settled at a different steady-state, i.e., not x_s.

$\bar{J}_E$ under LEMPC	$\bar{J}_E$ under $k(x)$	$\bar{J}_E$ under u_s
14.17	14.10	14.09
14.18	14.11	14.09
14.17	14.10	14.08
14.17	14.09	14.06
14.18	14.10	14.10
14.17	14.09	14.08
14.18	14.09	14.10
14.18	14.08	14.08
14.19	14.08	14.10
14.18	14.07	14.07
14.18	14.11	14.11
14.18	14.08	14.07
14.17	14.06	0.36*
14.19	14.06	14.10

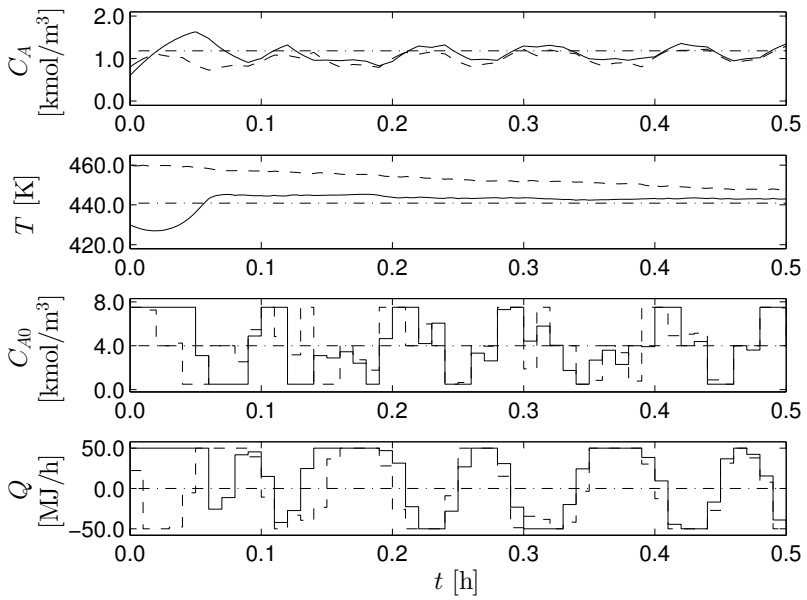

Figure 3.4: The closed-loop state and input trajectories of the CSTR under the LEMPC of Eq. 3.44 for two initial conditions (solid and dashed trajectories) and the steady-state is the dashed-dotted line.

where x and u denote the closed-loop state and input trajectories. The average economic cost over each of these simulations is reported in Table 3.2. Owing to the fact that the simulations were performed over many operating periods, the average closed-loop performance index is essentially a measure of the asymptotic average performance. The transient performance is also discussed below. From these results, an average of 0.6 percent closed-loop performance benefit was observed with the LEMPC over the Lyapunov-based controller and the constant input u_s^*. It is important to note that for one of the simulations that was initialized outside Ω_u the CSTR under the constant input u_s^* settled on an offsetting steady-state which is denoted with an asterisk in Table 3.2.

Fig. 3.4 gives the state and input trajectories of the CSTR under the LEMPC of Eq. 3.44 for two initial conditions: (0.6 kmol m^{-3}, 430.0 K), referred to as the low temperature initial condition, and (0.8 kmol m^{-3}, 460.0 K), referred to as the high temperature initial con-

dition. One of the most interesting results of these simulations is the asymmetric responses about the temperature set-point dictated by the LEMPC. For the low temperature initial condition, the heat rate input computed by the LEMPC is initially at the maximum admissible value to force the temperature to the set-point as fast as possible. This behavior is desirable with respect to the economic cost because the production rate is monotonically increasing with temperature. On the other hand, for the high temperature initial condition, the rate at which the computed input trajectory of the LEMPC forces the temperature to the set-point is much slower rate than that of the case with the lower initial temperature. Again, this type of behavior is desirable owing to the fact that the production rate of B is greater at higher temperature.

To quantify the difference in the transient closed-loop performance under LEMPC relative to the transient closed-loop performance achieved under the Lyapunov-based controller and under the constant input equal to u_s, the closed-loop economic performance over the first operating period is used, i.e., the index $\bar{J}_e$ with $t_f = 0.2\,\text{h}$. The performance benefit under the LEMPC relative to that achieved under the Lyapunov-based controller and under the constant input is 12.15 percent and 20.79 percent, respectively, and a clear advantage on transient performance is realized under LEMPC. Moreover, the asymmetric response dictated by the LEMPC is a unique property of EMPC that addresses a potential drawback of tracking MPC methodologies. In particular, the stage cost of tracking MPC typically penalize positive and negative deviation from the set-point equally even though from an economic stand-point this may not be appropriate.

3.4 Closed-loop Performance under LEMPC

Owing to the availability of the explicit stabilizing (Lyapunov-based) controller, the corresponding Lyapunov function, and the stability region used to design LEMPC, a terminal

equality constraint may be readily designed for the LEMPC problem. The terminal equality constraint allows for guaranteed closed-loop performance properties, while maintaining the unique recursive feasibility property of LEMPC. Nominally operated systems are considered, i.e., the system of Eq. 3.1 with $w \equiv 0$ and with slight abuse of notation, the nominally operated system will be written as

$$\dot{x} = f(x,u) \tag{3.46}$$

where $x \in \mathbb{X}$ and $u \in \mathbb{U}$. The system of Eq. 3.46 satisfies all of the relevant assumptions as the system of Eq. 3.1.

An economic cost $l_e : \mathbb{X} \times \mathbb{U} \to \mathbb{R}$ is assumed for the system of Eq. 3.46 which is continuous on $\mathbb{X} \times \mathbb{U}$. The existence of a steady-state and steady-state input pair, denoted as (x_s^*, u_s^*), that minimizes the economic cost in the sense that the minimum of l_e is attained at the pair (x_s^*, u_s^*) is assumed. For simplicity, the minimizing pair is assumed to be unique. With these assumptions, the minimizing steady-state pair is given by:

$$(x_s^*, u_s^*) = \underset{x_s \in \mathbb{X}, u_s \in \mathbb{U}}{\arg\min} \{ l_e(x_s, u_s) : f(x_s, u_s) = 0 \} \ .$$

Without loss of generality, the minimizing pair will be taken to be the origin of Eq. 3.46, i.e., $f(0,0) = 0$.

3.4.1 Stabilizability Assumption

A terminal equality constraint imposed in the LEMPC optimization problem will be computed at each sampling time based on the solution of the sampled-data system consisting of the continuous-time system of Eq. 3.46 with an explicit controller applied in a sample-and-hold fashion. To consider infinite-time closed-loop economic performance (to be made precise below), a stronger assumption is considered on the explicit controller (Lyapunov-

based controller). A relaxation of the assumption is discussed in a remark below.

Assumption 3.1. *There exists a locally Lipschitz feedback controller $h : \mathbb{X} \to \mathbb{U}$ with $h(0) = 0$ for the system of Eq. 3.1 that renders the origin of the closed-loop system under continuous implementation of the controller locally exponentially stable. More specifically, there exist constants $\rho > 0$, $c_i > 0$, $i = 1,2,3,4$ and a continuously differentiable Lyapunov function $V : \mathbb{X} \to \mathbb{R}_+$ such that the following inequalities hold:*

$$c_1 |x|^2 \leq V(x) \leq c_2 |x|^2, \tag{3.47a}$$

$$\frac{\partial V(x)}{\partial x} f(x, h(x)) \leq -c_3 |x|^2, \tag{3.47b}$$

$$\left| \frac{\partial V(x)}{\partial x} \right| \leq c_4 |x|, \tag{3.47c}$$

for all $x \in \Omega_\rho \subseteq \mathbb{X}$.

When the controller of Assumption 3.1 is applied in a sample-and-hold (zeroth-order hold) fashion, i.e., the controller is an emulation controller, the resulting closed-loop system is a sampled-data system. To distinguish from the state and input trajectories of the system under the emulation controller and the state and input trajectories of the closed-loop system under LEMPC, z and v will be used for the former, and x and u^* will be used for the latter, respectively. The sampled-data system consisting of the system of Eq. 3.46 under the sample-and-hold implementation of the explicit controller is given by:

$$\begin{aligned} \dot{z}(t) &= f(z(t), v(t)) \\ v(t) &= h(z(t_k)) \end{aligned} \tag{3.48}$$

for $t \in [t_k, t_{k+1})$ where $t_k = k\Delta$ and $k = 0, 1, \ldots$ with initial condition $z(0) = z_0 \in \Omega_\rho$. From Corollary 2.1, the origin of the closed-loop system of Eq. 3.48 is exponentially stable under

sufficiently fast sampling, i.e., the sampling period, Δ, is sufficiently small. Moreover, from the proof of Corollary 2.1, V is a Lyapunov function for the closed-loop sampled-data system in the sense that there exists a constant $\hat{c}_3 > 0$ such that

$$\frac{\partial V(z(t))}{\partial z} f(z(t), h(z(t_k))) \leq -\hat{c}_3 |z(t)|^2 \tag{3.49}$$

for all $t \in [t_k, t_{k+1})$ and integers $k \geq 0$ where $z(t)$ is the solution of Eq. 3.48 at time t with initial condition $z(0) = x(0) \in \Omega_\rho$ where $x(0)$ denotes a state measurement of the system of Eq. 3.46 at the initial time.

3.4.2 Formulation and Implementation of the LEMPC with a Terminal Equality Constraint

The solution of Eq. 3.48 may be leveraged in the design of a terminal equality constraint. Specifically, the system of Eq. 3.48 is initialized with a state measurement of the system of Eq. 3.46 at $t = 0$. Using forward simulation of the system of Eq. 3.48, the state may be computed at t_{k+N}. The computed state is then used as a terminal constraint in LEMPC in the sense that the predicted state of the LEMPC must converge to the state of Eq. 3.48, i.e., $\tilde{x}(t_{k+N}) = z(t_{k+N})$. Using this design principle, the formulation of the LEMPC with a

terminal equality constraint formulated based on z is given by the problem:

$$\min_{u\in S(\Delta)} \int_{t_k}^{t_{k+N}} l_e(\tilde{x}(\tau),u(\tau))\, d\tau \tag{3.50a}$$

$$\text{s.t.} \quad \dot{\tilde{x}}(t) = f(\tilde{x}(t),u(t)) \tag{3.50b}$$

$$\tilde{x}(t_k) = x(t_k) \tag{3.50c}$$

$$\tilde{x}(t_{k+N}) = z(t_{k+N}) \tag{3.50d}$$

$$u(t) \in \mathbb{U},\ \forall\, t \in [t_k, t_{k+N}) \tag{3.50e}$$

$$V(\tilde{x}(t)) \leq \rho_e,\ \forall\, t \in [t_k, t_{k+N})$$

$$\text{if } V(x(t_k)) \leq \rho_e \text{ and } t_k < t_s \tag{3.50f}$$

$$\frac{\partial V(x(t_k))}{\partial x} f(x(t_k),u(t_k)) \leq \frac{\partial V(x(t_k))}{\partial x} f(x(t_k),h(x(t_k)))$$

$$\text{if } V(x(t_k)) > \rho_e \text{ or } t_k \geq t_s \tag{3.50g}$$

where all the components of the LEMPC optimization problem of Eq. 3.50 are similar to that of the problem of Eq. 3.3 except for the additional constraint of Eq. 3.50d. The terminal constraint of Eq. 3.50d enforces that the computed input trajectory steers the predicted state trajectory to the state $z(t_{k+N})$ at the end of the prediction horizon. The terminal constraint of Eq. 3.50d differs from traditional terminal equality constraints in the sense that it is not necessarily a steady-state. However, it is important to note that the terminal constraint in the LEMPC of Eq. 3.50 exponentially converges to the steady-state owing to the stability properties of the explicit controller.

The implementation of the LEMPC of Eq. 3.50 is similar to that of the LEMPC of Eq. 3.3. Before the optimization problem of Eq. 3.50 is solved, the terminal constraint, $z(t_{k+N})$, is computed by recursively solving the system of Eq. 3.48 over t_{k+N-1} to t_{k+N} and is initialized with $z(t_{k+N-1})$, which corresponds to the terminal constraint at the previous sampling time. At the initial time ($t = 0$), $z(t_N)$ is computed by first initializing the system

of Eq. 3.48 with $x(0)$ and recursively solving this system from the initial time to $t_N = N\Delta$. For added robustness, especially to numerical and discretization error, one may reinitialize the system of Eq. 3.48 with a state measurement at each sampling time, i.e., initialize the system of Eq. 3.48 with $x(t_k)$ and use forward simulation to compute $z(t_{k+N})$. However, in the nominal scenario considered here, numerical error is not considered.

3.4.3 Closed-loop Performance and Stability Analysis

The closed-loop stability properties of the LEMPC follows from the results of the previous section and are stated in the following corollary.

Corollary 3.1. *Let the conditions of Theorem 3.1 be satisfied. If $x(0) \in \Omega_\rho$, then the closed-loop state trajectory of the system of Eq. 3.46 under the LEMPC of Eq. 3.50 based on the Lyapunov-based controller that satisfies Eq. 3.2 is always bounded in Ω_ρ for all $t \geq 0$. Moreover, the LEMPC problem of Eq. 3.50 is recursively feasible.*

Proof. If similar conditions are satisfied as that of Theorem 3.1 and the LEMPC problem of Eq. 3.50 is feasible, it follows from Theorem 3.1 that the closed-loop state is bounded in Ω_ρ. Initial feasibility at $t = 0$ follows from the fact that the sample-and-hold input trajectory used to compute the terminal constraint, $z(t_N)$, is a feasible solution to the optimization problem because (1) it forces the predicted state to the terminal constraint, (2) satisfies the input constraint, (3) maintains the state in Ω_{ρ_e} if $x(0) \in \Omega_{\rho_e}$ or trivially satisfies the contractive constraint of Eq. 3.50g. For the subsequent sampling time ($t = \Delta$), the piecewise defined input trajectory consisting of $u^*(t|0)$ for $t \in [\Delta, N\Delta)$ and $u(t) = h(z(t_N))$ for $t \in [N\Delta, (N+1)\Delta)$ is a feasible solution to the optimization problem at $t = \Delta$. Applying this result recursively for all future sampling times, recursive feasibility follows. □

Finite-time and infinite-time economic performance is considered. The analysis follows closely that of [6], which analyzes closed-loop performance of EMPC formulated with an

equality terminal constraint equal to x_s^*. Let $J_e^*(x(t_k))$ denote the optimal value of Eq. 3.50a at time t_k given the state measurement $x(t_k)$. The first result gives the finite-time average performance under the LEMPC of Eq. 3.50. Without loss of generality, take $l_e(x,u) \geq 0$ for all $x \in \Omega_\rho$ and $u \in \mathbb{U}$.

Theorem 3.2. *Consider the system of Eq. 3.48 under the LEMPC of Eq. 3.50 based on the Lyapunov-based controller that satisfies Eq. 3.2. For any T strictly positive finite integer, the closed-loop average economic performance is bounded by:*

$$\int_0^{T\Delta} l_e(x(t),u^*(t))\,dt \leq \int_0^{(T+N)\Delta} l_e(z(t),v(t))\,dt \tag{3.51}$$

where x and u^* denote the closed-loop state and input trajectories and z and v denote the resulting state and input trajectories of the system of Eq. 3.48.

Proof. Let $u^*(t|t_k)$ for $t \in [t_k, t_{k+N})$ be the optimal input trajectory of Eq. 3.50 at t_k. The piecewise defined input trajectory consisting of $u^*(t|t_k)$ for $t \in [t_{k+1}, t_{k+N})$ and $u(t) = h(z(t_{k+N}))$ for $t \in [t_{k+N}, t_{k+N+1})$ is a feasible solution to the optimization problem at the next sampling time (t_{k+1}). Utilizing the feasible solution to the problem of Eq. 3.50 at t_{k+1}, the difference between the optimal value of Eq. 3.50a at any two successive sampling times may be bounded as follows:

$$\begin{aligned} &J_e^*(x(t_{k+1})) - J_e^*(x(t_k)) \\ &\quad \leq \int_{t_{k+N}}^{t_{k+N+1}} l_e(z(t),h(z(t_{k+N})))\,dt - \int_{t_k}^{t_{k+1}} l_e(x(t),u^*(t_k|t_k))\,dt\ . \end{aligned} \tag{3.52}$$

Let T be any strictly positive integer. Summing the difference of the optimal value of

Eq. 3.50a at two subsequent sampling times, the sum may be lower bounded by:

$$\sum_{k=0}^{T-1} [J_e^*(x(t_{k+1})) - J_e^*(x(t_k))] = J_e^*(x(T\Delta)) - J_e^*(x(0))$$
$$\geq -J_e^*(x(0)) \tag{3.53}$$

where the inequality follows from the fact that $l_e(x,u) \geq 0$ for all $x \in \Omega_\rho$ and $u \in \mathbb{U}$. At the initial time, the optimal value of Eq. 3.50a may be bounded by the cost under the explicit controller over the prediction horizon:

$$J_e^*(x(0)) \leq \int_0^{t_N} l_e(z(t), v(t))\, dt\ . \tag{3.54}$$

Moreover, the left-hand side of Eq. 3.53 may be upper bounded as follows:

$$\begin{aligned}
&\sum_{k=0}^{T-1} [J_e^*(x(t_{k+1})) - J_e^*(x(t_k))] \\
&\quad \leq \sum_{k=0}^{T-1} \left(\int_{t_{k+N}}^{t_{k+N+1}} l_e(z(t), h(z(t_{k+N})))\, dt - \int_{t_k}^{t_{k+1}} l_e(x(t), u^*(t_k|t_k))\, dt \right) \\
&\quad = \int_{t_N}^{(T+N)\Delta} l_e(z(t), v(t))\, dt - \int_0^{T\Delta} l_e(x(t), u^*(t))\, dt
\end{aligned} \tag{3.55}$$

From Eq. 3.53 and Eq. 3.55, the closed-loop economic performance over the initial time to $T\Delta$ is no worse than the closed-loop performance under the explicit control from initial time to $(T+N)\Delta$:

$$\begin{aligned}
\int_0^{T\Delta} l_e(x(t), u^*(t))\, dt &\leq J_e^*(x(0)) + \int_{t_N}^{T\Delta+N\Delta} l_e(z(t), v(t))\, dt \\
&\leq \int_0^{(T+N)\Delta} l_e(z(t), v(t))\, dt
\end{aligned} \tag{3.56}$$

where the second inequality follows from Eq. 3.54. This proves the bound of Eq. 3.51. □

The upper limit of integration of the right-hand side of Eq. 3.51, i.e., $(T+N)\Delta$, arises from the fact that a fixed prediction horizon is used in the LEMPC of Eq. 3.50. If, instead, $T\Delta$ represents the final operating time of a given system, one could employ a shrinking horizon from $(T-N)\Delta$ to $T\Delta$ in the LEMPC and the upper limit of integration of the right-hand side of Eq. 3.51 would be $T\Delta$. Also, as a consequence of the performance bound of Eq. 3.51, the average finite-time economic performance may be bounded as follows:

$$\begin{aligned}&\frac{1}{T\Delta}\int_0^{T\Delta} l_e(x(t),u^*(t))\,dt \\ &\quad\leq \frac{1}{T\Delta}\int_0^{T\Delta} l_e(z(t),v(t))\,dt + \frac{1}{T\Delta}\int_{T\Delta}^{(T+N)\Delta} l_e(z(t),v(t))\,dt \end{aligned} \tag{3.57}$$

for any integer $T > 0$. From the right-hand side of Eq. 3.57, the second term of the right-hand side is less significant as T gets large.

To consider asymptotic average closed-loop economic performance of the system under the LEMPC of Eq. 3.50, the asymptotic average closed-loop performance under the explicit controller needs to be considered. Because the state and input trajectory asymptotically converge to (x_s^*, u_s^*), it is straightforward to show that the asymptotic average economic performance under the explicit controller is no worse than the economic cost at the optimal steady-state pair, which is stated in the lemma below.

Lemma 3.1. *The asymptotic average economic cost of the system of Eq. 3.48 under the Lyapunov-based controller that satisfies Assumption 3.1 for any initial condition $z(0) \in \Omega_\rho$ is*

$$\lim_{T\to\infty} \frac{1}{T\Delta}\int_0^{T\Delta} l_e(z(t),v(t))\,dt = l_e(x_s^*,u_s^*) \tag{3.58}$$

where $\Delta \in (0,\Delta^*)$ ($\Delta^* > 0$ is defined according to Corollary 2.1) and z and v denote the state and input trajectories of the system of Eq. 3.48.

Proof. Recall, the economic stage cost function l_e is continuous on the compact set $\Omega_\rho \times \mathbb{U}$

and $z(t) \in \Omega_\rho$ and $v(t) \in \mathbb{U}$ for all $t \geq 0$. Thus, the integral:

$$\frac{1}{T\Delta}\int_0^{T\Delta} l_e(z(t), v(t))\, dt < \infty \tag{3.59}$$

for any integer $T > 0$. Since $z(t)$ and $v(t)$ exponentially converge to the optimal steady-state pair (x_s^*, u_s^*) as $t \to \infty$, the limit of the integral of Eq. 3.59 as T tends to infinity exists and is equal to $l_e(x_s^*, u_s^*)$. To prove the limit, it is sufficient to show that for any $\varepsilon > 0$, there exists a T^* such that for $T > T^*$, the following holds:

$$\left|\frac{1}{T\Delta}\int_0^{T\Delta} l_e(z(t), v(t))\, dt - l_e(x_s^*, u_s^*)\right| < \varepsilon \tag{3.60}$$

To simplify the presentation, define $I(T_1, T_2)$ as the following integral:

$$I(T_1, T_2) := \int_{T_1\Delta}^{T_2\Delta} l_e(z(t), v(t))\, dt \tag{3.61}$$

where the arguments of I are integers representing the integers of the lower and upper limits of integration, respectively. Since $z(t)$ and $v(t)$ converge to x_s^* and u_s^* as t tends to infinity, respectively, $l_e(x(t), v(t)) \to l_e(x_s^*, u_s^*)$ as t tends to infinity. Furthermore, $z(t) \in \Omega_\rho$ and $v(t) \in \mathbb{U}$ for all $t \geq 0$, so for every $\varepsilon > 0$, there exists an integer $\tilde{T} > 0$ such that

$$|l_e(z(t), v(t)) - l_e(x_s^*, u_s^*)| < \varepsilon/2 \tag{3.62}$$

for $t \geq \tilde{T}\Delta$. For any $T > \tilde{T}$,

$$\begin{aligned} |I(0,T) - T\Delta l_e(x_s^*,u_s^*)| &= |I(0,\tilde{T}) + I(\tilde{T},T) - T\Delta l_e(x_s^*,u_s^*)| \\ &\leq \int_0^{\tilde{T}\Delta} |l_e(z(t),v(t)) - l_e(x_s^*,u_s^*)|\, dt \\ &\quad + \int_{\tilde{T}\Delta}^{T\Delta} |l_e(z(t),v(t)) - l_e(x_s^*,u_s^*)|\, dt \\ &\leq \tilde{T}\tilde{M} + (T-\tilde{T})\varepsilon/2 \end{aligned} \tag{3.63}$$

where

$$\tilde{M} := \sup_{t\in[0,\tilde{T}\Delta]} \{|l_e(z(t),v(t)) - l_e(x_s^*,u_s^*)|\} \ .$$

For any $T > T^* = 2\tilde{T}(\tilde{M} - \varepsilon/2)/\varepsilon$ (which implies $(\tilde{M} - \varepsilon/2)\tilde{T}/T < \varepsilon/2$), the following inequality is satisfied:

$$\begin{aligned} |I(0,T)/T - l_e(x_s^*,u_s^*)| &\leq \tilde{T}\tilde{M}/T + (1-\tilde{T}/T)\varepsilon/2 \\ &= (\tilde{M} - \varepsilon/2)\tilde{T}/T + \varepsilon/2 < \varepsilon \end{aligned} \tag{3.64}$$

which proves the limit of Eq. 3.58. □

With Lemma 3.1, the asymptotic average closed-loop economic performance under the LEMPC is no worse than the closed-loop performance at the economically optimal steady-state.

Theorem 3.3. *Consider the system of Eq. 3.48 under the LEMPC of Eq. 3.50 based on the Lyapunov-based controller that satisfies Assumption 3.1. Let* $\Delta \in (0,\Delta^*)$ *(*$\Delta^* > 0$ *is defined according to Corollary 2.1). The closed-loop asymptotic average economic performance*

is no worse than the economic cost at steady-state, i.e., the following bound holds:

$$\limsup_{T\to\infty} \frac{1}{T\Delta} \int_0^{T\Delta} l_e(x(t), u^*(t))\, dt \leq l_e(x_s^*, u_s^*) \tag{3.65}$$

Proof. From Theorem 3.2, for any $T > 0$:

$$\frac{1}{T\Delta} \int_0^{T\Delta} l_e(x(t), u^*(t))\, dt \leq \frac{1}{T\Delta} \int_0^{(T+N)\Delta} l_e(z(t), v(t))\, dt\ . \tag{3.66}$$

As T increases, both sides of the inequality of Eq. 3.66 remain finite owing to the fact that l_e is continuous and the state and input trajectories are bounded in compact sets. The limit of the right-hand side as $T \to \infty$ is equal to $l_e(x_s^*, u_s^*)$ (Lemma 3.1). Therefore, one may readily obtain that:

$$\limsup_{T\to\infty} \frac{1}{T\Delta} \int_0^{T\Delta} l_e(x(t), u^*(t))\, dt \leq l_e(x_s^*, u_s^*) \tag{3.67}$$

which proves the desired result. □

While the finite-time performance results of Theorem 3.2 require that the Lyapunov-based controller be designed such that Eq. 3.2 is satisfied, the infinite-time average performance results of Theorem 3.3 require that the Lyapunov-based controller satisfies the stronger assumption (Assumption 3.1), which is required to obtain the performance bound of Eq. 3.65. A Lyapunov-based controller that satisfies Eq. 3.2 when implemented in a sample-and-hold fashion with a sufficiently small sampling period will force the state to a small compact set containing the steady-state. When the LEMPC of Eq. 3.50 is designed with a Lyapunov-based controller that only satisfies Eq. 3.2, a weaker result on the asymptotic average economic closed-loop performance is obtained. Namely, the closed-

loop asymptotic average performance may be bounded as follows:

$$\limsup_{T\to\infty} \frac{1}{T\Delta} \int_0^{T\Delta} l_e(x(t), u^*(t))\, dt \leq \max_{x,z\in\Omega_{\rho_{\min}}} l_e(x, h(z)) \tag{3.68}$$

where $\Omega_{\rho_{\min}}$ is defined as in Theorem 3.1. Note that the size of set $\Omega_{\rho_{\min}}$ may be made arbitrarily small by making the sampling period arbitrarily small.

Remark 3.1. For systems with average constraints e.g., like that imposed in the example of Section 3.3.2, the average constraint design methodologies for asymptotic average constraints [6] and for transient average constraints [137], which were presented for EMPC with a terminal equality constraint equal to x_s^*, may be extended to the LEMPC of Eq. 3.50 when the average constraint is satisfied under the explicit controller. The methods of [6, 137] go beyond imposing the average constraint over successive operating periods, which is the method employed in Section 3.3.2.

Remark 3.2. The performance results of this section hold for any prediction horizon size even when $N = 1$. The use of a short horizon may be computationally advantageous for real-time application. Also, owing to the fact that the terminal equality constraint of Eq. 3.50d may be a point in the state-space away from the steady-state, it is expected that the feasible region of the LEMPC of Eq. 3.50 would be larger than the feasible region of EMPC with a terminal equality constraint equal to the steady-state for most cases especially when a short prediction horizon is used in the EMPC formulation.

3.5 LEMPC with a Time-varying Stage Cost

One of the unique advantages of EMPC relative to other control methodologies is the integration of economic objectives directly within a control framework. For stability purposes, most of the EMPC schemes use a steady-state to impose constraints in the EMPC optimiza-

tion problem to ensure closed-loop stability in their formulations, e.g., the EMPC formulated with a terminal constraint described in Chapter 2 and the Lyapunov-based constraints of Eq. 3.3e-3.3f used in the LEMPC of Eq. 3.3. Also, these EMPC schemes have been formulated with time-invariant economic cost functions. However, when the time-scale or update frequency of time-varying economic considerations arising from, for example, variable energy pricing or product demand changes is comparable to the time-scale of the process/system dynamics, it may be desirable to formulate the EMPC scheme with a time-dependent cost function.

In this section, an LEMPC scheme is developed that may accommodate an explicitly time-varying economic cost function. First, the formulation of the LEMPC scheme is presented. Second, closed-loop stability, in the sense of boundedness of the closed-loop state, is proven through a theoretical treatment of the LEMPC scheme. The LEMPC scheme is applied to a chemical process example to demonstrate that the LEMPC with time-varying economic cost achieves closed-loop stability and results in improved closed-loop economic performance over a conventional approach to optimization and control.

3.5.1 Class of Economic Costs and Stabilizability Assumption

Consider the class of systems described by the system of Eq. 3.1 with all of the relevant assumptions. Instead of the time-invariant economic cost, the system of Eq. 3.1 is assumed to be equipped with a time-dependent economic cost function, which has the following form $l_e(t,x,u)$ (the function l_e maps time and the state and input vectors to a scalar that is a measure of the economics, i.e., $l_e : [0,\infty) \times \mathbb{X} \times \mathbb{U}$). No restriction on the form of the cost function is required for stability. However, some limitations to the cost function that may be considered must be made to solve the optimization problem. From a practical point-of-view, many of the cost functions that would be used to describe the economics of a system

may be piecewise continuous functions of time and continuous with respect to the state and input vectors.

In a traditional or conventional approach, if the economics change results in a change in the optimal operating steady-state, the optimal steady-state is updated and the updated optimal steady-state is sent down to a feedback controller, e.g., tracking MPC, to force the system to operate at this new steady-state. To account for the various potentially operating steady-states, the existence of a set of steady-states for the system of Eq. 3.1, which is denoted as $\Gamma = \{x_s \in \mathbb{R}^n : \exists\ u_s \in \mathbb{U} \text{ s.t. } f(x_s, u_s, 0) = 0\} \subset \mathbb{X}$, is assumed for the system of Eq. 3.1. An additional assumption is made on the set Γ to ensure that the acceptable operating region is non-empty which is stated below. For a given system, the equilibrium manifold Γ may be taken as the set of admissible operating steady-states, i.e., the set of possible operating points under the conventional approach to optimization and control.

As in the case for the LEMPC formulated with a time-invariant economic stage cost, a stabilizability assumption is needed. For each $x_s \in \Gamma$, the existence of a Lyapunov-based controller that renders x_s of the nominal system of Eq. 3.1 asymptotically stable under continuous implementation is assumed. More specifically, the set of Lyapunov-based controllers are mappings that map the state to the set $\mathbb{U}$. For simplicity of notation, the notation $h(x;x_s)$ where x_s is a parameter which is used to denote the Lyapunov-based controller with respect to $x_s \in \Gamma$, i.e., the control law $h(x;x_s)$ renders the steady-state x_s asymptotically stable for the nominally operated closed-loop system. Also, for two points in Γ, e.g., $x_{s,1}$, $x_{s,2} \in \Gamma$, no relationship is assumed between the two controllers $h(x;x_{s,1})$ and $h(x;x_{s,2})$ other than the former renders the steady-state $x_{s,1}$ asymptotically stable and the latter renders the steady-state $x_{s,2}$ asymptotically stable. Thus, the two controllers may be designed utilizing different techniques.

Using converse theorems, the existence of Lyapunov functions $V(\cdot;x_s)$ for all $x_s \in \Gamma$ follows from the stabilizability assumption. The Lyapunov functions satisfy the following

conditions:

$$\alpha_1(|x-x_s|;x_s) \leq V(x;x_s) \leq \alpha_2(|x-x_s|;x_s) \tag{3.69a}$$

$$\frac{\partial V(x;x_s)}{\partial x} f(x,h(x;x_s),0) \leq -\alpha_3(|x-x_s|;x_s) \tag{3.69b}$$

$$\left|\frac{\partial V(x;x_s)}{\partial x}\right| \leq \alpha_4(|x-x_s|;x_s) \tag{3.69c}$$

for $(x-x_s) \in D(x_s)$ and each $x_s \in \Gamma$ where $\alpha_i(\cdot;x_s)$, $i = 1,2,3,4$ are class $\mathscr{K}$ function and $D(x_s)$ is an open neighborhood of the origin that depends on x_s. Owing to the fact that there exists a Lyapunov function for each x_s, different class $\mathscr{K}$ function exist for each Lyapunov function. This is captured by the parameterization of the functions α_i, $i = 1,2,3,4$, and $\alpha_i(\cdot;x_s)$ denotes the ith class $\mathscr{K}$ function for the Lyapunov function with respect to the steady-state x_s.

For each $x_s \in \Gamma$, the stability region $\Omega_{\rho(x_s)}$ may be characterized for the closed-loop system of Eq. 3.1 with the Lyapunov-based controller $h(x;x_s)$. The symbol $\Omega_{\rho(x_s)}$ where $x_s \in \Gamma \subset \mathbb{R}^n$ is a fixed parameter denotes a level set of the Lyapunov function with respect to x_s, i.e., $\Omega_{\rho(x_s)} = \{x \in \mathbb{R}^n : V(x;x_s) \leq \rho(x_s)\}$ where $\rho(x_s)$ depends on x_s. The union of the stability regions is denoted as $\mathscr{X} = \bigcup_{x_s \in \Gamma} \Omega_{\rho(x_s)}$ and it is assumed to be a non-empty compact set.

3.5.2 The Union of the Stability Regions

A simple demonstration of the construction of the set $\mathscr{X}$ is provided to embellish the concept of the union set $\mathscr{X}$. The stability region of a closed-loop system under an explicit stabilizing control law may be estimated for a steady-state in Γ through the off-line computation described below. After the stability regions of sufficiently many steady-states in Γ are computed, the union of these sets may be described algebraically through various mathematical techniques, e.g., curve fitting and convex optimization techniques. The basic

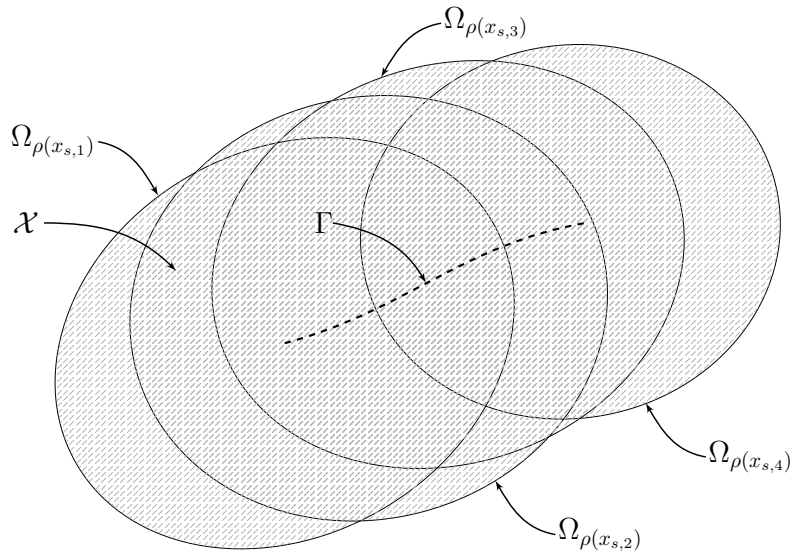

Figure 3.5: An illustration of the construction of the stability region $\mathscr{X}$. The shaded region corresponds to the set $\mathscr{X}$.

algorithm is

1. For $j = 1$ to J (if Γ consists of an infinite number of points, J is a sufficiently large positive integer).

   1.1 Select a steady-state, $x_{s,j}$, in the set Γ.

   1.2 Partition the state-space near $x_{s,j}$ into I discrete points (I is a sufficiently large positive integer).

   1.3 Initialize $\rho(x_{s,j}) := \infty$.

   1.4 For $i = 1$ to I:

      1.4.1 Compute $\dot{V}(x_i; x_{s,j})$ where x_i denotes the i discrete point from the partitioning of the state-space. If $\dot{V}(x_i; x_{s,j}) \geq 0$, go to Step 1.4.2. Else, go to Step 1.4.3.

      1.4.2 If $V(x_i; x_{s,j}) < \rho(x_{s,j})$, set $\rho(x_{s,j}) := V(x_i; x_{s,j})$. Go to Step 1.4.3.

1.4.3 If $i+1 \leq I$, go to Step 1.4.1 and $i \leftarrow i+1$. Else, go to Step 2.

2. Save $\rho(x_{s,j})$ (if necessary, reduce $\rho(x_{s,j})$ such that the set $\Omega_{\rho(x_{s,j})}$ only includes points where the time-derivative of the Lyapunov function is negative).

3. If $j+1 \leq J$, go to Step 1 and $j \leftarrow j+1$. Else, go to Step 4.

4. Approximate the union set with analytic algebraic expressions (constraints) using appropriate techniques.

If Γ consists of a finite number of points, then J could be taken as the number of points in Γ. If the number of points in Γ is large or infinite, J could be a sufficiently large integer. From a practical stand-point, these numbers need to be small enough such that this type of calculation may be implemented. Fig. 3.5 gives an illustration of the construction of $\mathscr{X}$ using this procedure. The following example provides a tractable illustration of the construction of $\mathscr{X}$ for a scalar system.

Example 3.2. Consider the nonlinear scalar system described by

$$\dot{x} = x - 2x^2 + xu \tag{3.70}$$

with admissible inputs in the set $\mathbb{U} = [-100, 100]$ and with the set of admissible operating steady-states defined as $\Gamma = \{x_s \in [-25, 25]\}$. The steady-states in Γ are open-loop unstable. For any $x_s \in \Gamma$, the system of Eq. 3.70 may be written in the following input-affine form:

$$\dot{\bar{x}} = f(\bar{x}) + g(\bar{x})\bar{u} \tag{3.71}$$

where $\bar{x} = x - x_s$ and $\bar{u} = u - u_s$. Consider a quadratic Lyapunov function of the form:

$$V(x; x_s) = \frac{1}{2}(x - x_s)^2 \tag{3.72}$$

for the closed system of Eq. 3.70 under the following Lyapunov-based feedback control law [175]:

$$\hat{h}(x;x_s) = \begin{cases} -\dfrac{L_f V + \sqrt{L_f V^2 + L_g V^4}}{L_g V} & \text{if } L_g V \neq 0 \\ 0 & \text{if } L_g V = 0 \end{cases} \tag{3.73}$$

for a $x_s \in \Gamma$ where $L_f V$ and $L_g V$ are the Lie derivatives of the function V with respect to f and g, respectively (these functions depend on x_s). To account for the bound on the available control energy, the controller is formulated as

$$h(x;x_s) = 100 \text{ sat}\left(\frac{\hat{h}(x;x_s)}{100}\right) \tag{3.74}$$

where sat$(\cdot)$ denotes the standard saturation function.

For this particular case, the stability region of the system of Eq. 3.70 with the stabilizing controller of Eq. 3.74 for the minimum and maximum steady-state in the set Γ are used to approximate the set $\mathscr{X}$. For the steady-state $x_{s,1} = -25$ with corresponding steady-state input $u_{s,1} = -51$, the largest level set of the Lyapunov function where the Lyapunov function is decreasing along the state trajectory with respect to the steady-state $x_{s,1}$ is $\Omega_{\rho(x_{s,1})} = \{x \in \mathbb{R} : V(x;-25) \leq 300.25\}$, i.e., $\rho(x_{s,1}) = 300.25$. For the steady-state $x_{s,2} = 25$ and $u_{s,2} = 49$, the level set is $\Omega_{\rho(x_{s,2})} = \{x \in \mathbb{R} : V(x,25) \leq 2775.49\}$, i.e., $\rho(x_{s,2}) = 2775.49$. Therefore, the union of the stability region is described as $\mathscr{X} = \{x \in [-49.5, 99.5]\}$.

3.5.3 Formulation of LEMPC with Time-Varying Economic Cost

The formulation of the LEMPC with the time-varying economic stage cost is given in this subsection. First, the overall methodology of employing the set $\mathscr{X}$ in the design of the LEMPC is described. As a consequence of the construction method used for $\mathscr{X}$, any state in $\mathscr{X}$ is in a stability region of at least one steady-state. This means that there exists

an input trajectory that satisfies the input constraint and that maintains operation in $\mathscr{X}$ is guaranteed because the input trajectory obtained from the Lyapunov-based controller with respect to the steady-state x_s such that the current state $x(t_k) \in \Omega_{\rho(x_s)}$ is a feasible input trajectory. The stability properties of $\mathscr{X}$ make it an attractive choice to use in the formulation of a LEMPC. Namely, use $\mathscr{X}$ to formulate a region constraint that is imposed in the optimization problem of EMPC to ensure that $\mathscr{X}$ is an invariant set.

In any practical setting, the closed-loop system is subjected to disturbances and uncertainties causing the closed-loop state trajectory to deviate from the predicted (open-loop) nominal trajectory. Enforcing that the predicted state to be in $\mathscr{X}$ is not sufficient for maintaining the closed-loop state trajectory in $\mathscr{X}$ because disturbances may force the state out of $\mathscr{X}$. To make $\mathscr{X}$ an invariant set, a subset of $\mathscr{X}$ is defined and is denoted as $\hat{\mathscr{X}}$. The set $\hat{\mathscr{X}}$ is designed such that any state starting in $\hat{\mathscr{X}}$, which may be forced outside of $\hat{\mathscr{X}}$ by the disturbances, will be maintained in $\mathscr{X}$ over the sampling period when the computed control action is such that the predicted state is maintained in $\hat{\mathscr{X}}$.

Any state $x(t_k) \in \mathscr{X} \setminus \hat{\mathscr{X}}$ where $x(t_k)$ denotes a measurement of the state at sampling time t_k may be forced back into the set $\hat{\mathscr{X}}$. This statement holds as a result of the method used to construct $\hat{\mathscr{X}}$ and $\mathscr{X}$. Specifically, a steady-state $\hat{x}_s \in \Gamma$ may be found such that $x(t_k) \in \Omega_{\rho(\hat{x}_s)}$. Then, a contractive Lyapunov-based constraint like that of Eq. 3.3f is imposed in the formulation of the LEMPC to ensure that the computed control action decreases the Lyapunov function by at least the rate given by the Lyapunov-based controller. This guarantees that the closed-loop state will converge to $\hat{\mathscr{X}}$ in finite-time. Here, $\hat{\mathscr{X}}$ and $\mathscr{X}$ are analogous to Ω_{ρ_e} and Ω_ρ in the LEMPC design of Eq. 3.3 with a time-invariant economic cost.

Given the overview and purposes of the sets $\mathscr{X}$ and $\hat{\mathscr{X}}$, a slight clarification must be made on the sets Γ, $\mathscr{X}$, and $\hat{\mathscr{X}}$. First, the set Γ is the set of points in state-space that satisfies the steady-state model equation for some $u_s \in U$, i.e., $f(x_s, u_s, 0) = 0$. Second, $\mathscr{X}$,

which is the union of the stability regions $\Omega_{\rho(x_s)}$ constructed for each steady-state in Γ, is assumed to be a non-empty, compact set. Third, the set $\hat{\mathscr{X}}$ is assumed to be a non-empty compact set with $\hat{\mathscr{X}} \subset \mathscr{X}$, and it is further clarified in Section 3.5.5.

Using the sets Γ, $\mathscr{X}$, and $\hat{\mathscr{X}}$, the LEMPC formulation with an explicitly time-varying cost is given by the following optimization problem:

$$\min_{u\in S(\Delta)} \int_{t_k}^{t_{k+N}} l_e(\tau,\tilde{x}(\tau),u(\tau))\, d\tau \tag{3.75a}$$

$$\text{s.t. } \dot{\tilde{x}}(t) = f(\tilde{x}(t),u(t),0) \tag{3.75b}$$

$$\tilde{x}(t_k) = x(t_k) \tag{3.75c}$$

$$u(t) \in U,\ \forall t \in [t_k,t_{k+N}) \tag{3.75d}$$

$$\tilde{x}(t) \in \hat{\mathscr{X}},\ \forall\, t \in [t_k,t_{k+N}) \text{ if } x(t_k) \in \hat{\mathscr{X}} \tag{3.75e}$$

$$\tilde{x}(t) \in \mathscr{X},\ \forall\, t \in [t_k,t_{k+N}) \text{ if } x(t_k) \in \mathscr{X} \setminus \hat{\mathscr{X}} \tag{3.75f}$$

$$\frac{\partial V(x(t_k);\hat{x}_s)}{\partial x} f(x(t_k),u(t_k),0) \leq \frac{\partial V(x(t_k);\hat{x}_s)}{\partial x} f(x(t_k),h(x(t_k);\hat{x}_s),0)$$
$$\text{if } x(t_k) \notin \hat{\mathscr{X}},\ x(t_k) \in \Omega_{\rho(\hat{x}_s)} \text{ with } \hat{x}_s \in \Gamma \tag{3.75g}$$

where all of the notation used is similar to that used in the LEMPC formulation of Eq. 3.3. The optimal solution of this optimization problem is denoted as $u^*(t|t_k)$ and it is defined for $t \in [t_k,t_{k+N})$. The control action computed for the first sampling period of the prediction horizon is denoted as $u^*(t_k|t_k)$. In the optimization problem of Eq. 3.75, Eq. 3.75a defines the time-dependent economic cost functional to be minimized over the prediction horizon. The constraint of Eq. 3.75b is the nominal model of the system of Eq. 3.1 which is used to predict the evolution of the system with input trajectory $u(t)$ computed by the LEMPC. The dynamic model is initialized with a measurement of the current state (Eq. 3.75c). The constraint of Eq. 3.75d restricts the input trajectory take values within the admissible input set.

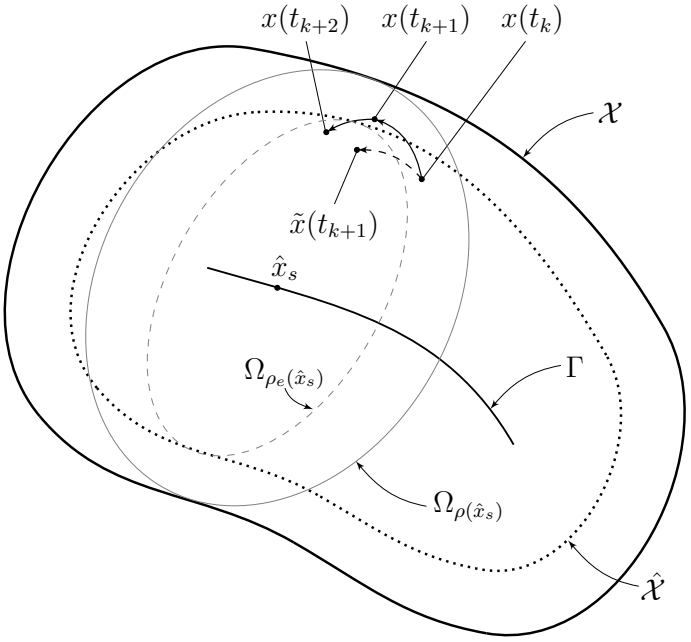

Figure 3.6: This illustration gives the state evolution over two sampling periods. Over the first sampling period, the LEMPC, operating in mode 1, computes a control action that maintains the predicted state $\tilde{x}(t_{k+1})$ inside $\hat{\mathcal{X}}$. However, the closed-loop state at the next sampling time $x(t_{k+1})$ is driven outside of $\hat{\mathcal{X}}$ by disturbances. The LEMPC, operating in mode 2, ensures that the computed control action decreases the Lyapunov function based on the steady-state $\hat{x}_s$ over the next sampling period to force the state back into $\hat{\mathcal{X}}$.

Similar to the LEMPC design of Eq. 3.3, the LEMPC of Eq. 3.75 is a dual-mode controller. The constraint of Eq. 3.75e defines mode 1 operation of the LEMPC and is active when the state at the current sampling time $x(t_k) \in \hat{\mathscr{X}}$. It enforces that the predicted state trajectory be maintained in $\hat{\mathscr{X}}$. The constraint of Eq. 3.75g defines mode 2 operation of the LEMPC and is active when the state is outside $\hat{\mathscr{X}}$. It is used to force the state back into the $\hat{\mathscr{X}}$ which is guaranteed for any $x(t_k) \in \mathscr{X}$. The constraint of Eq. 3.75f is active when $x(t_k) \in \mathscr{X} \setminus \hat{\mathscr{X}}$ and ensures the predicted state be contained in the set $\mathscr{X}$. Although Eq. 3.75f is not needed for stability, it is used to ensure that the LEMPC optimizes the input trajectory with knowledge that the state must be contained in $\mathscr{X}$, and potentially improves the closed-loop economic performance when the LEMPC is operating under mode 2 operation compared to not imposing such a constraint. Fig. 3.6 illustrates the sets and different operation modes of the closed-loop system under the LEMPC of Eq. 3.75.

3.5.4 Implementation Strategy

The LEMPC of Eq. 3.75 is implemented in a receding horizon fashion. The optimization problem is repeatedly solved every sampling time after receiving state feedback from the system. The implementation strategy may be summarized as follows:

1. At sampling time t_k, the LEMPC receives a state measurement $x(t_k)$ from the sensors.
2. If $x(t_k) \in \hat{\mathscr{X}}$, go to Step 2.1. Else, go to Step 2.2.
    - 2.1 LEMPC operates in mode 1: the constraint of Eq. 3.75e is active and the constraints of Eqs. 3.75f-3.75g are inactive, go to Step 3.
    - 2.2 Find $\hat{x}_s \in \Gamma$ such that $x(t_k) \in \Omega_{\rho(\hat{x}_s)}$, go to Step 2.3.
    - 2.3 LEMPC operates in mode 2: the constraint of Eq. 3.75e is inactive and the constraints of Eqs. 3.75f-3.75g are active, go to Step 3.

3. The LEMPC computes the optimal input trajectory $u^*(t|t_k)$ for $t \in [t_k, t_{k+N})$, go to Step 4.

4. The LEMPC sends the control action, $u^*(t_k|t_k)$, computed for the first sampling period of the prediction horizon to the control actuators to apply to the system in a sample-and-hold fashion from t_k to t_{k+1}. Go to Step 5.

5. Set $k \leftarrow k+1$. Go to Step 1.

3.5.5 Stability Analysis

In this subsection, Theorem 3.4 provides sufficient conditions for closed-loop stability, in the sense of boundedness of the closed-loop system state inside the set $\mathscr{X}$, under the LEMPC of Eq. 3.75 for any initial condition $x(0) \in \mathscr{X}$. It follows the ideas of the analysis of Theorem 3.1 of Section 3.3. The assumption on the set $\hat{\mathscr{X}}$ that is needed to ensure closed-loop stability is given below.

Assumption 3.2. *Let $\hat{\mathscr{X}} \subset \mathscr{X}$ be a compact set such that if $x(0) \in \hat{\mathscr{X}}$ and the constant control $\hat{u} \in \mathbb{U}$ is such that $\tilde{x}(t) \in \hat{\mathscr{X}}$ for all $t \in [0, \Delta]$ where $\tilde{x}(t)$ is the solution to*

$$\dot{\tilde{x}}(t) = f(\tilde{x}(t), \hat{u}, 0) \tag{3.76}$$

for $t \in [0, \Delta]$ and $\tilde{x}(0) = x(0)$, then $x(\Delta) \in \mathscr{X}$ where $x(\Delta)$ denotes the closed-loop state of Eq. 3.3 under the constant control $\hat{u}$.

Assumption 3.2 is satisfied for the case that instead of using the mode 1 constraint of Eq. 3.75e, the constraint $\tilde{x}(t) \in \Omega_{\rho_e(x_s)}$ for $t \in [t_k, t_{k+N})$ where $\Omega_{\rho_e(x_s)}$ is designed according to a similar condition as in Eq. 3.21 for some $x_s \in \Gamma$ such that $x(t_k) \in \Omega_{\rho_e(x_s)}$. For this case, $\hat{\mathscr{X}}$ may be constructed by taking the union of sets $\Omega_{\rho_e(x_s)}$ for all $x_s \in \Gamma$ where $\Omega_{\rho_e(x_s)}$ is sim-

ilar to the set Ω_{ρ_e} (for each $x_s \in \Gamma$) in the LEMPC of Eq. 3.3. Nevertheless, Assumption 3.2 is needed to cover the more general case with the mode 1 constraint of Eq. 3.75e.

To avoid introducing convoluted notation, the sufficient conditions of the Theorem are stated as similar conditions as Eqs. 3.22-3.23 must hold for each $x_s \in \Gamma$. This means that there exists positive constants: ρ, $\rho_{\min}$, ρ_s, L'_x, L'_w, M, and ε_w that satisfy similar conditions for each $x_s \in \Gamma$. Moreover, all of these parameters depend on x_s.

Theorem 3.4. *Consider the system of Eq. 3.1 in closed-loop under the LEMPC design of Eq. 5 based on the set of controllers that satisfy the conditions of Eq. 3.69 for each* $x_s \in \Gamma$. *Let* $\varepsilon_w(x_s) > 0$, $\Delta > 0$, $\rho(x_s) > \rho_e(x_s) \geq \rho_{\min}(x_s) > \rho_s(x_s) > 0$ *for all* $x_s \in \Gamma$ *satisfy a similar condition as Eqs. 3.22 for each* $x_s \in \Gamma$ *and let* $\mathscr{X} = \cup_{x_s \in \Gamma} \Omega_{\rho(x_s)}$ *be a non-empty compact set and* $\hat{\mathscr{X}}$ *satisfy Assumption 3.2. If* $x(0) \in \mathscr{X}$ *and* $N \geq 1$, *then the state* $x(t)$ *of the closed-loop system is always bounded in* $\mathscr{X}$ *for all* $t \geq 0$.

Proof. The proof of Theorem 3.4 consists of the following parts: first, the feasibility of the optimization problem of Eq. 3.75 is proven for any state $x(t_k) \in \mathscr{X}$. Second, boundedness of the closed-loop state trajectory $x(t) \in \mathscr{X}$ for all $t \geq 0$ is proven for any initial state starting in $\mathscr{X}$.

Part 1: Owing to the construction of $\mathscr{X}$, any state $x(t_k) \in \mathscr{X}$ is in the stability region $\Omega_{\rho(x_s)}$ of the Lyapunov-based controller designed for some steady-state $x_s \in \Gamma$. This implies that there exists an input trajectory that is a feasible solution because the input trajectory obtained from the Lyapunov-based controller is a feasible solution to the optimization of Eq. 3.75 as it satisfies the constraints (refer to Theorem 3.1, Part 1 on how this input trajectory is obtained). The latter claim is guaranteed by the closed-loop stability properties of the Lyapunov-based controller ($h(\cdot; x_s)$).

Part 2: If $x(t_k) \in \mathscr{X} \setminus \hat{\mathscr{X}}$, then the LEMPC of Eq. 3.75 operates in mode 2. Since $x(t_k) \in \mathscr{X}$, a steady-state $\hat{x}_s \in \Gamma$ may be found such that the current state $x(t_k) \in \Omega_{\rho(\hat{x}_s)}$.

Utilizing the Lyapunov-based controller $h(\cdot;\hat{x}_s)$, the LEMPC computes a control action that satisfies the constraint of Eq. 3.75g:

$$\frac{\partial V(x(t_k);\hat{x}_s)}{\partial x} f(x(t_k), u^*(t_k|t_k), 0) \leq \frac{\partial V(x(t_k);\hat{x}_s)}{\partial x} f(x(t_k), h(x(t_k);\hat{x}_s), 0) \tag{3.77}$$

for some $\hat{x}_s \in \Gamma$ where $u^*(t_k|t_k)$ is the optimal control action computed by the LEMPC to be applied in a sample-and-hold fashion to the system of Eq. 3.1 for $t \in [t_k, t_{k+1})$. From Eq. 3.69b, the term in the right-hand side of the inequality of Eq. 3.77 may be upper bounded by a class $\mathscr{K}$ function as follows:

$$\frac{\partial V(x(t_k),\hat{x}_s)}{\partial x} f(x(t_k), u^*(t_k), 0) \leq -\alpha_3(|x(t_k) - \hat{x}_s|;\hat{x}_s) \tag{3.78}$$

for all $x(t_k) \in \mathscr{X}$ and for some $\hat{x}_s \in \Gamma$. Following similar steps as that used in Theorem 3.4, Part 2, one may show that the Lyapunov function value, i.e., the Lyapunov function for the steady-state $\hat{x}_s$, will decay over the sampling period when a similar condition to Eq. 3.22 is satisfied for each $x_s \in \Gamma$.

If $x(t_k) \in \mathscr{X}^{\hat{}}$, then $x(t_{k+1}) \in \mathscr{X}$ owing to the construction of $\mathscr{X}^{\hat{}}$, i.e., if Assumption 3.2 is satisfied. If $x(t_k) \in \mathscr{X} \setminus \mathscr{X}^{\hat{}}$, then $x(t_{k+1}) \in \mathscr{X}$ because the state is forced to a smaller level set of the Lyapunov function with respect to the steady-state $\hat{x}_s \in \Gamma$ over the sampling period. Both of these results together imply that $x(t_{k+1}) \in \mathscr{X}$ for all $x(t_k)$ under the LEMPC of Eq. 3.75. Using this result recursively, the closed-loop state is always bounded in $\mathscr{X}$ when the initial state is in $\mathscr{X}$. □

Remark 3.3. The LEMPC of Eq. 3.75 does not have a switching time like the LEMPC of Eq. 3.3 whereby the mode 2 constraint is exclusively imposed after the switching time to enforce the closed-loop state to a specific steady-state. To ensure there exists a feasible path from any state in $\mathscr{X}$ to the desired operating steady-state more conditions are needed. The

Table 3.3: CSTR process parameters.

Feedstock volumetric flow rate	$F = 5.0\,\mathrm{m}^3\,\mathrm{h}^{-1}$
Feedstock temperature	$T_0 = 300\,\mathrm{K}$
Reactor volume	$V_R = 5.0\,\mathrm{m}^3$
Pre-exponential factor for reaction 1	$k_{01} = 6.0 \times 10^5\,\mathrm{h}^{-1}$
Pre-exponential factor for reaction 2	$k_{02} = 6.0 \times 10^4\,\mathrm{h}^{-1}$
Pre-exponential factor for reaction 3	$k_{03} = 6.0 \times 10^4\,\mathrm{h}^{-1}$
Reaction enthalpy change for reaction 1	$\Delta H_1 = -5.0 \times 10^4\,\mathrm{kJ\,kmol}^{-1}$
Reaction enthalpy change for reaction 2	$\Delta H_2 = -5.2 \times 10^4\,\mathrm{kJ\,kmol}^{-1}$
Reaction enthalpy change for reaction 3	$\Delta H_3 = -5.4 \times 10^4\,\mathrm{kJ\,kmol}^{-1}$
Activation energy for reaction 1	$E_1 = 5.0 \times 10^4\,\mathrm{kJ\,kmol}^{-1}$
Activation energy for reaction 2	$E_2 = 7.53 \times 10^4\,\mathrm{kJ\,kmol}^{-1}$
Activation energy for reaction 3	$E_3 = 7.53 \times 10^4\,\mathrm{kJ\,kmol}^{-1}$
Heat capacity	$C_p = 0.231\,\mathrm{kg\,m}^{-3}$
Density	$\rho_L = 1000\,\mathrm{kJ\,kg}^{-1}\,\mathrm{K}^{-1}$
Gas constant	$R = 8.314\,\mathrm{kJ\,kmol}^{-1}\,\mathrm{K}^{-1}$

interested reader may refer to [109] that provides some conditions that accomplish such a goal. Additionally, no guarantees are made that the closed-loop state will converge to $\mathscr{X}^{\hat{}}$ when the state is in $\mathscr{X} \setminus \mathscr{X}^{\hat{}}$ owing to the fact that the mode 2 constraint could be formulated with respect to a different steady-state at each sampling time. However, enforcing convergence to $\mathscr{X}^{\hat{}}$ may be readily accomplished through implementation by enforcing a mode 2 constraint formulated with respect to the same steady-state at each sampling time until the state converges to $\mathscr{X}^{\hat{}}$.

3.5.6 Application to a Chemical Process Example

Consider a non-isothermal continuous stirred-tank reactor (CSTR) where three parallel reactions take place. The reactions are elementary irreversible exothermic reactions of the form: $A \to B$, $A \to C$, and $A \to D$. The desired product is B; while, C and D are byproducts. The feed of the reactor consists of the reactant A in an inert solvent and does not contain any of the products. Using first principles and standard modeling assumptions, a nonlinear

dynamic model of the process is obtained:

$$\frac{dC_A}{dt} = \frac{F}{V_R}(C_{A0} - C_A) - \sum_{i=1}^{3} k_{0,i} e^{-E_i/RT} C_A \tag{3.79a}$$

$$\frac{dT}{dt} = \frac{F}{V_R}(T_0 - T) - \frac{1}{\rho_L C_p} \sum_{i=1}^{3} \Delta H_i k_{0,i} e^{-E_i/RT} C_A + \frac{Q}{\rho_L C_p V_R} \tag{3.79b}$$

where C_A is the concentration of the reactant A, T is the temperature of the reactor, Q is the rate of heat supplied or removed from the reactor, C_{A0} and T_0 are the reactor feed reactant concentration and temperature, respectively, F is a constant volumetric flow rate through the reactor, V_R is the constant liquid hold-up in the reactor, ΔH_i, $k_{0,i}$, and E_i, $i = 1,2,3$ denote the enthalpy changes, pre-exponential constants and activation energies of the three reactions, respectively, and C_p and ρ_L denote the heat capacity and the density of the fluid in the reactor. The process parameters are given in Table 3.3. The CSTR has two manipulated inputs: the inlet concentration C_{A0} with available control energy $0.5\,\mathrm{kmol\,m^{-3}} \leq C_{A0} \leq 7.5\,\mathrm{kmol\,m^{-3}}$ and the heat rate to/from the vessel Q with available control energy $-1.0 \times 10^5\,\mathrm{kJ\,h^{-1}} \leq Q \leq 1.0 \times 10^5\,\mathrm{kJ\,h^{-1}}$. The state vector is $x^T = [C_A\ T]$ and the input vector is $u^T = [C_{A0}\ Q]$.

Stability Region Construction

Supplying or removing significant amount of thermal energy to/from the reactor (nonzero Q) is considered to be undesirable from an economic perspective. Therefore, the set $\mathscr{X}$ is constructed considering steady-states with a steady-state reactant inlet concentration of $C_{A0s} \in [2.0, 6.0]\,\mathrm{kmol\,m^{-3}}$ and no heat rate supplied/removed from the reactor, i.e., $Q_s = 0.0\,\mathrm{kJ\,h^{-1}}$. The corresponding steady-states in the desired operating range form a set denoted as Γ of admissible operating steady-states. Several of these steady-states have been verified to be open-loop unstable, i.e., the eigenvalues of the linearization around the

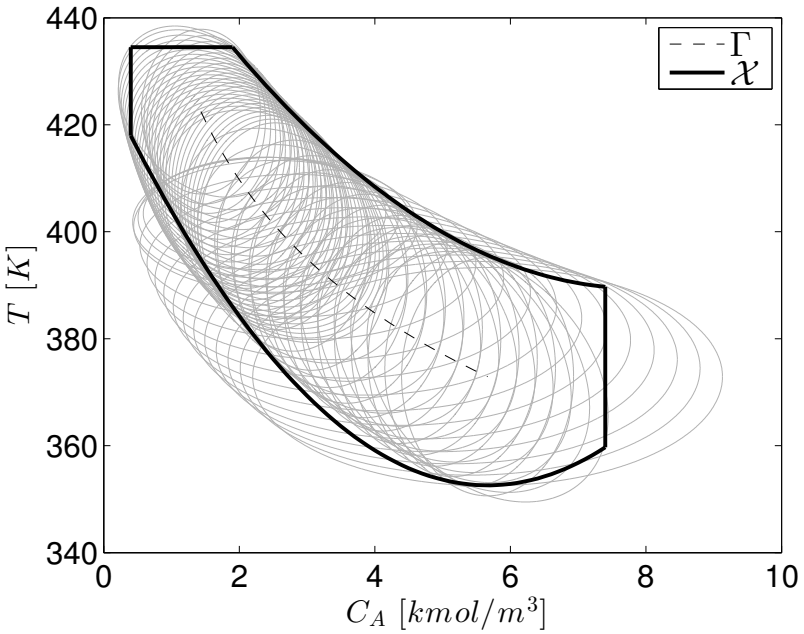

Figure 3.7: The construction of the set $\mathscr{X}$ for the CSTR of Eq. 3.79.

steady-states corresponding to the minimum and maximum steady-state inlet concentrations are $\lambda_{1,\min} = -1.00$, $\lambda_{2,\min} = 2.73$ and $\lambda_{1,\max} = -1.00$, $\lambda_{2,\max} = 2.10$, respectively. The set Γ covers approximately a temperature range of 50 K.

A set of two proportional controllers with saturation to account for the input constraints is used in the design of the Lyapunov-based controller:

$$h(x;x_s) = \begin{bmatrix} 3.5 \text{ sat}\left(\dfrac{K_1(x_{s,1}-x_1)+u_{1,s}-4.0}{3.5}\right)+4.0 \\ 10^5 \text{ sat}\left(\dfrac{K_2(x_{s,2}-x_2)+u_{2,s}}{10^5}\right) \end{bmatrix} \tag{3.80}$$

where $K_1 = 10$ and $K_2 = 8000$ are the gains of each proportional controller. The proportional controller gains have been tuned to give the largest estimate of the stability region for a given steady-state. A quadratic Lyapunov function of the form:

$$V(x;x_s) = (x-x_s)^T P(x-x_s) \tag{3.81}$$

where P is a positive definite matrix is used to estimate the stability regions of many steady-states in the set Γ, i.e., the stability region for a given steady-state in Γ is taken to be a level set of the Lyapunov function where the Lyapunov function is decreasing along the state trajectory. To estimate $\mathscr{X}$, the procedure outlined in Section 3.5.2 is employed. To obtain the largest estimate of the region $\mathscr{X}$, several P matrices were used. The results of this procedure are shown in Fig. 3.7. The union of these regions $\mathscr{X}$ was approximated with two quadratic polynomial inequalities and three linear state inequalities given by:

$$\begin{gathered} 1.26x_1^2 - 19.84x_1 + 467.66 - x_2 \geq 0 \\ 2.36x_1^2 - 26.72x_1 + 428.26 - x_2 \leq 0 \\ 0.4 \leq x_1 \leq 7.4 \\ x_2 \leq 434.5 \end{gathered} \tag{3.82}$$

which will be used in the formulation of the LEMPC to ensure that the state trajectories are maintained inside $\mathscr{X}$ (note that x_2 is lower bounded by the second inequality).

Closed-loop Simulation Results

The control objective of this chemical process example is to operate the CSTR in an economically optimal manner while accounting for changing economic factors and maintaining the system operation inside a bounded set. For this chemical process example, the economic measure being considered is

$$l_e(t,x,u) = A_1(t)u_2^2 + A_2(t)u_1 - A_3 r_1(x) + A_4(x_2 - 395)^2 \tag{3.83}$$

where $r_1(x)$ is the reaction rate of the first reaction that produces the desired product:

$$r_1(x) = k_{01} e^{-E_1/Rx_2} x_1 \ . \tag{3.84}$$

The economic measure of Eq. 3.83 penalizes energy usage/removal, penalizes reactant material consumption, credits the production rate of the desired product, and penalizes the deviation of the operating temperature from the median operating temperature. The fourth term of the economic cost is used to prevent the LEMPC from operating the CSTR at the boundary of the allowable operating range for long periods of time which is considered undesirable from a practical perspective. In this fashion, the economic cost consists of terms that are associated with the operating cost/profit (economic terms) as well as terms that ensure that the LEMPC operates the CSTR in a practical and safe fashion.

For this study, the weights A_1 and A_2 are considered to vary with time; while, $A_3 = 278$ and $A_4 = 0.4$ are constants over the 5.0 h simulated operation of the CSTR under the LEMPC. The weight A_1 is equal to 4.0×10^{-6} for $t = 0.0$ h to 4.0 h and 5.0×10^{-6} for 4.0 h to 5.0 h, and the time-dependent weight A_2 is given by the following piecewise constant relationship:

$$A_2(t) = \begin{cases} 333 & 0.0\,\text{h} \leq t < 1.0\,\text{h} \\ 167 & 1.0\,\text{h} \leq t < 2.0\,\text{h} \\ 83 & 2.0\,\text{h} \leq t < 3.0\,\text{h} \\ 17 & 3.0\,\text{h} \leq t < 4.0\,\text{h} \\ 167 & 4.0\,\text{h} \leq t < 5.0\,\text{h} \end{cases} \tag{3.85}$$

Since the economic cost is considered to account for more than just the operating cost/profit of the CSTR, the weights may be considered to account for more than the price of a particular resource. For instance, the variation of the weight A_2 may be caused by supply

and/or demand changes of the reactant A. While these weights may come from a higher level information technology system, careful tuning of these weights is critical to achieve both practical operation with LEMPC and economically optimal (with respect to the actual operating cost) operation. For this particular study, the economic cost has been chosen to vary on a time-scale comparable to the one of the process dynamics.

In the first set of simulations, nominal operation ($w \equiv 0$) is considered to understand the operation of the CSTR under the LEMPC operating in mode 1 only. The formulation of the LEMPC with explicitly time-varying cost function used to accomplish the desired control objective is

$$\begin{aligned}
\min_{u\in S(\Delta)} \quad & \int_{t_k}^{t_{k+N}} l_e(\tau,\tilde{x}(\tau),u(\tau))\, d\tau \\
\text{s.t.} \quad & \dot{\tilde{x}}(t) = f(\tilde{x}(t),u(t),0) \\
& \tilde{x}(t_k) = x(t_k) \\
& u(t) \in U,\ \forall\, t \in [t_k,t_{k+N}) \\
& 1.26\tilde{x}_1^2(t) - 19.84\tilde{x}_1(t) + 467.66 - \tilde{x}_2(t) \geq 0,\ \forall\, t \in [t_k,t_{k+N}) \\
& 2.36\tilde{x}_1^2(t) - 26.72\tilde{x}_1(t) + 428.26 - \tilde{x}_2(t) \leq 0,\ \forall\, t \in [t_k,t_{k+N}) \\
& 0.4 \leq \tilde{x}_1(t) \leq 7.4,\ \forall\, t \in [t_k,t_{k+N}) \\
& \tilde{x}_2(t) \leq 434.5,\ \forall\, t \in [t_k,t_{k+N})
\end{aligned} \tag{3.86}$$

where the economic measure l_e is given in Eq. 3.83. Since no disturbances or uncertainties are present, the set $\hat{\mathscr{X}}$ is taken to be $\mathscr{X}$ ($\hat{\mathscr{X}} = \mathscr{X}$). The sampling period and the prediction horizon of the LEMPC is $\Delta = 0.1\,\text{h}$ and $N = 10$, respectively. These parameters have been chosen through extensive simulations such that the total prediction horizon is sufficiently long to yield good economic performance of the closed-loop system. To solve the LEMPC optimization problem at each sampling period, the open-source interior point

solver Ipopt [187] was used. A fourth-order Runge-Kutta method with integration step of 5.0×10^{-4} h was used to numerically solve the nonlinear ODEs of Eq. 3.79. To assess the total economic performance of each simulation, the total economic measure over the simulated operation of the CSTR is defined as

$$\sum_{j=0}^{M-1} \left[A_1(t_j) u_2^2(t_j) + A_2(t_j) u_1(t_j) - A_3 r_1(x(t_j)) + A_4 (x_2(t_j) - 395)^2 \right] \tag{3.87}$$

where M is the number of integration steps over the entire simulated time t_f and t_j denotes an integration time step.

Since the exact future values of the cost weights may not be known exactly in a practical setting, two cases were simulated: (1) the LEMPC of Eq. 3.86 is formulated with a perfect forecast of time-varying economic weights and (2) the LEMPC of Eq. 3.86 is formulated with constant A_1 and A_2 (no forecasting). The two cases are denoted as LEMPC-1 and LEMPC-2, respectively. For LEMPC-2, the previously obtained weights A_1 and A_2 are used in the optimization problem until the LEMPC receives new weight values which are obtained at the time instance in which the weights change.

The CSTR is initialized at the initial condition of $C_A(0) = 2.0\,\text{kmol}\,\text{m}^{-3}$ and $T(0) = 410.0\,\text{K}$. The results of two simulations are shown in Figs. 3.8-3.9 under LEMPC-1 and LEMPC-2, respectively. Over the course of both of these simulations, the LEMPC schemes operate the CSTR in a time-varying (transient) fashion. If the economic weights become fixed or if a significant time-scale separation between economic cost change and the process dynamics existed, steady-state operation would become optimal for this particular economic cost and nonlinear model. Also, the LEMPC in this example is not formulated with any periodic, average, or integral input constraints, and is not formulated with any stabilizing constraints to enforce convergence to the economically optimal steady-state. Therefore, the reason for the time-varying operation is due to the economic cost changing

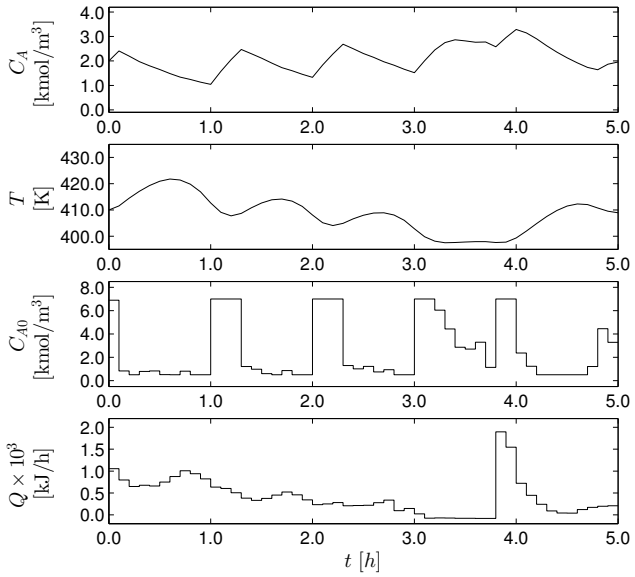

Figure 3.8: The states and inputs of the nominally operated CSTR under LEMPC-1 (mode 1 operation only) initialized at $C_A(0) = 2.0\,\text{kmol}\,\text{m}^{-3}$ and $T(0) = 410.0\,\text{K}$.

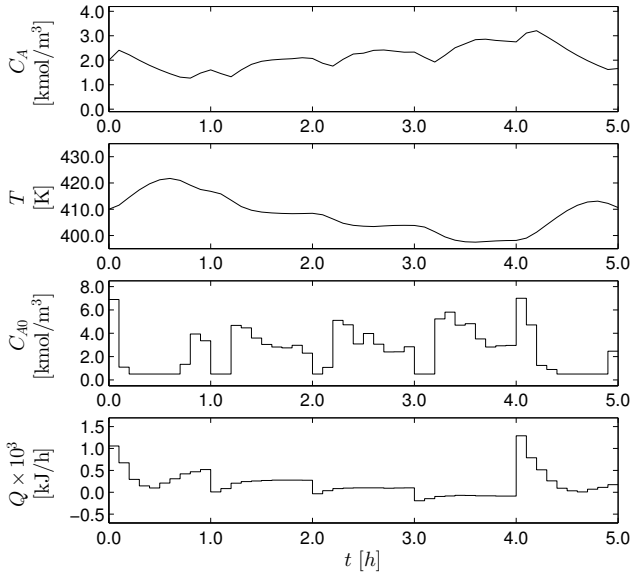

Figure 3.9: The states and inputs of the nominally operated CSTR under LEMPC-2 (mode 1 operation only) initialized at $C_A(0) = 2.0\,\text{kmol}\,\text{m}^{-3}$ and $T(0) = 410.0\,\text{K}$.

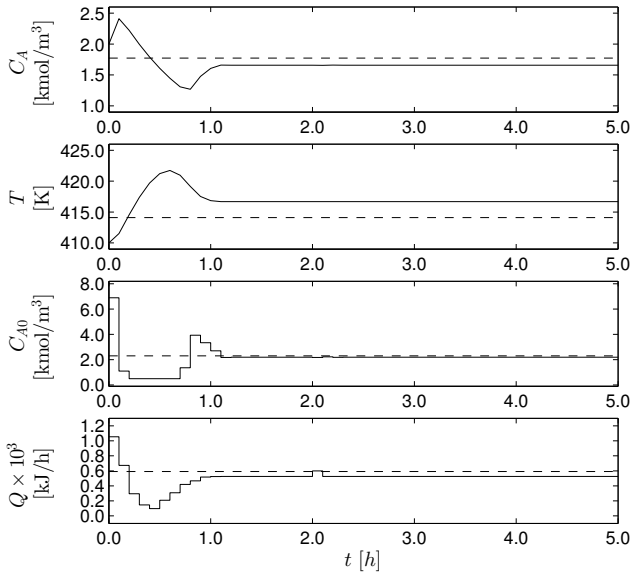

Figure 3.10: The states and inputs of the CSTR under the LEMPC of Eq. 3.86 (mode 1 operation only) when the economic cost weights are constant with time (solid line) with the economically optimal steady-state (dashed line).

with time on a time-scale comparable to the process dynamics. To demonstrate this point, Fig. 3.10 shows the state and input trajectories under LEMPC of Eq. 3.86 (mode 1 operation of the controller only) where the economic cost weights are constant with time. Recalling the LEMPC does not have any constraints that enforce convergence to the steady-state, the CSTR under the LEMPC with a prediction horizon of $N = 10$ settles on an offsetting steady-state from the economically optimal steady-state, i.e., the steady-state in Γ that optimizes the economic cost.

The total economic cost of the CSTR under LEMPC-1 is 2.37×10^4; while, the economic cost of the CSTR under LEMPC-2 is 2.91×10^4. The key factor that contributes to the performance degradation of the second simulation (as depicted in Figs. 3.8-3.9) may be observed in the input trajectories that the two LEMPC schemes compute. For the LEMPC-1 simulation, the LEMPC knows that the cost of the reactant material decreases at the beginning of each of the first four hours of operation so it waits to utilize this resource until the

Table 3.4: The optimal steady-state variation with respect to the time-varying economic weights.

t	$C_{A,s}^*$	T_s^*	$C_{A0,s}^*$	Q_s^*
$0.0\,\text{h} \leq t < 1.0\,\text{h}$	1.77	414.1	2.30	591.5
$1.0\,\text{h} \leq t < 2.0\,\text{h}$	2.12	407.5	2.61	300.9
$2.0\,\text{h} \leq t < 3.0\,\text{h}$	2.40	402.9	2.87	151.2
$3.0\,\text{h} \leq t < 4.0\,\text{h}$	2.75	398.1	3.20	-80.0
$4.0\,\text{h} \leq t < 5.0\,\text{h}$	2.12	407.5	2.61	240.6

beginning of each of these hours when the price is less than in the previous hour. For the LEMPC-2 simulation, the LEMPC uses the minimum amount of reactant material at the beginning of each of these four hours. Also, the cost of the thermal energy Q increases over the last hour of the simulated operation. In the first case, the LEMPC utilizes the thermal energy before the price increases to increase the reactor temperature, and then, uses less energy thereafter. In the second case, the LEMPC supplies heat to the reactor when the cost of thermal energy has already increased. Comparing the evolution of the states in both cases, the regions of operation in state-space between the two cases are similar.

To assess the economic performance of the CSTR under the LEMPC, a comparison between the CSTR under the LEMPC and under a conventional approach to optimization and control, i.e., steady-state optimization with tracking MPC, was carried out. The CSTR is simulated under a Lyapunov-based MPC (LMPC), formulated with a quadratic cost, where the LMPC works to drive the system to the economically optimal steady-state which is the minimizer of

$$\begin{aligned} \min_{(x_s,u_s)} \quad & l_e(t,x_s,u_s) \\ \text{s.t.} \quad & f(x_s,u_s,0)=0 \\ & u_s \in U, x_s \in \Gamma \end{aligned} \tag{3.88}$$

for a fixed t. The optimal steady-state at a given time t is denoted as $x_s^*(t)$ and the optimal

steady-state with time for the economic weights is given in Table 3.4.

The formulation of LMPC is as follows:

$$\begin{aligned}
\min_{u\in S(\Delta)} \quad & \int_{t_k}^{t_{k+N}} \left(|\tilde{x}(\tau) - x_s^*(\tau)|_{Q_c} + |u(\tau) - u_s^*(\tau)|_{R_c} \right) d\tau \\
\text{s.t.} \quad & \dot{\tilde{x}}(t) = f(\tilde{x}(t), u(t), 0) \\
& \tilde{x}(t_k) = x(t_k) \\
& u(t) \in U, \forall t \in [t_k, t_{k+N}) \\
& \frac{\partial V(x(t_k); x_s^*(t_k))}{\partial x} f(x(t_k), u(t_k), 0) \\
& \quad \leq \frac{\partial V(x(t_k); x_s^*(t_k))}{\partial x} f(x(t_k), h(x(t_k); x_s^*(t_k)), 0)
\end{aligned} \tag{3.89}$$

where the cost function is a quadratic cost function that penalizes the deviation of states and inputs from the optimal (time-varying) steady-state. The sampling period and prediction horizon of the LMPC are chosen to be the same as the ones of the LEMPC. The weighting matrices are $Q_c = \text{diag}([2788.0, 0.6])$ and $R_c = \text{diag}([27.8, 5.0 \times 10^{-7}])$. A quadratic Lyapunov function of the form given in Eq. 3.81 with a positive definite matrix $P = \text{diag}([280.0, 9.0])$ is considered. The Lyapunov-based controller used in the formulation of the Lyapunov-based constraint is a set of proportional controllers (P-controllers) like that of Eq. 3.80 with gains $K_1 = 1$ and $K_2 = 6000$. The P-controllers have been tuned less aggressively compared to the P-controllers used in the construction of the set $\mathscr{X}$ to allow the LMPC more freedom in the optimization of the control action.

The CSTR was initialized at several states in state-space and was simulated with three control strategies: (1) LEMPC-1, (2) LEMPC-2, and (3) LMPC. The total economic cost of each simulation is given in Table 3.5. The operating trajectories of a simulation under LMPC are also given in Fig. 3.11 to demonstrate the differences in achievable trajectories with the conventional MPC formulation working to track the economically optimal steady-

Table 3.5: The total economic cost of the closed-loop reactor over several simulations with different initial states. The performance improvement is relative to the economic performance under LMPC.

Initial State		Total Economic Cost ($\times 10^5$) and Performance Improvement				
$x_1(0)$	$x_2(0)$	LMPC	LEMPC-1	Improvement	LEMPC-2	Improvement
2.0	410.0	0.908	0.237	73.9%	0.291	68.0%
2.0	425.0	2.325	0.456	80.4%	0.507	78.2%
4.0	370.0	4.274	1.234	71.1%	1.075	74.8%
4.0	395.0	2.744	0.152	94.4%	0.192	93.0%
5.0	370.0	4.164	0.634	84.8%	0.643	84.6%
6.0	360.0	5.370	1.375	74.4%	1.225	77.2%

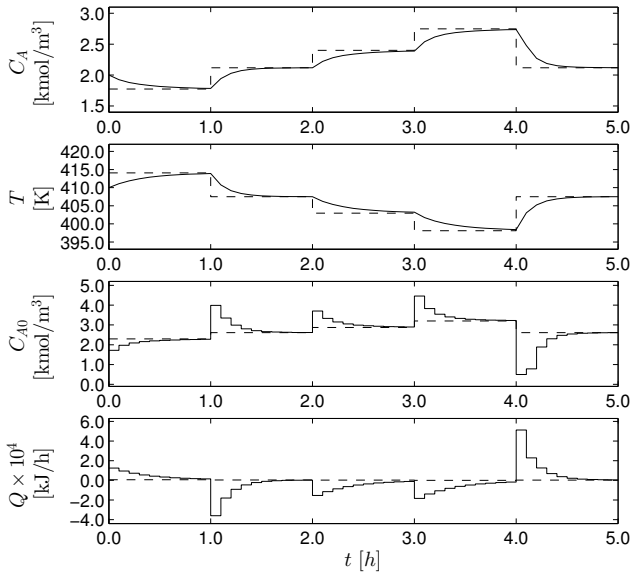

Figure 3.11: The states and inputs of the CSTR under the LMPC of Eq. 3.89 used to track the economically optimal steady-state (dashed line).

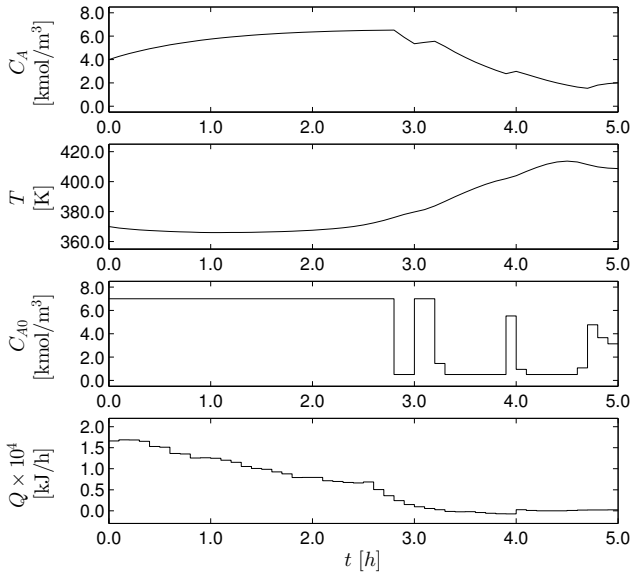

Figure 3.12: The states and inputs of the nominally operated CSTR under LEMPC-1 initialized at $C_A(0) = 4.0\,\text{kmol}\,\text{m}^{-3}$ and $T(0) = 370.0\,\text{K}$.

state. Clearly, the operating trajectories of the EMPC cannot be obtained by a tracking MPC, regardless of the tuning of the weighting matrices. From the results of Table 3.5, the economic performance of the system under both of the LEMPC schemes is better than the performance under the tracking LMPC.

For two of the initial conditions, the economic performance was better with LEMPC-2 compared to LEMPC-1 (Table 3.5). The closed-loop evolution of the CSTR with the two LEMPC schemes for one of these simulations is shown in Fig. 3.12-3.13. This is a result of not having a sufficiently long prediction horizon for these two initial conditions. More specifically, this behavior is caused by initializing the CSTR far away from the economically optimal region to operate the process. For this prediction horizon ($N = 10$), the LEMPC cannot simulate enough of the future evolution of the process to recognize that there is an economically better region to operate the process. As a result, the state is maintained away from this optimal region at the beginning of both simulations. For the

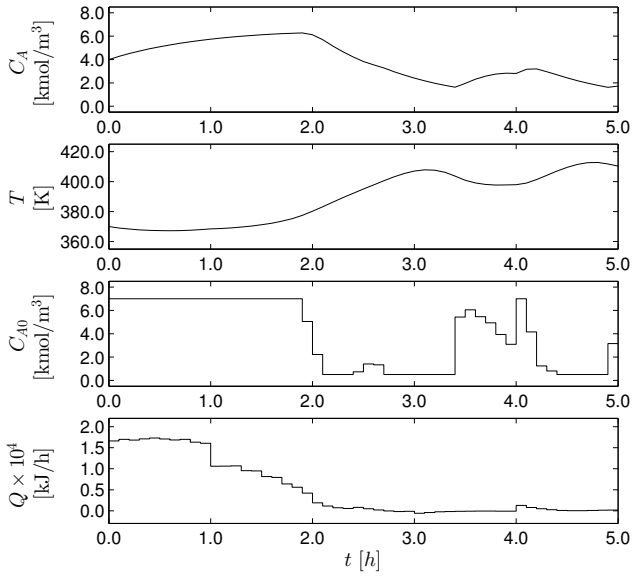

Figure 3.13: The states and inputs of the nominally operated CSTR under LEMPC-2 initialized at $C_A(0) = 4.0\,\text{kmol m}^{-3}$ and $T(0) = 370.0\,\text{K}$.

LEMPC-2 simulation, the maximum allowable amount of reactant concentration is fed to the process from 0.0 h to 1.8 h. This causes the rates of the three reactions to increase. Since the heat rate supplied/removed from the reactor is penalized in the cost and the LEMPC does not know that the price of the reactant material will decrease at 2.0 h, Q and C_{A0} decrease up to about 2.0 h to maintain stability. This decrease in Q and C_{A0} decreases the reactant concentration in the reactor while increasing the temperature bringing the states closer to the economically optimal region of operation. The LEMPC is then able to observe the economically optimal region of operation along its prediction horizon. Thus, it forces the states to this region. For LEMPC-1, the LEMPC knows that the reactant price will decrease at the beginning of each of the first four hours. Therefore, it maintains feeding the maximum allowable reactant material to maximize the reaction rate of the first reaction, and it supplies less heat to the reactor compared to LEMPC-2. As a result of this behavior, process operation is maintained far enough away from the optimal region of operation.

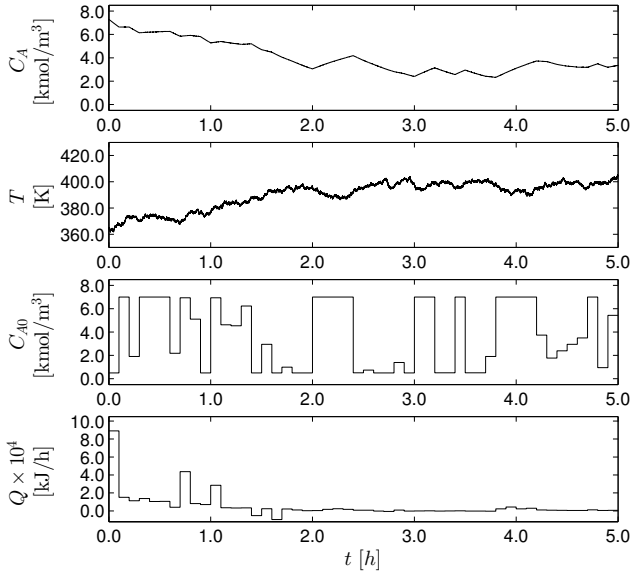

Figure 3.14: The states and inputs of the CSTR under the two-mode LEMPC with added process noise; evolution with respect to time.

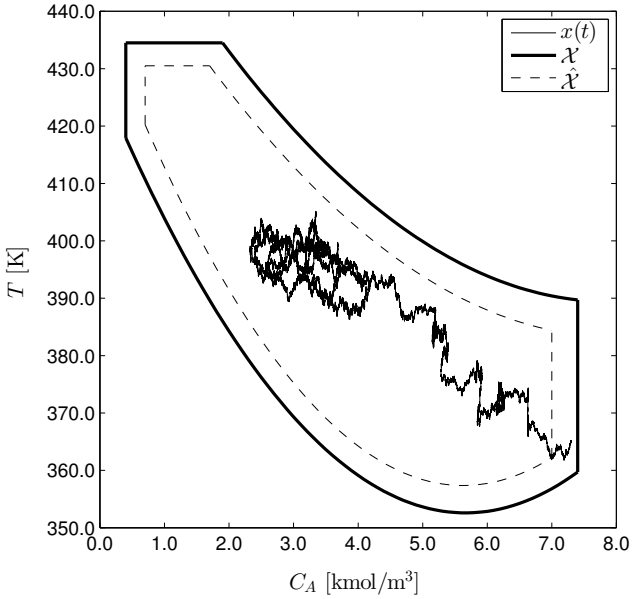

Figure 3.15: The states and inputs of the CSTR under the two-mode LEMPC with added process noise; state-space plot.

To assess the stability and robustness properties of the LEMPC of Eq. 3.75, the size where the LEMPC is able to operate the system in a time-varying manner to optimize the process economic cost is reduced and the two-mode control strategy is employed. Process noise is added to the closed-loop system and is modeled as bounded Gaussian white noise on the inlet reactant concentration and inlet temperature which has zero mean and the following standard deviation and bound: $0.5\,\mathrm{kmol\,m^{-3}}$ and $1.0\,\mathrm{kmol\,m^{-3}}$, respectively, for the inlet concentration noise and $3.0\,\mathrm{K}$ and $10.0\,\mathrm{K}$, respectively, for the inlet temperature noise. To simulate the noise, a new random number is generated and used to add noise in the process model over each integration step. The region $\hat{\mathscr{X}}$ is approximated through the following constraints:

$$\begin{aligned} 1.20x_1^2 - 19.17x_1 + 460.61 - x_2 \geq 0 \\ 2.59x_1^2 - 29.14x_1 + 438.36 - x_2 \leq 0 \\ 0.7 \leq x_1 \leq 7.1 \\ x_2 \leq 431.5 \end{aligned} \tag{3.90}$$

which has been estimated through extensive simulations with the given process model, economic cost, and process noise as the region whereby closed-loop stability may be maintained. The results of a closed-loop simulation of the CSTR are displayed in Figs. 3.14-3.15. The LEMPC does maintain the process inside the region $\mathscr{X}$ for the duration of the simulation as observed in Figs. 3.14-3.15.

3.6 Conclusions

In this chapter, various LEMPC designs were developed, which are capable of optimizing closed-loop performance with respect to general economic considerations for nonlinear

systems. Numerous issues arising in the context of chemical process control were considered including closed-loop stability, robustness, closed-loop performance, and explicitly time-varying economic cost functions. The formulations of the LEMPC schemes were provided as well as rigorous theoretical treatments of the schemes were carried out. Closed-loop stability, in the sense of boundedness of the closed-loop state, under the LEMPC designs was proven. Additionally, when desirable, the LEMPC designs may be used to enforce convergence of the closed-loop state to steady-state. Under a specific terminal constraint design, the closed-loop system under the resulting LEMPC scheme was shown to achieve at least as good closed-loop performance as that achieved under an explicit stabilizing controller. Demonstrations of the effectiveness of the LEMPC schemes on chemical process examples were also provided. Moreover, the closed-loop properties of these examples under the LEMPC schemes were compared with respect to existing approaches to optimization and control. In all cases considered, the closed-loop economic performance under the LEMPC designs was better relative to the conventional approaches.

Chapter 4

Two-layer EMPC Implementation

4.1 Introduction

As discussed in Chapter 1, in the traditional paradigm to optimization and control, a hierarchical strategy is employed using real-time optimization (RTO) to compute economically optimal steady-states that are subsequently sent down to a tracking MPC layer. The tracking MPC computes control actions that are applied to the closed-loop system to force the state to the optimal steady-state. If there is a shift in the optimal operating conditions, RTO updates the optimal steady-state and sends the updated steady-state to the MPC layer. On the other hand, the EMPC merges economic optimization and control, i.e., the methods discussed in Chapters 1-3, employing a one-layer approach to optimization and control. While EMPC merges optimization and control, the extent that EMPC takes on all the responsibilities of RTO remains to be seen. For example, many EMPC methods are formulated using a steady-state, which potentially could be the economically optimal steady-state. RTO is also responsible for other tasks besides optimization. Therefore, one may envision that future optimization and control structures will maintain some aspects of the hierarchical approach within the context of industrial applications. Moreover, in some applications, maintaining a

division between economic optimization and control is suitable, especially for applications where there is an explicit time-scale separation between the process/system dynamics and the update frequency or time-scale of evolution of economic factors and/or other factors that shift optimal operating conditions, e.g., disturbances.

In an industrial control architecture, which features a high degree of complexity, a hierarchical approach to dynamic economic optimization and control may be more applicable. Motivated by the aforementioned considerations, several two-layer approaches to dynamic economic optimization and control are discussed in this chapter. The upper layer, utilizing an EMPC, is used to compute economically optimal policies and potentially, also, control actions that are applied to the closed-loop system. The economically optimal policies are sent down to a lower layer MPC scheme which may be a tracking MPC or an EMPC. The lower layer MPC scheme forces the closed-loop state to closely follow the economically optimal policy computed in the upper layer EMPC.

The unifying themes of the two-layer EMPC implementations described in this chapter are as follows. First, the upper layer EMPC may employ a long prediction horizon. The long prediction horizon ideally prevents the EMPC from dictating an operating policy based on myopic decision-making, which may lead to poor closed-loop economic performance. Considering a one-layer EMPC approach with a long horizon, the computational time and complexity of the resulting optimization problem (thousands of decisions variables for large-scale systems) may make it unsuitable for real-time application. Second, the upper layer dynamic economic optimization problem, i.e., the EMPC problem, is formulated with explicit control-oriented constraints which allow for guaranteed closed-loop stability properties. This is a departure from other two-layer approaches to dynamic optimization and control such as those featuring dynamic-RTO, e.g. [80, 94, 122, 93, 185, 202, 92, 192, 195, 193], which may not be formulated with such constraints. Third, the upper layer is solved infrequently in the sense that it is not solved every sampling time like

a standard one-layer EMPC method with a receding horizon implementation. The rate that the upper layer EMPC is solved may be considered a tuning parameter of the optimization and control architectures. However, the upper layer does not need to wait until the system has reached steady-state owing to the fact that a dynamic model of the process is used in the optimization layer.

The lower layer MPC, which may be either a tracking MPC or an EMPC, may be formulated with a shorter prediction horizon and potentially smaller sampling period if state measurement feedback is available. It is used to force the closed-loop state to track the operating policy computed by the upper layer EMPC and to ensure closed-loop stability and robustness. Owing to the fact that the upper layer EMPC is solved infrequently and the lower layer MPC utilizes a shorter prediction horizon, the major benefit of a two-layer EMPC implementation is improved computational efficiency compared to a one-layer EMPC method.

The results of this chapter originally appeared in [51, 49, 50, 46].

4.1.1 Notation

Given that this chapter deals with control elements arranged in a multi-layer configuration, an extended amount of notation is needed to describe the control system. To aid the reader, Table 4.1 summarizes the notation used in this chapter. Some of the notation will be made more precise in what follows. To clarify the difference between open-loop and closed-loop trajectories, consider a time sequence: $\{\bar{t}_i\}_{i=k}^{k+\bar{N}}$ where $\bar{t}_i = i\bar{\Delta}$, $\bar{\Delta} > 0$ is a constant and $\bar{N} \geq 1$ is a positive integer. Given a function $\bar{u} : [\bar{t}_k, \bar{t}_{k+\bar{N}}) \to \mathbb{U}$, which is right-continuous piecewise constant with constant hold period $\bar{\Delta}$, the open-loop predicted state trajectory under the open-loop input trajectory $\bar{u}$ is the solution to the differential equation:

$$\dot{\bar{x}}(t) = f(\bar{x}(t), \bar{u}(t), 0) \tag{4.1}$$

Table 4.1: A summary of the notation used to describe the two-layer EMPC structure.

Notation	Description
Δ_E	Zeroth-order hold period used for the upper layer control parameterization
N_E	Number of zeroth-order hold periods in the upper layer EMPC prediction horizon
K_E	Number of hold periods, Δ_E, that the upper layer EMPC is solved
t'	Operating period length with $t' = K_E\Delta_E$
$\{\hat{t}_k\}_{k\geq 0}$	Computation time sequence of upper layer with $\hat{t}_k = kt'$ ($k \in \mathbb{I}_+$)
$z(\cdot\|\hat{t}_k)$	Open-loop predicted state trajectory under an auxiliary controller computed at $\hat{t}_k$
$v(\cdot\|\hat{t}_k)$	Open-loop input trajectory computed by an auxiliary controller computed at $\hat{t}_k$
$x_E(\cdot\|\hat{t}_k)$	Open-loop predicted state trajectory under the upper layer MPC at $\hat{t}_k$
$u_E(\cdot\|\hat{t}_k)$	Open-loop input trajectory computed by the upper layer MPC at $\hat{t}_k$
Δ	Sampling period size of the lower layer
N	Number of sampling periods in the lower layer MPC prediction horizon
$\{t_j\}_{j\geq 0}$	Sampling time sequence of lower layer with $t_j = j\Delta$ ($j \in \mathbb{I}_+$)
$\tilde{x}(\cdot\|t_j)$	Open-loop predicted state trajectory under the lower layer MPC at t_j
$u(\cdot\|t_j)$	Open-loop input trajectory computed by the upper layer MPC at t_j
$x(\cdot)$	Closed-loop state trajectory under the two-layer control structure
$u^*(t_j\|t_j)$	Control action applied to the closed-loop system computed at t_j and applied from t_j to t_{j+1}
(x_s, u_s)	Steady-state and steady-state input pair

for $t \in [\bar{t}_k, \bar{t}_{k+\bar{N}})$ with initial condition $\bar{x}(\bar{t}_k) = x(\bar{t}_k)$ where $x(\bar{t}_k)$ is a state measurement of the closed-loop system at time $\bar{t}_k$. In this context, existence of a solution for a given open-loop input trajectory is assumed. In the subsequent sections, existence and uniqueness of a solution to Eq. 4.1 is guaranteed under mild smoothness requirements on f and the fact that $\bar{u}(\cdot)$ is piecewise continuous and is computed such that the solution is maintained in a compact state-space set. The open-loop predicted state and input trajectories are denoted as $\bar{x}(\cdot|\bar{t}_k)$ and $\bar{u}(\cdot|\bar{t}_k)$ to make clear that both of these trajectories, which are functions of time, have been computed at $\bar{t}_k$ with a state measurement at $\bar{t}_k$.

The term closed-loop system refers to the resulting sampled-data system of Eq. 3.1 under an MPC scheme. The closed-loop state trajectory is the solution to:

$$\dot{x}(t) = f(x(t), k(x(t_j)), w(t)) \tag{4.2}$$

for $t \in [t_j, t_{j+1})$ with $t_j = j\Delta$ for some $\Delta > 0$ and $j = 0, 1, \ldots$. The mapping $k(\cdot)$ is a state feedback control law. In the context of MPC, the state feedback control law is implicitly defined from the solution of an optimization problem and the receding horizon implement ion Specifically, the MPC receives a state measurement at a sampling time t_j, computes a control action, and applies it in a sample-and-hold fashion over the sample period, i.e., from t_j to t_{j+1}. The notation $u^*(t_j|t_j)$ is used to denote the computed control action by the MPC scheme at sampling time t_j with a state measurement $x(t_j)$. Under an MPC scheme, the closed-loop system is written similarly to Eq. 4.2 by replacing $k(x(t_j))$ with $u^*(t_j|t_j)$. Finally, the notation $\cdot^*$, e.g., y^*, is used to denote that the quantity, which may be a vector with real elements or a function defined over an appropriate domain and range, is optimal with respect to a cost function (or cost functional) and some constraints.

4.2 Two-Layer Control and Optimization Framework

In this section, a two-layer dynamic economic optimization and control framework featuring EMPC in the upper layer and tracking MPC in the lower layer is discussed. The same nonlinear dynamic model is used in each layer to avoid modeling inconsistencies. Control-oriented constraints are employed in the dynamic optimization layer to ensure closed-loop stability. A rigorous theoretical treatment of the stability properties of the closed-loop system with the control architecture is provided. Variants and extensions of the two-layer optimization and control framework are discussed. The two-layer optimization and control framework is applied to a chemical process example.

4.2.1 Class of Systems

While a similar class of nonlinear systems is considered as that described by Eq. 3.1, the manipulated inputs are split into two groups, i.e., the input vector is given by $u := [u_1 \; u_2]^T$ where $u_1 \in \mathbb{R}^{m_1}$, $u_2 \in \mathbb{R}^{m_2}$, and $m_1 + m_2 = m$. Loosely speaking, the inputs are partitioned into two groups based on their main responsibility. The input u_1 is directly responsible for economic optimization and/or has the most significant impact on the closed-loop economic performance, while the input u_2 is responsible for maintaining closed-loop stability. In the chemical process example of Section 4.2.3, the inputs are partitioned using this rationale as a basis. Additional methods may be employed to help identify the inputs that have the most significant impact on the economic performance such as the methods presented in Chapter 7.

With the two sets of inputs, the following state-space model is written to emphasize the dependence of the vector field on each group of inputs:

$$\dot{x} = f(x, u_1, u_2, w) \tag{4.3}$$

where $x \in \mathbb{X} \subseteq \mathbb{R}^n$ denotes the state vector, $u_1 \in \mathbb{U}_1 \subset \mathbb{R}^{m_1}$ and $u_2 \in \mathbb{U}_2 \subset \mathbb{R}^{m_2}$ denote the two manipulated input vectors or the two sets of manipulated inputs, $w \in \mathbb{R}^l$ denotes the disturbance vector and f is assumed to be a locally Lipschitz vector function on $\mathbb{X} \times \mathbb{U}_1 \times \mathbb{U}_2 \times \mathbb{W}$. The sets $\mathbb{U}_1$ and $\mathbb{U}_2$ are assumed to be nonempty compact sets. The disturbance is assumed to be bounded, i.e., $\mathbb{W} := \{w \in \mathbb{R}^l : |w| \leq \theta\}$ where $\theta > 0$. The origin of the nominal unforced system of Eq. 4.3 is assumed to be an equilibrium point ($f(0,0,0,0) = 0$). The state of the system is sampled synchronously at the time instants indicated by the time sequence $\{t_j\}_{j \geq 0}$ where $t_j = j\Delta$, $j = 0, 1, \ldots$ and $\Delta > 0$ is the sampling period.

As before, a stabilizability assumption is imposed on the system of Eq. 4.3 in the sense that the existence of a stabilizing feedback control law that renders the origin of the system of Eq. 4.3 asymptotically stable is assumed. The stabilizing feedback control law is given by the pair:

$$(h_1(x), h_2(x)) \in \mathbb{U}_1 \times \mathbb{U}_2 \tag{4.4}$$

for all $x \in \mathbb{X}$. While the domain of the stabilizing controller is taken to be $\mathbb{X}$, it renders the origin asymptotically stable with some region of attraction that may be a subset of $\mathbb{X}$. Applying converse Lyapunov theorems [100, 123], there exists a continuous differentiable Lyapunov function $V : D \to \mathbb{R}_+$ that satisfies the following inequalities:

$$\alpha_1(|x|) \leq V(x) \leq \alpha_2(|x|) \tag{4.5a}$$

$$\frac{\partial V(x)}{\partial x} f(x, h_1(x), h_2(x), 0) \leq -\alpha_3(|x|) \tag{4.5b}$$

$$\left| \frac{\partial V(x)}{\partial x} \right| \leq \alpha_4(|x|) \tag{4.5c}$$

for all $x \in D$ where $\alpha_i \in \mathscr{K}$ for $i = 1, 2, 3, 4$ and D is an open neighborhood of the origin. The region $\Omega_\rho \subseteq D$ such that $\Omega_\rho \subseteq \mathbb{X}$ is the (estimated) stability region of the closed-loop

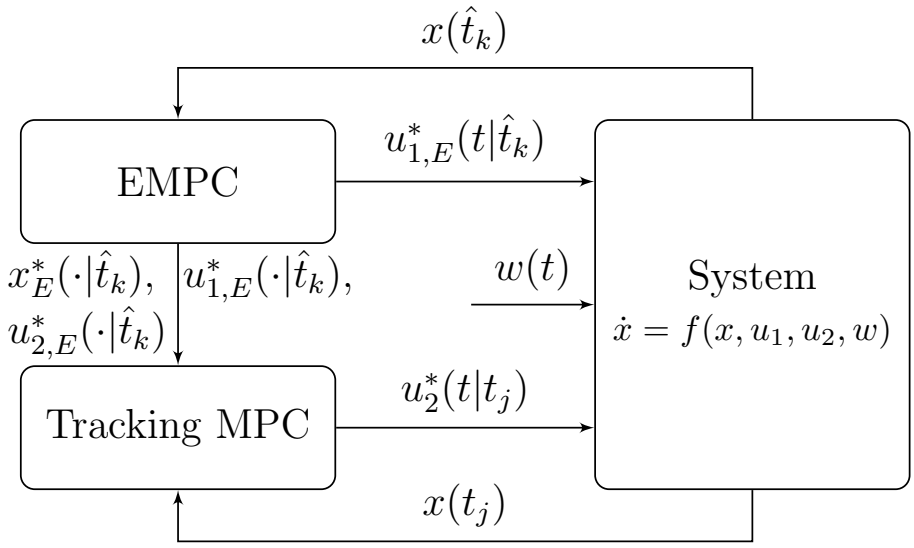

Figure 4.1: A block diagram of the two-layer integrated framework for dynamic economic optimization and control with EMPC in the upper layer and tracking MPC in the lower layer. Both the upper and lower layers compute control actions that are applied to the system.

system under the stabilizing controller.

4.2.2 Formulation and Implementation

The dynamic economic optimization and control framework consists of EMPC in the upper layer and tracking MPC in the lower layer. A block diagram of the framework is given in Fig. 4.1. The prediction horizons of the EMPC and the MPC may be different. This allows for the EMPC to be formulated with a long prediction horizon. The number of sampling periods in the prediction horizon of the EMPC is denoted as $N_E \in \mathbb{I}_{\geq 1}$, and that of the MPC is denoted as $N \in \mathbb{I}_{\geq 1}$. For simplicity, the sampling periods of the upper layer EMPC and lower layer MPC are assumed to be the same ($\Delta_E = \Delta$) and Δ will be used to denote the sampling period. The two-layer framework may be extended to the case where the sampling periods are not equal.

The upper layer EMPC problem is solved infrequently, i.e., not every sampling time. Let $K_E \geq \mathbb{I}_+$ be the number of sampling times that the upper layer is resolved. The time sequence $\{\hat{t}_k\}_{k\geq 0}$ denotes the time steps that the upper layer EMPC is solved. Owing to the implementation strategy, the time sequence is not necessarily a synchronous partitioning of time. For sake of simplicity, let $N \leq N_E - K_E$ to ensure that the upper layer EMPC problem is computed at a rate needed to ensure that the economically optimal trajectory is defined over the prediction horizon of the lower layer tracking MPC. If this is not satisfied, one could employ a shrinking horizon in the lower layer LMPC. While the upper layer EMPC computes optimal input trajectories for both sets of manipulated inputs, it sends control actions for the manipulated input u_1 to the control actuators to be applied in an open-loop fashion. The implementation strategy is described below. The optimal operating trajectory over the prediction horizon of the EMPC is computed by the upper layer EMPC and sent to the lower layer tracking MPC to force the closed-loop state to track the optimal operating trajectory. The optimal operating trajectory is defined below.

Definition 4.1. Let $(u^*_{1,E}(t|\hat{t}_k), u^*_{2,E}(t|\hat{t}_k))$, which is defined for $t \in [\hat{t}_k, \hat{t}_k + N_E\Delta)$, be the optimal input pair computed by the upper layer EMPC and let $x(\hat{t}_k)$ be the state measurement at the sampling time $\hat{t}_k$. The economically optimal state trajectory $x^*_E(t|\hat{t}_k)$ for $t \in [\hat{t}_k, \hat{t}_k + N_E\Delta)$ of the system of Eq. 4.3 is the solution of

$$\dot{x}^*_E(t) = f(x^*_E(t), u^*_{1,E}(\tau_i|\hat{t}_k), u^*_{2,E}(\tau_i|\hat{t}_k), 0), \quad t \in [\tau_i, \tau_{i+1}) \tag{4.6}$$

for $i = 0, 1, \ldots, N_E - 1$ with $x_E(\hat{t}_k) = x(\hat{t}_k)$ where $\tau_i := \hat{t}_k + i\Delta$.

The lower layer MPC is implemented with a receding horizon implementation and thus, is solved at every sampling time. The notation t_j will be reserved to denote a sampling time that the MPC problem is solved. To provide closed-loop stability guarantees on the resulting control framework, the upper layer EMPC is formulated as an LEMPC (Eq. 3.3)

and the lower layer MPC is formulated as a LMPC (Eq. 2.43). The advantage of this formulation is that the LEMPC computes a reference trajectory that the tracking LMPC layer may force the system to track and unreachable set-points are avoided.

An assumption is needed to ensure feasibility and stability with the resulting two-layer framework. Owing to the fact that the upper layer EMPC is solved infrequently and applies its computed trajectory for u_1 in an open-loop fashion, an assumption is needed to ensure that it is possible to maintain stability with the input u_2 in the sense that for any $u_1 \in \mathbb{U}_1$ it possible to find a $u_2 \in \mathbb{U}_2$ that ensures that the time-derivative of the Lyapunov function is negative. This is stated in the following assumption. Also, the assumption further clarifies how the manipulated inputs are divided into the two input groups.

Assumption 4.1. *For any fixed $u_{1,E} \in U_1$, there exists $u_2 \in U_2$ such that:*

$$\frac{\partial V(x)}{\partial x} f(x, u_{1,E}, u_2, 0) \leq \frac{\partial V(x)}{\partial x} f(x, h_1(x), h_2(x), 0) \tag{4.7}$$

for all $x \in \Omega_\rho$.

Variations of the assumption are discussed in Section 4.2.2.

The upper layer LEMPC has a similar formulation as that of Eq. 3.3 with one modification discussed below. The upper layer LEMPC problem is given by the following

optimization problem:

$$\min_{u_{1,E},u_{2,E}\in S(\Delta)} \int_{\hat{t}_k}^{\hat{t}_k+N_E\Delta} l_e(x_E(\tau),u_{1,E}(\tau),u_{2,E}(\tau))\, d\tau \tag{4.8a}$$

$$\text{s.t.} \quad \dot{x}_E(t) = f(x_E(t),u_{1,E}(t),u_{2,E}(t),0) \tag{4.8b}$$

$$x_E(\hat{t}_k) = x(\hat{t}_k) \tag{4.8c}$$

$$u_{1,E}(t) \in \mathbb{U}_1,\ u_{2,E}(t) \in \mathbb{U}_2,\ \forall\, t \in [\hat{t}_k,\hat{t}_k+N_E\Delta) \tag{4.8d}$$

$$V(x_E(t)) \leq \rho_e,\ \forall\, t \in [\hat{t}_k,\hat{t}_k+N_E\Delta),$$
$$\text{if } V(x(\hat{t}_k)) \leq \rho_e \text{ and } \hat{t}_k < t_s \tag{4.8e}$$

$$\frac{\partial V(x_E(\tau_i))}{\partial x} f(x_E(\tau_i),u_{1,E}(\tau_i),u_{2,E}(\tau_i),0)$$
$$\leq \frac{\partial V(x_E(\tau_i))}{\partial x} f(x_E(\tau_i),h_1(x_E(\tau_i)),h_2(x_E(\tau_i)),0),$$
$$i = 0,1,\ldots,N_E-1, \text{ if } V(x(\hat{t}_k)) > \rho_e \text{ or } \hat{t}_k \geq t_s \tag{4.8f}$$

where $\tau_i := \hat{t}_k + i\Delta$. The main difference between the upper layer LEMPC formulation and the LEMPC formulation of Eq. 3.3 is the mode 2 contractive constraint (Eq. 4.8f). In the upper layer LEMPC formulation, the mode 2 contractive constraint is imposed at each time instance of the prediction horizon. This ensures that the Lyapunov function value decays over the prediction horizon and thus, the lower layer LMPC attempts to force the closed-loop state along a reference trajectory that either converges to Ω_{ρ_e} if $\hat{t}_k < t_s$ or converges to a neighborhood of the origin if $\hat{t}_k \geq t_s$. The optimal trajectories computed by the upper layer LEMPC are denoted by $x_E^*(t|\hat{t}_k)$, $u_{E,1}^*(t|\hat{t}_k)$, and $u_{E,2}^*(t|\hat{t}_k)$ defined for $t \in [\hat{t}_k,\hat{t}_k+N_E\Delta)$.

The stage cost function used in the LMPC is formulated to penalize deviations of the state and inputs from the economically optimal trajectories. Additionally, the LMPC is equipped with dual-mode constraints similar to that imposed in LEMPC. The dual-mode

LMPC problem is given by the following optimization problem:

$$\min_{u_2 \in S(\Delta)} \int_{t_j}^{t_{j+N}} l_T(\tilde{x}(\tau), x_E^*(\tau|\hat{t}_k), u_2(\tau), u_{2,E}^*(\tau|\hat{t}_k))\, d\tau \tag{4.9a}$$

$$\text{s.t.} \quad \dot{\tilde{x}}(t) = f(\tilde{x}(t), u_{1,E}^*(t|\hat{t}_k), u_2(t), 0) \tag{4.9b}$$

$$\tilde{x}(t_j) = x(t_j) \tag{4.9c}$$

$$u_2(t) \in \mathbb{U}_2, \ \forall\, t \in [t_j, t_{j+N}) \tag{4.9d}$$

$$V(\tilde{x}(t)) \leq \rho_e, \ \forall\, t \in [t_j, t_{j+N}),$$

$$\text{if } V(x(t_j)) \leq \rho_e \text{ and } t_j < t_s \tag{4.9e}$$

$$\frac{\partial V(x(t_j))}{\partial x} f(x(t_j), u_{1,E}^*(t_j|\hat{t}_k), u_2(t_j), 0)$$
$$\leq \frac{\partial V(x(t_j))}{\partial x} f(x(t_j), h_1(x(t_j)), h_2(x(t_j)), 0),$$
$$\text{if } V(x(t_j)) > \rho_e \text{ and } t_j \geq t_s \tag{4.9f}$$

where the stage cost of LMPC is given by:

$$l_T(\tilde{x}, x_E^*, u_2, u_{2,E}^*) = |\tilde{x} - x_E^*|_{Q_c}^2 + \left|u_2 - u_{2,E}^*\right|_{R_{c,2}}^2 \tag{4.10}$$

and Q_c and R_c are positive definite tuning matrices. The constraint of Eq. 4.9e defines mode 1 operation of the LMPC and serves a similar purpose as the mode 1 constraint of LEMPC (Eq. 3.3e). Under mode 2 operation of the LMPC, which is defined when the constraint of Eq. 4.9f is active, the LMPC computes control actions to ensure that the contractive Lyapunov-based constraint is satisfied. The optimal solution of Eq. 4.9 is denoted as $u_2^*(t|t_j)$ for $t \in [t_j, t_{j+N})$.

The two-layer optimization and control framework has a number of tunable parameters. Specifically, the tuning parameters include the weighting matrices Q_c and R_c, the prediction horizons N and N_E, the number of sampling times that the upper layer recomputes a

solution K_E, the subset of the stability region that the control framework may operate the system in a time-varying fashion (Ω_{ρ_e}), the sampling period Δ and the triple (h_1, h_2, V), i.e., stabilizing controller design and Lyapunov function which are used in the Lyapunov-based constraints.

If the optimal state trajectory has been computed using mode 2 operation of the LEMPC and the current time is less than the switching time t_s, it is advantageous from a performance perspective, to recompute a new LEMPC solution using mode 1 once the state converges to the set Ω_{ρ_e}. This is captured in the implementation strategy of the two-layer optimization and control framework that is described by the following algorithm. Let the index $l \in \mathbb{I}_+$ be the number of sampling times since the last time that the upper layer LEMPC problem has been solved and m_k be the mode of operation of the LEMPC used to solve the LEMPC problem at $\hat{t}_k$. To initialize the algorithm, let $\hat{t}_0 = 0$, $k = 0$, and $j = 0$.

1. At $\hat{t}_k$, the upper layer LEMPC receives a state measurement $x(\hat{t}_k)$ and set $l = 0$. If $x(\hat{t}_k) \in \Omega_{\rho_e}$ and $\hat{t}_k < t_s$, go to Step 1.1. Else, go to Step 1.2.

   1.1 The mode 1 constraint (Eq. 4.8e) is active and the mode 2 constraint (Eq. 4.8f) is inactive. Set $m_k = 1$ and go to Step 1.3.

   1.2 The mode 2 constraint (Eq. 4.8f) is active and the mode 1 constraint (Eq. 4.8e) is inactive. Set $m_k = 2$ and go to Step 1.3.

   1.3 Solve the optimization problem of Eq. 4.8 to compute the optimal trajectories $x_E^*(t|\hat{t}_k)$, $u_{E,1}^*(t|\hat{t}_k)$, and $u_{E,2}^*(t|\hat{t}_k)$ defined for $t \in [\hat{t}_k, \hat{t}_k + N_E\Delta)$. Send these trajectories to the lower layer LMPC and go to Step 2.

2. At t_j, the lower layer LMPC receives a state measurement $x(t_j)$. If $x(t_j) \in \Omega_{\rho_e}$, $t_j < t_s$, and $m_k = 2$, set $\hat{t}_{k+1} = t_j$ and $k \leftarrow k+1$, and go to Step 1. Else if $x(t_j) \in \Omega_{\rho_e}$ and $t_j < t_s$, go to Step 2.1. Else, go to Step 2.2.

2.1 The mode 1 constraint (Eq. 4.9e) is active and the mode 2 constraint (Eq. 4.9f) is inactive. Go to Step 2.3.

2.2 The mode 2 constraint (Eq. 4.9f) is active and the mode 1 constraint (Eq. 4.9e) is inactive. Go to Step 2.3.

2.3 Solve the optimization problem of Eq. 4.9 to compute the optimal input trajectory $u^*(t|t_j)$ defined for $t \in [t_j, t_{j+N})$. Apply the input pair $(u^*_{1,E}(t_j|\hat{t}_k), u^*_2(t_j|t_j))$ to the system of Eq. 4.3 from t_j to t_{j+1}. Go to Step 3.

3. If $l+1 = K_E$, set $\hat{t}_{k+1} = t_{j+1}$, $k \leftarrow j+1$, and $j \leftarrow j+1$, and go to Step 1. Else, go to Step 2 and set $l \leftarrow l+1$ and $j \leftarrow j+1$.

The two-layer implementation strategy allows for computational advantages over one-layer EMPC structures. When the LEMPC is operating in mode 1, the LEMPC problem is only computed once every K_E sampling times. The LMPC is less computationally expensive to solve than the LEMPC because the LMPC does not compute control actions for all of the manipulated inputs. Additionally, the LMPC may use a smaller prediction horizon than the LEMPC. Owing to these considerations, the two-layer framework is more computationally efficient compared to one-layer EMPC structures.

It is important to point out the two limiting cases of the optimization and control framework. If all the inputs are in the group u_2, then the control framework is reminiscent of current two-layer frameworks where economic optimization, which in this case is a dynamic optimization problem, and control are divided into separate layers. If, on the other hand, all inputs are placed in the group u_1 or the upper layer LEMPC is solved every sampling time ($K_E = 1$), then this would correspond to a one-layer implementation of LEMPC. For the case that all inputs are in the u_1 group, the LEMPC would need to be computed every sampling time to ensure stability and robustness of the closed-loop system.

Variants of the Two-Layer Optimization and Control Framework

While the stability results presented in Section 4.2.2 apply to the two-layer framework described above, one may consider many variations to the two-layer framework design. A few such variants are listed here.

1. The upper layer EMPC does not compute input trajectories for all inputs. For instance, some inputs in the u_2 set may have little impact on the economic performance. For these inputs, a constant input profile, for instance, could be assumed in the upper layer EMPC. This could further improve the computational efficiency of the two-layer framework. The inputs that are held constant in the EMPC problem could be used as additional degrees of freedom in the lower layer MPC to help force the closed-loop state to track the economically optimal state trajectory.

2. The lower layer MPC computes control actions for all the inputs, i.e., the upper layer EMPC does not apply any control actions directly to the system, but rather, is used to compute reference trajectories for the lower layer MPC. This approach is similar to current optimization and control structures but employs dynamic economic optimization with explicit control-oriented constraints imposed in the optimization layer.

3. Other assumptions to ensure feasibility and stability of the two-layer framework than Assumption 4.1 may be considered. For example, it may be possible to consider the input u_1 as a perturbation to the system and derive the explicit stabilizing controller on the basis of the inputs u_2. Specifically, if there exists an explicit controller $h_2 : \mathbb{X} \to \mathbb{U}_2$ and Lyapunov function that satisfies:

$$\frac{\partial V(x)}{\partial x} f(x, u_1, h_2(x), 0) \leq -\bar{\alpha}_3(|x|) \tag{4.11}$$

for all $u_1 \in \mathbb{U}_1$ and $x \in \Omega_\rho \setminus B$ where $B \subset \Omega_\rho$ is some set containing the origin and $\bar{\alpha}(\cdot)$ is a class $\mathscr{K}$ function, then this assumption could be used to guarantee closed-loop stability and feasibility of the control problems. This assumption is essentially an input-to-state stability assumption of the closed-loop system of Eq. 4.3 under the controller h_2 with respect to the input u_1.

4. The two-layers could use a different sampling period size. In particular, the upper layer could use a larger sampling period than the lower layer.

5. One could use an EMPC scheme in the lower layer instead of tracking MPC. One such variant employing this concept is presented later in this chapter (Section 4.4).

Stability Analysis

In this section, sufficient conditions are presented that guarantee that the closed-loop system with the two-layer dynamic economic optimization and control framework is stable in the sense that the system state remains bounded in a compact set for all times. Two propositions are needed, which are straightforward extensions of Proposition 3.1 and Proposition 3.2, respectively. The propositions are restated here for convenience. The first proposition provides an upper bound on the deviation of the open-loop state trajectory, obtained using the nominal model (Eq. 4.3 with $w \equiv 0$), from the closed-loop state trajectory.

Proposition 4.1 (Proposition 3.1)**.** *Consider the systems*

$$\begin{aligned} \dot{x}_a(t) &= f(x_a(t), u_1(t), u_2(t), w(t)) \\ \dot{x}_b(t) &= f(x_b(t), u_1(t), u_2(t), 0) \end{aligned} \tag{4.12}$$

with initial states $x_a(t_0) = x_b(t_0) \in \Omega_\rho$ and inputs $u_1(t) \in \mathbb{U}_1$ and $u_2(t) \in \mathbb{U}_2$ for $t \geq t_0$. If the states of the two systems are maintained in Ω_ρ for all $t \in [t_0, t_1]$ ($t_1 > t_0$), there exists a

class $\mathscr{K}$ function $\alpha_w(\cdot)$ such that

$$|x_a(t) - x_b(t)| \leq \alpha_w(t - t_0), \tag{4.13}$$

for all $w(t) \in W$ and $t \in [t_0, t_1]$.

The following proposition bounds the difference between the Lyapunov function of two different states in Ω_ρ.

Proposition 4.2 (Proposition 3.2)**.** *Consider the Lyapunov function $V(\cdot)$ of the system of Eq. 4.3. There exists a quadratic function $\alpha_V(\cdot)$ such that:*

$$V(x) \leq V(\hat{x}) + \alpha_V(|x - \hat{x}|) \tag{4.14}$$

for all $x, \hat{x} \in \Omega_\rho$.

Theorem 1 provides sufficient conditions such that the two-layer dynamic economic optimization and control framework guarantees that the state of the closed-loop system is always bounded in Ω_ρ. The result is similar to that of the closed-loop stability properties under LEMPC.

Theorem 4.1. *Consider the system of Eq. 4.3 in closed-loop under the two-layer framework with the LEMPC of Eq. 4.8 in the upper layer and the LMPC of Eq. 4.9 in the lower layer both based on the explicit stabilizing controller that satisfies Eqs. 4.5a-4.5c. Let $\varepsilon_w > 0$, $\Delta > 0$, $N_E \geq 1$, $N \geq 1$ ($N \leq N_E - K_E$), $\rho > \rho_e > \rho_{\min} > \rho_s > 0$, and L'_x, L'_w and M are positive constants (the existence of these constants follows from the assumptions on the system of Eq. 4.3) satisfy:*

$$\rho_e < \rho - \alpha_V(\alpha_w(\Delta)), \tag{4.15}$$

$$-\alpha_3(\alpha_2^{-1}(\rho_s)) + L'_x M\Delta + L'_w\theta \leq -\varepsilon_w/\Delta\,, \tag{4.16}$$

and

$$\rho_{\min} = \max_{s\in[0,\Delta]} \{V(x(s)) : V(x(0)) \leq \rho_s\} \ . \tag{4.17}$$

If $x(0) \in \Omega_\rho$ and Assumption 4.1 is satisfied, then the state $x(t)$ of the closed-loop system is always bounded in Ω_ρ for all $t \geq 0$. Moreover, if t_s is finite, the closed-loop state is ultimately bounded in $\Omega_{\rho_{\min}}$.

Proof. The proof is organized into three parts. In part 1, feasibility of the optimization problems of Eq. 4.8 and Eq. 4.9 is proved when the state measurement given to each problem is in Ω_ρ. In part 2, boundedness of the closed-loop state in Ω_ρ is established. Finally, ultimate boundedness of the closed-loop state in a small state-space set containing the origin is proved when the switching time is finite.

Part 1: When the closed-loop state is maintained in Ω_ρ, which will be proved in Part 2, the sample-and-hold input trajectory obtained from the stabilizing feedback controller is a feasible solution to the upper layer LEMPC optimization problem of Eq. 4.8. Specifically, let $\hat{x}(t)$ denote the solution at time t to the system:

$$\dot{\hat{x}}(t) = f(\hat{x}(t), h_1(\hat{x}(\tau_i)), h_2(\hat{x}(\tau_i)), 0) \tag{4.18}$$

for $t \in [\tau_i, \tau_{i+1})$ ($\tau_i := \hat{t}_k + i\Delta$), $i = 0, 1, \ldots, N_E - 1$ with initial condition $\hat{x}(\hat{t}_k) = x(\hat{t}_k) \in \Omega_\rho$. Defining the pair $(\hat{u}_1(t), \hat{u}_2(t)) := (h_1(\hat{x}(\tau_i)), h_2(\hat{x}(\tau_i)))$ for $t \in [\tau_i, \tau_{i+1})$, $i = 0, 1, \ldots, N_E - 1$, the input trajectory pair $(\hat{u}_1, \hat{u}_2)$ is a feasible solution to the LEMPC problem. Specifically, for mode 2 operation of the LEMPC, the pair $(\hat{u}_1, \hat{u}_2)$ meets the input constraints since it is computed from the stabilizing controller, which satisfies the input constraints (Eq. 4.4). Also, the mode 2 contractive constraint of Eq. 4.8f is trivially satisfied with the input pair $(\hat{u}_1, \hat{u}_2)$. For mode 1 operation, the region Ω_{ρ_e} is forward invariant under the stabilizing controller applied in a sample-and-hold fashion when $\Omega_{\rho_{\min}} \subseteq \Omega_{\rho_e} \subset \Omega_\rho$ where $\Omega_{\rho_{\min}}$ will

be explained further in Parts 2 and 3.

If Assumption 4.1 is satisfied, the feasibility of the lower layer LMPC problem of Eq. 4.9 follows because there exists an input trajectory $u_1(t)$ for $t \in [t_j, t_{j+N})$ that decreases the Lyapunov function by at least the rate given by the Lyapunov-based controller at each sampling time instance along the prediction horizon. Using similar arguments as that used for feasibility of the LEMPC, mode 2 operation of the LMPC is feasible. Assumption 4.1 further implies that there exists a sample-and-hold input trajectory such that Ω_{ρ_e} is forward invariant when $\Omega_{\rho_{\min}} \subseteq \Omega_{\rho_e} \subset \Omega_\rho$ which guarantees that mode 1 operation of the LMPC is feasible.

Part 2: To show that the state is maintained in Ω_ρ when $x(0) \in \Omega_\rho$, two cases must be considered. The first case occurs when the state $x(t_j) \in \Omega_{\rho_e}$ and $t_j < t_s$ and the second case occurs when $x(t_j) \in \Omega_\rho \setminus \Omega_{\rho_e}$ or $t_j \geq t_s$. It is sufficient to show that $x(t) \in \Omega_\rho$ for all $t \in [t_j, t_{j+1}]$. Through recursive application of this result, boundedness of the closed-loop state in Ω_ρ for all $t \geq 0$ follows if the initial state is in Ω_ρ.

Case 1: If $x(t_j) \in \Omega_{\rho_e}$ and $t_j < t_s$, the lower layer LMPC operates in mode 1 operation. Regardless if the upper layer LEMPC has been computed under mode 1 or mode 2, there exists a control action $\hat{u}_2(t_j)$ such that when applied to the model of Eq. 4.9b in a sample-and-hold fashion over one sampling period the state at the next sampling time will be predicted to be in Ω_{ρ_e} (this follows from Part 1). However, the closed-loop system of Eq. 4.3 does not evolve according to the model of Eq. 4.9b owing to the forcing of the disturbance w.

Let ρ_e satisfy Eq. 4.15. The proof proceeds by contradiction. Assume there exists a time $\tau^* \in [t_j, t_{j+1}]$ such that $V(x(\tau^*)) > \rho$. Define $\tau_1 := \inf\{\tau \in [t_j, t_{j+1}] : V(x(\tau)) > \rho\}$. A standard continuity argument in conjunction with the fact that $V(x(t_j)) \leq \rho_e < \rho$ shows that $\tau_1 \in (t_j, t_{j+1}]$, $V(x(t)) \leq \rho$ for all $t \in [t_j, \tau_1]$ with $V(x(\tau_1)) = \rho$, and $V(x(t)) > \rho$ for

some $t \in (\tau_1, t_{j+1}]$. If ρ_e satisfies Eq. 4.15, then

$$\begin{aligned} \rho = V(x(\tau_1)) &\leq V(\tilde{x}(\tau_1)) + \alpha_V(\alpha_w(\tau_1)) \\ &\leq \rho_e + \alpha_V(\alpha_w(\Delta)) < \rho \end{aligned} \tag{4.19}$$

where the first inequality follows from Propositions 4.1-4.2 and the second inequality follows from the fact that $\alpha_V \circ \alpha_w \in \mathscr{K}$ and $\tau_1 \leq \Delta$. Eq. 4.19 leads to a contradiction. Thus, $x(t_{j+1}) \in \Omega_\rho$ if Eq. 4.15 is satisfied.

Case 2: When $x(t_j) \in \Omega_\rho \setminus \Omega_{\rho_e}$ or $t_j \geq t_s$, the lower layer LMPC operates in mode 2. To cover both possibilities, consider any $x(t_j) \in \Omega_\rho$ and that mode 2 operation of the LEMPC is active. From the constraint of Eq. 4.9f and the condition of Eq. 4.5b, the computed control action at t_j satisfies:

$$\begin{aligned} &\frac{\partial V(x(t_j))}{\partial x} f(x(t_j), u^*_{1,E}(t_j|\hat{t}_k), u^*_2(t_j|t_j), 0) \\ &\quad \leq \frac{\partial V(x(t_j))}{\partial x} f(x(t_j), h_1(x(t_j)), h_2(x(t_j)), 0) \leq -\alpha_3(|x(t_j)|) \end{aligned} \tag{4.20}$$

where $x(t_j)$ denotes the closed-loop state at sampling time t_j. Over the sampling period ($\tau \in [t_j, t_{j+1})$), the time derivative of the Lyapunov function of the closed-loop system is given by:

$$\dot{V}(x(\tau)) = \frac{\partial V(x(\tau))}{\partial x} f(x(\tau), u^*_{1,E}(t_j|\hat{t}_k), u^*_2(t_j|t_j), w(\tau)) \tag{4.21}$$

for $\tau \in [t_j, t_{j+1})$. Adding and subtracting the first term of Eq. 4.20 to/from Eq. 4.21 and accounting for the bound of Eq. 4.20, the time-derivative of the Lyapunov function over the

sampling period is bounded by:

$$\begin{aligned}\dot{V}(x(\tau)) \leq &-\alpha_3(|x(t_j)|) + \frac{\partial V(x(\tau))}{\partial x} f(x(\tau), u^*_{1,E}(t_j|\hat{t}_k), u^*_2(t_j|t_j), w(\tau)) \\ &- \frac{\partial V(x(t_j))}{\partial x} f(x(t_j), u^*_{1,E}(t_j|\hat{t}_k), u^*_2(t_j|t_j), 0)\end{aligned} \tag{4.22}$$

for all $\tau \in [t_j, t_{j+1})$.

Since the sets Ω_ρ, $\mathbb{U}_1$, $\mathbb{U}_2$, and $\mathbb{W}$ are compact, the vector field f is locally Lipschitz, and the Lyapunov function is continuously differentiable, there exist $L'_x > 0$ and $L'_w > 0$ such that:

$$\left| \frac{\partial V(x)}{\partial x} f(x, u_1, u_2, w) - \frac{\partial V(x')}{\partial x} f(x', u_1, u_2, 0) \right| \leq L'_x |x - x'| + L'_w |w| \tag{4.23}$$

for all x, $x' \in \Omega_\rho$, $u_1 \in \mathbb{U}_1$, $u_2 \in \mathbb{U}_2$, and $w \in \mathbb{W}$. From Eq. 4.22 and Eq. 4.23 and the fact that the disturbance is bounded in $\mathbb{W} = \{w \in \mathbb{R}^l : |w| \leq \theta\}$, the time-derivative of the Lyapunov function over the sampling period may be bounded as follows:

$$\dot{V}(x(\tau)) \leq -\alpha_3(|x(t_j)|) + L'_x \left| x(\tau) - x(t_j) \right| + L'_w \theta \tag{4.24}$$

for all $\tau \in [t_j, t_{j+1})$. Again, by the fact that the sets Ω_ρ, $\mathbb{U}_1$, $\mathbb{U}_2$, and $\mathbb{W}$ are compact and the vector field f is locally Lipschitz, there exists $M > 0$ such that

$$|f(x, u_1, u_2, w)| \leq M \tag{4.25}$$

for all $x \in \Omega_\rho$, $u_1 \in \mathbb{U}_1$, $u_2 \in \mathbb{U}_2$, and $w \in \mathbb{W}$. From Eq. 4.25 and continuity of $x(\tau)$ for $\tau \in [t_j, t_{j+1})$, the difference between the state at τ and t_j is bounded by:

$$\left| x(\tau) - x(t_j) \right| \leq M\Delta \tag{4.26}$$

for all $\tau \in [t_j, t_{j+1})$. From Eq. 4.24 and Eq. 4.26 and for any $x(t_j) \in \Omega_\rho \setminus \Omega_{\rho_s}$, the inequality below follows:

$$\dot{V}(x(\tau)) \leq -\alpha_3(\alpha_2^{-1}(\rho_s)) + L_x' M\Delta + L_w' \theta \tag{4.27}$$

for all $\tau \in [t_j, t_{j+1})$ where the fact that $|x| \geq \alpha_2^{-1}(\rho_s)$ for all $x \in \Omega_\rho \setminus \Omega_{\rho_s}$ follows from Eq. 4.5a.

If the condition of Eq. 4.16 is satisfied, there exists $\varepsilon_w > 0$ such that the following inequality holds for $x(t_j) \in \Omega_\rho \setminus \Omega_{\rho_s}$

$$\dot{V}(x(\tau)) \leq -\varepsilon_w/\Delta$$

for all $\tau \in [t_j, t_{j+1})$. Integrating the bound for $\tau \in [t_j, t_{j+1})$, the following two bounds on the Lyapunov function value are obtained:

$$V(x(t_{j+1})) \leq V(x(t_j)) - \varepsilon_w \tag{4.28}$$

$$V(x(\tau)) \leq V(x(t_j)),\ \forall\ \tau \in [t_j, t_{j+1}) \tag{4.29}$$

for all $x(t_j) \in \Omega_\rho \setminus \Omega_{\rho_s}$ and when mode 2 operation of the lower layer LMPC is active.

If $x(t_j) \in \Omega_\rho \setminus \Omega_{\rho_e}$, the closed-loop state converges to Ω_{ρ_e} in a finite number of sampling times without leaving the stability region Ω_ρ which follows by applying Eq. 4.28 recursively. If $t_j \geq t_s$ and $x(t_j) \in \Omega_\rho \setminus \Omega_{\rho_s}$, the closed-lop state converges to Ω_{ρ_s} in a finite number of sampling times without leaving the stability region Ω_ρ (again, by recursive application of Eq. 4.28). Moreover, once the state converges to Ω_{ρ_s}, it remains inside $\Omega_{\rho_{\min}}$ for all times. This statement holds by the definition of $\rho_{\min}$. Therefore, from Case 1 and Case 2, the fact that the closed-loop state is bounded in Ω_ρ for all $t \geq 0$ when $x(0) \in \Omega_\rho$ follows.

Part 3: If t_s is finite, the lower layer LMPC will switch to mode 2 operation only and

the closed-loop state will be ultimately bounded in $\Omega_{\rho_{\min}}$, which follows from Part 2. $\square$

4.2.3 Application to a Chemical Process

The two-layer framework for dynamic economic optimization and process control is implemented on the benchmark chemical reactor example presented in Section 1.3.1. Recall, the nonlinear dynamic model that describes the evolution of the reactor (Eqs. 1.5-1.8) has four states: the vapor density in the reactor (x_1), the ethylene concentration in the reactor (x_2), the ethylene oxide concentration in the reactor (x_3), and the reactor temperature (x_4) and three inputs: the volumetric flow rate of the reactor feed, the ethylene concentration in the reactor feed, and the reactant coolant temperature. With abuse of notation with the notation used to denote the two sets of inputs in Eq. 4.3, the notation u_1, u_2, and u_3 is used to denote the three inputs, respectively. The reactor has an asymptotically stable steady-state:

$$x_s^T = [0.998\ 0.424\ 0.032\ 1.002] \tag{4.30}$$

which corresponds to the steady-state input:

$$u_{1,s} = 0.35,\ u_{2,s} = 0.5,\ u_{3,s} = 1.0\ . \tag{4.31}$$

The control objective considered here is to optimize the time-averaged yield of ethylene oxide by operating the reactor in a time-varying fashion around the stable steady-state. Owing to the fact that closed-loop stability is not an issue for this application, the optimization and control framework operates with mode 1 operation only. The time-averaged

yield of ethylene oxide over an operating length of t_f is given by

$$Y = \frac{\int_0^{t_f} x_3(t)x_4(t)u_1(t)\ dt}{\int_0^{t_f} u_1(t)u_2(t)\ dt}\ . \tag{4.32}$$

Owing to practical considerations, the average amount of ethylene that may be fed into the process over the length of operation is constrained to be equal to that when uniformly distributing the reactant material to the reactor which is given by the following integral constraint:

$$\frac{1}{t_f}\int_0^{t_f} u_1(t)u_2(t)dt = u_{1,s}u_{2,s} = 0.175 \tag{4.33}$$

where $u_{1,s}$ and $u_{2,s}$ are the steady-state inlet volumetric flow rate and ethylene concentration, respectively. Since the average ethylene fed to the reactor is fixed, which fixes the denominator of the yield (Eq. 4.32), the economic stage cost used in the formulation of the upper layer LEMPC is

$$l_e(x,u) = -x_3x_4u_1\ . \tag{4.34}$$

In the implementation of the two-layer dynamic optimization and control framework, the manipulated inputs are partitioned into two sets. The first set of manipulated inputs consists of the inlet flow rate and ethylene feed concentration inputs. As pointed out in Section 2.2, periodic switching of these two inputs may improve economic performance. Additionally, these two inputs are constrained by the integral constraint of Eq. 4.33. Therefore, the first set of inputs is controlled by the upper layer LEMPC, i.e., the upper layer LEMPC computes control actions for these manipulated inputs that are applied to the reactor. The second set of manipulated inputs consists of the coolant temperature input that the lower layer LMPC (Eq. 4.9) controls.

To characterize the region Ω_{ρ_e}, which is used in the two-layer framework design, an

explicit stabilizing controller is designed and a Lyapunov function is constructed. Specifically, the explicit controller is designed as a proportional controller for the input u_3: $h_2(x) = K(x_3 - x_{s,3}) + u_{s,3}$ with $K = 0.1$. A quadratic Lyapunov function is found for the closed-loop reactor under the proportional controller, which is given by:

$$V(x) = (x - x_s)^T P (x - x_s)$$

where $P = \text{diag}([10\ 0.01\ 10\ 10])$. The closed-loop stability region of the reactor under the explicit controller with the inputs u_1 and u_2 fixed at their steady-state values is taken to be a level set of the Lyapunov function where the time-derivative of the Lyapunov function is negative definite for all points contained in the level set. The constructed level set is subsequently taken to be Ω_{ρ_e} with $\rho_e = 0.53$ and in this case, $\Omega_\rho = \Omega_{\rho_e}$. The prediction horizon of the upper layer LEMPC and lower layer LMPC are $N_E = 47$ and $N = 3$, respectively, the sampling period is $\Delta = 1.0$, the number of sampling times that the upper layer LEMPC is recomputed is $K_E = 47$, which is the same as the prediction horizon in this case, and a shrinking horizon employed in the lower layer LMPC when the prediction horizon extends past the time that the upper layer optimal trajectory is defined. To ensure that the integral constraint of Eq. 4.33 is satisfied over the length of operation, the computed input trajectory of the upper layer LEMPC must satisfy the integral constraint, i.e., it is enforced over each operating windows of length 47 (dimensionless time). The weighting matrices of the lower layer LMPC are $Q_c = P$, and $R_c = 0.01$ which have been tuned to achieve close tracking of the optimal trajectory. The optimization problems of upper layer LEMPC and lower layer LMPC are solved using Ipopt [187].

In the first set of simulations, the two-layer framework is applied to the reactor without disturbances or plant-model mismatch. The reactor is initialized at a transient initial

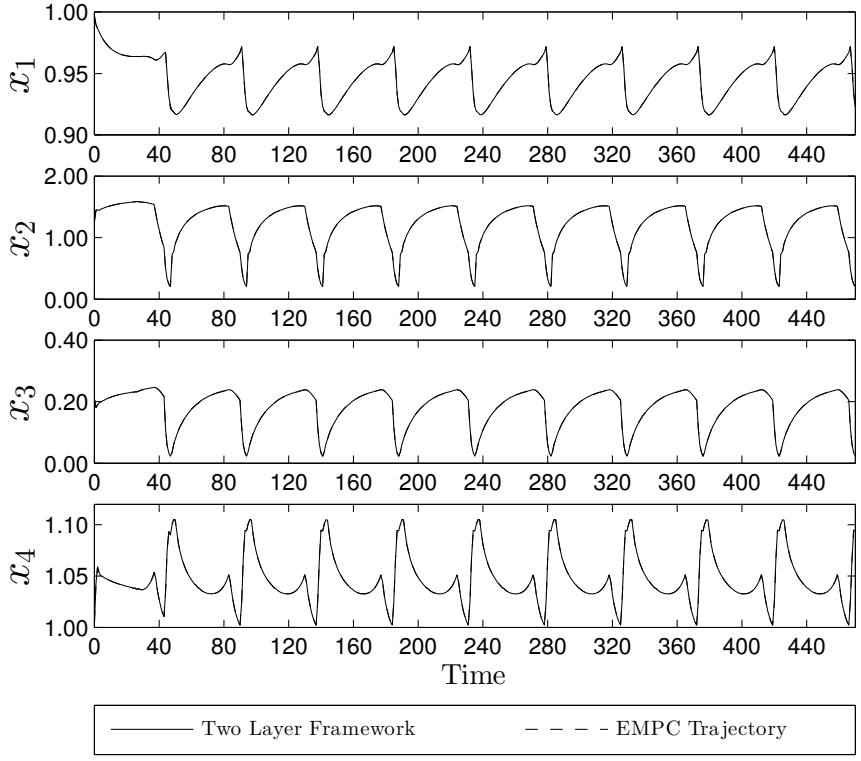

Figure 4.2: The closed-loop state trajectories of the reactor under the two-layer dynamic economic optimization and control framework (the two trajectories are overlapping).

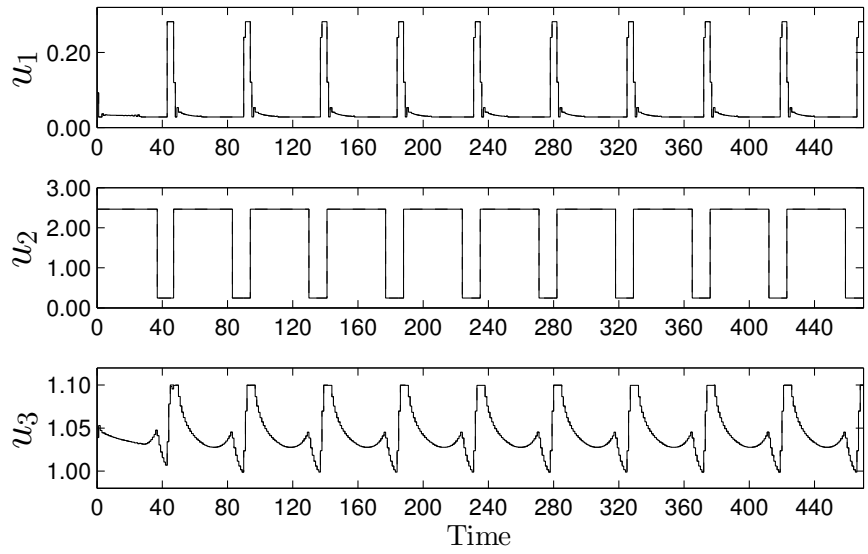

Figure 4.3: The closed-loop input trajectories computed by two-layer dynamic economic optimization and control framework (the two trajectories are overlapping).

condition given by:

$$x_0^T = [0.997\ 1.264\ 0.209\ 1.004]\ .$$

The closed-loop state and input trajectories of the reactor under the two-layer optimization and control framework are shown in Figs. 4.2-4.3, respectively. From the state trajectories (Fig. 4.2), the lower layer LMPC is able to force the system to track the optimal state trajectory. Recall, the sampling periods of the upper and lower layer are the same, and the closed-loop system is not subjected to any uncertainties or disturbances. Therefore, perfect tracking of the optimal trajectory is expected.

As described above, the main motivation for the design of a two-layer optimization and control architecture is to achieve a computation benefit relative to a one-layer EMPC approach. To compare the computational time of the two-layer framework with a one-layer EMPC approach, a one-layer LEMPC implementation is considered. The LEMPC is implemented with mode 1 operation only and with a shrinking prediction horizon. The shrinking

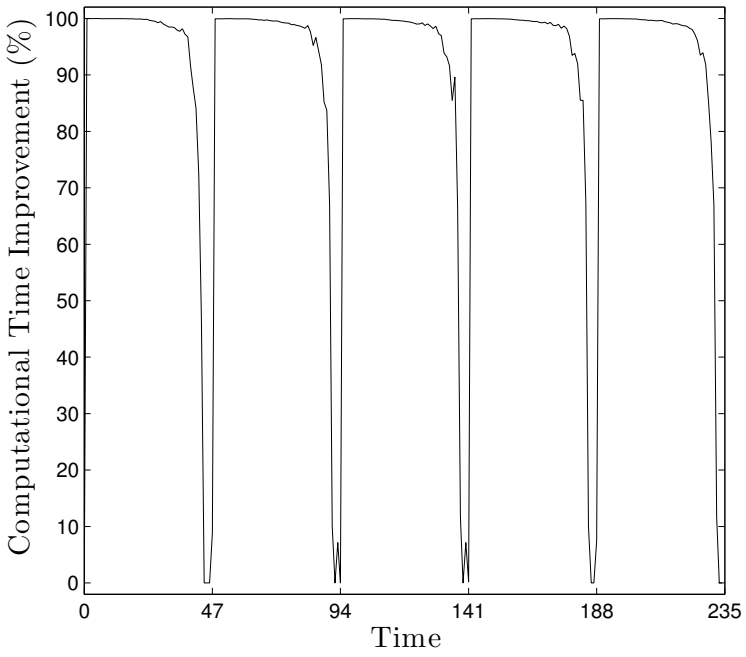

Figure 4.4: The computational time reduction of the two-layer optimization and control framework relative to the one-layer implementation of LEMPC.

horizon implementation is described as follows: the LEMPC is initialized with a prediction horizon of 47 (dimensionless time) and at every subsequent sampling time, the prediction horizon is decreased by one sampling period. Every 47 sampling times, the prediction horizon is reset to 47. It is important to point out that the closed-loop performance achieved under the two-layer LEMPC and that under the one-layer LEMPC are equal owing to the fact there is no plant-model mismatch. Also, a fixed-horizon one-layer LEMPC implementation strategy requires more computation time on average relative to the shrinking horizon implementation.

Fig. 4.4 gives the computational time reduction achieved with the two-layer optimization and control framework relative to the one-layer LEMPC implementation. For this example, the lower layer LMPC computation time is insignificant compared to the computation time of the upper layer LEMPC. The two-layer framework only solves the LEMPC

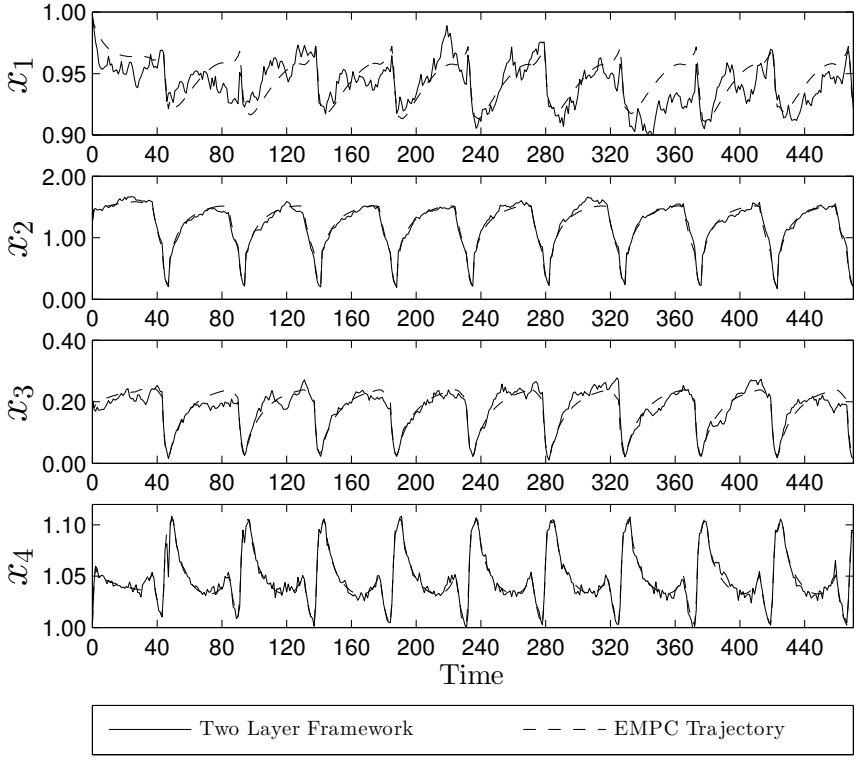

Figure 4.5: The closed-loop state trajectories of the catalytic reactor under the two-layer dynamic economic optimization and control framework and with process noise added to the states.

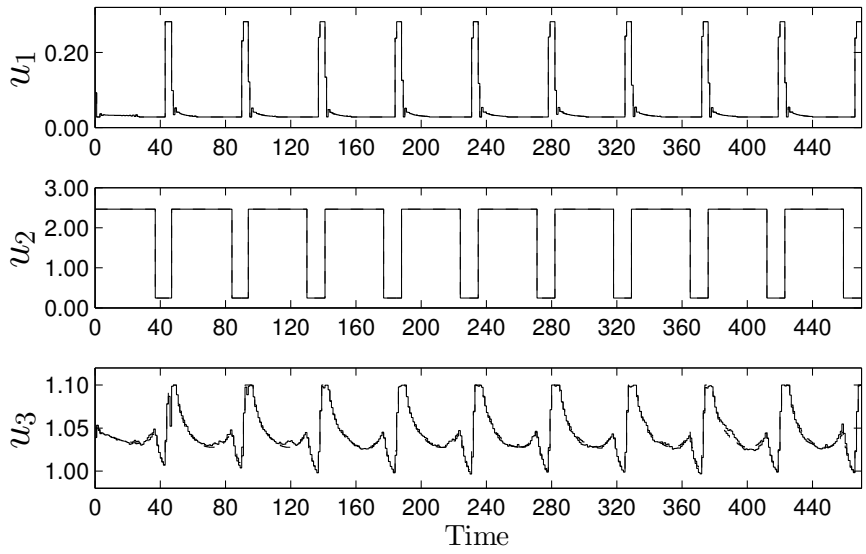

Figure 4.6: The closed-loop input trajectories computed by two-layer dynamic economic optimization and control framework and with process noise added to the states (the two trajectories are nearly overlapping).

optimization problem once every 47 sampling times. Every 47 sampling times when the upper layer LEMPC is solved and at the end of each operating interval of length 47 when the one-layer LEMPC horizon has decreased to a comparable length as the horizon of the lower layer LEMPC, the computational burden of the two-layer framework compared to that of the one-layer LEMPC is comparable, i.e., approximately a zero percent computational time improvement is achieved (Fig. 4.4). For the other sampling times, the computation of the LMPC which computes control actions for the set of manipulated inputs u_2 is much better than that compared to the one-layer LEMPC. For this case, an average of 89.4 percent reduction of the computational time with the two-layer framework was achieved relative to that of the one-layer LEMPC implementation.

In the second set of simulations, significant process noise was added to the system states. The noise is assumed to be bounded Gaussian white noise with zero mean and standard deviation of 0.005, 0.03, 0.01, and 0.02 and bounds given by 0.02, 0.1, 0.03, and

0.08 for the four states, respectively. To simulate the process noise, a new random number is generated and applied to the process over each sampling period. The results of a closed-loop simulation are shown in Figs. 4.5-4.6. Because of the added process noise, the lower layer LMPC is not able to force the closed-loop state to perfectly track the economically optimal state trajectory. The added process noise has an effect on the closed-loop economic performance. However, this effect was minimal in the sense that the time-averaged yield of the closed-loop system under the two-layer framework is 10.3 percent with the added process disturbance and 10.4 percent without the added process disturbance. Even with the process noise, the closed-loop reactor performance is better than that at the steady-state (the yield at steady-state is 6.4 percent).

4.3 Unifying Optimization with Time-Varying Economics and Control

In the previous section, a two-layer framework for dynamic optimization and control is presented. However, the framework treats the economic considerations, e.g., demand, energy pricing, variable feedstock quality, and product grade changes as time-invariant. This paradigm may be effective, especially for the applications where there is a sufficient time-scale separation between the time constants of the process/system dynamics and the update frequency of the economic parameters. However, including the time-variation of the economic considerations in the formulation of the economic stage cost may be needed to achieve good closed-loop performance when the time-scales are comparable. One class of examples where there may not be such a time-scale separation is energy systems where the energy price may change frequently.

In this section, a two-layer framework for optimization and control of systems of the

form of Eq. 3.1 is considered where the economic stage cost may be time-dependent in the sense that the system of Eq. 3.1 is equipped with a time-dependent economic cost $l_e : [0,\infty) \times \mathbb{X} \times \mathbb{U} \to \mathbb{R}$ that is continuous over its domain. The framework design is similar to that in the previous section. Specifically, the upper layer dynamic economic optimization problem (EMPC) is used to generate an economically optimal state trajectory defined over a finite-time horizon. In the lower layer, a tracking MPC is used to force the states to track the economically optimal trajectory. However, the main differences of the two-layer approach presented in this section compared to that of the previous section are the EMPC is formulated with an economic stage cost that may be explicitly time-dependent, the formulations of the layers are different, and the underlying theory and analysis are different.

Explicit constraints are used in the upper layer dynamic optimization problem to ensure that the lower layer tracking MPC may force the closed-loop state to track the trajectory computed in the optimization layer. In particular, the optimization layer is constrained to compute an optimal trajectory that is slowly time-varying. The resulting slowly time-varying trajectory vector is denoted as $x_E(t) \in \Gamma \subset \mathbb{R}^n$ for $t \geq 0$ where Γ is a compact set and the rate of change of the reference trajectory is bounded by

$$|\dot{x}_E(t)| \leq \gamma_E \tag{4.35}$$

for all $t \geq 0$. The deviation between the actual state trajectory and the slowly-varying reference trajectory is defined as $e := x - x_E$ with its dynamics described by

$$\begin{aligned} \dot{e} &= f(x,u,w) - \dot{x}_E \\ &= f(e + x_E, u, w) - \dot{x}_E \\ &=: g(e, x_E, \dot{x}_E, u, w) \ . \end{aligned} \tag{4.36}$$

The state e of the system of Eq. 4.36 will be referred to as the deviation state in the remainder of this section.

Assumption 4.2. *The system of Eq. 4.36 has a continuously differentiable, isolated equilibrium for each fixed $x_E \in \Gamma$, i.e., there exists a $\hat{u} \in \mathbb{U}$ for a fixed $x_E \in \Gamma$ to make $e = 0$ the equilibrium of Eq. 4.36 ($g(0, x_E, 0, \hat{u}, 0) = 0$).*

In what follows, the upper layer EMPC computes a reference trajectory that evolves according to the nominal system dynamics $\dot{x}_E = f(x_E, u_E, 0)$ while maintaining the state trajectory to be in the set Γ where Γ is an equilibrium manifold in the sense that $\Gamma = \{x_E \in \mathbb{X} : \exists\, u_E \in \mathbb{U} \text{ s.t. } f(x_E, u_E, 0) = 0\}$. Nevertheless, the theory applies to a more general case where the following hold: $|\dot{x}_E| \leq \gamma_E$, Γ is compact and Assumption 4.2 is satisfied. One conceptually straightforward extension of the two-layer framework is to consider steady-state optimization in the upper layer instead of dynamic optimization. Specifically, x_E could be taken as a steady-state and varied slowly to account for the time-varying economic considerations.

4.3.1 Stabilizability Assumption

For each fixed $x_E \in \Gamma$, there exists a Lyapunov-based controller that makes the origin of the nonlinear system given by Eq. 4.36 without uncertainty ($w \equiv 0$) asymptotically stable under continuous implementation. This assumption is essentially equivalent to the assumption that the nominal system of Eq. 3.1 is stabilizable at each $x_E \in \Gamma$. More specifically, for each fixed $x_E \in \Gamma$, the existence of a mapping $h : D_s \times \Gamma \to \mathbb{U}$ and a continuously differentiable function $V : D_s \times \Gamma \to \mathbb{R}_+$ is assumed that satisfies:

$$\alpha_1(|e|) \leq V(e, x_E) \leq \alpha_2(|e|), \tag{4.37a}$$

$$\frac{\partial V(e,x_E)}{\partial e} g(e,x_E,0,h(e,x_E),0) \leq -\alpha_3(|e|), \tag{4.37b}$$

$$\left| \frac{\partial V(e,x_E)}{\partial e} \right| \leq \alpha_4(|e|), \tag{4.37c}$$

$$\left| \frac{\partial V(e,x_E)}{\partial x_E} \right| \leq \alpha_5(|e|), \tag{4.37d}$$

for all $e \in D_s$ where $\alpha_i \in \mathscr{K}$, $i = 1,2,3,4,5$, D_s is an open neighborhood of the origin, and h is the Lyapunov-based controller. In this sense, the function V is a Lyapunov function for each $x_E \in \Gamma$. While the inequalities of Eqs. 4.37a-4.37c are similar to the inequalities of standard Lyapunov functions, Eq. 4.37d is needed to account for the time-varying nature of x_E. More precisely, the special requirement that the inequalities hold uniformly in x_E is required to handle the perturbation, which results from the fact that x_E is not constant, but rather, a time-varying function.

For a fixed $x_E \in \Gamma \subset \mathbb{R}^n$, the symbol $\Omega_{\rho(x_E)}$ is a level set of the Lyapunov function, i.e., $\Omega_{\rho(x_E)} := \{e \in \mathbb{R}^n : V(e,x_E) \leq \rho(x_E)\}$ where $\rho(x_E) > 0$ depends on x_E. The region $\Omega_{\rho*}$ is the intersection of stability regions $\Omega_{\rho(x_E)}$ of the closed-loop system under the Lyapunov-based controller for all $x_E \in \Gamma$.

For broad classes of nonlinear systems arising in the context of chemical process control applications, quadratic Lyapunov functions using state deviation variables, i.e., $V(x) = (x-x_s)^T P(x-x_s)$, where x_s is a steady-state, have been widely used and have been demonstrated to yield acceptable estimates of closed-loop stability regions (see [33] and the references therein). In the example of Section 4.3.3, a quadratic Lyapunov function is used where instead of a fixed equilibrium x_s a time-varying reference trajectory x_E is used, i.e., at time t, the Lyapunov function is given by: $V(e(t),x_E(t)) = e(t)Pe(t)$ where $e(t) = x(t) - x_E(t)$.

Remark 4.1. If the equilibrium point $e = 0$ of the frozen system forced by an explicit controller ($\dot{e} = g(e,x_E,0,h(e,x_E),0)$) is exponentially stable uniformly in x_E and under some

additional mild smoothness requirements, then there exists a Lyapunov function satisfying Eqs. 4.37a-4.37d [100, Lemma 9.8].

Remark 4.2. The set $\Omega_{\rho*}$ is such that for any $e \in \Omega_{\rho*}$, the ability to drive the state with the Lyapunov-based controller asymptotically to any fixed $x_E \in \Gamma$ is guaranteed. This set may be estimated in the following way: first, the set Γ is chosen. Second, the regions $\Omega_{\rho(x_E)}$ for a sufficiently large number of x_E in the set Γ are estimated. The regions $\Omega_{\rho(x_E)}$ may be estimated as the level set (ideally the largest) of V for a fixed $x_E \in \Gamma$ where $\dot{V} < 0$ with the Lyapunov-based controller. Lastly, the stability region $\Omega_{\rho*}$ may be constructed from the intersection of these computed regions. It is important to point out that the design of the upper layer EMPC does not employ $\Omega_{\rho*}$. Therefore, for practical design purposes, an explicit construction of $\Omega_{\rho*}$ is not needed.

4.3.2 Two-layer EMPC Scheme Addressing Time-Varying Economics

In this section, the two-layer framework for dynamic economic optimization and control for handling time-varying economics is described and the stability and robustness properties of the closed-loop system are given.

Formulation and Implementation

To address time-dependent economics, a two-layer framework is presented. The two-layer framework for optimization and control may be considered an intermediate approach between existing steady-state operation and one-layer EMPC schemes. A block diagram of the two-layer control framework is given in Fig. 4.7. In this framework, optimization and control are effectively divided into separate tasks. However, the upper optimization layer is formulated with specific control-oriented constraints to ensure stability. In the upper layer, an EMPC, formulated with a time-varying economic stage cost, computes economically

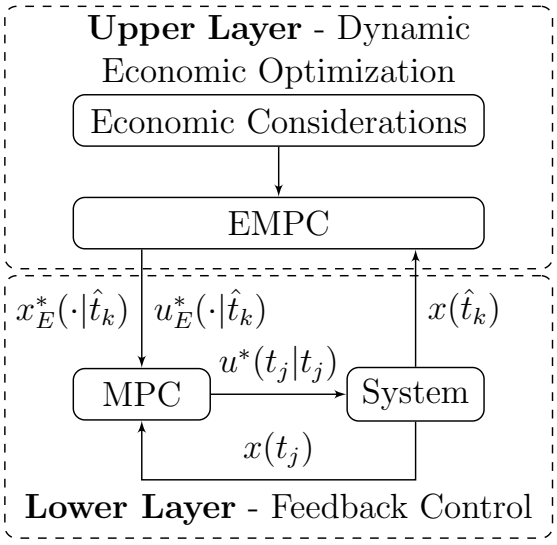

Figure 4.7: A block diagram of the dynamic economic optimization and control framework for handling time-varying economics.

optimal state and input trajectories over a finite-time horizon. The optimal trajectories are sent down to a lower layer tracking MPC to force the system to track the economically optimal state trajectory. For computational efficiency, the EMPC optimization problem is solved infrequently, i.e., it does not employ a standard receding horizon implementation strategy. Instead, the operating time is partitioned into finite-time intervals of length t' called operating periods. The operating period is chosen based on the time-scale of the process dynamics and update frequency of the economic parameters in the economic cost function, e.g., the update frequency of the energy price, product demand, or product transitions. The length of the operating period may be considered a tuning parameter of the control architecture. At the beginning of each operating period, the EMPC problem is initialized with a state measurement and is solved. The lower layer tracking MPC is solved every sampling time to maintain closed-loop stability and robustness and is formulated with a stage cost that penalizes deviations from the optimal trajectory. While in the lower layer any MPC tracking controller could be used, Lyapunov-based MPC (LMPC) is used here

owing to its unique stability and robustness properties.

An overview of the implementation strategy is as follows (a detailed algorithm is given below after the formulations of the control problems are given). The operating time is divided into finite-time operating periods of length $t' = K_E \Delta_E$ where K_E is some integer greater than or equal to one. At the beginning of the operating period denoted by $\hat{t}_k = kt'$ where $k = 0, 1, \ldots$, the upper layer EMPC, with hold period $\Delta_E > 0$ (zeroth-order control parameterization is employed in the upper layer EMPC) and prediction horizon of $T_E = N_E \Delta_E$ where $N_E \in \mathbb{I}_+$, receives a state measurement and computes the economically optimal state and input trajectories. The prediction horizon of the EMPC is chosen to be sufficiently large to cover the operating period plus the transition to the next operating period, i.e., $T_E \geq t' + T$ where $T = N\Delta$ is the prediction horizon of the lower layer LMPC, $\Delta > 0$ denotes the sampling period of the lower layer LMPC that is less than or equal to Δ_E, and $N \in \mathbb{I}_+$ is the number of sampling periods in the prediction horizon of the LMPC. Between $\hat{t}_k$ and $\hat{t}_k + t'$, the lower layer LMPC computes control actions that work to force the closed-loop state to track the optimal trajectories.

The upper layer EMPC optimization problem is as follows:

$$\min_{u_E \in S(\Delta_E)} \int_{\hat{t}_k}^{\hat{t}_k + T_E} l_e(\tau, x_E(\tau), u_E(\tau))\, d\tau \tag{4.38a}$$

$$\text{s.t.} \quad \dot{x}_E(t) = f(x_E(t), u_E(t), 0) \tag{4.38b}$$

$$x_E(\hat{t}_k) = \operatorname*{proj}_{\Gamma}(x(\hat{t}_k)) \tag{4.38c}$$

$$u_E(t) \in \mathbb{U},\ \forall\, t \in [\hat{t}_k, \hat{t}_k + T_E) \tag{4.38d}$$

$$|\dot{x}_E(t)| \leq \gamma_E,\ \forall\, t \in [\hat{t}_k, \hat{t}_k + T_E) \tag{4.38e}$$

$$x_E(t) \in \Gamma,\ \forall\, t \in [\hat{t}_k, \hat{t}_k + T_E) \tag{4.38f}$$

where $S(\Delta_E)$ is the family of piecewise constant functions with period Δ_E, l_e is the time-

dependent economic measure which defines the cost function, the state x_E is the predicted trajectory of the system with the input trajectory u_E computed by the EMPC and $x(\hat{t}_k)$ is the state measurement obtained at time $\hat{t}_k$. The optimal state and input trajectory computed by the EMPC are denoted as $x_E^*(t|\hat{t}_k)$ and $u_E^*(t|\hat{t}_k)$ defined for $t \in [\hat{t}_k, \hat{t}_k + T_E)$, respectively.

In the optimization problem of Eq. 4.38, the constraint of Eq. 4.38b is the nominal dynamic model of the system ($w \equiv 0$) used to predict the future evolution under the sample-and-hold input trajectory. The constraint of Eq. 4.38c defines the initial condition of the optimization problem which is a projection of the state measurement at $\hat{t}_k$ onto the set Γ where the symbol $\text{proj}_\Gamma(x)$ denotes the projection of x onto the set Γ. The constraint of Eq. 4.38d ensures that the computed input trajectory take values in the set of admissible inputs. The constraint of Eq. 4.38f limits the rate of change of the economically optimal state trajectory. Finally, the constraint of Eq. 4.38f ensures that the state evolution is maintained in the region Γ.

The constraint of Eq. 4.38c is used to ensure that the optimization problem is feasible. The projection operator may be any projection operator that projects the current state $x(\hat{t}_k)$ onto a near (ideally the nearest) point in the set Γ. In some cases, when the sampling periods of the upper and lower layers and the bounded disturbance are sufficiently small, it may also be sufficient to use the predicted state $x_E^*(\hat{t}_k|\hat{t}_{k-1})$ derived from the solution of the optimization problem of Eq. 4.38 that was solved at the beginning of the preceding operating period. Another potential option is to allow for the initial condition $x_E(\hat{t}_k)$ be a decision variable in the optimization problem by including another term in the objective function penalizing the deviation of the computed initial condition from the current state $x(\hat{t}_k)$. In this sense, the framework offers a degree of flexibility in the selection of the projection operator.

The last two constraints of the optimization problem of Eq. 4.38 are used to guarantee closed-loop stability under the integrated framework and to ensure that the lower layer may

force the system to track the optimal state trajectory, i.e., they are control-oriented constraints. This is a departure from other types of two-layer dynamic economic optimization and control architectures featuring, for example, dynamic real-time optimization in the upper optimization layer. Also, the constraint imposed in the upper layer EMPC on the rate of change of the optimal trajectory (Eq. 4.38e) does pose a restriction on the feasible set of the optimization problem of Eq. 4.38 and could affect closed-loop economic performance achieved under the resulting two-layer framework. However, allowing the optimal state trajectory to have a large rate of change may be undesirable for many applications based on practical considerations like excessive strain on control actuators as well as the difficulty of forcing the system to track a rapidly changing reference trajectory in the presence of disturbances.

At the lower feedback control level, LMPC is employed to force the state to track the economically optimal state trajectory. The LMPC is implemented with a standard receding horizon implementation, i.e., LMPC recomputes an updated input trajectory synchronously every sampling time. Let $\{t_j\}_{j\geq 0}$ where $t_j = j\Delta,\ j = 0,1,\ldots$ denote the sampling time sequence of the LMPC. Also, the dynamic model used in the LMPC is that of Eq. 4.36, which is the deviation system. The LMPC optimization problem is given by:

$$\min_{u\in S(\Delta)} \int_{t_j}^{t_j+T} \left(|\tilde{e}(\tau)|^2_{Q_c} + |u(\tau) - u^*_E(\tau|\hat{t}_k)|^2_{R_c} \right) d\tau \tag{4.39a}$$

$$\text{s.t} \quad \dot{\tilde{e}}(t) = g(\tilde{e}(t), x^*_E(t|\hat{t}_k), \dot{x}^*_E(t|\hat{t}_k), u(t), 0) \tag{4.39b}$$

$$\tilde{e}(t_j) = x(t_j) - x^*_E(t_j|\hat{t}_k) \tag{4.39c}$$

$$u(t) \in \mathbb{U},\ \forall\, t \in [t_j, t_j + T) \tag{4.39d}$$

$$\begin{aligned} &\frac{\partial V(\tilde{e}(t_j), x^*_E(t_j|\hat{t}_k))}{\partial e} g(\tilde{e}(t_j), x^*_E(t_j|\hat{t}_k), 0, u(t_j), 0) \\ &\quad \leq \frac{\partial V(\tilde{e}(t_j), x^*_E(t_j|\hat{t}_k))}{\partial e} g(\tilde{e}(t_j), x^*_E(t_j|\hat{t}_k), 0, h(\tilde{e}(t_j), x_E(t_j|\hat{t}_k)), 0) \end{aligned} \tag{4.39e}$$

where $S(\Delta)$ is the family of piecewise constant functions with sampling period Δ, N is the prediction horizon of the LMPC, $\tilde{e}$ is the predicted deviation between the state trajectory predicted by the nominal model under the input trajectory computed by the LMPC and the economically optimal state trajectory $x_E^*(\cdot|\hat{t}_k)$. The optimal solution of the optimization problem of Eq. 4.39 is denoted by $u^*(t|t_j)$ defined for $t \in [t_j, t_{j+N})$.

In the optimization problem of Eq. 4.39, the constraint of Eq. 4.39b is the nominal model of the deviation system. The constraint of Eq. 4.39c is the initial condition to the dynamic optimization problem. The constraint of Eq. 4.39d defines the control energy available to all manipulated inputs. The constraint of Eq. 4.39e ensures that the Lyapunov function of the closed-loop system with LMPC decreases by at least the rate achieved by the Lyapunov-based controller. The last constraint ensures that the closed-loop state trajectory converges to a neighborhood of the optimal state trajectory computed by the upper layer EMPC.

The implementation strategy of the dynamic economic optimization and control framework is summarized by the following algorithm.

1. At $\hat{t}_k$, the EMPC receives a state measurement $x(\hat{t}_k)$ and projects the current state $x(\hat{t}_k)$ onto the set Γ. Go to Step 2.

2. The EMPC computes the economically optimal state and input trajectories: $x_E^*(t|\hat{t}_k)$ and $u_E^*(t|\hat{t}_k)$ defined for $t \in [\hat{t}_k, \hat{t}_k + T_E)$. Go to Step 3.

3. For $\hat{t}_k$ to $\hat{t}_k + t'$ (one operating period), repeat:

    3.1 The LMPC receives a state measurement $x(t_j)$ and computes the deviation of the current state from the optimal state trajectory. The error $e(t_j)$ is used to initialize the dynamic model of the LMPC. Go to Step 3.2.

3.2 The LMPC optimization problem is solved to compute an optimal input trajectory $u^*(t|t_j)$ defined for $t \in [t_j, t_j + T)$. Go to Step 3.3.

3.3 The control action computed for the first sampling period of the prediction horizon is sent to the control actuators to be applied from t_j to t_{j+1}. If $t_{j+1} > \hat{t}_k + t'$, go to Step 4 and let $j \leftarrow j+1$. Else, go to 3.1 and let $j \leftarrow j+1$.

4. Go to Step 1, $k \leftarrow k+1$.

Stability Analysis

In this subsection, the stability properties of the two-layer control framework with the EMPC of Eq. 4.38 in the upper layer and the LMPC of Eq. 4.39 in the lower layer when applied the system of Eq. 3.1. Before these properties may be presented, several properties are presented that are needed in the analysis. Owing to the fact that $\Omega_{\rho*}$, Γ, $\mathbb{U}$, and $\mathbb{W}$ are compact sets and f is locally Lipschitz, there exists $M_x > 0$ such that

$$|f(e + x_E, u, w)| \leq M_x \tag{4.40}$$

for all $e \in \Omega_{\rho*}$, $x_E \in \Gamma$, $u \in \mathbb{U}$, and $w \in \mathbb{W}$. From similar conditions and since the rate of change of x_E is bounded, there exists $M > 0$ such that

$$|g(e, x_E, \dot{x}_E, u, w)| \leq M \tag{4.41}$$

for all $e \in \Omega_{\rho*}$, $x_E \in \Gamma$, $u \in \mathbb{U}$, $w \in \mathbb{W}$ and $|\dot{x}_E| \leq \gamma_E$. In addition, since the Lyapunov function V is continuously differentiable (in both arguments) and the fact that f is locally Lipschitz, there exist positive constants L_e, L_w, L'_e, L'_E, L''_E, L'_w such that

$$\left|g(e, x_E, \dot{x}_E, u, w) - g(e', x_E, \dot{x}_E, u, 0)\right| \leq L_e|e - e'| + L_w|w|, \tag{4.42}$$

$$\begin{aligned}&\left|\frac{\partial V(e,x_E)}{\partial e}g(e,x_E,\dot{x}_E,u,w)-\frac{\partial V(e',x'_E)}{\partial e}g(e',x'_E,\dot{x}'_E,u,0)\right|\\&\leq L'_e|e-e'|+L'_E|x_E-x'_E|+L''_E|\dot{x}_E-\dot{x}'_E|+L'_w|w|\end{aligned}\tag{4.43}$$

for all e, $e' \in \Omega_{\rho*}$, x_E, $x'_E \in \Gamma$, $u \in \mathbb{U}$, $w \in \mathbb{W}$, $|\dot{x}_E| \leq \gamma_E$, and $|\dot{x}'_E| \leq \gamma_E$.

The following Lemma gives the feasibility properties of the EMPC and therefore, by the constraint of Eq. 4.38f, the optimal state trajectory $x_E^*(t|\hat{t}_k)$ is embedded in the set Γ for $t \in [\hat{t}_k, \hat{t}_{k+1}]$.

Lemma 4.1. *Consider the system of Eq. 4.38b over the prediction horizon. If Assumption 4.2 is satisfied, the optimization problem of Eq. 4.38 is feasible and therefore, the optimal state trajectory $x_E^*(t|\hat{t}_k)$ for $t \in [\hat{t}_k, \hat{t}_k + T_E]$ computed by applying the optimal input trajectory $u_E^*(t|\hat{t}_k)$ defined for $t \in [\hat{t}_k, \hat{t}_k + T_E)$ is always embedded in the set Γ.*

Proof. When the EMPC optimization problem of Eq. 4.38 is solved with an initial condition satisfying $x_E(\hat{t}_k) \in \Gamma$ (this is guaranteed through the projection procedure), the feasibility of the optimization problem follows if Assumption 4.2 is satisfied because maintaining the state at the initial condition along the predicted horizon is a feasible solution to the optimization problem as it satisfies all the constraints, i.e., there exists a constant input trajectory $u_E(t) = \bar{u}_E \in \mathbb{U}$ for $t \in [\hat{t}_k, \hat{t}_k + T_E)$ that maintains the state trajectory at its initial condition: $x_E(t) = \text{proj}_\Gamma(x(\hat{t}_k))$ for $t \in [\hat{t}_k, \hat{t}_k + T_E)$. Owing to the fact that the problem is feasible and imposing the constraint of Eq. 4.38f, the optimal state trajectory $x_E^*(t|\hat{t}_k)$ is bounded in the set Γ for $t \in [\hat{t}_k, \hat{t}_k + T_E]$. □

Theorem 4.2 provides sufficient conditions such that the LMPC may track the economically optimal trajectory x_E^*. More specifically, the deviation state gets small over time until it is bounded in a small ball containing the origin.

Theorem 4.2. *Consider the system of Eq. 3.1 in closed-loop under the tracking LMPC of Eq. 4.39 based on the Lyapunov-based controller that satisfies the conditions of Eqs. 4.37a-*

4.37d with the reference trajectory x_E^* computed by the upper layer EMPC of Eq. 4.38. Let $\varepsilon_{error} > 0$, $\mu > 0$, $\varepsilon_w > 0$, $\Delta > 0$, $\Delta_E > 0$, $N \geq 1$, $N_E \geq 1$, $N_E \Delta_E \geq t' + N\Delta$, *and* $\gamma_E > 0$ *satisfy*

$$\mu > \alpha_3^{-1}\left(\frac{(L_x' M + L_E' \gamma_E)\Delta + \alpha_5(\alpha_1^{-1}(\rho*))\gamma_E + L_w'\theta}{\hat{\theta}}\right) \tag{4.44}$$

for some $\hat{\theta} \in (0,1)$,

$$\varepsilon_{error} = \max_{s\in[0,\Delta]} \{|e(s)| : e(0) \in B_\mu \text{ for all } x_E \in \Gamma\}\ , \tag{4.45}$$

and $B_\mu \subset B_{\varepsilon_{error}} \subset \Omega_{\rho*}$. *If* $(x(0) - x_E^*(0)) \in \Omega_{\rho*}$, *then the deviation state of the system of Eq. 4.36 is always bounded in* $\Omega_{\rho*}$ *and therefore, also, the closed-loop state trajectory x is always bounded. Furthermore, the deviation between the state trajectory of Eq. 3.1 and the economically optimal trajectory is ultimately bounded in* $B_{\varepsilon_{error}}$.

Proof. The proof consists of two parts. First, the LMPC optimization problem of Eq. 4.39 is shown to be feasible for all deviation states in $\Omega_{\rho*}$. Subsequently, the deviation state is proved to be bounded in $\Omega_{\rho*}$ and to be ultimately bounded in $B_{\varepsilon_{\text{error}}}$.

Part 1: When the deviation state is maintained in $\Omega_{\rho*}$ (which will be proved in Part 2), the feasibility of the LMPC of Eq. 4.39 follows because the input trajectory obtained from the Lyapunov-based controller is a feasible solution. Specifically, define the trajectory v such that:

$$\dot{z}(t) = g(z(t), x_E^*(t|\hat{t}_k), \dot{x}_E^*(t|\hat{t}_k), v(t), 0)$$
$$v(t) = h(z(t_i), x_E^*(t_i|\hat{t}_k))$$

for $t \in [t_i, t_{i+1})$, $i = j, j+1, \ldots, N-1$ where $z(t_j) = e(t_j)$. The trajectory v is a feasible solution to the optimization problem of Eq. 4.39 since the trajectory satisfies the input

and the Lyapunov function constraints of Eq. 4.39. This is guaranteed by the closed-loop stability property of the Lyapunov-based controller.

Part 2: At $\hat{t}_k$, the EMPC computes an optimal trajectory $x_E^*(\cdot|\hat{t}_k)$ for the LMPC to track for one operating period. The computed trajectory is such that $x_E^*(t|\hat{t}_k)$ and $|\dot{x}_E^*(t|\hat{t}_k)| \leq \gamma_E$ for all $t \in [\hat{t}_k, \hat{t}_{k+1}]$ (Lemma 4.1). For simplicity of notation, let $x_E(\tau) = x_E^*(\tau|\hat{t}_k)$, $\dot{x}_E(\tau) = \dot{x}_E^*(\tau|\hat{t}_k)$,

$$\frac{\partial V(\tau)}{\partial e} := \frac{\partial V(e(\tau), x_E(\tau))}{\partial e}, \text{ and } \frac{\partial V(\tau)}{\partial x_E} := \frac{\partial V(e(\tau), x_E(\tau))}{\partial x_E} \tag{4.46}$$

for any $\tau \in [t_j, t_{j+1})$. At any sampling time $t_j \in [\hat{t}_k, \hat{t}_k + t')$ of the LMPC, consider $e(t_j) \in \Omega_{\rho*}$ (recursive arguments will be applied to show this is always the case when $e(0) \in \Omega_{\rho*}$). The computed control action at t_j satisfies:

$$\begin{aligned} \frac{\partial V(t_j)}{\partial e} g(e(t_j), x_E(t_j), 0, u^*(t_j|t_j), 0) &\leq \frac{\partial V(t_j)}{\partial e} g(e(t_j), x_E(t_j), 0, h(e(t_j), x_E(t_j)), 0) \\ &\leq -\alpha_3(|e(t_j)|) \end{aligned} \tag{4.47}$$

for all $e(t_j) \in \Omega_{\rho*}$. For all $\tau \in [t_j, t_{j+1})$, the time derivative of the Lyapunov function is given by:

$$\dot{V}(e(\tau), x_E(\tau)) = \frac{\partial V(\tau)}{\partial e} \dot{e}(\tau) + \frac{\partial V(\tau)}{\partial x_E} \dot{x}_E(\tau) \, . \tag{4.48}$$

Adding and subtracting the left-hand term of Eq. 4.47 and from the bound of Eq. 4.47, the time-derivative of the Lyapunov function may be upper bounded as follows:

$$\begin{aligned} \dot{V}(e(\tau), x_E(\tau)) \leq &-\alpha_3(|e(t_j)|) + \frac{\partial V(\tau)}{\partial e} g(e(\tau), x_E(\tau), \dot{x}_E(\tau), u^*(t_j|t_j), w(\tau)) \\ &- \frac{\partial V(t_j)}{\partial e} g(e(t_j), x_E(t_j), 0, u^*(t_j|t_j), 0) + \frac{\partial V(\tau)}{\partial x_E} \dot{x}_E(\tau) \end{aligned} \tag{4.49}$$

for all $\tau \in [t_j, t_{j+1})$. From Eq. 4.43, the time derivative of the Lyapunov function (Eq. 4.49)

may be further upper bounded:

$$\begin{aligned}\dot{V}(e(\tau),x_E(\tau)) &\leq -\alpha_3(|e(t_j)|)+L'_x|e(\tau)-e(t_j)|+L'_E|x_E(\tau)-x_E(t_j)| \\ &\quad +L''_E|\dot{x}_E(\tau)|+L'_w|w(\tau)|+\alpha_5(|e(\tau)|)|\dot{x}_E(\tau)| \\ &\leq -\alpha_3(|e(t_j)|)+L'_x|e(\tau)-e(t_j)|+L'_E|x_E(\tau)-x_E(t_j)| \\ &\quad +(L''_E+\alpha_5(|e(\tau)|))\gamma_E+L'_w\theta \end{aligned} \tag{4.50}$$

for all $e(t_j)\in\Omega_{\rho*}$ and $\tau\in[t_j,t_{j+1})$ where the second inequality follows from the fact that $|\dot{x}_E(\tau)|\leq\gamma_E$ and $w(\tau)\in\mathbb{W}$.

Taking into account Eq. 4.41 and the fact that $|\dot{x}_E(\tau)|\leq\gamma_E$ and the continuity of e and x_E, the following bounds may be derived for all $\tau\in[t_j,t_{j+1})$:

$$\left|e(\tau)-e(t_j)\right|\leq M\Delta\,, \tag{4.51}$$

$$\left|x_E(\tau)-x_E(t_j)\right|\leq\gamma_E\Delta\,. \tag{4.52}$$

From Eqs. 4.50-4.52, the following inequality is obtained:

$$\begin{aligned}\dot{V}(e(\tau),x_E(\tau)) &\leq -\alpha_3(|e(t_j)|)+(L'_xM+L'_E\gamma_E)\Delta \\ &\quad +(L''_E+\alpha_5(|e(\tau)|))\gamma_E+L'_w\theta \end{aligned} \tag{4.53}$$

for all $\tau\in[t_j,t_{j+1})$.

If Δ, γ_E and θ are sufficiently small such that there exist $\hat{\theta}\in(0,1)$ and $(\mu,\varepsilon_{\text{error}})$ satisfying Eqs. 4.44-4.45 with $B_\mu\subset B_{\varepsilon_{\text{error}}}\subset\Omega_{\rho*}$, the following bound on the time-derivative of the Lyapunov function follows:

$$\dot{V}(e(\tau),x_E(\tau))\leq-(1-\hat{\theta})\alpha_3(|e(t_j)|) \tag{4.54}$$

for all $\tau \in [t_j, t_{j+1})$ and $e(t_j) \in \Omega_{\rho*} \setminus B_\mu$. Integrating this bound on $t \in [t_j, t_{j+1})$, one obtains that:

$$V(e(t_{j+1}), x_E(t_{j+1})) \leq V(e(t_j), x_E(t_j)) - (1-\hat{\theta})\Delta\alpha_3(|e(t_j)|) \tag{4.55}$$

$$V(e(t), x_E(t)) \leq V(e(t_j), x_E(t_j)) \; \forall \; t \in [t_j, t_{j+1}) \tag{4.56}$$

for all $e(t_j) \in \Omega_{\rho*} \setminus B_\mu$. Using the above inequalities recursively, it may be proved that if $e(t_j) \in \Omega_{\rho*} \setminus B_\mu$, the deviation between the actual state trajectory and the economic optimal trajectory converges to B_μ in a finite number of sampling times without going outside the set $\Omega_{\rho*}$. Since the deviation state is always embedded in the set $\Omega_{\rho*}$ and from Lemma 4.1, the economically optimal state trajectory is always embedded in the set Γ, the boundedness of the closed-loop state trajectory of Eq. 3.1 under the lower layer LMPC follows because $\Omega_{\rho*}$ and Γ are compact sets.

To summarize, if $e(t_j) \in \Omega_{\rho*} \setminus B_\mu$, then

$$V(e(t_{j+1}), x_E(t_{j+1})) < V(e(t_j), x_E(t_j)) \; . \tag{4.57}$$

Furthermore, the deviation between the state trajectory and the economic optimal trajectory is ultimately bounded in $B_{\varepsilon_{\text{error}}}$ where satisfies Eq. 4.45 and $B_\mu \subset B_{\varepsilon_{\text{error}}} \subset \Omega_{\rho*}$. This statement holds because if the deviation state comes out of the ball B_μ, the deviation state is maintained within the ball $B_{\varepsilon_{\text{error}}}$ owing to Eq. 4.45. Once the deviation comes out of the ball B_μ, the Lyapunov function becomes decreasing. □

Notes and remarks on results:

- Three factors influences the time-derivative of the Lyapunov function when $e(t_j) \in \Omega_{\rho*} \setminus B_\mu$ as observed in Eq. 4.53: the sampling period of the lower layer LMPC, the bound on the disturbance, and the bound on the rate of change of the econom-

Table 4.2: Process parameters of the CSTR of Eq. 4.58.

F	5.0	$\mathrm{m^3\,h^{-1}}$	ΔH	-1.2×10^4	$\mathrm{kJ\,kmol^{-1}}$
V_R	1.0	$\mathrm{m^3}$	k_0	3.0×10^7	$\mathrm{h^{-1}}$
T_0	300	K	E	5.0×10^4	$\mathrm{kJ\,kmol^{-1}}$
R	8.314	$\mathrm{kJ\,kmol^{-1}\,K^{-1}}$	ρ_L	1000	$\mathrm{kg\,m^{-3}}$
C_p	0.231	$\mathrm{kJ\,kg^{-1}\,K^{-1}}$			

ically optimal trajectory. While the bound on the disturbance is a property of the system, two of the other properties may be used to achieve a desired level of tracking: the sampling period of the lower level control loop and the rate of change of the economically optimal tracking trajectory.

- Theorem 4.2 clarifies how the parameter γ_E arises and why it is needed in the formulation of the EMPC of Eq. 4.38.

- No guarantee is made that the closed-loop economic performance with the two-layer framework is better compared to the performance using a steady-state model in the upper layer. In some cases, it may be the case that closed-loop performance is the same or possibly better using a steady-state model in the upper layer EMPC. In this case, the stability result presented here may be extended to the case where the optimal steady-state varies sufficiently slow.

4.3.3 Application to a Chemical Process Example

Consider a well-mixed, non-isothermal continuous stirred tank reactor (CSTR) where an elementary (first-order) reaction takes place of the form $A \rightarrow B$. The feed to the reactor consists of pure A at volumetric flow rate F, temperature $T_0 + \Delta T_0$ and molar concentration $C_{A0} + \Delta C_{A0}$ where ΔT_0 and ΔC_{A0} are disturbances. A jacket around the reactor is used to provide/remove heat to the reactor. The dynamic equations describing the behavior

of the system, obtained through material and energy balances under standard modeling assumptions, are given below:

$$\frac{dT}{dt} = \frac{F}{V_R}(T_0 + \Delta T_0 - T) - \frac{\Delta H k_0}{\rho_L C_p} e^{\frac{-E}{RT}} C_A + \frac{Q}{\rho_L C_p V_R} \tag{4.58a}$$

$$\frac{dC_A}{dt} = \frac{F}{V_R}(C_{A0} + \Delta C_{A0} - C_A) - k_0 e^{\frac{-E}{RT}} C_A \tag{4.58b}$$

where C_A is the concentration of the reactant A in the reactor, T is the reactor temperature, Q is the rate of heat input/removal, V_R is the reactor volume, ΔH is the heat of the reaction, k_0 and E are the pre-exponential constant and activation energy of the reaction, respectively, C_p and ρ_L denote the heat capacity and the density of the fluid in the reactor, respectively. The values of the process parameters are given in Table 4.2. The state vector is $x = [T\ C_A]^T$ and the manipulated inputs are the heat rate $u_1 = Q$ where $u_1 \in [-2,2] \times 10^5$ kJ h^{-1} and the inlet reactant concentration $u_2 = C_{A0}$ where $u_2 \in [0.5, 8.0]$ kmol m^{-3}. The feed disturbances are modeled as bounded Gaussian white noise with zero mean, variances 20 K^2 and 0.1 kmol^2 m^{-6}, and bounds given by $|\Delta T_0| \leq 15$ K and $|\Delta C_{A0}| \leq 1.0$ kmol m^{-3}.

The control objective is to force the system to track the economically optimal time-varying operating trajectories computed by the upper layer EMPC. The set Γ is defined as

$$\Gamma := \{x \in \mathbb{R}^2 : 340 \leq x_1 \leq 390\,\text{K},\ 0.5 \leq x_2 \leq 3.0\,\text{kmol m}^{-3}\}\ . \tag{4.59}$$

In this example, the time-varying economic stage cost penalizes energy consumption, credits conversion of the reactant to the product, and penalizes the deviation of temperature from 365.0 K and is given by:

$$l_e(t,x,u) = A_1(t)u_1^2 - A_2(t)\frac{(u_2 - x_2)}{u_2} + A_3(t)(x_1 - 365.0\,\text{K})^2 \tag{4.60}$$

where A_1, A_2, and A_3 are the potentially time-varying weighting factors. The last term in the economic stage cost is used to prevent the system from operating on the boundary of Γ for long periods of time. The magnitudes of the economic weighting factors have been chosen so that all terms in the economic cost have the same order of magnitude. For this example, A_1 and A_3 are chosen to be time-varying and $A_2 = 10$ is constant. The time-varying weight $A_1(t)$, over four hours of operation, is given by

$$A_1(t) = \begin{cases} 1.0 \times 10^{-7}, & t < 1.0\,\text{h} \\ 5.0 \times 10^{-8}, & 1.0\,\text{h} \leq t < 2.0\,\text{h} \\ 1.0 \times 10^{-8}, & 2.0\,\text{h} \leq t < 3.0\,\text{h} \\ 5.0 \times 10^{-8}, & 3.0\,\text{h} \leq t \leq 4.0\,\text{h} \end{cases}$$

and is used to model the time-varying energy cost. The time-varying weight $A_3(t)$ is given by

$$A_3(t) = \begin{cases} 1.0 \times 10^{-2}, & t < 1.0\,\text{h} \\ 7.5 \times 10^{-3}, & 1.0\,\text{h} \leq t < 2.0\,\text{h} \\ 5.0 \times 10^{-3}, & 2.0\,\text{h} \leq t < 3.0\,\text{h} \\ 7.5 \times 10^{-3}, & 3.0\,\text{h} \leq t \leq 4.0\,\text{h} \end{cases}$$

The rationale for varying A_3 is to allow the CSTR be operated over a larger temperature range when the energy cost decreases and thus, take advantage of the decreased energy cost. The upper layer EMPC is implemented with a sampling period of $\Delta_E = 36\,\text{s}$ and prediction horizon of $N_E = 60$ sampling periods. It is solved every 0.50 h, i.e., the operating period is chosen to be $t' = 0.50\,\text{h}$. The prediction horizon and operating period were chosen to account for the update frequency of the economic weighting parameters. It was found that defining and imposing a rate of change constraint in the upper layer EMPC, i.e., defining the

parameter γ_E, was not needed for this particular example because the closed-loop system under the lower layer LMPC was able to achieve acceptable tracking performance without imposing a rate of change constraint in the upper layer EMPC. The projection operator is such that it projects the current state to the closest boundary of Γ if the current state is outside the set Γ, e.g., if $x = [400\,\mathrm{K}\ 2.0\,\mathrm{kmol\,m^{-3}}]^T$, then $\mathrm{proj}_\Gamma(x) = [390\,\mathrm{K}\ 2.0\,\mathrm{kmol\,m^{-3}}]^T$.

To design the lower layer LMPC, a Lyapunov-based controller is designed for the CSTR, which is essentially two proportional controllers that account for the input constraints. Specifically, the two proportional controllers are given by:

$$\begin{aligned} &-K_1(x_1 - x^*_{E,1}) + u_{s,1}, \\ &-K_2(x_2 - x^*_{E,2}) + u_{s,2} \end{aligned} \tag{4.61}$$

where $K_1 = 8000$, $K_2 = 0.01$, and u_s is the steady-state input corresponding to the steady-state x^*_E, i.e., the input vector that makes the right-hand side of Eqs. 4.58a-4.58b equal to zero with the state vector x^*_E. The resulting Lyapunov-based controller design for the CSTR is derived by accounting for the input constraints in the controller design of Eq. 4.61 as well as for the fact that u_s may be written as a function of x_E, i.e., the resulting Lyapunov-based controller is a mapping h that maps the pair (e, x_E) to $h(e, x_E) \in \mathbb{U}$. A quadratic Lyapunov function of the form $V(e, x_E) = e^T P e$ is constructed for the closed-loop system under the Lyapunov-based controller with

$$P = \begin{bmatrix} 10 & 1 \\ 1 & 100 \end{bmatrix}. \tag{4.62}$$

The LMPC is implemented with a sampling time $\Delta = 36\,\mathrm{s}$, prediction horizon $N = 5$, and weighting matrices of $Q_c = P$ and $R_c = \mathrm{diag}\begin{bmatrix} 10^{-7} & 10 \end{bmatrix}$. The prediction horizon and weighting matrices of the lower layer LMPC were tuned to achieve a close tracking of the

optimal state trajectory.

With the nonlinear system of Eqs. 4.58a-4.58b, the Lyapunov-based controller, and the Lyapunov function, the stability regions of the closed-system under the Lyapunov-based controller may be estimated for a sufficiently large number of points in Γ. This procedure was carried out as follows: fix $x_E \in \Gamma$ and compute a level set of the Lyapunov function where $\dot{V} < 0$ for all points contained in the level set. The intersection of all these level sets is taken to be an estimate of the closed-loop stability region Ω_{ρ^*} of the CSTR under the Lyapunov-based controller. In this example, Ω_{ρ^*} is estimated to be $\rho^* = 110$. Through the Lyapunov-based constraint on the LMPC of (Eq. 4.39e), the closed-loop system with the two-layer framework inherits the stability region Ω_{ρ^*}.

To simulate the closed-loop system, explicit Euler method with integration step 0.36 s was used to integrate the ODEs and the open source interior point solver Ipopt [187] was used to solve the optimization problems. Three sets of closed-loop simulations were completed. In the first set of closed-loop simulations, the stability properties of the closed-loop system under the two-layer dynamic economic optimization and control framework are demonstrated. Second, time-varying operation with the two-layer dynamic economic optimization and control framework is analyzed. Third, the closed-loop economic performance of the CSTR under the two-layer framework is compared to the CSTR under a conventional approach to optimization and control.

To demonstrate the closed-loop stability properties of the proposed two-layer framework, the CSTR is initialized at $x_0 = [400\,\mathrm{K},\ 0.1\,\mathrm{kmol\,m^{-3}}]$ which is outside of Γ, but inside the stability region Ω_{ρ^*}. The projection operator of the upper layer EMPC projects the initial state onto the state $x_{E,0} = [390\,\mathrm{K},\ 0.5\,\mathrm{kmol\,m^{-3}}] \in \Gamma$ to use as an initial condition to the upper layer EMPC problem of Eq. 4.38. The evolution of the closed-loop system under the two-layer framework and with the inlet temperature and reactant concentration disturbance is shown in Figs. 4.8-4.9. From Fig. 4.9, the deviation of the actual closed-loop

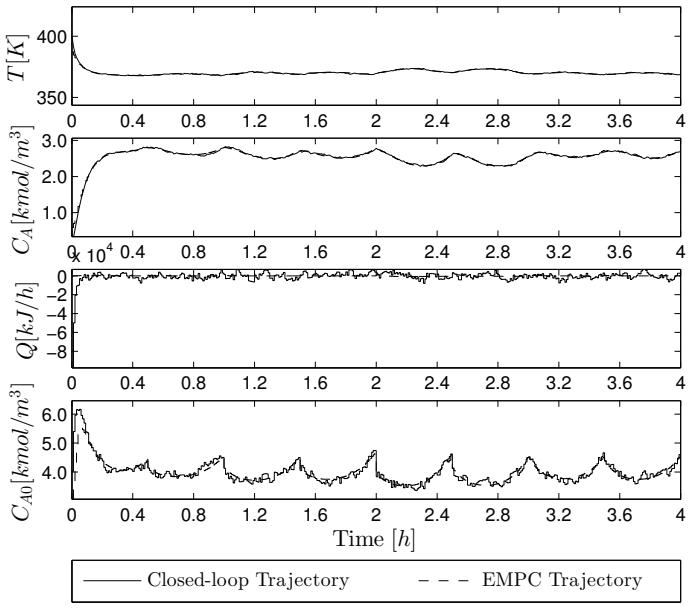

Figure 4.8: The closed-loop state and input trajectories of Eq. 4.58a-4.58b under the two-layer optimization and control framework with the feed disturbances and starting from 400 K and 0.1 kmol m^{-3}.

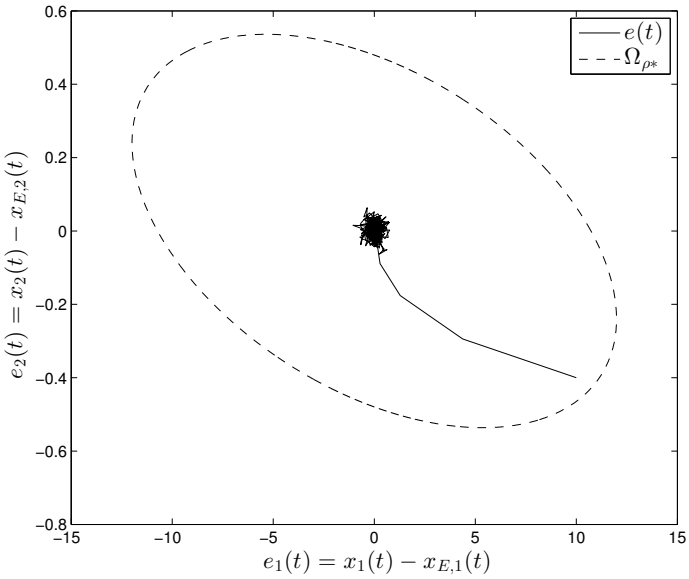

Figure 4.9: The closed-loop state trajectory of Eq. 4.58a-4.58b under the two-layer optimization and control framework with the feed disturbances and starting from 400 K and 0.1 kmol m^{-3} shown in deviation state-space.

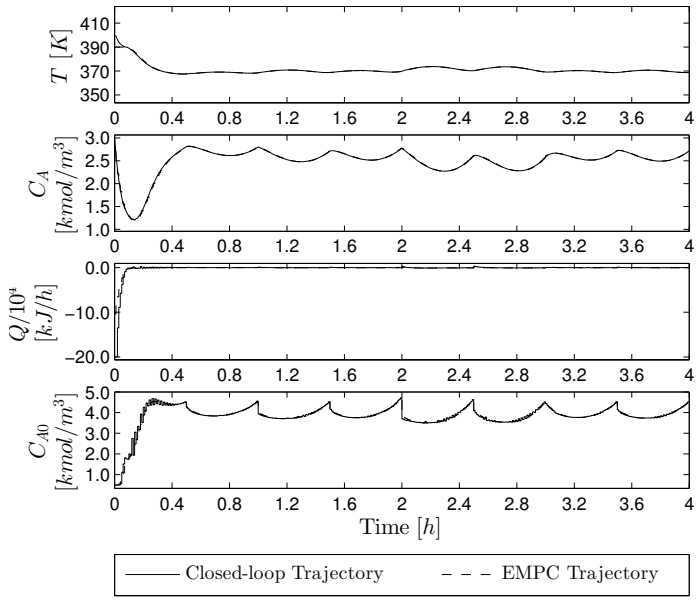

Figure 4.10: The closed-loop system states and inputs of Eq. 4.58a-4.58b without the feed disturbances and starting from 400 K and 3.0 kmol m^{-3}.

state and the economically optimal state is always maintained inside $\Omega_{\rho*}$. Moreover, the deviation becomes small over time until it is ultimately bounded in a small ball.

Two simulations of the closed-loop system without the feed disturbances added are shown in Figs. 4.10-4.11 with two different initial conditions to analyze the time-varying operation with the two-layer dynamic economic optimization and process control framework. The initial state in Fig. 4.10 is $x_0 = [400\,\text{K},\ 3.0\,\text{kmol m}^{-3}]^T$, while the initial state in Fig. 4.11 is $x_0 = [320\,\text{K},\ 3.0\,\text{kmol m}^{-3}]^T$. The closed-loop evolution of the two cases is initially different. For the CSTR starting at the larger temperature, heat should be removed from the reactor and the minimum amount of reactant material should be supplied to the reactor to decrease the temperature of the reactor. In contrast, when the CSTR is initialized at the smaller temperature, heat should be supplied to the reactor and reactant material should be fed to the reactor to increase the reactor temperature. After a sufficiently long length of operation, the effect of the initial condition diminishes and the closed-loop

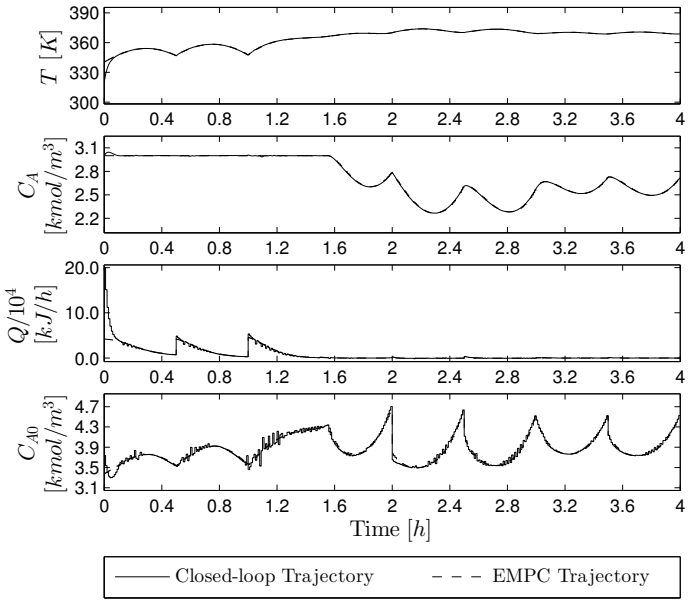

Figure 4.11: The closed-loop system states and inputs of Eq. 4.58a-4.58b without the feed disturbances and starting from 320 K and 3.0 kmol m^{-3}.

evolution of the two cases becomes similar. For both of these cases, the reactor is operated in a time-varying fashion, i.e., never converges to a steady-state.

To compare the closed-loop economic performance under the dynamic economic optimization and control framework and under a conventional approach to optimization and control, the total economic cost over the length of operation is defined as

$$J_E = \sum_{j=0}^{M} \left(A_1(t_j)Q^2(t_j) + A_2\frac{C_A(t_j)}{C_{A0}(t_j)} + A_3(T(t_j) - 365)^2 \right) \tag{4.63}$$

where t_0 is the initial time of the simulation and $t_M = 4.0$ h is the end of the simulation. The conventional approach to optimization and control uses a steady-state economic optimization problem to compute the optimal steady-states with respect to the time-varying economic cost weights. The optimal steady-states are used in a tracking MPC, which in this case is an LMPC, to force the CSTR states to the optimal steady-states. The optimal

Table 4.3: Comparison of the total economic cost, given by Eq. 4.63, of the closed-loop system with and without the feed disturbances for four hours of operation.

Initial Conditions		Total Economic Cost					
$T(0)$ K	$C_A(0)$ kmol m^{-3}	Steady-State Optimization without Disturbance	Two-layer Framework without Disturbance	Cost Decrease	Steady-State Optimization with Disturbance	Two-layer Framework with Disturbance	Cost Decrease
400.0	3.0	21970.5	14531.1	51.2 %	21642.4	14130.7	53.2 %
380.0	3.0	5235.4	3409.5	53.6 %	5060.1	3037.9	66.6 %
360.0	3.0	4261.8	3308.6	28.8 %	4083.2	2997.1	36.2 %
340.0	3.0	13732.2	10997.3	24.9 %	13554.9	10882.3	24.6 %
320.0	3.0	23719.4	19315.9	22.8 %	23729.1	19210.3	23.5 %
400.0	2.5	18546.8	10062.1	84.3 %	18283.4	9691.4	88.7 %
380.0	2.5	4558.7	3163.3	44.1 %	4387.2	2811.9	56.0 %
360.0	2.5	4496.4	3335.6	34.8 %	4322.7	3030.3	42.6 %
340.0	2.5	14078.3	11034.4	27.6 %	13910.2	10928.8	27.3 %
320.0	2.5	24052.2	19293.4	24.7 %	24002.2	19193.8	25.1 %
400.0	2.0	14831.5	6774.0	118.9 %	14682.4	6412.6	129.0 %
380.0	2.0	4073.2	3085.1	32.0 %	3905.0	2739.8	42.5 %
360.0	2.0	4765.4	3431.2	38.9 %	4596.4	3139.3	46.4 %
340.0	2.0	14395.5	11162.3	29.0 %	14236.8	11068.2	28.6 %
320.0	2.0	24202.7	19241.2	25.8 %	24223.5	19146.7	26.5 %
400.0	0.1	8146.1	4360.5	86.8 %	7999.4	4025.7	98.7 %

(time-varying) steady-state from steady-state economic optimization is

$$x_s^*(t) = \begin{cases} [370.0\,\text{K},\ 2.576\,\text{kmol}\,\text{m}^{-3}]^T, & t < 1.0\,\text{h} \\ [371.7\,\text{K},\ 2.447\,\text{kmol}\,\text{m}^{-3}]^T, & 1.0\,\text{h} \leq t < 2.0\,\text{h} \\ [375.2\,\text{K},\ 2.205\,\text{kmol}\,\text{m}^{-3}]^T, & 2.0\,\text{h} \leq t < 3.0\,\text{h} \\ [371.7\,\text{K},\ 2.447\,\text{kmol}\,\text{m}^{-3}]^T, & 3.0\,\text{h} \leq t \leq 4.0\,\text{h} \end{cases}$$

with the corresponding steady-state input of

$$u_s^*(t) = \begin{cases} [0.0\,\text{kJ}\,\text{h}^{-1},\ 3.923\,\text{kmol}\,\text{m}^{-3}]^T, & t < 1.0\,\text{h} \\ [-0.5\,\text{kJ}\,\text{h}^{-1},\ 3.827\,\text{kmol}\,\text{m}^{-3}]^T, & 1.0\,\text{h} \leq t < 2.0\,\text{h} \\ [0.0\,\text{kJ}\,\text{h}^{-1},\ 3.653\,\text{kmol}\,\text{m}^{-3}]^T, & 2.0\,\text{h} \leq t < 3.0\,\text{h} \\ [-0.5\,\text{kJ}\,\text{h}^{-1},\ 3.827\,\text{kmol}\,\text{m}^{-3}]^T, & 3.0\,\text{h} \leq t \leq 4.0\,\text{h} \end{cases}$$

An LMPC is implemented to drive the system to the time-varying optimal steady-state, which is formulated as follows:

$$
\begin{aligned}
\min_{u\in S(\Delta)} \quad & \int_{t_j}^{t_{j+N}} \left(|\tilde{x}(\tau) - x_s^*(\tau)|_{Q_c} + |u(\tau) - u_s^*(\tau)|_{R_c} \right) d\tau \\
\text{s.t.} \quad & \dot{\tilde{x}}(t) = f(\tilde{x}(t), u(t), 0), \\
& \tilde{x}(t_j) = x(t_j), \\
& -2\times 10^5 \leq u_1(t) \leq 2\times 10^5, \ \forall\, t \in [t_j, t_{j+N}), \\
& 0.5 \leq u_2(t) \leq 8, \ \forall\, t \in [t_j, t_{j+N}), \\
& \frac{\partial V(x(t_j))}{\partial x} f(x(t_j), u(t_j), 0) \\
& \quad \leq \frac{\partial V(x(t_j))}{\partial x} f(x(t_j), h(x(t_j), x_s^*(t_j)), 0)
\end{aligned}
\tag{4.64}
$$

where the Lyapunov function, the Lyapunov-based controller, the weighting matrices R_c and Q_c, the sampling period Δ, and the prediction horizon N are all the same as the ones used in the tracking LMPC scheme. To make a fair comparison, the same realization of the feed disturbances was applied to each closed-loop system simulation. The total economic cost values of several closed-loop simulations starting from different initial conditions and with and without the feed disturbances are given in Table 4.3. From the results of Table 4.3, the largest economic cost decrease occurs when the CSTR is initialized at higher temperature. When the CSTR starts from a lower temperature, the amount of heat that needs to be supplied to the reactor initially is less than the amount of heat that needs to be initially removed when the CSTR starts at a higher temperature as explained above and demonstrated in Figs. 4.10-4.11. Thus, when the CSTR starts from a higher temperature, better closed-loop performance is achieved because less energy is required to be supplied/removed from the reactor.

4.4 Addressing Closed-loop Performance and Computational Efficiency

An important theoretical consideration is the closed-loop performance of systems under EMPC because EMPC is formulated with a finite prediction horizon. The achievable closed-loop economic performance may strongly depend on the prediction horizon length. To address guaranteed closed-loop economic performance while formulating a computationally efficient control structure, a two-layer EMPC structure is presented in this section. In contrast to the two-layer EMPC methodologies presented in the previous sections, EMPC schemes are used in both layers of the two-layer EMPC structure to ensure economic performance improvement over a tracking controller, e.g., tracking MPC.

Each layer is formulated as an LEMPC scheme. The core idea of the two-layer LEMPC implementation is to solve the upper layer LEMPC infrequently (not every sampling period) while employing a long prediction horizon. Then, the solution generated by the upper layer LEMPC is subsequently used in the formulation of a lower layer LEMPC. The lower layer LEMPC is formulated with a shorter prediction horizon and smaller sampling time than the upper layer LEMPC and computes control actions that are applied to the closed-loop system. The control actions of the lower layer LEMPC are constrained to maintain the state near the economically optimal trajectories computed in the upper layer. For guaranteed performance improvement with the two-layer LEMPC implementation scheme, both layers are formulated with explicit performance-based constraints computed by taking advantage of the availability of an auxiliary stabilizing controller. The performance-based constraints, i.e., terminal constraints, are similar to that presented in Section 3.4, and guarantee that both the finite-time and infinite-time closed-loop economic performance under the two-layer LEMPC scheme are at least as good as that under the stabilizing controller. The use of the two-layer control implementation allows for the control architecture to be

computationally efficient. The two-layer LEMPC structure is applied to a chemical process example to demonstrate the closed-loop performance, stability, and robustness properties of the two-layer LEMPC structure.

4.4.1 Class of Systems

In this section, nominally operated systems are considered, i.e., the system of Eq. 3.1 with $w \equiv 0$. Specifically, the class of continuous-time nonlinear systems considered is described by the following state-space form:

$$\dot{x} = f(x,u) \tag{4.65}$$

where the state vector is $x \in \mathbb{X} \subseteq \mathbb{R}^n$ and the input vector is $u \in \mathbb{U} \subset \mathbb{R}^m$. The vector function $f : \mathbb{X} \times \mathbb{U} \to \mathbb{X}$ is a locally Lipschitz vector function on $\mathbb{X} \times \mathbb{U}$. The set of admissible inputs $\mathbb{U}$ is assumed to be a compact set, and the state is synchronously sampled at time instances $j\Delta$ with $j = 0,1,2,\ldots$ where $\Delta > 0$ is the sampling period. As before, the initial time is taken to be zero, and the notation t will be used for the continuous-time, while the time sequence $\{t_j\}_{j\geq 0}$ is the discrete sampling time sequence which is a synchronous partitioning of $\mathbb{R}_+$ with $t_j = j\Delta$.

A time-invariant economic measure $l_e : \mathbb{X} \times \mathbb{U} \to \mathbb{R}$ is assumed for the system of Eq. 4.3 that describes the real-time system economics. The economic measure is assumed to be continuous on $\mathbb{X} \times \mathbb{U}$. The optimal steady-state x_s^* and steady-state input u_s^* pair with respect to the economic cost function is computed as follows:

$$(x_s^*, u_s^*) = \underset{x_s \in \mathbb{X}, u_s \in \mathbb{U}}{\arg\min} \{ l_e(x_s,u_s) : f(x_s,u_s) = 0 \} \ .$$

The existence of a minimizing pair where the minimum is attained and such that the minimizing pair lies in the interior of $\mathbb{X} \times \mathbb{U}$ is assumed. For the sake of simplicity, the optimal

steady-state pair is assumed to be unique and to be $(x_s^*, u_s^*) = (0,0)$.

4.4.2 Existence of a Stabilizing Controller

A stronger stabilizability-like assumption than the assumption imposed in previous sections and chapters is needed here (stated in Assumption 4.3). In this section, the existence of a stabilizing controller that renders the origin of the closed-loop system exponentially stable under continuous implementation is assumed whereas, previously, the existence of a stabilizing controller is assumed that renders the closed-loop system only asymptotically stable under continuous implementation. The stronger assumption is needed to ensure that the stabilizing controller renders the origin of the closed-loop system exponentially (and therefore, asymptotically) stable under sample-and-hold implementation. This will be required to consider infinite-time closed-loop economic performance. Specifically, asymptotic convergence to the origin and not just convergence to a neighborhood of the steady-state (practical stability of the origin) will be required.

Assumption 4.3. *There exists a locally Lipschitz feedback controller $h : \mathbb{X} \to \mathbb{U}$ with $h(0) = 0$ for the system of Eq. 4.65 that renders the origin of the closed-loop system under continuous implementation of the controller locally exponentially stable. More specifically, there exist constants $\rho > 0$, $c_i > 0$, $i = 1,2,3,4$ and a continuously differentiable Lyapunov function $V : \mathbb{X} \to \mathbb{R}_+$ such that the following inequalities hold:*

$$c_1 |x|^2 \leq V(x) \leq c_2 |x|^2, \tag{4.66a}$$

$$\frac{\partial V(x)}{\partial x} f(x, h(x)) \leq -c_3 |x|^2, \tag{4.66b}$$

$$\left| \frac{\partial V(x)}{\partial x} \right| \leq c_4 |x|, \tag{4.66c}$$

for all $x \in \Omega_\rho \subseteq \mathbb{X}$.

Explicit feedback controllers that may be designed to satisfy Assumption 4.3 are, for example, feedback linearizing controller and some Lyapunov-based controllers, e.g., [100, 101]. The origin of the closed-loop system of Eq. 4.65 under the feedback controller, $h(x)$, implemented in a zeroth-order sample-and-hold fashion with a sufficiently small sampling period $\Delta > 0$, i.e., the controller is applied as an emulation controller may be shown to be exponentially stable (Corollary 2.1). Moreover, the proof of Corollary 2.1 shows that V is a Lyapunov function for the closed-loop sampled-data system in the sense that there exists a constant $\hat{c}_3 > 0$ such that

$$\frac{\partial V(x(t))}{\partial x} f(x(t), h(x(t_j))) \leq -\hat{c}_3 |x(t)|^2 \tag{4.67}$$

for all $t \in [t_j, t_{j+1})$ and integers $j \geq 0$ where $x(t)$ is the solution of Eq. 4.65 at time t starting from $x(t_j) \in \Omega_\rho$ and with the input $u(t) = h(x(t_j))$ for $t \in [t_j, t_{j+1})$. The stability region of the closed-loop system under the controller is defined as $\Omega_\rho \subseteq X$.

4.4.3 Two-layer EMPC Structure

A detailed description of the two-layer LEMPC structure is provided which includes descriptions of the implementation strategy, the formulations of the upper and lower layer LEMPC schemes, and the provable stability and performance properties.

Implementation Strategy

The objective of the two-layer LEMPC design is to ensure that both the finite-time and infinite-time closed-loop economic performance of the resulting closed-loop system will be at least as good the closed-loop performance under a stabilizing controller. To address

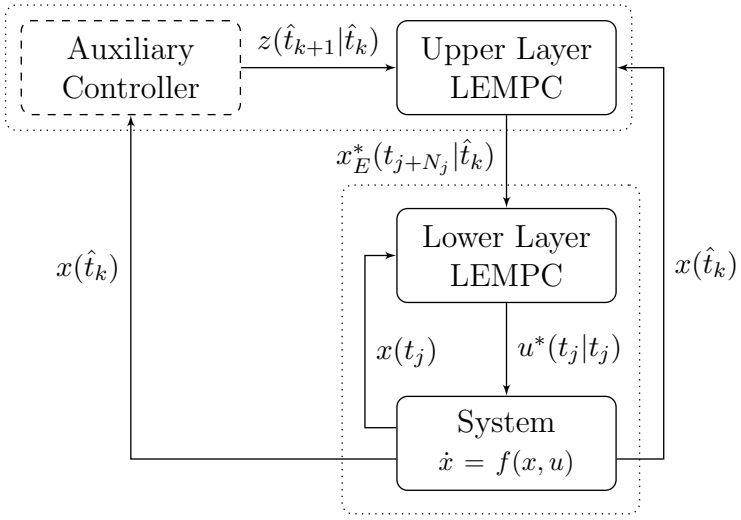

Figure 4.12: Block diagram of the two-layer EMPC structure addressing closed-loop performance and computational efficiency.

this objective, performance-based constraints are employed in the formulation of the upper and lower layer LEMPC that have been computed from the stabilizing controller. The stabilizing controller may be any controller that satisfies Assumption 4.3. For example, the stabilizing controller may be an explicit controller that satisfies Assumption 4.3 or an LMPC scheme, which is equipped with a contractive Lyapunov constraint designed using an explicit controller that satisfies Assumption 4.3. The formulation of such a LMPC scheme is provided below. However, it is important to point out that the amount of computation required to solve the LMPC is generally greater than that required for an explicit controller. The stabilizing controller will be referred as the auxiliary controller for the remainder.

A block diagram of the two-layer LEMPC is given in Fig. 4.12. In the upper layer, an LEMPC is used to optimize dynamic operation over a long horizon while accounting for the performance-based constraints generated from the auxiliary controller. Both the auxiliary controller and the upper layer LEMPC compute their input trajectories at the beginning

of some operating window, and thus, the auxiliary controller and upper layer LEMPC are computed once each operating window for computational efficiency. In the lower layer, an LEMPC, using a shorter prediction horizon and a smaller sampling period than the upper layer LEMPC, computes control inputs that are applied to the process. Terminal constraints that have been generated from the upper layer LEMPC optimal solution are used to ensure that the lower layer LEMPC guides the system along the optimal solution computed in the upper layer since it uses a shorter prediction horizon and a smaller sampling period. In this manner, the lower layer LEMPC is used to improve robustness of the closed-loop system (recomputes its optimal trajectory every sampling period to incorporate feedback) as well as for possibly providing additional economic cost improvement over the upper layer LEMPC solution owing to the use of a smaller sampling time.

To maintain consistency of the notation, the operating window is denoted as t' and is equal to $N_E\Delta_E$ where $N_E \in \mathbb{I}_+$ is the number of hold periods in the prediction horizon of the upper layer LEMPC and $\Delta_E > 0$ is the hold period of the piecewise constant input trajectory computed in the upper layer (here, $K_E = N_E$). The time sequence $\{\hat{t}_k\}_{k\geq 0}$ denotes the discrete time steps that the upper layer computes a solution to its control problem where $\hat{t}_k = kt'$ and $k = 0, 1, \ldots$.

At the beginning of each operating window, the upper layer control problems are solved in a sequential manner: first, the auxiliary controller is solved to obtain its corresponding open-loop predicted state and input trajectories over the operating window and second, the upper layer LEMPC is solved to obtain its corresponding open-loop predicted state and input trajectories over the operation window. Specifically, the auxiliary controller computes the open-loop (predicted) input trajectory that it would apply to the system over the time $\hat{t}_k$ to $\hat{t}_{k+1} = (k+1)t'$ along with the open-loop state trajectory under the computed input trajectory. If the auxiliary controller is an explicit controller, then the open-loop state

trajectory is computed by recursively solving:

$$\dot{z}(t) = f(z(t), h(z(\tau_i))) \tag{4.68}$$

for $t \in [\tau_i, \tau_{i+1})$, $i = 0, 1, \ldots, N_E - 1$ where $\tau_i := \hat{t}_k + i\Delta_E$, $z(\hat{t}_k) = x(\hat{t}_k)$ is the initial condition, and $x(\hat{t}_k)$ is a state measurement obtained at $\hat{t}_k$. If, instead, the auxiliary controller is an LMPC, then the open-loop state trajectory may be obtained directly from the solution of the optimization problem. The open-loop state and input trajectories under the auxiliary controller are denoted as $z(t|\hat{t}_k)$ and $v(t|\hat{t}_k)$ for $t \in [\hat{t}_k, \hat{t}_{k+1}) = [kt', kt' + N_E\Delta_E)$, respectively. The terminal state of the open-loop state trajectory, $z(\hat{t}_{k+1}|\hat{t}_k)$, is then sent to the upper level LEMPC.

The upper layer LEMPC subsequently uses $z(\hat{t}_{k+1}|\hat{t}_k)$ as a terminal equality constraint in the optimization problem. In this framework, no restrictions are placed on the type of operation achieved under the two-layer framework, i.e., it could be steady-state type operation or some more general time-varying operating behavior. Therefore, the upper level LEMPC is a LEMPC (Eq. 3.3) equipped with mode 1 operation only. If steady-state operation is desirable, one could formulate the upper level LEMPC with a mode 2 constraint similar to that of Eq. 4.8f to ensure that the optimal steady-state is asymptotically stable under the two-layer LEMPC. However, the mode 2 constraint of LEMPC is not discussed further. After receiving $z(\hat{t}_{k+1}|\hat{t}_k)$ from the auxiliary controller and a state measurement at $\hat{t}_k$, the upper layer LEMPC is solved to compute its optimal state and input trajectories over the operating window, which are denoted as $x_E^*(t|\hat{t}_k)$ and $u_E^*(t|\hat{t}_k)$ for $t \in [\hat{t}_k, \hat{t}_{k+1})$, respectively.

The upper layer hold period is divided into $\bar{N}$ subintervals of length Δ ($\Delta = \Delta_E/\bar{N}$ where $\bar{N}$ is a positive integer). The subintervals define the sampling period of the lower layer LEMPC and correspond to the sampling time sequence $\{t_j\}_{j\geq 0}$. The lower layer LEMPC recomputes its optimal input trajectory employing a shrinking horizon. Namely,

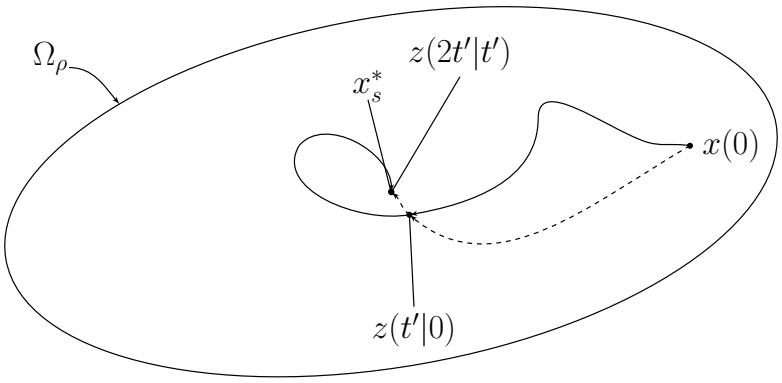

Figure 4.13: A state-space illustration of the evolution of the closed-loop system (solid line) in the stability region Ω_ρ over two operating periods. The open-loop predicted state trajectory under the auxiliary controller is also given (dashed line). At the beginning of each operating window, the closed-loop state converges to the open-loop state under the auxiliary controller.

at the beginning of each hold period of the upper layer, the lower layer is initialized with a prediction horizon $N_j = \bar{N}$. The lower layer LEMPC receives a state measurement, denoted as $x(t_j)$, as well as $x_E^*(t_{j+N_j}|\hat{t}_k)$ from the upper layer LEMPC. Using $x_E^*(t_{j+N_j}|\hat{t}_k)$ as a terminal equality constraint in the lower layer LEMPC, the lower layer LEMPC is solved. The optimal input trajectory computed by the lower layer LEMPC is denoted as $u^*(t|t_j)$, $t \in [t_j, t_{j+N_j})$. At the subsequent sampling period of the lower layer LEMPC, the prediction horizon decreases by one ($N_{j+1} = N_j - 1$). If decreasing the horizon results in the horizon being set to zero, the prediction horizon is reset to $\bar{N} = \Delta_E/\Delta$. This happens at the beginning of the next hold period of the upper layer LEMPC.

The implementation strategy is summarized below and an illustration of the closed-loop system is given in Figure 4.13. The lower layer LMPC is initialized with a prediction horizon of $N_0 = \bar{N} = \Delta_E/\Delta$. To initialize the algorithm, let $k = 0$ and $j = 0$.

1. **Upper layer:** At $\hat{t}_k$, the auxiliary controller and the upper layer LEMPC are initial-

ized with the state measurement $x(\hat{t}_k)$. Go to Step 1.1.

1.1 The auxiliary controller computes its optimal input trajectory denoted as $v(t|\hat{t}_k)$ defined for $t \in [\hat{t}_k, \hat{t}_{k+1})$ and corresponding state trajectory denoted as $z(t|\hat{t}_k)$ defined for $t \in [\hat{t}_k, \hat{t}_{k+1})$. The terminal state $z(\hat{t}_{k+1}|\hat{t}_k)$ is sent to the upper layer LEMPC. Go to Step 1.2.

1.2 The upper layer LEMPC receives $z(\hat{t}_{k+1}|\hat{t}_k)$ from the auxiliary controller and computes its optimal input trajectory $u_E^*(t|\hat{t}_k)$ defined for $t \in [\hat{t}_k, \hat{t}_{k+1})$ and state trajectory $x_E^*(t|\hat{t}_k)$ defined for $t \in [\hat{t}_k, \hat{t}_{k+1})$. Go to Step 2.

2. **Lower layer:** At t_j, the lower layer LEMPC receives a state measurement $x(t_j)$ and the terminal state $x_E^*(t_{j+N_j}|\hat{t}_k)$ from the upper layer LEMPC. Go to Step 2.1.

2.1 The lower layer LEMPC computes its optimal input trajectory $u^*(t|t_j)$ defined for $t \in [t_j, t_{j+N_j})$. Go to Step 2.2.

2.2 The control action $u^*(t_j|t_j)$, which is the computed input for the first sampling period of the lower layer LEMPC prediction horizon, is applied to the system from t_j to t_{j+1}. If $N_j - 1 = 0$, reset $N_{j+1} = \bar{N}$; else, let $N_{j+1} = N_j - 1$. If $t_{j+1} = \hat{t}_{k+1}$, set $j \leftarrow j+1$ and $k \leftarrow k+1$ and go to Step 1. Else, set $j \leftarrow j+1$ and go to Step 2.

Remark 4.3. Even though the lower layer LEMPC uses a shrinking horizon and nominal operation is considered, recomputing the lower layer LEMPC input at every subsequent sampling time is necessary regardless if the solution to the lower level LEMPC is the same or not. The incorporation of feedback allows for stabilization of open-loop unstable systems that cannot be accomplished with an open-loop implementation and ensures the robustness of the control solution with respect to infinitesimally small disturbances/uncertainty. For further explanation on this point, see, for example, [176].

Formulation

The formulations of the two LEMPC schemes are given. For convenience, the specific formulation of the LMPC needed if the auxiliary controller is chosen to be an LMPC scheme is given first. Specifically, the LMPC is given by the following optimization problem:

$$\min_{v\in S(\Delta_E)} \int_{\hat{t}_k}^{\hat{t}_{k+1}} (|z(t)|_{Q_c} + |v(t)|_{R_c})\, dt \tag{4.69a}$$

$$\text{s.t.} \quad \dot{z}(t) = f(z(t), v(t)) \tag{4.69b}$$

$$z(\hat{t}_k) = x(\hat{t}_k) \tag{4.69c}$$

$$v(t) \in \mathbb{U},\ \forall\, t \in [\hat{t}_k, \hat{t}_{k+1}) \tag{4.69d}$$

$$\frac{\partial V(z(\tau_i))}{\partial z} f(z(\tau_i), v(\tau_i)) \leq \frac{\partial V(z(\tau_i))}{\partial z} f(z(\tau_i), h(x(\tau_i)))$$

$$\text{for } i = 0, 1, \ldots, N_E - 1 \tag{4.69e}$$

where $\tau_i := \hat{t}_k + i\Delta_E$ and z is the state trajectory of the system with input trajectory v calculated by the LMPC. The Lyapunov-based constraint of Eq. 4.69e differs from the Lyapunov-based constraint of Eq. 4.69e as it is imposed at each sampling period along the prediction horizon of the LMPC to ensure that the state trajectory with input computed by the LMPC converges to the steady-state. Through enforcement of the Lyapunov-based constraint, the LMPC inherits the same stability properties as that of the explicit controller. The optimal solution of the optimization problem of Eq. 4.69 is denoted as $v^*(t|\hat{t}_k)$ and is defined for $t \in [\hat{t}_k, \hat{t}_{k+1})$. From the optimal input trajectory, the optimal state trajectory $z^*(t|\hat{t}_k)$, $t \in [\hat{t}_k, \hat{t}_{k+1})$ may be computed for the operating window. When the LMPC is used as the auxiliary controller, the terminal state $z^*(\hat{t}_{k+1}|\hat{t}_k)$ is sent to the upper layer LEMPC.

The formulation of the upper layer LEMPC is similar to the mode 1 LEMPC formula-

tion with a terminal equality constraint computed from the auxiliary controller:

$$\min_{u_E \in S(\Delta_E)} \int_{\hat{t}_k}^{\hat{t}_{k+1}} l_e(x_E(t), u_E(t))\, dt \tag{4.70a}$$

$$\text{s.t.} \quad \dot{x}_E(t) = f(x_E(t), u_E(t)) \tag{4.70b}$$

$$x_E(\hat{t}_k) = x(\hat{t}_k) \tag{4.70c}$$

$$u_E(t) \in \mathbb{U},\ \forall\, t \in [\hat{t}_k, \hat{t}_{k+1}) \tag{4.70d}$$

$$x_E(t) \in \Omega_\rho,\ \forall\, t \in [\hat{t}_k, \hat{t}_{k+1}) \tag{4.70e}$$

$$x_E(\hat{t}_{k+1}) = z(\hat{t}_{k+1}|\hat{t}_k) \tag{4.70f}$$

where x_E is the predicted state trajectory with the input trajectory u_E computed by the upper layer LEMPC. To ensure the existence of an input trajectory that has at least as good economic performance as the auxiliary LMPC input trajectory over the entire length of operation, the terminal constraint of Eq. 4.70f based on the auxiliary controller is used. The terminal constraint differs from traditional terminal equality constraints because $z(\hat{t}_{k+1}|\hat{t}_k)$ is not necessarily the steady-state. It does, however, asymptotically converge to the economically optimal steady-state. The optimal solution to the optimization problem of the upper layer LEMPC is denoted as $u_E^*(t|\hat{t}_k)$ and is defined for $t \in [\hat{t}_k, \hat{t}_{k+1})$. With the optimal solution, the optimal (open-loop) state trajectory may be computed and is denoted as $x_E^*(t|\hat{t}_k)$, for $t \in [\hat{t}_k, \hat{t}_{k+1})$.

The lower layer LEMPC formulation, which uses a terminal constraint computed from

$x_E^*(\cdot|\hat{t}_k)$, is given by:

$$\min_{u\in S(\Delta)} \int_{t_j}^{t_{j+N_j}} l_e(\tilde{x}(t), u(t))\, dt \tag{4.71a}$$

$$\text{s.t.} \quad \dot{\tilde{x}}(t) = f(\tilde{x}(t), u(t)) \tag{4.71b}$$

$$\tilde{x}(t_j) = x(t_j) \tag{4.71c}$$

$$u(t) \in \mathbb{U},\ \forall\, t \in [t_j, t_{j+N_j}) \tag{4.71d}$$

$$\tilde{x}(t) \in \Omega_\rho,\ \forall\, t \in [t_j, t_{j+N_j}] \tag{4.71e}$$

$$\tilde{x}(t_{j+N_j}) = x_E^*(t_{j+N_j}|\hat{t}_k) \tag{4.71f}$$

where $\tilde{x}$ is the predicted state trajectory under the input trajectory u. The terminal constraint of Eq. 4.71f is computed from the upper layer LEMPC solution, and serves the same purpose as the terminal constraint of Eq. 4.70f. The optimal solution to the lower layer LEMPC is denoted as $u^*(t|t_j)$ which is defined for $t \in [t_j, t_{j+N_j})$. The control input $u^*(t_j|t_j)$ is sent to the control actuators to be applied to the system of Eq. 4.65 in a sample-and-hold fashion until the next sampling period.

Remark 4.4. When the economic stage cost does not penalize the use of control energy, one may consider formulating constraints in the LEMPC problems to prevent the LEMPC from computing an input trajectory that uses excessive control energy. In particular, one straightforward extension of the two-layer LEMPC structure is to compute the total control energy used by the auxiliary controller over the operating window, i.e, integral of the input trajectory v over $\hat{t}_k$ to $\hat{t}_{k+1}$. Then, enforce that the upper and lower layer LEMPCs compute an input trajectory that uses no more control energy than the auxiliary controller input profile over the operating window. This approach was employed in [78].

Closed-loop Stability and Performance

The following proposition proves that the closed-loop system state under the two-layer EMPC structure is always bounded in the invariant set Ω_ρ and the economic performance is at least as good as the closed-loop state with the auxiliary LMPC over each operating period.

Proposition 4.3. *Consider the system of Eq. 4.65 in closed-loop under the lower layer LEMPC of Eq. 4.71. Let the terminal constraint of Eq. 4.71f computed from the upper layer LEMPC of Eq. 4.70, which has a terminal constraint formulated from the auxiliary controller that satisfies Assumption 4.3. Let* $\Delta_E \in (0,\ \Delta^*]$ *where* Δ^* *is defined according to Corollary 2.1,* $N_E \geq 1$, $\bar{N} \geq 1$, *and* $\Delta = \Delta_E/\bar{N}$. *If* $x(\hat{t}_k) \in \Omega_\rho$, *then the state remains bounded in* Ω_ρ *over the operating window with* $x(\hat{t}_{k+1}) = z(\hat{t}_{k+1}|\hat{t}_k) \in \Omega_\rho$, *the upper and lower LEMPCs remain feasible for all* $t \in [\hat{t}_k, \hat{t}_{k+1})$, *and the following inequality holds:*

$$\int_{\hat{t}_k}^{\hat{t}_{k+1}} l_e(x(t), u^*(t))\, dt \leq \int_{\hat{t}_k}^{\hat{t}_{k+1}} l_e(z(t|\hat{t}_k), v(t|\hat{t}_k))\, dt \tag{4.72}$$

where x and u^* *are the closed-loop state and input trajectories and* $z(\cdot|\hat{t}_k)$ *and* $v(\cdot|\hat{t}_k)$ *denote the open-loop predicted state and input trajectories under the auxiliary computed at* $\hat{t}_k$.

Proof. Stability: If $\Delta_E \in (0,\ \Delta^*]$ and the auxiliary controller satisfies Assumption 4.3, Eq. 4.67 implies forward invariance of the set Ω_ρ under the auxiliary controller. The terminal constraint $z(\hat{t}_{k+1}|\hat{t}_k)$ computed by the auxiliary controller is therefore in Ω_ρ. If the optimization problems are feasible, boundedness of the closed-loop state in Ω_ρ over the operating window follows when $x(\hat{t}_k) \in \Omega_\rho$ owing to the fact that the constraint of Eq. 4.71e is imposed in the lower layer LEMPC, which is responsible for computing control action for the closed-loop system. Also, the terminal constraint of Eq. 4.71f imposed in the lower layer LEMPC is always in Ω_ρ as a result of the constraint of Eq. 4.70e imposed in the upper

layer LEMPC.

Feasibility: Regarding feasibility of the upper layer LEMPC problem, the input trajectory $v(\cdot|\hat{t}_k)$ obtained from the auxiliary controller is a feasible solution to the upper layer LEMPC for any $x(\hat{t}_k) \in \Omega_\rho$ because it maintains the predicted state inside Ω_ρ and forces the predicted state to the terminal constraint of Eq. 4.70f. More specifically, if the auxiliary controller is an explicit controller that satisfies Assumption 4.3, then the input trajectory v is obtained from recursively solving Eq. 4.68. On the other hand, if the LMPC of Eq. 4.69 is used as the auxiliary controller, then v is the solution to the optimization problem of Eq. 4.69.

Consider any sampling time $t_j \in [\hat{t}_k, \hat{t}_{k+1})$ such that $t_j = \hat{t}_k + i\Delta_E$ for some i in the set $\{0, \ldots, N_E - 1\}$, i.e., consider a sampling time of the lower layer LEMPC that corresponds to the beginning of a hold time of the upper layer. Let $\{\bar{t}_i\}_{i=0}^{N_E-1}$ denote the sequence of such times. The constant input trajectory $u(t) = u_E^*(t_j|\hat{t}_k)$ for all $t \in [t_j, t_{j+\bar{N}})$ where $t_{j+\bar{N}} = \bar{t}_{i+1} = \hat{t}_k + (i+1)\Delta_E$ is a feasible solution to the optimization problem of Eq. 4.71 because it maintains the state in Ω_ρ and it forces the state to the terminal constraint of Eq. 4.71f. Owing to the shrinking horizon implementation of the lower layer LEMPC, the computed input trajectory by the lower layer LEMPC at $t_j = \bar{t}_i$ is a feasible solution to the optimization problem at the next sampling time (t_{j+1}) in the sense that if $u^*(t|t_j)$ defined for $t \in [t_j, t_j + \bar{N}\Delta)$ is the optimal solution at t_j, then $u^*(t|t_j)$ for $t \in [t_{j+1}, t_{j+1} + (\bar{N}-1)\Delta)$ is a feasible solution at t_{j+1}. Using this argument recursively until the sampling time $\bar{t}_{i+1} = \hat{t}_k + (i+1)\Delta_E$ when the horizon is reinitialized to $\bar{N}$ and then, repeating the arguments for $\bar{t}_{i+1}$, it follows that the lower layer LEMPC is feasible.

Performance: At $\bar{t}_i$, the lower layer LEMPC computes an optimal input trajectory that satisfies (by optimality):

$$\int_{\bar{t}_i}^{\bar{t}_{i+1}} l_e(x^*(t|\bar{t}_i), u^*(t|\bar{t}_i))\, dt \leq \int_{\bar{t}_i}^{\bar{t}_{i+1}} l_e(x_E^*(t|\hat{t}_k), u_E^*(\bar{t}_i|\hat{t}_k))\, dt \tag{4.73}$$

for all $i \in \{0,\ldots,N_E-1\}$ (recall, $\bar{t}_{i+1} = \bar{t}_i + \bar{N}\Delta$). Owing to the shrinking horizon and the principle of optimality, the closed-loop state and input trajectories are equal to the computed open-loop state and input trajectories computed at $\bar{t}_i$ and thus,

$$\int_{\bar{t}_i}^{\bar{t}_{i+1}} l_e(x^*(t|\bar{t}_i), u^*(t|\bar{t}_i))\, dt = \int_{\bar{t}_i}^{\bar{t}_{i+1}} l_e(x(t), u^*(t))\, dt \tag{4.74}$$

where $x^*(\cdot|\bar{t}_i)$ and $u^*(\cdot|\bar{t}_i)$ denote the optimal open-loop state and input trajectories computed at $\bar{t}_i$ and x and u^* are the closed-loop state and input trajectories. Therefore, from Eqs. 4.73-4.74, the closed-loop performance over one operating period is bounded by:

$$\begin{aligned}\int_{\hat{t}_k}^{\hat{t}_{k+1}} l_e(x(t), u^*(t))\, dt &= \sum_{i=0}^{N_E-1} \int_{\bar{t}_i}^{\bar{t}_{i+1}} l_e(x(t), u^*(t|\bar{t}_i))\, dt \\ &\leq \sum_{i=0}^{N_E-1} \int_{\bar{t}_i}^{\bar{t}_{i+1}} l_e(x_E^*(t|\hat{t}_k), u_E^*(t|\hat{t}_k))\, dt \\ &= \int_{\hat{t}_k}^{\hat{t}_{k+1}} l_e(x_E^*(t|\hat{t}_k), u_E^*(t|\hat{t}_k))\, dt\ . \end{aligned} \tag{4.75}$$

At $\hat{t}_k$, the upper layer LEMPC computes an optimal input trajectory. Owing to optimality, the computed (open-loop) state and input trajectories of the upper layer LEMPC satisfies:

$$\int_{\hat{t}_k}^{\hat{t}_{k+1}} l_e(x_E^*(t|\hat{t}_k), u_E^*(t|\hat{t}_k))\, dt \leq \int_{\hat{t}_k}^{\hat{t}_{k+1}} l_e(z(t|\hat{t}_k), v(t|\hat{t}_k))\, dt\ . \tag{4.76}$$

From Eq. 4.75 and Eq. 4.76, the result of Eq. 4.72 follows. □

The following theorem provides sufficient conditions such that the two-layer EMPC structure maintains the closed-loop state inside the region Ω_ρ and the closed-loop economic performance is at least as good as if the auxiliary LMPC was applied to the system of Eq. 4.65 over the entire length of operation which may be finite or infinite.

Theorem 4.3. *Consider the closed-loop system of Eq. 4.65 under the lower layer LEMPC*

of Eq. 4.71. Let the terminal constraint of Eq. 4.71f computed from the upper layer LEMPC of Eq. 4.70, which has a terminal constraint formulated from the auxiliary controller that satisfies Assumption 4.3, and let the assumptions of Proposition 4.3 hold. If $x(0) \in \Omega_\rho$*, then* $x(t) \in \Omega_\rho$ *for all* $t \geq 0$ *and the following inequality holds for finite-time operation:*

$$\int_0^T l_e(x(t), u^*(t))\, dt \leq \int_0^T l_e(z(t), v(t))\, dt \tag{4.77}$$

where $T = KN_E\Delta_E$ *and* K *is any strictly positive integer and* x *and* u^* *are the closed-loop state and input trajectory and* z *and* v *are the resulting state and input trajectory from the auxiliary controller defined over the interval* $[0, T]$ *with initial condition* $z(0) = x(0) \in \Omega_\rho$*. The following inequality holds for infinite-time operation:*

$$\limsup_{K\to\infty} \frac{1}{KN_E\Delta_E} \int_0^{KN_E\Delta_E} l_e(x(t), u^*(t))\, dt \leq l_e(x_s^*, u_s^*)\ . \tag{4.78}$$

Proof. Applying the results of Proposition 4.3 recursively over K operating periods, recursive feasibility of the optimization problems follows, and the closed-loop state is always bounded in Ω_ρ if $x(0) \in \Omega_\rho$, and $x(\hat{t}_k) = z(\hat{t}_k)$ for $k = 1, 2, \ldots, K$. To show the result of Eq. 4.77, the length of operation is divided into K operating periods and let $T = KN_E\Delta_E$:

$$\int_0^T l_e(x(t), u^*(t))\, dt = \int_0^{\hat{t}_1} l_e(x(t), u^*(t))\, dt + \cdots + \int_{\hat{t}_{K-1}}^{\hat{t}_K} l_e(x(t), u^*(t))\, dt \tag{4.79}$$

where $\hat{t}_K = T$. By Proposition 4.3, the inequality of Eq. 4.72 holds over each operating window when $x(\hat{t}_k) = z(\hat{t}_k)$ for $k = 1, 2, \ldots, K$ and thus, the inequality of Eq. 4.77 follows.

Owing to the result of Eq. 4.77, the average finite-time economic cost is given by:

$$\frac{1}{T}\int_0^T l_e(x(t), u^*(t))\, dt \geq \frac{1}{T}\int_0^T l_e(z(t), v(t))\, dt \tag{4.80}$$

for $T = KN_E\Delta_E$ where K is any strictly positive integer. Recall, the economic cost function l_e is continuous on the compact set $\Omega_\rho \times \mathbb{U}$ and $x(t), z(t) \in \Omega_\rho$ and $u^*(t), v(t) \in \mathbb{U}$ for all $t \geq 0$. Thus, both integrals of Eq. 4.80 are bounded for any $T > 0$. Owing to the fact that the auxiliary controller satisfies Assumption 4.3 and $\Delta \in (0, \Delta^*]$, z and v asymptotically converge to the steady-state (x_s^*, u_s^*) (this follows from the inequality of Eq. 4.67).

Considering the limit of the right-hand side of Eq. 4.80 as T tends to infinity (or similarly, as K tends to infinity), the limit exists and is equal to $l_e(x_s^*, u_s^*)$ owing to the fact that z and v asymptotically converge to optimal steady-state (x_s^*, u_s^*) while remaining bounded for all $t \geq 0$. To prove this limit, the definition of the limit is invoked in the sense that given any $\varepsilon > 0$, the existence of a $T^* > 0$ such that for all $T > T^*$, the following holds:

$$\left| \frac{1}{T} \int_0^T l_e(z(t), v(t))\, dt - l_e(x_s^*, u_s^*) \right| < \varepsilon \tag{4.81}$$

needs to be established.

Define $I(0,T)$ as the following integral:

$$I(0,T) := \int_0^T l_e(z(t), v(t))\, dt \tag{4.82}$$

where the arguments of I represent the lower and upper limits of integration, respectively. Since $z(t)$ and $v(t)$ converge to x_s^* and u_s^*, respectively, as t tends to infinity, i.e., $l_e(z(t), v(t)) \to l_e(x_s^*, u_s^*)$ as t tends to infinity. Furthermore, $z(t) \in \Omega_\rho$ and $v(t) \in \mathbb{U}$ for all $t \geq 0$, so for every $\varepsilon > 0$, there exists a $\tilde{T} > 0$ such that

$$|l_e(z^*(t), v^*(t)) - l_e(x_s^*, u_s^*)| < \varepsilon/2 \tag{4.83}$$

for $t \geq \tilde{T}$. For any $T > \tilde{T}$:

$$\begin{aligned} |I(0,T) - T l_e(x_s^*, u_s^*)| &= \left|I(0,\tilde{T}) + I(\tilde{T},T) - T l_e(x_s^*, u_s^*)\right| \\ &\leq \int_0^{\tilde{T}} |l_e(z(t),v(t)) - l_e(x_s^*,u_s^*)| \ dt \\ &\quad + \int_{\tilde{T}}^{T} |l_e(z(t),v(t)) - l_e(x_s^*,u_s^*)| \ dt \\ &\leq \tilde{T}\tilde{M} + (T-\tilde{T})\varepsilon/2 \end{aligned} \tag{4.84}$$

where $\tilde{M} := \sup_{t\in[0,\tilde{T}]} \{|l_e(z(t),v(t)) - l_e(x_s^*,u_s^*)|\}$. For any $T > T^*$ where $T^* = 2\tilde{T}(\tilde{M} - \varepsilon/2)/\varepsilon$, the following inequality is satisfied:

$$|I(0,T)/T - l_e(x_s^*,u_s^*)| \leq (1-\tilde{T}/T)\varepsilon/2 + \tilde{T}\tilde{M}/T < \varepsilon \tag{4.85}$$

which proves that the asymptotic average economic cost under the auxiliary controller is $l_e(x_s^*,u_s^*)$.

Considering the left hand side of Eq. 4.80, the limit as $K \to \infty$ may not exist owing to the possible time-varying system operation under the proposed two-layer LEMPC scheme. Therefore, an upper bound on the asymptotic average performance under the LEMPC scheme is considered. Since the limit superior is equal to the limit when the limit exists, the following is obtained:

$$\begin{aligned} &\limsup_{K\to\infty} \frac{1}{KN_E\Delta_E} \int_0^{KN_E\Delta_E} l_e(x(t),u^*(t)) \ dt \\ &\quad \leq \limsup_{K\to\infty} \frac{1}{KN_E\Delta_E} \int_0^{KN_E\Delta_E} l_e(z(t),v(t)) \ dt = l_e(x_s^*,u_s^*) \end{aligned} \tag{4.86}$$

which is the desired result of Eq. 4.78. □

Remark 4.5. The finite-time result of Theorem 4.3 may be extended to any $T > 0$ by, for

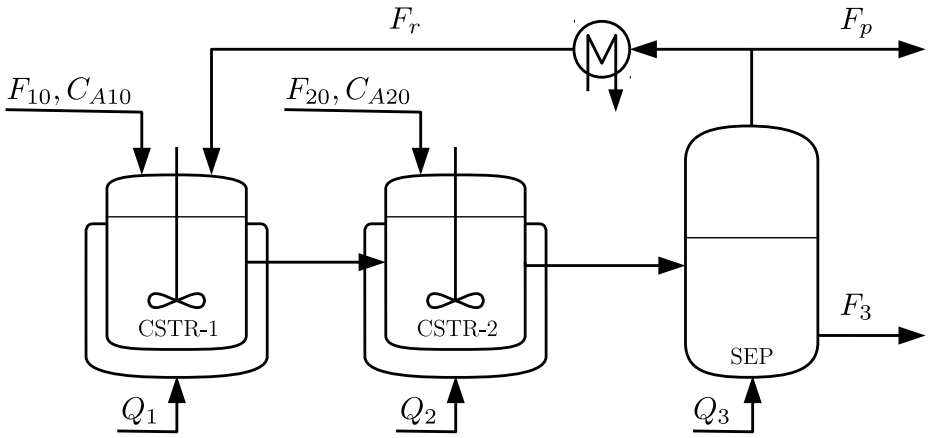

Figure 4.14: Process flow diagram of the reactor and separator process network.

instance, adjusting N_E and/or Δ_E in the last operating window.

4.4.4 Application to Chemical Process Example

Consider a three vessel chemical process network consisting of two non-isothermal continuously stirred tank reactors (CSTRs) in series followed by a flash tank separator. The process flow diagram of the process network is shown in Fig. 4.14. In each of the reactors, an irreversible second-order reaction of the form $A \rightarrow B$ takes place in an inert solvent D (A is the reactant and B is the desired product). The bottom stream of the flash tank is the product stream of the process network. Part of the overhead vapor stream from the flash tank is purged from the process, while, the remainder is fully condensed and recycled back to the first reactor. Each of the vessels have a heating/cooling jacket to supply/remove heat from the liquid contents of the vessel. The following indices are used to refer to each vessel: $i = 1$ denotes CSTR-1, $i = 2$ denotes CSTR-2, and $i = 3$ denotes SEP-1. The heat rate supplied/removed from the ith vessel is Q_i, $i = 1,2,3$. Furthermore, each reactor is fed with fresh feedstock containing A in the solvent D with concentration C_{Ai0}, volumetric flow rate F_{i0}, and constant temperature T_{i0} where $i = 1,2$. Applying first principles and standard

Table 4.4: Process parameters of the reactor and separator process network.

Symbol / Value	Description
$T_{10} = 300\,\mathrm{K}$	Temp.: CSTR-1 inlet
$T_{20} = 300\,\mathrm{K}$	Temp.: CSTR-2 inlet
$F_{10} = 5.0\,\mathrm{m^3\,h^{-1}}$	Flow rate: CSTR-1 inlet
$F_{20} = 5.0\,\mathrm{m^3\,h^{-1}}$	Flow rate: CSTR-2 inlet
$F_r = 3.0\,\mathrm{m^3\,h^{-1}}$	Flow rate: SEP-1 vapor
$F_p = 0.5\,\mathrm{m^3\,h^{-1}}$	Flow rate: purge stream
$V_1 = 1.5\,\mathrm{m^3}$	Volume: CSTR-1
$V_2 = 1.0\,\mathrm{m^3}$	Volume: CSTR-2
$V_3 = 1.0\,\mathrm{m^3}$	Volume: SEP-1
$k_0 = 3.0 \times 10^6\,\mathrm{m^3\,kmol^{-1}\,h^{-1}}$	Pre-exponential factor
$E = 3.0 \times 10^4\,\mathrm{kJ\,kmol^{-1}}$	Activation energy
$\Delta H = -5.0 \times 10^3\,\mathrm{kJ\,kmol^{-1}}$	Heat of reaction
$\Delta H_{\mathrm{vap}} = 5.0\,\mathrm{kJ\,kmol^{-1}}$	Heat of vaporization
$C_p = 0.231\,\mathrm{kJ\,kg^{-1}\,K^{-1}}$	Heat capacity
$R = 8.314\,\mathrm{kJ\,kmol^{-1}\,K^{-1}}$	Gas constant
$\rho_L = 1000\,\mathrm{kg\,m^{-3}}$	Density
$\alpha_A = 5.0$	Relative volatility: A
$\alpha_B = 0.5$	Relative volatility: B
$\alpha_D = 1.0$	Relative volatility: D
$MW_A = 18.0\,\mathrm{kg\,kmol^{-1}}$	Molecular weight: A
$MW_B = 18.0\,\mathrm{kg\,kmol^{-1}}$	Molecular weight: B
$MW_D = 40.0\,\mathrm{kg\,kmol^{-1}}$	Molecular weight: D

modeling assumptions, a dynamic model of the reactor-separator process network may be obtained (neglecting the dynamics of the condenser) and is given by the following ODEs (see Table 4.4 for variable definitions and values):

$$\frac{dT_1}{dt} = \frac{F_{10}}{V_1}(T_{10} - T_1) + \frac{F_r - F_p}{V_1}(T_3 - T_1) - \frac{\Delta H k_0}{\rho_L C_p} e^{-E/RT_1} C_{A1}^2 + \frac{Q_1}{\rho_L C_p V_1} \tag{4.87a}$$

$$\frac{dC_{A1}}{dt} = \frac{F_{10}}{V_1}(C_{A10} - C_{A1}) + \frac{F_r - F_p}{V_1}(C_{Ar} - C_{A1}) - k_0 e^{-E/RT_1} C_{A1}^2 \tag{4.87b}$$

$$\frac{dC_{B1}}{dt} = -\frac{F_{10}}{V_1} C_{B1} + \frac{F_r - F_p}{V_1}(C_{Br} - C_{B1}) + k_0 e^{-E/RT_1} C_{A1}^2 \tag{4.87c}$$

$$\frac{dT_2}{dt} = \frac{F_{20}}{V_2}(T_{20} - T_2) + \frac{F_1}{V_2}(T_1 - T_2) - \frac{\Delta H k_0}{\rho_L C_p} e^{-E/RT_2} C_{A2}^2 + \frac{Q_2}{\rho_L C_p V_2} \tag{4.87d}$$

$$\frac{dC_{A2}}{dt} = \frac{F_{20}}{V_2}(C_{A20} - C_{A2}) + \frac{F_1}{V_2}(C_{A1} - C_{A2}) - k_0 e^{-E/RT_2} C_{A2}^2 \tag{4.87e}$$

$$\frac{dC_{B2}}{dt} = -\frac{F_{20}}{V_2} C_{B2} + \frac{F_1}{V_2}(C_{B1} - C_{B2}) + k_0 e^{-E/RT_2} C_{A2}^2 \tag{4.87f}$$

$$\frac{dT_3}{dt} = \frac{F_2}{V_3}(T_2 - T_3) - \frac{\Delta H_{\text{vap}} F_r}{\rho_L C_p V_3} + \frac{Q_3}{\rho_L C_p V_3} \tag{4.87g}$$

$$\frac{dC_{A3}}{dt} = \frac{F_2}{V_3} C_{A2} - \frac{F_r}{V_3} C_{Ar} - \frac{F_3}{V_3} C_{A3} \tag{4.87h}$$

$$\frac{dC_{B3}}{dt} = \frac{F_2}{V_3} C_{B2} - \frac{F_r}{V_3} C_{Br} - \frac{F_3}{V_3} C_{B3} \tag{4.87i}$$

and the following algebraic equations:

$$K = \frac{1}{\rho_L} \sum_{i \in \{A,B,D\}} \alpha_i C_{i3} MW_i, \tag{4.88a}$$

$$C_{ir} = \alpha_i C_{i3}/K, \quad i = A, B, D, \tag{4.88b}$$

$$F_1 = F_r - F_p + F_{10},\ F_2 = F_1 + F_{20}, \tag{4.88c}$$

$$F_3 = F_2 - F_r\ . \tag{4.88d}$$

where C_{ir} is the concentration of the ith component ($i = A, B, D$) in the flash separator overhead, purge, and recycle streams. The state variables of the process network include the temperatures and concentrations of A and B in each of the vessels:

$$x^T = \begin{bmatrix} T_1 & C_{A1} & C_{B1} & T_2 & C_{A2} & C_{B2} & T_3 & C_{A3} & C_{B3} \end{bmatrix} .$$

The manipulated inputs are the heat inputs to the three vessels, Q_1, Q_2, and Q_3, and the concentration of A in the inlet streams, C_{A10} and C_{A20}:

$$u^T = \begin{bmatrix} Q_1 & Q_2 & Q_3 & C_{A10} & C_{A20} \end{bmatrix} .$$

The control objective is to regulate the process in an economically optimal time-varying fashion to maximize the average amount of product B in the product stream F_3. Continuously feeding in the maximum concentration of A into each reactor maximizes the production of B owing to the second-order reaction. However, this may not be practical from an economic stand-point. Instead, the average amount of reactant material that may be fed to each reactor is fixed motivating the use of EMPC to control the process network. In addition, supplying/removing heat to/from the vessels is considered undesirable. To accomplish these economic considerations, the two-layer LEMPC structure is applied and the upper and lower layer LEMPCs are formulated with the following economic stage cost function and constraint, respectively:

$$l_e(x,u) = -F_3 C_{B3} + A_1 Q_1^2 + A_2 Q_2^2 + A_3 Q_3^2 \tag{4.89}$$

$$\frac{1}{t'} \int_{\hat{t}_k}^{\hat{t}_{k+1}} (C_{A10} + C_{A20}) \, dt = 8.0 \, \text{kmol m}^3 \tag{4.90}$$

where $t' = 1.0\,\text{h}$ is the operating period length and $A_i = 10^{-6}$, $i = 1,2,3$ are the penalty weights for using energy. The value for the heat rate penalty has been chosen to account for the different numerical range of the heat rate and the first term in the economic cost (molar flow rate of B in the product stream). The economically optimal steady-state with respect to the economic cost function of Eq. 4.89 is open-loop asymptotically stable and is the only steady-state in the operating region of interest. Therefore, an explicit characterization of Ω_ρ is not needed for the LEMPC implementation.

The two-layer LEMPC structure, formulated with the cost function and reactant material constraint of Eqs. 4.89-4.90, respectively, is applied to the reactor-separator chemical process network. To numerically integrate the dynamic model of Eq. 4.87, explicit Euler method is used with an integration step of $1.0 \times 10^{-3}\,\text{h}$. The auxiliary controller is formulated as an auxiliary LMPC. The prediction horizon and sampling period of the auxiliary LMPC and upper layer LEMPC are $N_E = 10$ and $\Delta_E = 0.1\,\text{h}$, respectively, while, the lower layer LEMPC is formulated with a prediction horizon of $\bar{N} = 2$ and sampling period $\Delta = 0.05\,\text{h}$. Since the upper layer prediction horizon length is one hour, the reactant material constraint is enforced over each one hour operating period. However, the lower layer LEMPC prediction horizon does not cover the entire one hour operating window. Instead of using the material constraint of Eq. 4.90 directly in the lower layer LEMPC, a constraint is formulated on the basis of the upper layer LEMPC solution. Namely, over the prediction horizon of the lower layer LEMPC, the lower layer LEMPC solution must use the same amount of reactant material as that of the upper layer LEMPC solution over the same time so that the material constraint is satisfied over the operating window. To solve the optimization problems, Ipopt [187] was used and the simulations were completed on a desktop PC with an Intel® Core™ 2 Quad 2.66 GHz processor and a Linux operating system.

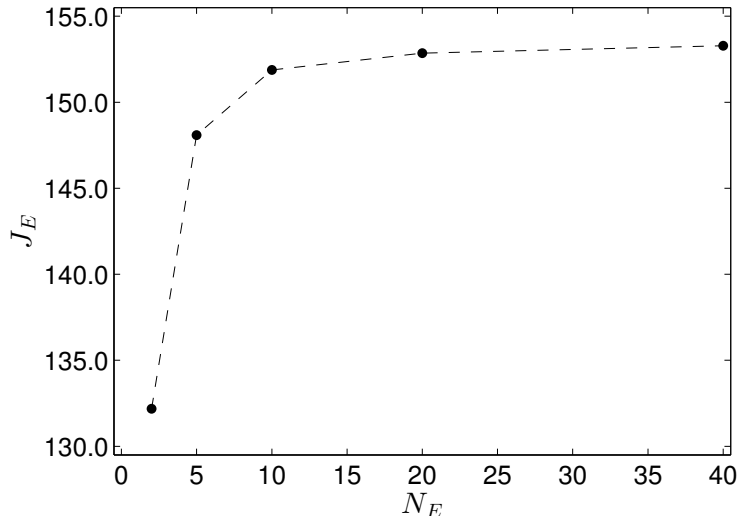

Figure 4.15: The closed-loop economic performance (J_E) with the length of prediction horizon (N_E) for the reactor-separator process under the upper layer LEMPC with a terminal constraint computed from an auxiliary LMPC.

Effect of Horizon Length

In the first set of simulations, the length of the prediction horizon on closed-loop performance is considered. The closed-loop economic performance over 4.0 h is defined by the total economic cost given by:

$$J_E = \int_0^{4.0} \left(F_3 C_{B3} - A_1 Q_1^2 - A_2 Q_2^2 - A_3 Q_3^2 \right) \, dt \, . \tag{4.91}$$

In these simulations, only the upper layer LEMPC, formulated with a terminal constraint computed from the auxiliary LMPC, is considered. Fig. 4.15 depicts the observed trend. As the prediction horizon increases, the closed-loop economic performance increases, which motivates the use of a long prediction horizon in EMPC.

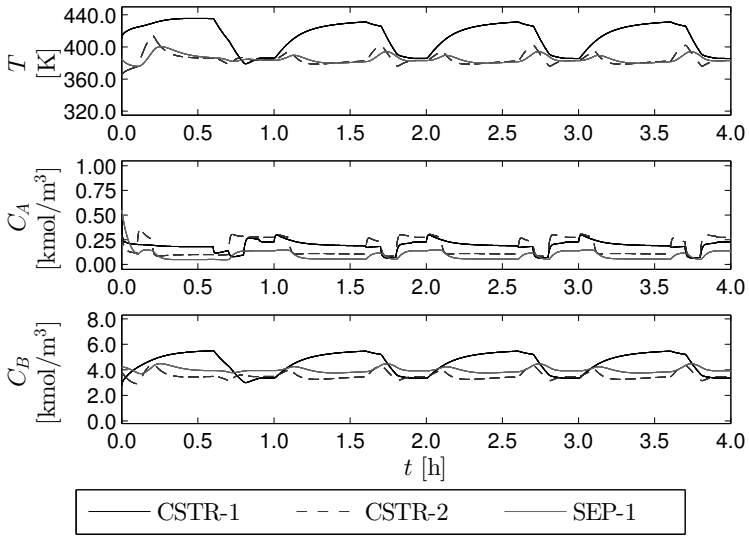

Figure 4.16: Closed-loop state trajectories of the reactor-separator process network with the upper layer LEMPC formulated with a terminal constraint computed by the auxiliary LMPC.

Effect of the Terminal Constraint

Since for any optimization problem, the addition of constraints may restrict the feasible region of the optimization problem, a reasonable consideration is the effect of the terminal constraint on closed-loop performance. To address this issue, consider the closed-loop system under the upper layer LEMPC formulated with a terminal equality constraint computed by the auxiliary LMPC and under an LEMPC (mode 1 operation only) formulated with the economic cost of Eq. 4.89 and the material constraint of Eq. 4.90, but without terminal constraints. Both use a prediction horizon of $N_E = 10$ and a sampling period of $\Delta = 0.01$ h. Figs. 4.16-4.17 display the closed-loop state and input trajectories of the reactor-separator process network with the upper layer LEMPC; while, Figs. 4.18-4.19 display the closed-loop trajectories under LEMPC with no terminal constraints.

The reactor-separator process network under the LEMPC with the terminal constraint evolves in a smaller operating range (370 K to 430 K) than the evolution under the LEMPC

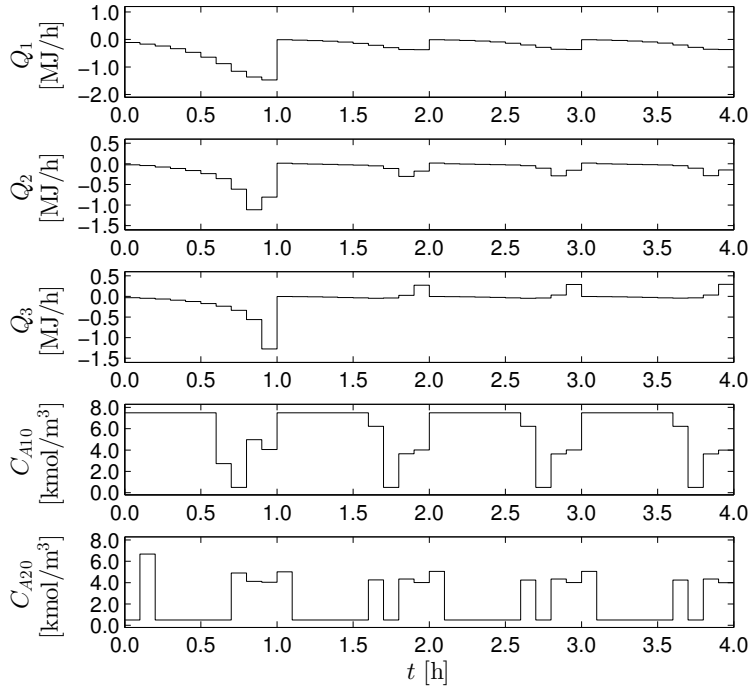

Figure 4.17: Input trajectories of the reactor-separator process network computed by the upper layer LEMPC formulated with a terminal constraint computed by the auxiliary LMPC.

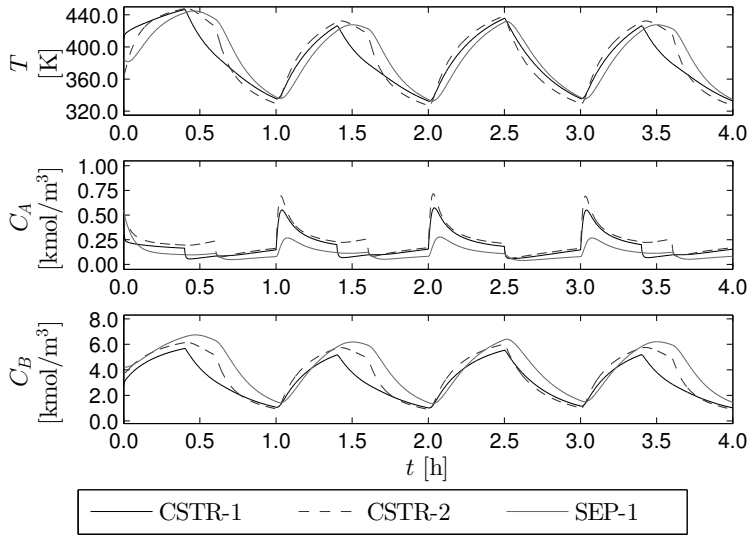

Figure 4.18: Closed-loop state trajectories of the reactor-separator process network with an LEMPC formulated without terminal constraints.

without the terminal constraint (325 K to 440 K). The total economic cost with the upper layer LEMPC (based on the auxiliary LMPC) is 151.2, while the total economic cost with LEMPC formulated without terminal constraints is 159.3. Clearly, the terminal constraint imposed in the LEMPC problem affects the achievable performance. However, the key advantage of the addition of this constraint is that for any system and any prediction horizon the closed-loop economic performance under the two-layer LEMPC structure is guaranteed to be at least as good as a stabilizing controller for both finite-time and infinite-time operating intervals.

Two-layer LEMPC Structure

The two-layer LEMPC structure with a terminal constraint computed from an auxiliary LMPC is applied to the reactor-separator process network. Several closed-loop simulations over a 4.0 h length of operation were completed. The closed-loop state and input trajectories of one of the simulations are shown in Figs. 4.20-4.21, respectively and demonstrate

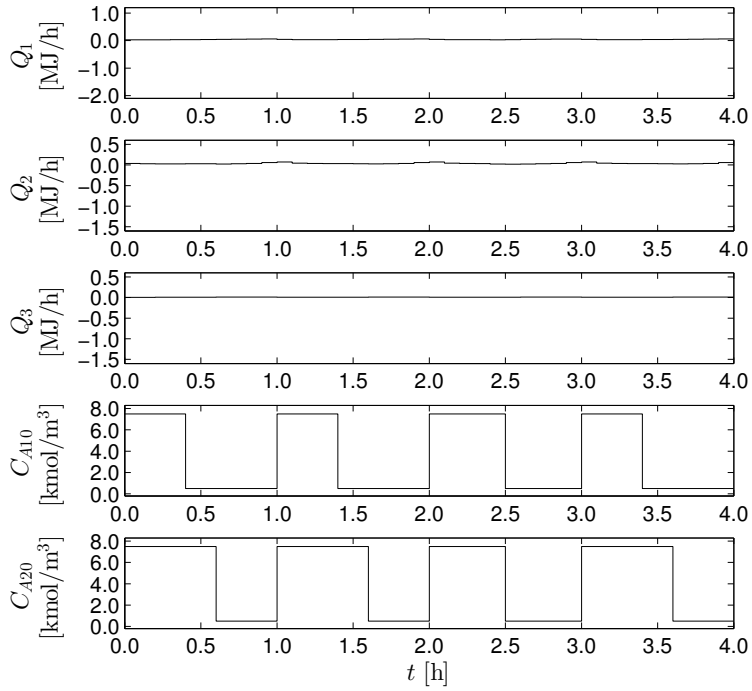

Figure 4.19: Input trajectories of the reactor-separator process network computed by an LEMPC formulated without terminal constraints.

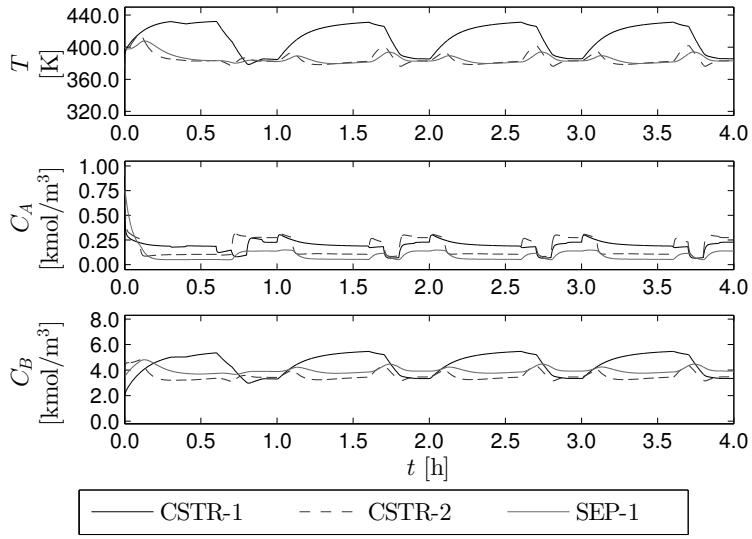

Figure 4.20: Closed-loop state trajectories of the reactor-separator process network with the two-layer LEMPC structure.

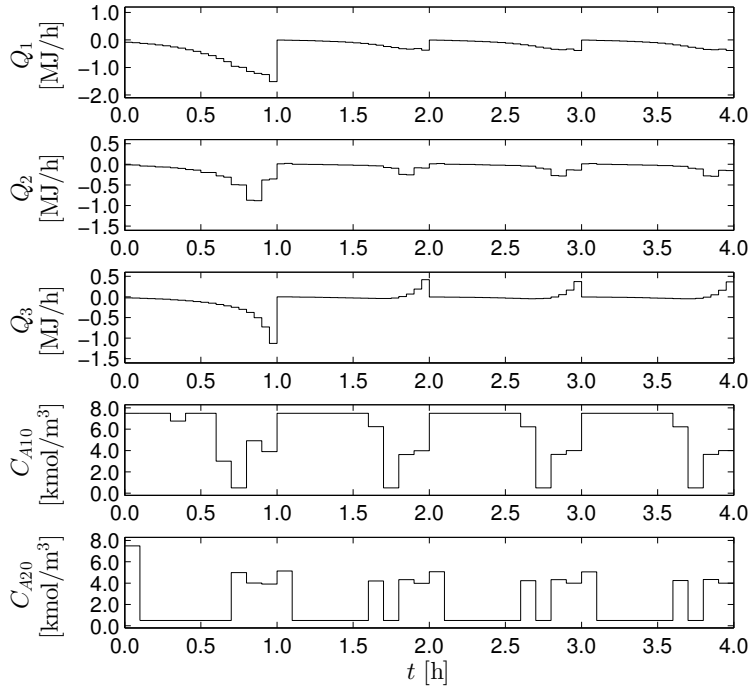

Figure 4.21: Input trajectories of the reactor-separator process network computed by the two-layer LEMPC structure.

Table 4.5: Total economic cost and average computational time in seconds per sampling period for several 4.0 h simulations with: (a) the auxiliary LMPC, (b) the one-layer LEMPC and (c) the two-layer LEMPC structure.

	LMPC	One-layer EMPC		Two-layer EMPC	
Sim.	Cost	CPU Time	Cost	CPU Time	Cost
1	140.1	5.68	151.5	1.10	151.1
2	150.3	4.24	153.9	1.05	153.4
3	142.0	4.65	152.4	0.98	152.0
4	130.7	6.45	152.3	1.24	151.9
5	126.0	4.67	151.9	1.11	151.5
6	140.2	4.63	151.6	1.33	151.2
7	144.6	4.60	150.6	1.08	150.2
8	138.1	5.01	152.5	1.06	152.1

time-varying operation of the process network. The economic performance (Eq. 4.91) is compared to the economic performance with the auxiliary LMPC (Table 4.5). From this comparison, an average of 10 percent benefit with the two-layer LEMPC structure was realized over operation under the auxiliary LMPC, i.e., resulting in steady-state operation.

Additionally, a comparison between the computational time required to solve the two-layer LEMPC system and that of a one-layer LEMPC system was completed. The one-layer LEMPC system consists of the upper layer LEMPC with a terminal constraint computed from the auxiliary LMPC. In the one-layer LEMPC system, the LEMPC applies its computed control actions directly to the process network, and there is no lower layer LEMPC. To make the comparison consistent, the one layer LEMPC is implemented with a prediction horizon of $N_E = 20$ and a sampling period of $\Delta_E = 0.05\,\text{h}$, which are the same sampling period and horizon used in the lower layer LEMPC of the two-layer LEMPC system. Since the upper and lower layer controllers are sequentially computed, the computational time at the beginning of each operating window is measured as the sum of the computational time to solve the auxiliary LMPC, the upper layer LEMPC, and the lower layer LEMPC for the two-layer LEMPC system and as the sum of the time to solve the auxiliary LMPC and the LEMPC for the one-layer LEMPC system. From Table 4.5, the one-layer LEMPC achieves slightly better closed-loop economic performance because the one-layer LEMPC uses a smaller sampling period than the upper layer LEMPC in the two-layer LEMPC structure. However, the computational time required to solve the one-layer LEMPC structure is greater than the computational time of the two-layer LEMPC structure. The two-layer LEMPC structure is able to reduce the computational time by about 75 percent on average.

Handling Disturbances

While the two-layer EMPC has been designed for nominal operation to guarantee finite-time and infinite-time closed-loop performance as is at least as good as that achieved under

a stabilizing controller, it may be applied to the process model in the presence of disturbances, plant/model mismatch, and other uncertainties with some modifications to improve recursive feasibility of the optimization problems and to ensure greater robustness of the controller to uncertainties. For instance, if the disturbances are relatively small, it may be sufficient to relax the terminal constraints or treat them as soft constraints. If one were to simply relax the terminal constraints, e.g., use a terminal region instead of a point-wise terminal constraint, it is difficult to guarantee recursive feasibility of the optimization problem. Another potential methodology is to use the terminal state constraints in the cost function instead of imposing them as constraints. For example, use a cost functional in the lower layer LEMPC of the form:

$$\frac{\alpha}{N}\left(\int_{t_j}^{t_{j+N}} l_e(\tilde{x}(t),u(t))\,dt\right)+\beta\left|\tilde{x}(t_{j+N})-x_E^*(t_j|t_k)\right|_Q \tag{4.92}$$

where α and β are tuning parameters and Q is a positive definite weighting matrix. The cost functional works to optimize the economic performance while ensuring the predicted evolution is near the terminal state through the quadratic terminal cost. The resulting lower layer LEMPC has the same stability and robustness to bounded disturbances properties as the LEMPC (without terminal constraints), i.e., recursive feasibility and boundedness of the closed-loop state for all initial states starting in Ω_ρ. While no provable performance guarantees may be made on closed-loop performance in the presence of disturbances, the closed-loop performance benefit may be evaluated through simulations.

The two-layer LEMPC with the lower layer LEMPC designed with the cost described above in Eq. 4.92 and without terminal constraints is applied to the example with significant process noise added. The noise is modeled as bounded Gaussian white noise and is introduced additively to each model state. The closed-loop state and input trajectories are shown in Figs. 4.22-4.23, respectively. The closed-loop system performance under the

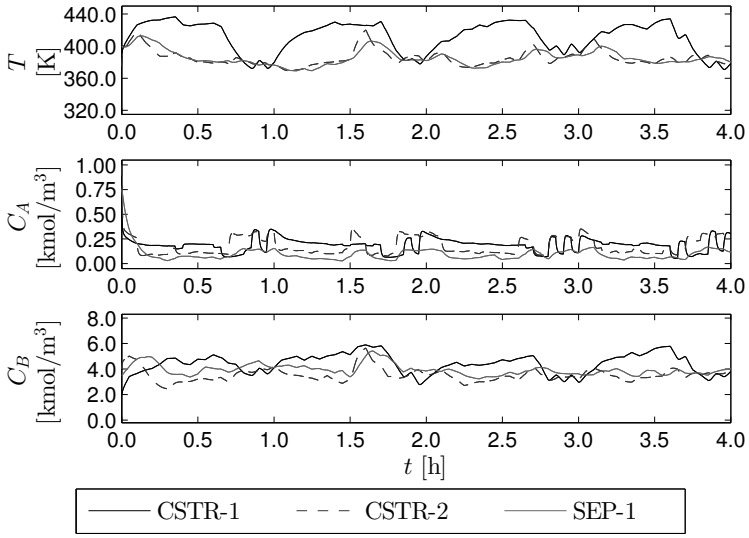

Figure 4.22: Closed-loop state trajectories of the reactor-separator process network with process noise added with the two-layer LEMPC structure.

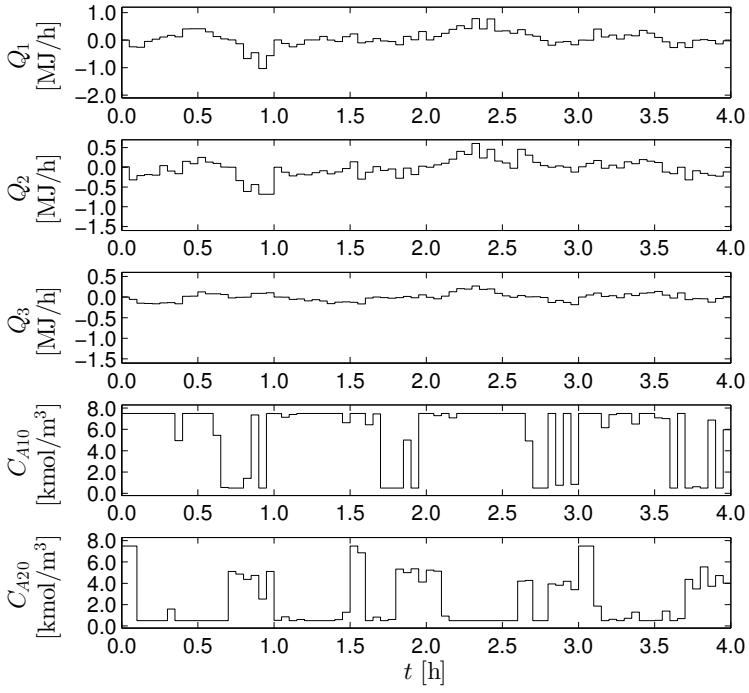

Figure 4.23: Input trajectories of the reactor-separator process network with process noise added computed by the two-layer LEMPC structure.

two-layer LEMPC is compared to the system under auxiliary LMPC with the same realization of the process noise. The LMPC is formulated with a prediction horizon of $N = 2$ and sampling period $\Delta = 0.05\,\text{h}$ which is the same horizon and sampling period as the lower layer LEMPC. The closed-loop performance under the two-layer LEMPC is 2.6 percent better than that under the LMPC for this particular realization of the process noise.

4.5 Conclusions

In this chapter, several computationally-efficient two-layer frameworks for integrating dynamic economic optimization and control of nonlinear systems were presented. In the upper layer, EMPC is used to compute economically optimal time-varying operating trajectories. Explicit control-oriented constraints were employed in the upper layer EMPC. In the lower layer, an MPC scheme is used to force the system to track the optimal time-varying trajectory computed by the upper layer EMPC. The properties, i.e., stability, performance, and robustness, of closed-loop systems under the two-layer EMPC methods were rigorously analyzed. The two-layer EMPC methods were applied to chemical process examples to demonstrate the closed-loop properties. In all the examples considered, closed-loop stability was achieved, the closed-loop economic performance under the two-layer EMPC framework was better than that achieved under conventional approaches to optimization and control, and the total on-line computational time was better with the two-layer EMPC methods compared to that under one-layer EMPC methods.

Chapter 5

Real-Time Economic Model Predictive Control of Nonlinear Process Systems

5.1 Introduction

While the two-layer EMPC structures of Chapter 4 were shown to successfully reduce the on-line computation time relative to that required for a centralized, one-layer EMPC scheme, EMPC optimization problems are nonlinear and non-convex because a nonlinear dynamic model is embedded in the optimization problem, which manifests itself as nonlinear equality constraints in the optimization problem. Although many advances have been made in solving such problems and modern computers may perform complex calculations in an efficient manner, it is possible that computation delay will occur that may approach or exceed the sampling time. If the computational delay is significant relative to the sampling period, closed-loop performance degradation and/or closed-loop instability may occur.

Some of the early work addressing computational delay within tracking MPC includes developing an implementation strategy of solving the MPC problem intermittently to account for the computational delay [162] and predicting the future state after an assumed

constant computational delay to compute an input trajectory to be implemented after the optimization problem is solved [31, 64]. Nominal feasibility and stability has been proved for tracking MPC subject to computational delay formulated with a positive definite stage cost (with respect to the set-point or steady-state), a terminal cost, and a terminal region constraint [31, 64]. Another option to handle computational delay would be to force the optimization solver to terminate after a pre-specified time to ensure that the solver returns a solution by the time needed to ensure closed-loop stability. This concept is typically referred to as suboptimal MPC [164] because the returned solution will likely be suboptimal. It was shown that when the returned solution of the MPC with a terminal constraint is any feasible solution, the origin of the closed-loop system is asymptotically stable [164].

More recently, more advanced strategies have been proposed. Particularly, nonlinear programming (NLP) sensitivity analysis has demonstrated to be a useful tool to handle computational delay by splitting the MPC optimization problem into two parts: (1) solving a computationally intensive nonlinear optimization problem which is completed before state feedback is received and (2) performing a fast on-line update of the precomputed input trajectories using NLP sensitivities (when the active-set does not change) after the current state measurement is obtained, e.g., [192, 200]; see, also, the review [21]. If the active-set changes, various methods have been proposed to cope with changing active-sets, e.g., solving a quadratic program like that proposed in [65]. In this direction, the advanced-step MPC [200] has been proposed which computes the solution of the optimization problem one sampling period in advance using a prediction of the state at the next sampling period. At the next sampling period (when the precomputed control action will be applied), the optimal solution is updated employing NLP sensitivities after state feedback is received. The advanced-step (tracking) MPC has been extended to handle computation spanning multiple sampling periods [198] and to EMPC [91]. Another related approach involves a hierarchical control structure [193, 191]. The upper layer is the full optimization problem which is

solved infrequently. In the lower layer, NLP sensitivities are used to update the control actions at each sampling period that are applied to the system. The aforementioned schemes solve an optimization problem to (local) optimality using a prediction of the state at the sampling time the control action is to be applied to the system.

As another way, the so-called real-time nonlinear MPC (NMPC) scheme [40] only takes one Newton-step of the NLP solver instead of solving the optimization problem to optimality at each sampling period. To accomplish this, the structure of the resulting dynamic optimization program, which is solved using a direct multiple shooting method, is exploited to divide the program into a preparation phase and a feedback phase. In the preparation phase, the computationally expensive calculations are completed before the state feedback is received. In the feedback phase, a state measurement is received and the remaining fast computations of the Newton-step are completed on-line to compute the control action to apply to the system. The advantage of such a strategy is that the on-line computation after a feedback measurement is obtained is insignificant compared to solving the optimization problem to optimality. The disadvantage is one would expect to sacrifice at least some closed-loop performance as a result of not solving the problem to optimality.

Clearly, the available computing power has significantly increased since the early work on computational delay of MPC and if this trend continues, one may expect a significant increase in computing power over the next decade. Moreover, more efficient solution strategies for nonlinear dynamic optimization problems continue to be developed (see, for example, the overview paper [41] and the book [20] for results in this direction). However, the ability to guarantee that a solver will converge within the time needed for closed-loop stability remains an open problem especially for nonlinear, non-convex dynamic optimization problems and systems with fast dynamics. Additionally, EMPC is generally more computationally intensive compared to tracking MPC given the additional possible nonlinearities in the stage cost of EMPC.

In this chapter, a real-time implementation strategy for LEMPC, referred to as real-time LEMPC, is developed to account for possibly unknown and time-varying computational delay. The underlying implementation strategy is inspired by event-triggered control concepts [181] since the LEMPC is only recomputed when stability conditions dictate that it must recompute a new input trajectory. If the precomputed control action satisfies the stability conditions, the control action is applied to the closed-loop system. If not, a back-up explicit controller, which has negligible computation time, is used to compute the control action for the system at the current sampling instance. This type of implementation strategy has the advantage of being easy to implement and the strategy avoids potential complications of active-set changes because the re-computation condition is only formulated to account for closed-loop stability considerations. Closed-loop stability under the real-time LEMPC scheme is analyzed and specific stability conditions are derived. The real-time LEMPC scheme is applied to an illustrative chemical process network to demonstrate closed-loop stability under the control scheme. The example also demonstrates that real-time LEMPC improves closed-loop economic performance compared to operation at the economically optimal steady-state. The results of this chapter were first presented in [54, 53].

5.2 Real-time Economic Model Predictive Control

In this section, the formulation and implementation strategy of the real-time LEMPC is presented along with sufficient conditions such that the closed-loop system under the real-time LEMPC renders the closed-loop state trajectory bounded in Ω_ρ. For the reader's convenience, the class of systems considered and the relevant assumptions are stated in the next subsection.

5.2.1 Class of Systems

The class of nonlinear systems considered has the following state-space form:

$$\dot{x}(t) = f(x(t), u(t), w(t)) \tag{5.1}$$

where $x(t) \in \mathbb{R}^n$ is the state vector, $u(t) \in \mathbb{U} \subset \mathbb{R}^m$ is the manipulated input vector, $w(t) \in \mathbb{W} \subset \mathbb{R}^l$ is the disturbance vector, and $f(\cdot,\cdot,\cdot)$ is a locally Lipschitz vector function. The input and disturbance vectors are bounded in the following sets:

$$\mathbb{U} := \{u \in \mathbb{R}^m : u_{\min,i} \leq u_i \leq u_{\max,i},\ i = 1,\ \ldots,\ m\}, \tag{5.2}$$

$$\mathbb{W} := \{w \in \mathbb{R}^l : |w| \leq \theta\}\ , \tag{5.3}$$

where $\theta > 0$ bounds the norm of the disturbance vector. Without loss of generality, the origin of the unforced system is assumed to be the equilibrium point of Eq. 5.1, i.e., $f(0,0,0) = 0$.

The following stabilizability assumption further qualifies the class of systems considered and is similar to the assumption that the pair (A,B) is stabilizable in linear systems.

Assumption 5.1. *There exists a feedback controller $h(x) \in \mathbb{U}$ with $h(0) = 0$ that renders the origin of the closed-loop system of Eq. 5.1 with $u(t) = h(x(t))$ and $w \equiv 0$ asymptotically stable for all $x \in D_0$ where D_0 is an open neighborhood of the origin.*

Applying converse theorems [123, 100], Assumption 5.1 implies that there exists a continuously differentiable Lyapunov function, $V : D \to \mathbb{R}^n$, for the closed-loop system of Eq. 5.1 with $u = h(x) \in \mathbb{U}$ and $w \equiv 0$ such that the following inequalities hold:

$$\alpha_1(|x|) \leq V(x) \leq \alpha_2(|x|), \tag{5.4a}$$

$$\frac{\partial V(x)}{\partial x} f(x, h(x), 0) \leq -\alpha_3(|x|), \tag{5.4b}$$

$$\left| \frac{\partial V(x)}{\partial x} \right| \leq \alpha_4(|x|) \tag{5.4c}$$

for all $x \in D$ where D is an open neighborhood of the origin and α_i, $i = 1,\ 2,\ 3,\ 4$ are functions of class $\mathscr{K}$. A level set of the Lyapunov function Ω_ρ, which defines a subset of D (ideally the largest subset contained in D), is taken to be the stability region of the closed-loop system under the controller $h(x)$.

Measurements of the state vector of Eq. 5.1 are assumed to be available synchronously at sampling instances denoted as $t_k := k\Delta$ where $\Delta > 0$ is the sampling period and $k = 0,\ 1, \ldots$. As described below, the EMPC computes sample-and-hold control actions and thus, the resulting closed-loop system, which consists of the continuous-time system of Eq. 5.1 under a sample-and-hold controller, is a sampled-data system. If the controller $h(x)$ is implemented in a sample-and-hold fashion, it possesses a certain degree of robustness to uncertainty in the sense that the origin of the closed-loop system is rendered practically stable when a sufficiently small sampling period is used and the bound θ on the disturbance vector is sufficiently small; see, for example, [133] for more discussion on this point.

5.2.2 Real-time LEMPC Formulation

The overall objective of the real-time LEMPC is to account for the real-time computation time required to solve the optimization problem for a (local) solution. Particularly, the case when the average computation time, which is denoted as $\bar{t}_s$, is greater than one sampling period is considered, i.e., $N_s = \lceil \bar{t}_s/\Delta \rceil \geq 1$ where N_s is the average number of sampling periods required to solve the optimization problem. During the time the solver is solving the optimization problem, the control actions computed at a previous sampling period are applied to the system if there are precomputed control actions available and if the stability

conditions described below are satisfied. If no precomputed control actions are available or the stability conditions are violated, the explicit controller $h(x)$ is used to compute and apply control actions during the time that the real-time LEMPC is computing. In this fashion, the LEMPC is used to compute control actions to improve the economic performance when possible.

Specifically, when the closed-loop state is in the subset of the stability region $\Omega_{\rho_e} \subset \Omega_\rho$, the control actions of the precomputed LEMPC problem may be applied to the system. When the state is outside the subset, the explicit controller is used because maintaining the closed-loop state in Ω_ρ is required for guaranteeing the existence of a feasible input trajectory that maintains closed-loop stability (in the sense that the closed-loop state trajectory is always bounded in Ω_ρ). To force the state back to the subset of the stability region Ω_{ρ_e}, the Lyapunov function must decrease over each sampling period in the presence of uncertainty. This requires the incorporation of feedback, i.e., recomputing the control action at each sampling period using a measurement of the current state. Owing to the computational burden of solving the LEMPC optimization problem, it may not be possible to achieve convergence of the optimization solver within one sampling period. Hence, the controller $h(x)$ is used when the state is outside of Ω_{ρ_e}.

For real-time implementation, only mode 1 of the LEMPC of Eq. 3.3 is used and the LEMPC is solved infrequently (not every sampling period) which will be made clear when

the implementation strategy is discussed. The real-time LEMPC is formulated as follows:

$$\min_{u\in S(\Delta)} \quad \int_{t_{j+1}}^{t_{j+N}} l_e(\tilde{x}(t),u(t))\,dt \tag{5.5a}$$

$$\text{s.t.} \quad \dot{\tilde{x}}(t) = f(\tilde{x}(t),u(t),0) \tag{5.5b}$$

$$\tilde{x}(t_j) = x(t_j) \tag{5.5c}$$

$$u(t) = \tilde{u}(t_j),\ \forall\, t\in[t_j,t_{j+1}) \tag{5.5d}$$

$$u(t)\in\mathbb{U},\ \forall\, t\in[t_{j+1},t_{j+N}) \tag{5.5e}$$

$$V(\tilde{x}(t))\le\rho_e,\ \forall\, t\in[t_{j+1},t_{j+N}) \tag{5.5f}$$

where the notation and constraints are similar to that used in LEMPC of Eq. 3.3 except for an additional constraint of Eq. 5.5d. This additional constraint is used because a predetermined control action is applied to the system over the first sampling period of the prediction horizon. The predetermined control action is either the control action computed by the LEMPC at a previous sampling period or the control action from the explicit controller $h(x)$, i.e., the input trajectory over the first sampling period of the prediction horizon is not a degree of freedom in the optimization problem. The LEMPC of Eq. 5.5 may dictate a time-varying operating policy to optimize the economic cost as long as the predicted evolution is maintained in the level set $\Omega_{\rho_e}\subset\Omega_\rho$. The notation t_j denotes the sampling time at which the LEMPC problem is initialized with a state measurement and the solver begins solving the resulting optimization problem. The optimal solution of the LEMPC is denoted as $u^*(t|t_j)$ and is defined for $t\in[t_{j+1},t_{j+N})$. Feasibility of the optimization problem is considered in Section 5.2.4 below. However, it is important to point out that $x(t_j)\in\Omega_{\rho_e}$ and $\tilde{x}(t_{j+1})\in\Omega_{\rho_e}$ owing to the real-time implementation strategy, and thus, the real-time LEMPC has a feasible solution (refer to the proof of Theorem 5.1).

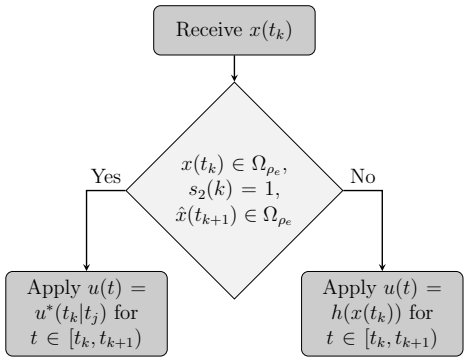

Figure 5.1: Implementation strategy for determining the control action at each sampling period.

The notation $u^*(t_k|t_j)$ is used to denote the control action to be applied over the sampling period t_k to t_{k+1} from the precomputed input solution of the real-time LEMPC of Eq. 5.5 solved at time step t_j.

5.2.3 Implementation Strategy

Before the implementation strategy is presented, the following discrete-time signals are defined to simplify the presentation of the implementation strategy. The first signal is used to keep track of whether the solver is currently solving an LEMPC optimization problem:

$$s_1(k) = \begin{cases} 1, & \text{solving the LEMPC} \\ 0, & \text{not solving the LEMPC} \end{cases} \tag{5.6}$$

where k denotes the k-th sampling period, i.e., t_k. The second signal keeps track if there is a previously computed input trajectory currently stored in memory:

$$s_2(k) = \begin{cases} 1, & \text{previous input solution stored} \\ 0, & \text{no previous input solution stored} \end{cases} \tag{5.7}$$

At each sampling period, a state measurement $x(t_k)$ is received from the sensors and three conditions are used to determine if a precomputed control action from LEMPC or if

the control action from the explicit controller $h(x)$ is applied to the system. If the following three conditions are satisfied the control action applied to the system in a sample-and-hold fashion is the precomputed control action from the LEMPC: (1) the current state must be in Ω_{ρ_e} ($x(t_k) \in \Omega_{\rho_e}$), (2) there must be a precomputed control action available for the sampling instance t_k, i.e., $s_2(k) = 1$, and (3) the predicted state under the precomputed control action must satisfy: $\hat{x}(t_{k+1}) \in \Omega_{\rho_e}$ where $\hat{x}(t_{k+1})$ denotes the predicted state. To obtain a prediction of the state at the next sampling period, the nominal model of Eq. 5.1 with $w \equiv 0$ is recursively solved with the input $u(t) = u^*(t_k|t_j)$ for $t \in [t_k, t_{k+1})$ (the on-line computation time to accomplish this step is assumed to be negligible). The control action decision at a given sampling instance t_k is summarized by the flow chart of Fig. 5.1.

A series of decisions are made at each sampling period to determine if the LEMPC should begin resolving, continue solving, or terminate solving the optimization problem and is illustrated in the flow chart of Fig. 5.2. The computation strategy is summarized in the following algorithm. To initialize the algorithm at $t_0 = 0$, get the state measurement $x(0) \in \Omega_\rho$. If $x(0) \in \Omega_{\rho_e}$, begin solving the LEMPC problem with $j = 0$ and $x(0)$. Set $s_1(0) = 1$, $s_2(0) = 0$, and $\tilde{u}(t_j) = h(x(0))$. Go to Step 8. Else, set $s_1(0) = s_1(1) = s_2(0) = s_2(1) = 0$ and go to Step 9.

1. Receive a measurement of the current state $x(t_k)$ from the sensors; go to Step 2.

2. If $x(t_k) \in \Omega_{\rho_e}$, then go to Step 2.1. Else, go to Step 2.2.

   2.1 If $s_2(k) = 1$, go to Step 3. Else, go to Step 6.

   2.2 Terminate solver if $s_1(k) = 1$, set $s_1(k+1) = 0$ and $s_2(k+1) = 0$, and go to Step 9.

3. If $\hat{x}(t_{k+1}) \in \Omega_{\rho_e}$, go to Step 4. Else, set $s_2(k) = 0$ and $\tilde{u}(t_j) = h(x(t_k))$; go to Step 7.

4. If $s_1(k) = 1$, go to Step 8. Else, go to Step 5.

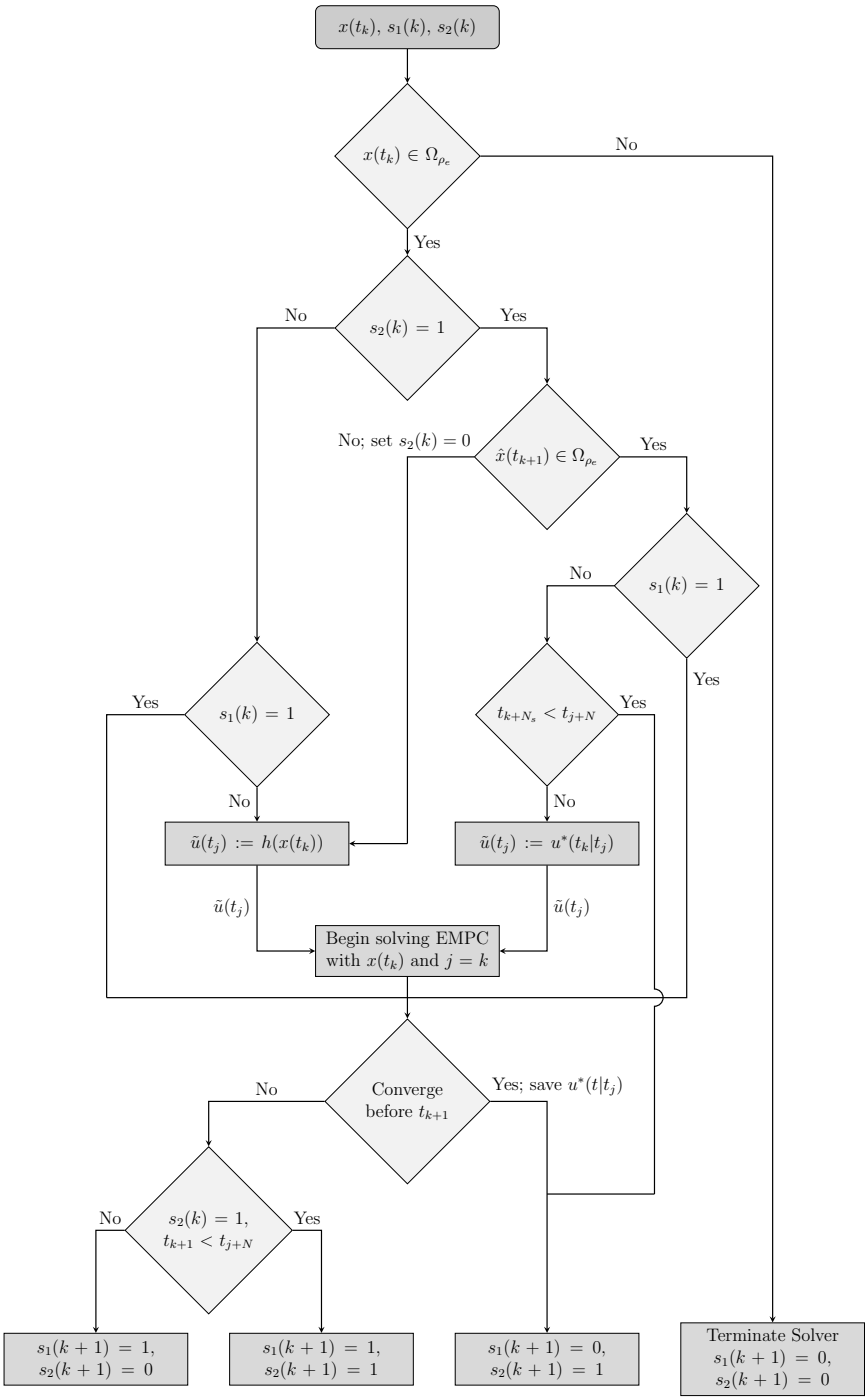

Figure 5.2: Computation strategy for the real-time LEMPC scheme.

5. If $t_{k+N_s} < t_{j+N}$, set $s_1(k+1) = 0$ and $s_2(k+1) = 1$, and go to Step 9. Else, set $\tilde{u}(t_j) = u^*(t_k|t_j)$; go to Step 7.

6. If $s_1(k) = 1$, go to Step 8. Else, set $\tilde{u}(t_j) = h(x(t_k))$; go to Step 7.

7. If the solver is currently solving a problem ($s_1(k) = 1$), terminate the solver. Begin solving the LEMPC problem with $j = k$ and $x(t_j) = x(t_k)$. Go to Step 8.

8. If the solver converges before t_{k+1}, then go to Step 8.1. Else, go to Step 8.2.

   8.1 Save $u^*(t|t_j)$ for $t \in [t_k, t_{j+N})$. Set $s_1(k+1) = 0$ and $s_2(k+1) = 1$. Go to Step 9.

   8.2 Set $s_1(k+1) = 1$. If $s_2(k) = 1$ and $t_{k+1} < t_{j+N}$, the go to Step 8.2.1. Else, go to Step 8.2.2.

      8.2.1 Set $s_2(k+1) = 1$. Go to Step 9.

      8.2.2 Set $s_2(k+1) = 0$. Go to Step 9.

9. Go to Step 1 ($k \leftarrow k+1$).

In practice, N_s may be unknown or possibly time varying. If N_s is unknown, then one may specify the number of sampling periods that the real-time LEMPC may apply a precomputed input trajectory before it must start re-computing a new input trajectory as a design parameter. This condition may be used instead of Step 5 of the algorithm above. Additionally, it may be beneficial from a closed-loop performance perspective to force the LEMPC to recompute its solution more often than prescribed by the implementation strategy described above.

A possible input trajectory resulting under the real-time LEMPC scheme is given in Fig. 5.3. In the illustration, the solver begins to solve an LEMPC optimization problem at t_0 and returns a solution at t_5. It is assumed that the closed-loop state is maintained in Ω_{ρ_e}

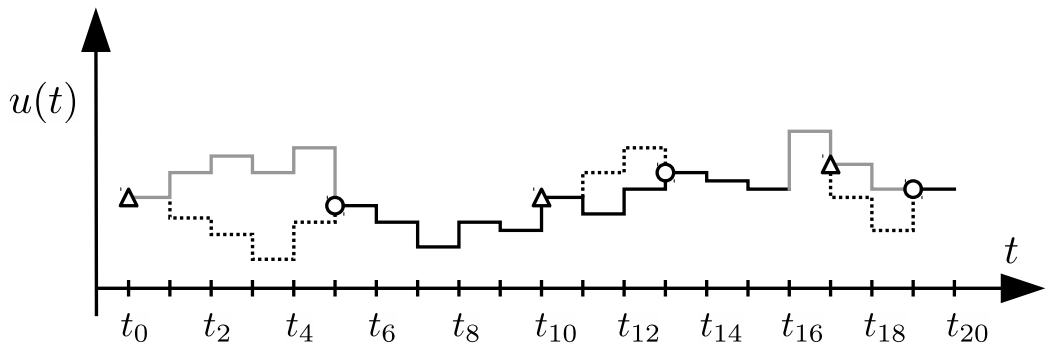

Figure 5.3: An illustration of an example input trajectory resulting under the real-time LEMPC scheme.
The triangles are used to denote the time instances when the LEMPC begins to solve the optimization problem, while the circles are used to denote when the solver converges to a solution. The solid black trajectory represents the control actions computed by the LEMPC which are applied to the system, the dotted trajectory represents the computed input trajectory by the LEMPC (not applied to the system), and the solid gray trajectory is the input trajectory of the explicit controller which is applied to the system.

from t_0 to t_5 so that the solver is not terminated. Over the time the solver is solving, the explicit controller is applied to the system since a precomputed LEMPC input trajectory is not available. The precomputed LEMPC solution is applied from t_5 to t_{13}. At t_{10}, the solver begins to solve a new LEMPC problem. The solver returns a solution at t_{13}. At t_{16}, the stability conditions are not satisfied for the precomputed LEMPC input trajectory, so the explicit controller computes a control action and applies it to the system.

5.2.4 Stability Analysis

In this section, sufficient conditions such that the closed-loop state under the real-time LEMPC is bounded in Ω_ρ are presented which make use of the following properties. Since $f(\cdot,\cdot,\cdot)$ is a locally Lipschitz vector function and the Lyapunov function $V(\cdot)$ is a continuously differentiable function, there exist positive constants L_x, L_w, L'_x, and L'_w such that the

following bounds hold:

$$|f(x_a,u,w)-f(x_b,u,0)| \leq L_x\,|x_a-x_b|+L_w\,|w| \tag{5.8}$$

$$\left|\frac{\partial V(x_a)}{\partial x}f(x_a,u,w)-\frac{\partial V(x_b)}{\partial x}f(x_b,u,0)\right| \leq L'_x\,|x_a-x_b|+L'_w\,|w| \tag{5.9}$$

for all x_a, $x_b \in \Omega_\rho$, $u \in \mathbb{U}$ and $w \in \mathbb{W}$. Furthermore, there exists $M > 0$ such that

$$|f(x,u,w)| \leq M \tag{5.10}$$

for all $x \in \Omega_\rho$, $u \in \mathbb{U}$ and $w \in \mathbb{W}$ owing to the compactness of the sets Ω_ρ, $\mathbb{U}$, and $\mathbb{W}$ and the locally Lipschitz property of the vector field.

The following proposition bounds the difference between the actual state trajectory of the system of Eq. 5.1 ($w \not\equiv 0$) and the nominal state trajectory ($w \equiv 0$).

Proposition 5.1 (c.f. Proposition 3.1)**.** *Consider the state trajectories $x(t)$ and $\hat{x}(t)$ with dynamics:*

$$\dot{x}(t) = f(x(t),u(t),w(t)), \tag{5.11}$$

$$\dot{\hat{x}}(t) = f(\hat{x}(t),u(t),0), \tag{5.12}$$

input trajectory $u(t) \in \mathbb{U}$, $w(t) \in \mathbb{W}$, and initial condition $x(0) = \hat{x}(0) \in \Omega_\rho$. If $x(t)$, $\hat{x}(t) \in \Omega_\rho$ for all $t \in [0,T]$ where $T \geq 0$, then the difference between $x(T)$ and $\hat{x}(T)$ is bounded by the function $\gamma_e(\cdot)$:

$$|x(T)-\hat{x}(T)| \leq \gamma_e(T) := \frac{L_w\theta}{L_x}\left(e^{L_xT}-1\right)\ . \tag{5.13}$$

Owing to the compactness of the set Ω_ρ, the difference in Lyapunov function values for any two points in Ω_ρ may be bounded by a quadratic function which is stated in the following proposition.

Proposition 5.2 (c.f. Proposition 3.2)**.** *Consider the Lyapunov function $V(\cdot)$ of the closed-loop system of Eq. 5.1 under the controller $h(x)$. There exists a scalar-valued quadratic function $f_V(\cdot)$ such that*

$$V(x_a) \leq V(x_b) + f_V(|x_a - x_b|) \tag{5.14}$$

for all x_a, $x_b \in \Omega_\rho$ where

$$f_V(s) := \alpha_4(\alpha_1^{-1}(\rho))s + \beta s^2 \tag{5.15}$$

and β is a positive constant.

Theorem 5.1 below provides sufficient conditions such that the real-time LEMPC renders the closed-loop state trajectory bounded in Ω_ρ for all times. The conditions such that the closed-loop state trajectory is maintained in Ω_ρ are independent of the computation time required to solve the LEMPC optimization problem. From the perspective of closed-loop stability, computational delay of arbitrary size may be handled with the real-time LEMPC methodology. In the case where the computational delay is always greater than the prediction horizon, the real-time LEMPC scheme would return the input trajectory under the explicit controller applied in a sample-and-hold fashion.

Theorem 5.1. *Consider the system of Eq. 5.1 in closed-loop under the real-time LEMPC of Eq. 5.5 based on a controller $h(x)$ that satisfies the conditions of Eq. 5.4 that is implemented according to the implementation strategy of Fig. 5.1. Let $\varepsilon_w > 0$, $\Delta > 0$ and $\rho > \rho_e \geq \rho_{\min} > \rho_s > 0$ satisfy*

$$-\alpha_3(\alpha_2^{-1}(\rho_s)) + L_x' M\Delta + L_w'\theta \leq -\varepsilon_w/\Delta\,, \tag{5.16}$$

$$\rho_{\min} = \max\{V(x(t+\Delta) \mid V(x(t)) \leq \rho_s\}\,, \tag{5.17}$$

and

$$\rho_e < \rho - f_V(\gamma_e(\Delta))\,. \tag{5.18}$$

If $x(t_0) \in \Omega_\rho$ and $N \geq 1$, then the state trajectory $x(t)$ of the closed-loop system is always bounded in Ω_ρ for $t \geq t_0$.

Proof. If the real-time LEMPC is implemented according to the implementation strategy of Fig. 5.1, the control action to be applied over the sampling period either comes from the precomputed LEMPC input trajectory or the explicit controller $h(x)$. To prove that the closed-loop state is bounded in Ω_ρ, we will show that when the control action is computed from the explicit controller and $x(t_k) \in \Omega_\rho$, then the state at the next sampling period will be contained in Ω_ρ. If the control action comes from a precomputed LEMPC solution, we will show that if $x(t_k) \in \Omega_{\rho_e}$, then $x(t_{k+1}) \in \Omega_\rho$ owing to the stability conditions imposed on applying the precomputed LEMPC solution. The proof consists of two parts. In the first part, the closed-loop properties when the control action is computed by the explicit controller $h(x)$ are analyzed. This part of the proof is based on the proof of [133] which considers the stability properties of an explicit controller of the form assumed for $h(x)$ implemented in a sample-and-hold fashion. In the second part, the closed-loop stability properties of the precomputed control actions by the LEMPC are considered. In both cases, the closed-loop state trajectory is shown to be maintained in Ω_ρ for $t \geq t_0$ when $x(t_0) \in \Omega_\rho$.

Part 1: First, consider the properties of the control action computed by the explicit controller $h(x)$ applied to the system of Eq. 5.1 in a sample-and-hold fashion. Let $x(t_k) \in \Omega_\rho \setminus \Omega_{\rho_s}$ for some $\rho_s > 0$ such that the conditions of Theorem 5.1 are satisfied, i.e., Eq. 5.16. The explicit controller $h(x)$ computes a control action that has the following property (from condition of Eq. 5.4):

$$\frac{\partial V(x(t_k))}{\partial x} f(x(t_k), h(x(t_k)), 0) \leq -\alpha_3(|x(t_k)|) \leq -\alpha_3(\alpha_2^{-1}(\rho_s)) \tag{5.19}$$

for any $x(t_k) \in \Omega_\rho \setminus \Omega_{\rho_s}$. Over the sampling period, the time-derivative of the Lyapunov

function is:

$$\dot{V}(x(t)) = \frac{\partial V(x(t_k))}{\partial x} f(x(t_k), h(x(t_k)), 0) + \frac{\partial V(x(t))}{\partial x} f(x(t), h(x(t_k)), w(t)) - \frac{\partial V(x(t_k))}{\partial x} f(x(t_k), h(x(t_k)), 0) \tag{5.20}$$

for all $t \in [t_k, t_{k+1})$. From the bound on the time-derivative of Lyapunov function of Eq. 5.19, the Lipschitz bound of Eq. 5.9, and the bound on the norm of the disturbance vector, the time-derivative of the Lyapunov function is bounded for $t \in [t_k, t_{k+1})$ as follows:

$$\begin{aligned}
\dot{V}(x(t)) &\leq -\alpha_3(\alpha_2^{-1}(\rho_s)) \\
&\quad + \left| \frac{\partial V(x(t))}{\partial x} f(x(t), h(x(t_k)), w(t)) - \frac{\partial V(x(t_k))}{\partial x} f(x(t_k), h(x(t_k)), 0) \right| \\
&\leq -\alpha_3(\alpha_2^{-1}(\rho_s)) + L'_x |x(t) - x(t_k)| + L'_w |w(t)| \\
&\leq -\alpha_3(\alpha_2^{-1}(\rho_s)) + L'_x |x(t) - x(t_k)| + L'_w \theta
\end{aligned} \tag{5.21}$$

for all $t \in [t_k, t_{k+1})$. Taking into account of Eq. 5.10 and the continuity of $x(t)$, the following bound may be written for all $t \in [t_k, t_{k+1})$:

$$|x(t) - x(t_k)| \leq M\Delta \,. \tag{5.22}$$

From Eq. 5.21 and Eq. 5.22, the bound below follows:

$$\dot{V}(x(t)) \leq -\alpha_3(\alpha_2^{-1}(\rho_s)) + L'_x M\Delta + L'_w \theta \tag{5.23}$$

for all $t \in [t_k, t_{k+1})$. If the condition of Eq. 5.16 is satisfied, i.e., Δ and θ is sufficiently

small, then there exists $\varepsilon_w > 0$ such that:

$$\dot{V}(x(t)) \leq -\varepsilon_w/\Delta \tag{5.24}$$

for all $t \in [t_k, t_{k+1})$. Integrating the above bound, yields:

$$V(x(t)) \leq V(x(t_k)), \quad \forall\, t \in [t_k, t_{k+1}), \tag{5.25}$$

$$V(x(t_{k+1})) \leq V(x(t_k)) - \varepsilon_w\ . \tag{5.26}$$

For any state $x(t_k) \in \Omega_\rho \setminus \Omega_{\rho_s}$, the state at the next sampling period will be in a smaller level set when the control action $u(t) = h(x(t_k))$ is applied for $t \in [t_k, t_{k+1})$. Also, the state will not come out of Ω_ρ over the sampling period owing to Eq. 5.24. Once the closed-loop state under the explicit controller $h(x)$ implemented in a sample-and-hold fashion has converged to Ω_{ρ_s}, the closed-loop state trajectory will be maintained in $\Omega_{\rho_{\min}}$ if $\rho_{\min} \leq \rho$ and $\rho_{\min}$ is defined according to Eq. 5.17. Thus, the sets Ω_ρ and $\Omega_{\rho_{\min}}$ are forward invariant sets under the controller $h(x)$ and if $x(t_k) \in \Omega_\rho$, then $x(t_{k+1}) \in \Omega_\rho$ under the explicit controller $h(x)$.

Part 2: In this part, the closed-loop stability properties of the input precomputed by the LEMPC for the sampling period t_k to t_{k+1} are considered. For clarity of presentation, the notation $\hat{x}(t)$ denotes the prediction of closed-loop state at time t, i.e., this prediction used in the implementation strategy to determine which control action to apply to the system, while the notation $\tilde{x}(t)$ will be reserved to denote the predicted state in the LEMPC of Eq. 5.5. The predicted state in the LEMPC of Eq. 5.5 at t_{j+1}, which is denoted as $\tilde{x}(t_{j+1})$, satisfies $\hat{x}(t_{j+1}) = \tilde{x}(t_{j+1})$ because both predicted states use the nominal model with the same initial condition and same piecewise constant input applied from t_j to t_{j+1}.

First, feasibility of the optimization problem is considered. Owing to the formulation of the LEMPC of Eq. 5.5, the optimization problem is always feasible if ρ_e satisfies: $\rho >$

$\rho_e \geq \rho_{\min}$. Recall, the input over the sampling period t_j to t_{j+1} is not a degree of freedom in the optimization problem. If this control action is precomputed from a previous LEMPC solution, it must have the property that $\hat{x}(t_{j+1}) = \tilde{x}(t_{j+1}) \in \Omega_{\rho_e}$ which is imposed as a condition of the implementation strategy of Fig. 5.1. If the control action is computed by the explicit controller, the control action over the sampling period t_j to t_{j+1} will maintain $\tilde{x}(t_{j+1}) \in \Omega_{\rho_e}$. Thus, $\tilde{x}(t_{j+1}) \in \Omega_{\rho_e}$ in the LEMPC of Eq. 5.5. Feasibility of the optimization problem follows from the fact that the input trajectory obtained from the explicit controller $h(x)$ over the prediction horizon is a feasible solution, that is $u(t) = h(\hat{x}(t_i))$ for $t \in [t_i, t_{i+1})$, $i = j+1,\ j+2,\ \ldots,\ j+N-1$ where $\hat{x}(t)$ is obtained by recursively solving the model:

$$\dot{\hat{x}}(t) = f(\hat{x}(t), h(\hat{x}(t_i)), 0) \tag{5.27}$$

for $t \in [t_i, t_{i+1})$ and $i = j+1,\ j+1\ \ldots,\ j+N-1$ with the initial condition $\hat{x}(t_{j+1}) = \tilde{x}(t_{j+1})$. Furthermore, the set Ω_{ρ_e} is forward invariant under the controller $h(x)$ (the proof is analogous to Part 1 where the set Ω_{ρ_e} is used instead of Ω_ρ). Thus, the LEMPC of Eq. 5.5 is always feasible for any $x(t_j) \in \Omega_{\rho_e}$.

If the LEMPC is implemented according to the implementation strategy of Fig. 5.1, then the precomputed input for t_k by the LEMPC is only used when $x(t_k) \in \Omega_{\rho_e}$ and the predicted state at the next sampling period $\hat{x}(t_{k+1}) \in \Omega_{\rho_e}$. When $x(t) \in \Omega_\rho$ for $t \in [t_k, t_{k+1})$, i.e., a sufficiently small sampling period is used, the following bound on the Lyapunov function value at the next sampling period t_{k+1} may be derived from Propositions 5.1-5.2:

$$V(x(t_{k+1})) \leq V(\hat{x}(t_{k+1})) + f_V(\gamma_e(\Delta))\ . \tag{5.28}$$

Since $\hat{x}(t_{k+1}) \in \Omega_{\rho_e}$ and if the condition of Eq. 5.18 is satisfied, $x(t_{k+1}) \in \Omega_\rho$.

To summarize, if the control action to be applied over the sampling period t_k to t_{k+1}

is $u(t_k) = h(x(t_k))$, the state at the next sampling period will be in Ω_ρ ($x(t_{k+1}) \in \Omega_\rho$). If the control action to be applied over the sampling period t_k to t_{k+1} is from a precomputed LEMPC input, the state at the next sampling period will also be contained in Ω_ρ which completes the proof of boundedness of the closed-loop state trajectory $x(t) \in \Omega_\rho$ under the real-time LEMPC for $t \geq t_0$. □

Remark 5.1. No closed-loop performance guarantees may be made because performance constraints, e.g., terminal constraints, are not imposed on the LEMPC and the closed-loop performance may be adversely affected with greater computation time. The latter point is associated with the fact that the LEMPC problem allows for the input trajectory from t_{j+1} to t_{j+N_s}, i.e., the time the solver converges, to be degrees of freedom in the optimization problem. However, the actual closed-loop input trajectory applied over this period may be different from that computed by the LEMPC over the same time period. Potentially, one may also employ sensitivity-based corrections to the precomputed control actions after receiving state feedback like that employed in [192, 200] to improve closed-loop performance. However, active set changes must be handled appropriately which may introduce additional on-line computation. It is important to point out that the computed solution of the LEMPC may dictate a time-varying operating policy to optimize the process economics. Even in the presence of uncertainty, the time-varying operating policy dictated by the real-time LEMPC may be substantially better (with respect to the economic cost) than steady-state operation which is the case for the chemical process network considered in Section 5.3.

Remark 5.2. In the current chapter, unknown and possibly time-varying computational delay is considered for operation affected by unknown bounded disturbance. If, instead of the computation algorithm described above, a hard cap was placed on the solver to terminate and return a (suboptimal) solution by a certain number of sampling times, one

could account for the control actions that are applied to the system over the computation time by setting the input trajectory in the LEMPC problem over the specified number of sampling periods of the prediction horizon be equal to a predetermined input trajectory. This potential strategy, however, does not account for the fact that the solver may return a solution before the end of specified number of sampling periods.

Remark 5.3. From the proof of Theorem 5.1, recursive feasibility of the LEMPC in the presence of bounded uncertainty is guaranteed if the initial state is in Ω_ρ. It is difficult in general to characterize the feasible set under EMPC formulated with a terminal constraint, i.e., the set of points where recursive feasibility is maintained in the presence of uncertainty. Thus, it may be difficult to ensure that the closed-loop state is maintained in the feasible set under EMPC with a terminal constraint in the presence of uncertainty and computational delay. In this respect, LEMPC has a unique advantage for real-time implementation compared to EMPC with a terminal constraint in that LEMPC maintains the closed-loop state inside Ω_ρ where recursive feasibility is guaranteed.

Remark 5.4. The number of times that the explicit controller is applied to the closed-loop system may be a factor in the closed-loop economic performance. Whether the control action is from a precomputed LEMPC problem or the explicit controller is mainly influenced by how close the state measurement is to the boundary of Ω_{ρ_e}. To decrease the number of times that the explicit controller is applied to the system, one could potentially add penalization terms to the stage cost of the LEMPC to penalize the closeness of the state to the boundary of Ω_{ρ_e}.

5.3 Application to a Chemical Process Network

Consider a chemical process network consisting of two continuous stirred-tank reactors (CSTRs) in series followed by a flash separator shown in Fig. 5.4. In each of the reactors,

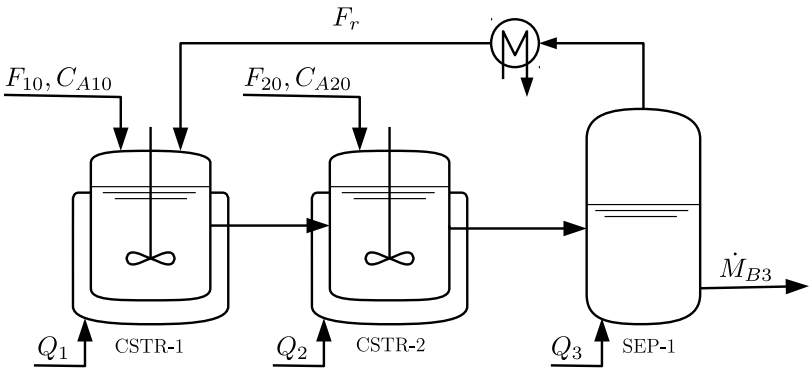

Figure 5.4: Process flow diagram of the reactor and separator process network.

the reactant A is converted to the desired product B through an exothermic and irreversible reaction of the form $A \rightarrow B$. A fresh feedstock containing a dilute solution of the reactant A in an inert solvent D is fed to each reactor. The reaction rate is second-order in the reactant concentration. The CSTRs are denoted as CSTR-1 and CSTR-2, respectively. A flash separator, which is denoted as SEP-1, is used to recover some unreacted A. The overhead vapor from the flash tank is condensed and recycled back to CSTR-1. The bottom stream is the product stream of the process network which contains the desired product B. In the separator, a negligible amount of A is assumed to be converted to B through the reaction. The two reactors have both heating and cooling capabilities and the rate of heat supplied to or removed from the reactors is denoted as $Q_j,\ j = 1,\ 2$. While the heat supplied to or removed from the vessel contents is modeled with one variable, two different actuators may be used in practice for supplying heat to and removing heat from each vessel. To vaporize some contents of the separator, heat is supplied to the separator at a rate of Q_3. The liquid holdup of each vessel is assumed to be constant and the liquid density throughout the process network is assumed to be constant.

Table 5.1: Process parameters of the reactor and separator process network.

Symbol / Value	Description	Symbol / Value	Description
$T_{10} = 300\,\mathrm{K}$	Temp.: CSTR-1 inlet	$k_0 = 1.9 \times 10^9\,\mathrm{m^3\,kmol^{-1}\,h^{-1}}$	Pre-exponential factor
$T_{20} = 300\,\mathrm{K}$	Temp.: CSTR-2 inlet	$E = 7.1 \times 10^4\,\mathrm{kJ\,kmol^{-1}}$	Activation energy
$F_{10} = 5.0\,\mathrm{m^3\,h^{-1}}$	Flow rate: CSTR-1 inlet	$\Delta H = -7.8 \times 10^3\,\mathrm{kJ\,kmol^{-1}}$	Heat of reaction
$F_{20} = 5.0\,\mathrm{m^3\,h^{-1}}$	Flow rate: CSTR-2 inlet	$\Delta H_{\mathrm{vap}} = 4.02 \times 10^4\,\mathrm{kJ\,kmol^{-1}}$	Heat of vaporization
$F_r = 2.0\,\mathrm{m^3\,h^{-1}}$	Flow rate: SEP-1 vapor	$C_p = 0.231\,\mathrm{kJ\,kg^{-1}\,K^{-1}}$	Heat capacity
$V_1 = 5.0\,\mathrm{m^3}$	Volume: CSTR-1	$R = 8.314\,\mathrm{kJ\,kmol^{-1}\,K^{-1}}$	Gas constant
$V_2 = 5.0\,\mathrm{m^3}$	Volume: CSTR-2	$\rho_L = 1000\,\mathrm{kg\,m^{-3}}$	Liquid solution density
$V_3 = 3.0\,\mathrm{m^3}$	Volume: SEP-1	$MW_A = 18\,\mathrm{kg\,kmol^{-1}}$	Molecular weight: A
$\alpha_A = 3.0$	Relative volatility: A	$MW_B = 18\,\mathrm{kg\,kmol^{-1}}$	Molecular weight: B
$\alpha_B = 0.8$	Relative volatility: B	$MW_D = 40.0\,\mathrm{kg\,kmol^{-1}}$	Molecular weight: D
$\alpha_D = 1.0$	Relative volatility: D		

Applying first principles, a dynamic model of the process network may be obtained (neglecting the dynamics of the condenser and the solvent) and is given by the following ordinary differential equations (ODEs) (see Table 5.1 for parameter notation and values):

$$\frac{dT_1}{dt} = \frac{F_{10}}{V_1}T_{10} + \frac{F_r}{V_1}T_3 - \frac{F_1}{V_1}T_1 - \frac{\Delta H k_0}{\rho_L C_p}e^{-E/RT_1}C_{A1}^2 + \frac{Q_1}{\rho_L C_p V_1} \tag{5.29a}$$

$$\frac{dC_{A1}}{dt} = \frac{F_{10}}{V_1}C_{A10} + \frac{F_r}{V_1}C_{Ar} - \frac{F_1}{V_1}C_{A1} - k_0 e^{-E/RT_1}C_{A1}^2 \tag{5.29b}$$

$$\frac{dC_{B1}}{dt} = \frac{F_r}{V_1}C_{Br} - \frac{F_1}{V_1}C_{B1} + k_0 e^{-E/RT_1}C_{A1}^2 \tag{5.29c}$$

$$\frac{dT_2}{dt} = \frac{F_{20}}{V_2}T_{20} + \frac{F_1}{V_2}T_1 - \frac{F_2}{V_2}T_2 - \frac{\Delta H k_0}{\rho_L C_p}e^{-E/RT_2}C_{A2}^2 + \frac{Q_2}{\rho_L C_p V_2} \tag{5.29d}$$

$$\frac{dC_{A2}}{dt} = \frac{F_{20}}{V_2}C_{A20} + \frac{F_1}{V_2}C_{A1} - \frac{F_2}{V_2}C_{A2} - k_0 e^{-E/RT_2}C_{A2}^2 \tag{5.29e}$$

$$\frac{dC_{B2}}{dt} = \frac{F_1}{V_2}C_{B1} - \frac{F_2}{V_2}C_{B2} + k_0 e^{-E/RT_2}C_{A2}^2 \tag{5.29f}$$

$$\frac{dT_3}{dt} = \frac{F_2}{V_3}(T_2 - T_3) - \frac{\Delta H_{\text{vap}}\dot{M}_r}{\rho_L C_p V_3} + \frac{Q_3}{\rho_L C_p V_3} \tag{5.29g}$$

$$\frac{dC_{A3}}{dt} = \frac{F_2}{V_3}C_{A2} - \frac{F_r}{V_3}C_{Ar} - \frac{F_3}{V_3}C_{A3} \tag{5.29h}$$

$$\frac{dC_{B3}}{dt} = \frac{F_2}{V_3}C_{B2} - \frac{F_r}{V_3}C_{Br} - \frac{F_3}{V_3}C_{B3} \tag{5.29i}$$

where T_j denotes the temperature of the j-th vessel ($j = 1$ denotes CSTR-1, $j = 2$ denotes CSTR-2, and $j = 3$ denotes SEP-1), C_{ij} denotes the concentration of the i-th species ($i = A,\ B$) in the j-th vessel, and $\dot{M}_r$ denotes the molar flow rate of the recycle stream.

The relative volatility of each species is assumed to be constant within the operating temperature range of the flash tank. The following algebraic equations are used to model

the composition of the recycle stream:

$$C_{D3} = \left(\rho_L - C_{A3}MW_A - C_{B3}MW_B\right)/MW_D \tag{5.30a}$$

$$C_{ir} = \frac{\alpha_i \rho_L C_{i3}}{\sum_{j\in\{A,B,D\}} \alpha_j C_{j3} MW_j}, \quad i = A,\ B,\ D \tag{5.30b}$$

$$\dot{M}_r = F_r\left(C_{Ar} + C_{Br} + C_{Dr}\right) \tag{5.30c}$$

where C_{ir} is the overhead vapor concentration of the separator. Given the assumption of constant liquid hold-up and constant liquid density, the volumetric flow rates are given by the following equations:

$$F_1 = F_r + F_{10} \tag{5.31a}$$

$$F_2 = F_1 + F_{20} \tag{5.31b}$$

$$F_3 = F_2 - F_r \tag{5.31c}$$

where F_j is the volumetric flow rate of the outlet stream of the j-th vessel.

The process network has five manipulated inputs: the three heat rates Q_j, $j = 1,\ 2,\ 3$ and the inlet concentration of the reactant A in the feedstock to each reactor (C_{A10} and C_{A20}). The bounds on the available control action are $Q_j \in [-1.0,\ 1.0] \times 10^5$ kJ h^{-1} for $j = 1,\ 2$, $Q_3 \in [2.2,\ 2.5]\ \times 10^6$ kJ h^{-1}, and $C_{Aj0} \in [0.5,\ 7.5]$ kmol m^{-3} $j = 1,\ 2$. In addition to the input constraints, the reactions take place within the temperature range from 370.0 to 395.0 K and thus, the reactors are to be operated within this temperature range. The separation occurs at 390.0 K.

The real-time economics of the process network are assumed to be described by the molar flow rate of desired product B leaving the process network which is denoted as $\dot{M}_{B3}$. The time-averaged amount of reactant that may be fed to each reactor is constrained to

an average amount of $20.0\,\text{kmol}\,\text{h}^{-1}$ which gives rise to the following two input average constraints:

$$\frac{1}{t_f}\int_{t_0}^{t_f} F_{j0}C_{Aj0}(t)\,dt = 20.0\,\text{kmol}\,\text{h}^{-1} \tag{5.32}$$

for $j = 1,\ 2$ where t_0 and t_f are the initial and final time of the operation of the process network. Since the inlet flow rates F_{10} and F_{20} are constant, the average input constraint may be written in terms of the inlet concentration of A only such that the time-averaged value of C_{Aj0} must be equal to $4.0\,\text{kmol}\,\text{m}^{-3}$.

The economically optimal steady-state (which is simply referred to as the optimal steady-state for the remainder) will be used in the design of a real-time LEMPC, i.e., the stability region for the optimal steady-state will be used in the LEMPC formulation. Since the reaction rate is maximized at high temperature, computing the optimal steady-state with the exact acceptable temperature operating range will give an optimal steady-state with the greatest acceptable reactor operating temperature. Much like current practice, the optimal steady-state is computed with a degree of conservativeness or "back-off" introduced in the acceptable operating temperature range, so that the reactor temperature is maintained within the acceptable operating range over the length of operation in the presence of uncertainty and disturbances (see [102] and the references therein, for instance, for more details on the back-off methodology). Thus, the optimal steady-state must satisfy a restricted temperature range of $T_{js} \in [370.0, 380.0]$ K for $j = 1,\ 2$. The steady-state optimization problem

is given by:

$$
\begin{aligned}
\max_{x_s,u_s} \quad & F_3 C_{B3s} \\
\text{s.t.} \quad & f(x_s,u_s) = 0 \\
& 370.0\,\text{K} \leq T_{1s} \leq 380.0\,\text{K} \\
& 370.0\,\text{K} \leq T_{2s} \leq 380.0\,\text{K} \\
& T_{3s} = 390.0\,\text{K} \\
& -1.0\times10^5\,\text{kJ h}^{-1} \leq Q_{1s} \leq 1.0\times10^5\,\text{kJ h}^{-1} \\
& -1.0\times10^5\,\text{kJ h}^{-1} \leq Q_{2s} \leq 1.0\times10^5\,\text{kJ h}^{-1} \\
& 2.2\times10^6\,\text{kJ h}^{-1} \leq Q_{3s} \leq 2.5\times10^6\,\text{kJ h}^{-1} \\
& C_{A10s} = C_{A20s} = 4.0\,\text{kmol m}^{-3}
\end{aligned}
\tag{5.33}
$$

where $f(x_s,u_s)=0$ represents the steady-state model. The optimal steady-state vector (omitting units) is:

$$
\begin{aligned}
x_s^* &= \begin{bmatrix} T_{1s}^* & C_{A1s}^* & C_{B1s}^* & T_{2s}^* & C_{A2s}^* & C_{B2s}^* & T_{3s}^* & C_{A3s}^* & C_{B3s}^* \end{bmatrix}^T \\
&= \begin{bmatrix} 380.0 & 2.67 & 2.15 & 380.0 & 2.42 & 2.06 & 390.0 & 1.85 & 2.15 \end{bmatrix}^T,
\end{aligned}
\tag{5.34}
$$

and the optimal steady-state input vector is

$$
\begin{aligned}
u_s^* &= \begin{bmatrix} Q_{1s}^* & Q_{2s}^* & Q_{3s}^* & C_{A10s}^* & C_{A20s}^* \end{bmatrix}^T \\
&= \begin{bmatrix} -4.21\times10^3 & 1.70\times10^4 & 2.34\times10^6 & 4.0 & 4.0 \end{bmatrix}^T.
\end{aligned}
\tag{5.35}
$$

The optimal steady-state is open-loop unstable.

The control objective of the process network is to optimize the economics through real-time operation while maintaining the closed-loop state trajectory inside a well-defined

state-space set. To accomplish this objective, the real-time LEMPC scheme is applied to the process network. In stark contrast to traditional tracking control that forces the closed-loop state to converge to the (optimal) steady-state, applying LEMPC to the process network is not expected to achieve convergence to the optimal steady-state. Instead, LEMPC may force the process network to operate in a consistently transient manner to achieve better closed-loop performance compared to the closed-loop performance at the optimal steady-state.

For the implementation of the LEMPC, the acceptable temperature range is not treated as a hard constraint. Instead, the acceptable temperature range is accounted for by imposing quadratic penalty terms in the stage cost of the LEMPC. Thus, the stage cost used in the objective function of the LEMPC is

$$l_e(x,u) = -F_3 C_{B3} + \sum_{i=1}^{3} Q_{c,i}(T_i - T_{is}^*)^2 \tag{5.36}$$

where T_{is}^*, $i = 1,\ 2,\ 3$ are the optimal steady-state temperatures. The stage cost of Eq. 5.36 includes the economics and the quadratic penalty terms for the temperature. The weight coefficients are $Q_{c,1} = 0.018$, $Q_{c,2} = 0.022$, and $Q_{c,3} = 0.01$ and have been tuned such that the closed-loop temperatures are maintained near the optimal steady-state temperature. Since no hard or soft constraints are imposed on the temperature in the LEMPC, it is emphasized that there is no guarantee that the temperatures are maintained within the acceptable temperature range described above ($T_j \in [370.0,\ 395.0]$ K for $j = 1,\ 2$ and $T_3 \approx 390.0$ K). In this example, small violations over a short period are considered acceptable. If maintaining the operation within the acceptable operating temperature range is considered critical, one may add various modifications to the LEMPC to achieve this objective such as decreasing the size of Ω_{ρ_e}, adding hard or soft constraints on the temperature in the LEMPC, or adding a contractive constraint on the temperature ODEs.

An explicit stabilizing controller is designed using feedback linearization techniques to make the dynamics of the temperature ODEs linear (in a state-space region where the input constraints are satisfied) under the explicit controller. Specifically, the temperature ODEs are input-affine in the heat rate input and have the form:

$$\dot{T}_j = f_j(x) + b_j Q_j \tag{5.37}$$

where $f_j(x)$ is a nonlinear scalar-valued function, b_j is constant and $j = 1,\ 2,\ 3$. The controller that makes the closed-loop temperature dynamics linear is:

$$Q_j = -\frac{1}{b_j}\left(f_j(x) + K_j(T_j - T_{js}^*)\right) \tag{5.38}$$

where K_j denotes the controller gain. In this case, the controller gains are $K_1 = 5$, $K_2 = 5$, and $K_3 = 7$, respectively. The inlet concentration input values are fixed to the average values ($4.0\,\mathrm{kmol\,m^{-3}}$). Through extensive closed-loop simulations under the state feedback controller, a quadratic Lyapunov function for the process network under the feedback controller $h(x)$ was determined. An estimate of the stability region of the process network under the feedback controller was characterized by computing the state-space points where $\dot{V} < 0$ and taking the stability region to be a level set of the Lyapunov function containing only state-space points where the time-derivative of the Lyapunov function is negative. The quadratic Lyapunov function has the form:

$$V(x) = (x - x_s^*)^T P (x - x_s^*) \tag{5.39}$$

where P is the following positive definite matrix:

$$P = \mathrm{diag}\begin{bmatrix} 0.001 & 1.5 & 0.05 & 0.001 & 1.5 & 0.05 & 0.001 & 1.5 & 0.05 \end{bmatrix}. \tag{5.40}$$

The estimated stability region Ω_ρ is the level set of the Lyapunov function where $V(x) \leq 11.0$, i.e., $\rho = 11.0$. The subset of the stability region which defines the mode 1 constraint of the LEMPC is $\rho_e = 10.0$ and has been determined through extensive closed-loop simulation under LEMPC as the subset of the stability region Ω_ρ where the closed-loop state under LEMPC is maintained in Ω_ρ.

The input average constraint is imposed over successive, finite-length operating periods. Specifically, the average constraint must be satisfied over each operating period $t_M = M\Delta$ where M is the number of sampling periods in the operating period. This ensures that over the entire length of operation the average constraint will be satisfied. For this example, the operating period was chosen to be $t_M = 2.4\,\text{h}$ which leads to better asymptotic average economic performance under LEMPC (assuming no computational delay) than the asymptotic average performance at the economically optimal steady-state. To solve the dynamic optimization problem of the LEMPC, orthogonal collocation with three Radau collocation points per sampling period is employed for discretization of the ODEs (see, for instance, [20] for details on solving a dynamic optimization problem using a simultaneous approach). The open-source nonlinear optimization solver Ipopt [187] was employed owing to its ability to exploit the high degree of sparsity of the resulting optimization problem. Analytical first and second-order derivative information was provided to the solver. The closed-loop simulations were coded in C++ and performed on an Intel® Core™ 2 Quad 2.66 GHz processor running an Ubuntu Linux operating system. The sampling period of the LEMPC used in the simulations below is $\Delta = 0.01\,\text{h}$. To simulate forward in time the closed-loop process network, the fourth-order Runge-Kutta method was used with a time step of 0.0001 h.

In the first set of simulations, nominal operation of the process network under LEMPC implemented in a typical receding horizon fashion is considered under ideal computation, i.e., assuming no computational delay. The closed-loop economic performance under

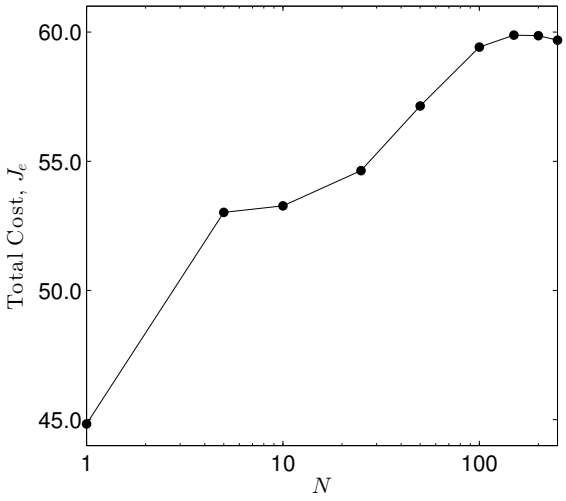

Figure 5.5: The total economic cost J_e over one operating window length of operation (2.4 h) of the process network under LEMPC with the prediction horizon length.

LEMPC is assessed using the economic performance index which is defined as:

$$J_e = \int_0^{t_f} F_3 C_{B3} \, dt \ . \tag{5.41}$$

Since the LEMPC does not directly optimize the molar flow rate of product out of the process network, the stage cost index will also be considered as a measure of the closed-loop performance and is given by:

$$L_e = -\int_0^{t_f} l_e(x,u) \, dt \ . \tag{5.42}$$

First, the effect of the prediction horizon on the closed-loop economic performance over one operating period (2.4 h) is considered. The closed-loop performance index of Eq. 5.41 plotted against the prediction horizon length is given in Fig. 5.5. A significant increase in closed-loop performance is observed initially with increasing prediction horizon length until the closed-loop performance becomes approximately constant. Owing to this fact, a pre-

diction horizon of $N = 200$ is used in all subsequent simulations. A simulation over many operating periods such that the effect of the initial condition on closed-loop performance becomes negligible is performed (with $N = 200$). The asymptotic average closed-loop economic performance, which is the time-averaged economic cost after the effect of the initial condition becomes negligible, was determined from this simulation to be $25.0\,\mathrm{kmol\,h^{-1}}$ (in this case, the time-averaged production rate over each operating window becomes constant after a sufficiently long length of operation). The optimal steady-state production rate of B is $21.5\,\mathrm{kmol\,h^{-1}}$. Thus, the asymptotic production rate of the process network under the LEMPC is 16.3% better than the production rate at the economically optimal steady-state.

The effect of computational delay is considered in the next set of simulations, and two scenarios are considered: (1) the closed-loop process network under LEMPC implemented in a typical receding horizon fashion where the control action is subject to real-time computational delay (for the sake of simplicity, this case will be referred to as the closed-loop process network under LEMPC for the remainder) and (2) the closed-loop process network under the real-time LEMPC scheme (also, subject to real-time computational delay). For the former scenario, the LEMPC begins to compute a control action at each sampling instance after receiving a state measurement. Owing to the computational delay, the control action applied to the process network is the most up-to-date control action. For example, if it takes 0.002 h to compute the control action at the sampling instance t_k, then $u(t_{k-1})$ is applied to the process network from t_k to $t_k + 0.002\,\mathrm{h}$ (assuming $u(t_{k-1})$ is available at t_k) and applies $u(t_k)$ to the process network from $t_k + 0.002\,\mathrm{h}$ to $t_{k+1} = t_k + \Delta$. For each scenario, a 12.0 h length of closed-loop operation was simulated. For the real-time LEMPC case, the LEMPC is forced to recompute a new solution after three sampling periods have elapsed since the last time an LEMPC solution was computed, i.e., the solver starts computing a new solution at the beginning of the fourth sampling period.

The average computation time required to solve the LEMPC (of scenario (1)) at each

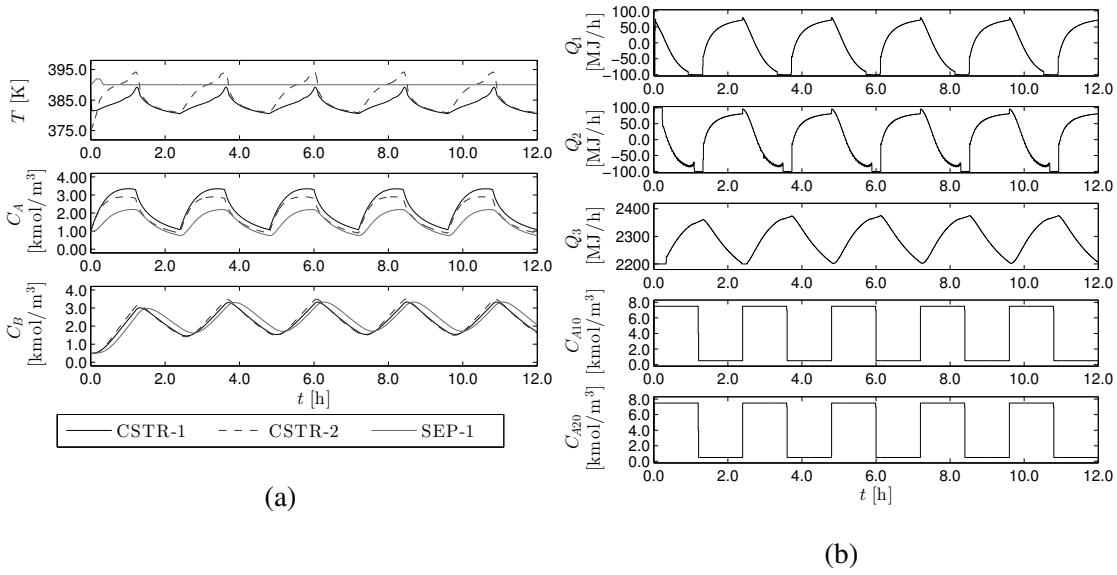

(a) (b)

Figure 5.6: The closed-loop (a) state and (b) input trajectories of the nominally operated process network under the real-time LEMPC scheme.

sampling time was 11.2 s (31.2% of the sampling period) with a standard deviation of 7.42 s. The maximum computation time over the simulation was 61.9 s which is almost double the sampling period. The computation time exceeded the sampling period ten out of the 1,200 sampling periods in the simulation. Over the course of both simulations, the closed-loop state was maintained in Ω_ρ. The closed-loop trajectories under the real-time LEMPC scheme are given in Fig. 5.6 (the closed-loop behavior under the LEMPC subject to real-time computational delay was similar). The difference between the performance index of the two cases was less than 0.5% (the performance indices for case (1) and case (2) were 284.3 and 283.3, respectively).

While little difference between the two cases in terms of closed-loop performance was realized, it is important to note that an *a priori* guarantee on closed-loop stability under the real-time LEMPC may be made, while, under the LEMPC with computational delay, it is difficult to guarantee closed-loop stability *a priori*. Also, the total on-line computation

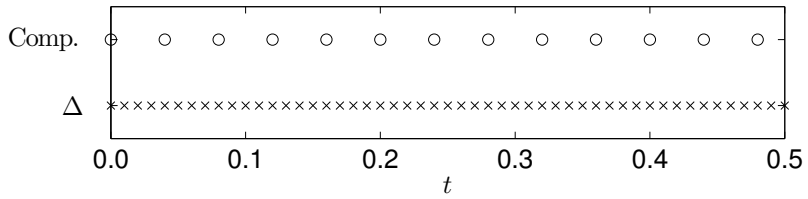

Figure 5.7: The number of times the LEMPC problem was solved (Comp.) as dictated by the real-time implementation strategy compared to the sampling period (Δ) over the first 0.5 h of operation.

time to solve the LEMPC over the two simulations was 3.74 h and 0.94 h, respectively. The real-time LEMPC reduces the total on-line computation requirement by 75% compared to LEMPC implemented in a receding horizon fashion because the real-time LEMPC does not recompute a control action at each sampling instance, while LEMPC, implemented in a receding horizon fashion, recomputes a control action at each sampling instance. To better illustrate this point, Fig. 5.7 shows the frequency the LEMPC problem was solved under the real-time implementation strategy with respect to the sampling period over the first 0.5 h of operation. Over this time, the LEMPC optimization problem was solved at a rate of one out of every four sampling periods. This trend continues over the remainder of the 12.0 h length of operation and hence, the 75% reduction in total computational time.

Since the computational delay depends on many factors, e.g., model dimension, prediction horizon, solution strategy used to solve the dynamic optimization problem, the nonlinear optimization solver used, computer hardware, it is also important to consider computational delay greater than one sampling period to demonstrate that the real-time LEMPC scheme may handle computation delay of arbitrary length. Therefore, another set of simulations is considered where longer computational delay is simulated. The computation delay is modeled as a bounded uniformly-distributed random number and the maximum computational delay is assumed to be less than 10 sampling periods. Both the LEMPC (receding horizon implementation) and the real-time LEMPC scheme are considered. To

Table 5.2: The performance indices of the process network under the back-up explicit controller, under the LEMPC subject to computational delay, and under the real-time LEMPC for several simulations.

Sim.	Back-up Controller		LEMPC		Real-time LEMPC	
	J_e	L_e	J_e	L_e	J_e	L_e
1	225.5	225.4	277.0	245.0	295.1	216.5
2	254.2	254.1	318.7	278.6	307.3	279.6
3	260.5	260.4	319.9	286.3	318.1	294.7
4	232.7	230.6	290.7	255.7	299.2	266.4
5	250.0	250.0	308.7	276.9	322.8	282.9

make the comparison as consistent as possible, the computational delay, at the time steps the real-time LEMPC is solved, is simulated to be the same as the computation delay to solve the LEMPC at the same time step (recall the real-time LEMPC is not solved at each sampling period). Given the computational delay is much greater for this set of simulations than in the previous set of simulations, the real-time LEMPC is forced to recompute a new solution after 15 sampling periods have elapsed since the last time it computed a solution.

Several simulations were performed, each starting at a different initial condition, and the performance indices of these simulations are given in Table 5.2. Applying the back-up explicit controller $h(x)$ implemented in a sample-and-hold fashion to the chemical process network was also considered and the performance indices of these simulations are given in Table 5.2 as well. The average improvement in economic performance compared to the process network under the back-up controller was 26.1% under the real-time LEMPC scheme and 23.9% under the LEMPC (implemented in a receding horizon). Thus, a substantial economic benefit is achieved by applying LEMPC to the process network. While the real-time LEMPC did not always achieve better performance (either measured in terms of the economic performance index or stage cost index) compared to the performance under LEMPC, the closed-loop trajectories between the two cases are significantly different.

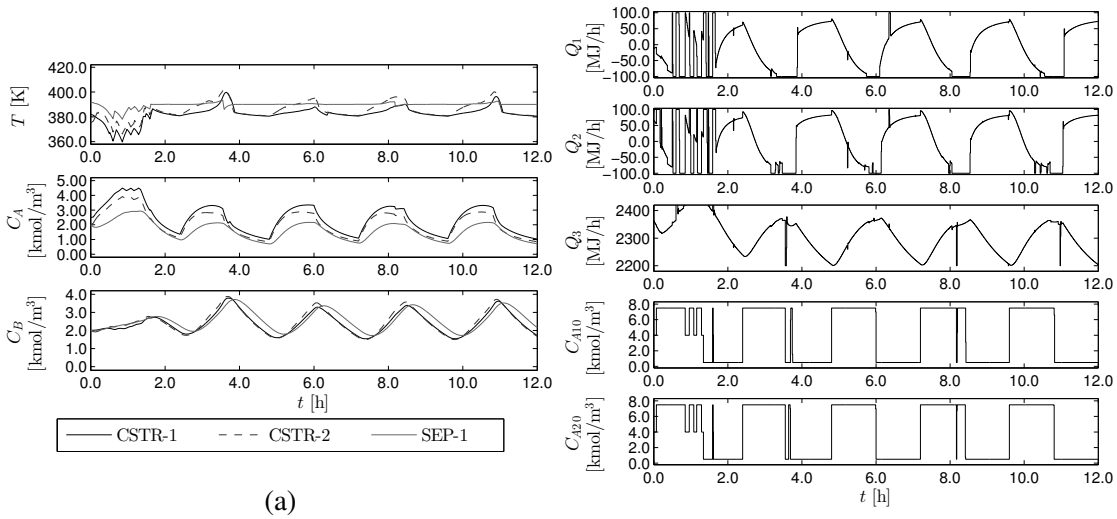

(a) (b)

Figure 5.8: The closed-loop (a) state and (b) input trajectories of process network under the real-time LEMPC scheme where the computational delay is modeled as a bounded random number.

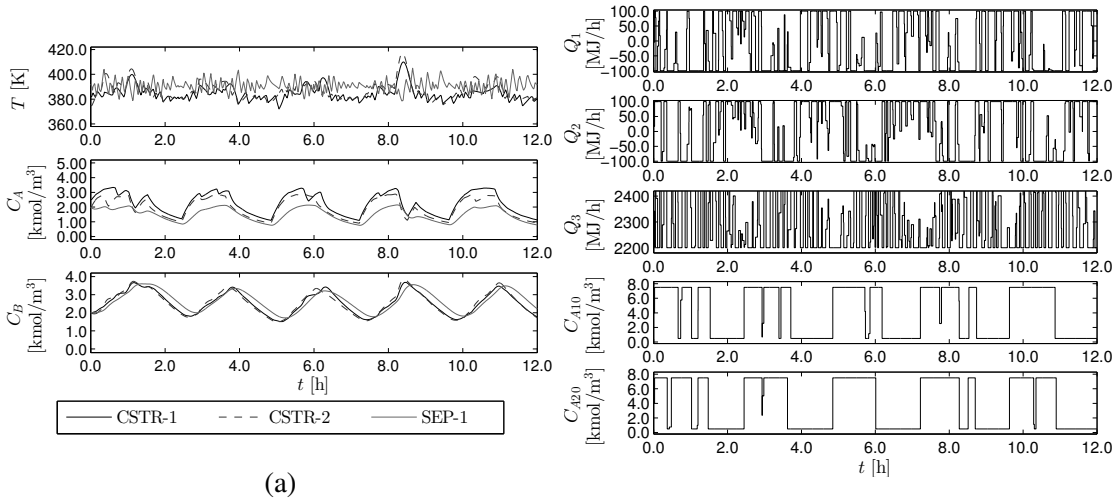

(a) (b)

Figure 5.9: The closed-loop (a) state and (b) input trajectories of process network under LEMPC subject to computational delay where the computational delay is modeled as a bounded random number.

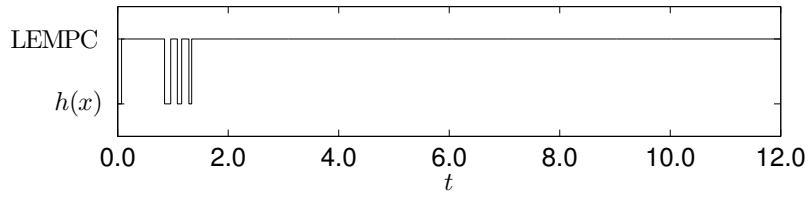

Figure 5.10: A discrete trajectory depicting when the control action applied to the process network over each sampling period was from a precomputed LEMPC solution or from the back-up controller for the closed-loop simulation of Fig. 5.8.

Figures 5.8-5.9 give the closed-loop trajectories of simulation 2 (as labeled in Table 5.2). The input trajectory computed by the real-time LEMPC has chattering initially over the first operating period because of the effect of the initial condition, but after the first operating period when the effect of the initial condition dissipates, the computed input trajectory is significantly smoother. On the other hand, chattering in the input profiles is observed throughout the entire simulation under the LEMPC. If we compare the performance index of operation from $t = 2.4\,\text{h}$ to $t = 12.0\,\text{h}$ (after the first operating period) for simulation 2, the indices are $J_e = 249.8$ and $L_e = 227.9$ for operation under the real-time LEMPC and $J_e = 248.5$ and $L_e = 217.4$ for operation under the LEMPC; the performance under the real-time LEMPC is better over this period than under LEMPC.

Over the five simulations under the real-time LEMPC strategy, the explicit controller was applied on average 19 out of 1200 sampling periods. For the simulation of Fig. 5.8, a discrete trajectory showing when the control action applied to the process network under the real-time LEMPC strategy was from a precomputed LEMPC solution or from the back-up controller is given in Fig. 5.10. For this case, the back-up controller is used 31 out of 1200 sampling periods (2.7% of the sampling periods). From Fig. 5.10, the back-up controller is only applied over the first operating period and is not used in any subsequent sampling period. Thus, the source of performance degradation for this case (Sim. 2 in Table 5.2) is due to applying the explicit back-up controller to maintain the closed-loop

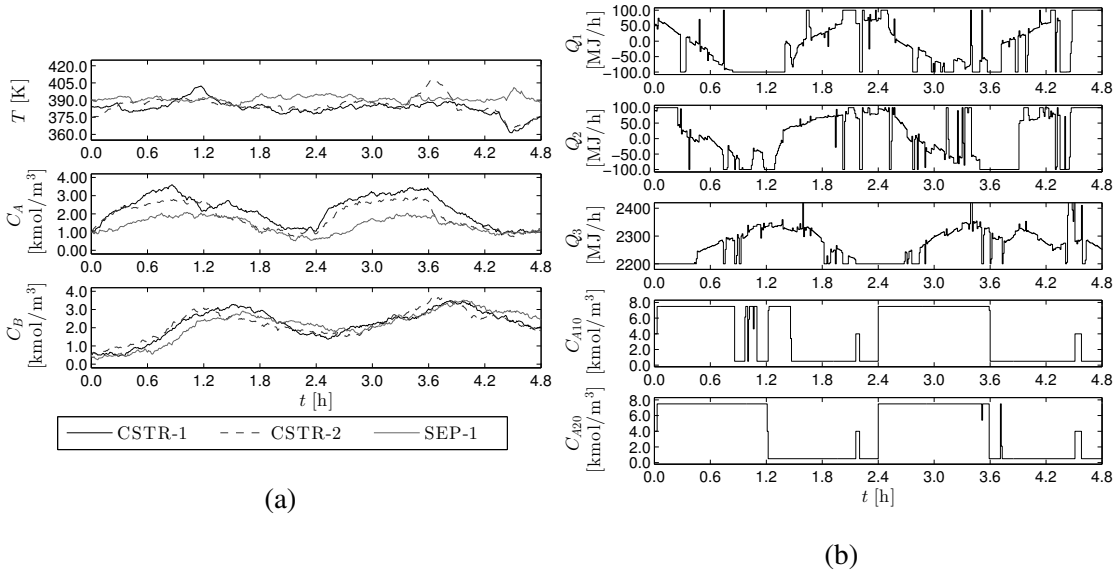

Figure 5.11: The closed-loop (a) state and (b) input trajectories of process network under the real-time LEMPC scheme with bounded process noise.

state in Ω_ρ. Again, it is emphasized that there is no *a priori* guarantee that the LEMPC implemented in a receding horizon fashion subject to computational delay could maintain the closed-loop state inside Ω_ρ.

In the last set of simulations, significant bounded Gaussian process noise with zero mean was added to the model states. The standard deviations of the noise added to the temperature and concentration states were 5.0 and 0.5, respectively and the bounds on the noise were 2.0 and 15.0, respectively. Two closed-loop simulations over 12.0 h length of operation were completed with the same realization of the process noise. In the first simulation, the process network was controlled by the real-time LEMPC and the closed-loop trajectories are given in Fig. 5.11 over the first two operating periods. For this case, the back-up controller is applied 69 out of 1200 sampling periods (5.8% of the sampling periods). In the second simulation, the process network was controlled by LEMPC subject to computation delay (trajectories shown in Fig. 5.12).

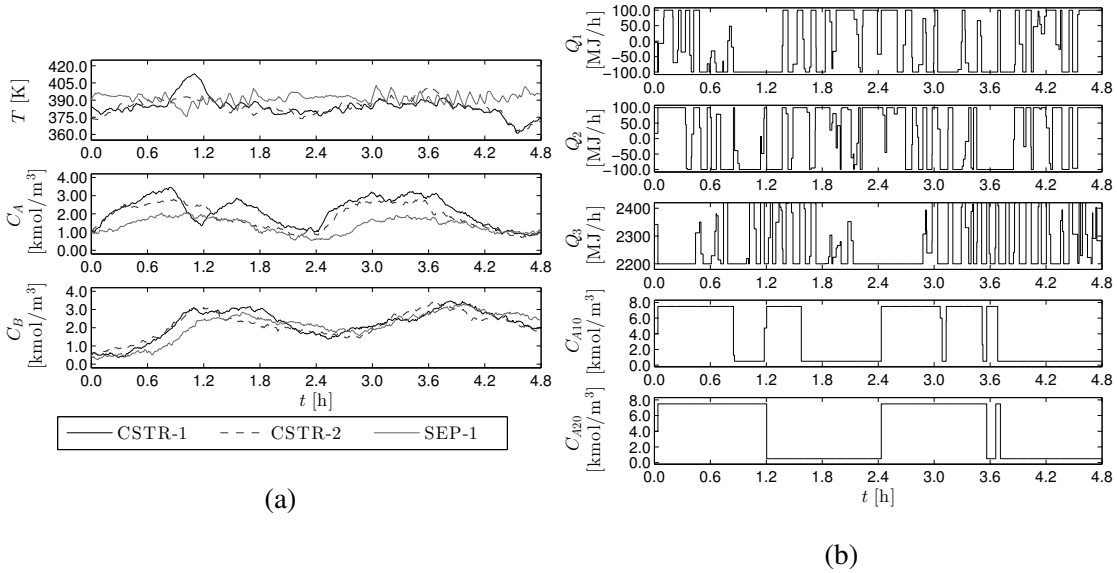

(a) (b)

Figure 5.12: The closed-loop (a) state and (b) input trajectories of process network under LEMPC subject to computational delay with bounded process noise.

From Fig. 5.12, a significant degree of chattering and bang-bang type actuation in the input trajectory is observed. This behavior tries to combat the effect of the added process noise and is due to not penalizing control actions in the stage cost and not imposing rate of change constraints on the control actions. In practice, one could add one or both of these elements to the LEMPC if the computed input trajectory is not implementable. On the other hand, the real-time LEMPC implements a much smoother input trajectory (Fig. 5.11) because the precomputed input trajectory of the real-time LEMPC has a degree of smoothness like the closed-loop trajectory of the nominally operated process network (Fig. 5.6). If the precomputed input trajectory satisfies the stability conditions, it will be applied to the closed-loop process network with disturbances. The closed-loop system under the real-time LEMPC has guaranteed stability properties, but is not recomputed at each sampling period like the receding horizon implementation of LEMPC which will try to combat the effect of the disturbance on performance. In both cases, the state is maintained in Ω_ρ.

The performance indices of the two cases are 301.6 under the real-time LEMPC and 295.5 under the LEMPC; the closed-loop performance under the real-time LEMPC scheme is 2.0% better than applying LEMPC without accounting for the computational delay. Moreover, the back-up controller was also applied to the process network subject to the same realization of the process noise. The economic performance index for this case was 242.3. For operation with process noise, the economic performance improvement over the process network under the back-up controller was 24.4% under the real-time LEMPC strategy and 21.9% under the receding horizon LEMPC for the same initial condition.

5.4 Conclusions

In this chapter, a strategy for implementing Lyapunov-based economic model predictive control (LEMPC) in real-time with computation delay was developed. The implementation strategy uses a triggering condition to precompute an input trajectory from LEMPC over a finite-time horizon. At each sampling period, if a certain stability (triggering) condition is satisfied, then the precomputed control action by LEMPC is applied to the closed-loop system. If the stability condition is violated, then a backup explicit stabilizing controller is used to compute the control action for the sampling period. In this fashion, the LEMPC is used when possible to optimize the economics of the process. Conditions such that the closed-loop state under the real-time LEMPC is always bounded in a compact set were derived. The real-time LEMPC scheme was applied to a chemical process network and demonstrated that it may maintain closed-loop stability in the presence of significant computation delay and process noise while also, improving the closed-loop economic performance compared to the economic performance at the economically optimal steady-state.

Chapter 6

EMPC of Time-Delay Systems: Closed-loop Stability and Delay Compensation

6.1 Introduction

Within the context of control of chemical process systems, time-delays resulting from computation and communication delays are enviable albeit they may be small and insignificant depending on the magnitude of the time-delay relative to the time-constants of the process dynamics. From a modeling perspective, time-delays are often employed to describe and/or to approximate the dynamics of transportation of material through the process system, control actuator dynamics, measurement sensor dynamics, and high-order dynamic behavior. Thus, robustness with respect to closed-loop stability and performance of control systems to time-delays is an important consideration. Moreover, many chemical process systems have significant nonlinear behavior owing to complex reaction mechanisms, Arrhenius reaction-rate dependence on temperature, and thermodynamic relationships which

adds additional complexity in considering the closed-loop behavior of the system resulting from a nonlinear time-delay system under a control law.

Dynamic models of systems that involve nonlinearities and time-delays are systems of nonlinear differential difference equations (DDEs). Systems described by DDEs are fundamentally different from systems described by ordinary differential equations (ODEs) (see, for example, [74] for more details on this point). One important difference is that a dynamic system with an arbitrarily small delay is an infinite-dimensional system even though the dimension of the state vector may be finite. For nonlinear DDEs, there are typically two approaches employed to analyze stability that are analogous to Lyapunov stability theory employed to assess stability of equilibria and solutions of ODEs. The first method uses Lyapunov-Krasovski functionals, which is the direct analog to Lyapunov functions for ODEs, and the second method uses Lyapunov-Razumikhin functions [74]. While Razumikhin theorems are typically more conservative than Krasovski theorems, Razumikhin theorems require the construction of a function which is typically less challenging than the construction of a functional. Various extensions of stability theory for DDE systems exist including input-to-state stability using Razumikhin-type arguments and extending the notion of control Lyapunov functions to control Lyapunov-Krasovski functionals and control Lyapunov-Razumikhin functions, e.g., [197, 182, 89, 90, 161].

One approach to design a controller for a time-delay system is to neglect the delays in the model used for controller design and employ controller design methods used for systems described by ODEs. This may lead to acceptable closed-loop properties especially when the time-delays are small. However, employing these methods, in general, may pose unacceptable limitations on the achievable control quality and performance, e.g., sluggish response, oscillations, and even instability [178]. Perhaps, one of the most well-known results to cope with time-delay in the control input or sensor measurement is the classical Smith predictor structure designed for linear time-delay systems which eliminates the de-

lay from the characteristic polynomial of the closed-loop system and allows for larger controller gains to be used [174]. Many extensions of the Smith predictor exist in the literature including extensions to nonlinear systems [106, 82]. With respect to control design and/or input delay compensation for nonlinear systems, many results exist in the literature including state and output feedback control designs for nonlinear DDE systems [7, 8, 33, 148], input delay compensation for nonlinear systems [107, 96], and nonlinear sampled-data systems with time-delays [183, 84, 30, 98], see, also, the reviews [71, 161] for more references on control of time-delay systems.

In addition to nonlinearities and time-delays, other important considerations within the context of chemical process control are process constraints and performance considerations. As described in the previous chapters, EMPC may be used to control nonlinear systems in an economically optimal manner while accounting for state and control constraints. While there has been some work completed on tracking MPC of nonlinear time-delay systems, e.g., [142, 153, 119, 160, 37], to the best of our knowledge, no work on EMPC for time-delay systems has been completed.

In this chapter, we first consider the robustness of LEMPC, formulated with an ODE model, for nonlinear systems with state and input delays in the sense that closed-loop stability (to be made precise below) will be maintained when the state and input delays are sufficiently small. Since LEMPC is designed with an explicit stabilizing control law and LEMPC is applied in a sample-and-hold fashion, we first consider the closed-loop stability of the nonlinear sampled-data time-delay system resulting from the continuous-time delay system under the nonlinear control law applied in a sample-and-hold fashion. Leveraging the aforementioned results, closed-loop stability is shown for the closed-loop time-delay system under LEMPC when the time-delays are sufficiently small. Using a chemical process example, we demonstrate that the LEMPC maintains closed-loop stability when the time-delays in both inputs and states are sufficiently small. To address economic perfor-

mance deterioration due to time-delays, in the second part, we develop a predictor feedback based LEMPC scheme, formulated with a DDE model, that compensates for the effect of the input delay. The results of this chapter were first presented in [56].

6.2 Preliminaries

6.2.1 Notation and Preliminary Results

In this chapter, the following notation will be used. The notation $x(t) \in \mathbb{R}^n$ is a time dependent vector and $x_d(t) : [-t_d, 0] \to \mathbb{R}^n$ is a time-dependent function where $x_d(t)(\tau) := x(t+\tau)$ for $\tau \in [-t_d, 0]$. The explicit dependence of t on $x(t)$ and $x_d(t)$ may be omitted and we may simply write x and x_d when convenient. The symbol $|\cdot|$ denotes the Euclidean norm of a real vector. The floor and ceiling functions, denoted as $\lfloor a \rfloor$ and $\lceil a \rceil$ ($a \in \mathbb{R}$), respectively, are the largest integer not greater than a and the smallest integer not less than a, respectively. The symbol B_δ denotes a norm-ball of radius δ, and the symbol Ω_ρ is a level set or level surface of a scalar positive definite function $V : \mathbb{R}^n \to \mathbb{R}_{\geq 0}$, i.e., $\Omega_\rho := \{x \in \mathbb{R}^n : V(x) \leq \rho\}$. The family of piecewise constant, right-continuous functions with period Δ (defined over the appropriate interval) is denoted as $S(\Delta)$.

A function $\gamma : [0, a) \to \mathbb{R}_{\geq 0}$ is said to be of class-$\mathscr{G}$ if it is a nondecreasing continuous function and $\gamma(0) = 0$. The symbol $C([a,b], \mathbb{R}^n)$ is the Banach space of continuous functions mapping the interval $[a,b]$ into $\mathbb{R}^n$ with topology of uniform convergence and equipped with the norm:

$$\|\phi\| := \max_{a \leq s \leq b} |\phi(s)|,$$

where $\phi \in C([a,b], \mathbb{R}^n)$.

To present some preliminary definitions and results, consider the class of systems de-

scribed by functional differential equations:

$$\dot{x}(t) = f(x_d(t), w_d(t)), \quad x_d(t_0) = \xi \tag{6.1}$$

where $f : C([-t_d, 0], \mathbb{R}^n) \times C([-t_d, 0], \mathbb{R}^m) \to \mathbb{R}^n$ with $f(0,0) = 0$ and the initial data is $\xi \in C([-t_d, 0], \mathbb{R}^n)$, and w is a bounded, piecewise continuous input. For each initial data and initial time $t_0 \geq 0$, we suppose there exists $T_f \geq 0$ and a unique maximal solution $x(\cdot)$ defined on $[t_0 - t_d, t_0 + T_f]$. We define the following norm:

$$\|x_d\|_{t_0} := \sup_{s \geq t_0} \|x_d(s)\| .$$

We will make use of the following definition and results on input-to-state stability of the zero solution of the system of Eq. 6.1 from [182]. The definition and results are stated here for the reader's convenience.

Definition 6.1 ([182])**.** Let $\gamma \in \mathscr{G}$, $\nu \in \mathbb{R}_{\geq 0}$ and $\Delta_x, \Delta_w \in \mathbb{R}_{\geq 0}$. The zero solution of Eq. 6.1 is said to be *uniform input-to-state stable (ISS)* with gain γ, offset ν, and restriction (Δ_x, Δ_w) if $\|x_d(t_0)\| < \delta_x$ imply $T_f = \infty$ and that the following properties hold uniformly in t_0: 1) for each $\varepsilon > 0$ there exists $\delta > 0$ such that $\|x_d(t_0)\| \leq \delta$ implies $\|x_d\|_{t_0} \leq \max\{\varepsilon, \gamma(\|w_d\|_{t_0}), \nu\}$ and 2) for each $\varepsilon > 0$ and $\eta_x \in (0, \Delta_x)$ and $\eta_w \in (0, \Delta_w)$ there exists $T > 0$ such that $\|x_d(t_0)\| \leq \eta_x$ and $\|w_d\|_{t_0} \leq \eta_w$ imply $\|x_d\|_{t_0+T} \leq \max\{\varepsilon, \gamma(\|w_d\|_{t_0}), \nu\}$.

If $V : [-t_d, \infty) \times \mathbb{R}^n \to \mathbb{R}_{\geq 0}$ is a continuous function, then we use $\dot{V}(t, x(t))$ to denote the upper right-hand derivative of V along the solution of Eq. 6.1 and is defined as

$$\dot{V}(t, x(t)) := \limsup_{h \to 0^+} \frac{V(t+h, x(t+h) - V(t, x(t))}{h} . \tag{6.2}$$

The following two results are needed:

Lemma 6.1 ([100, 182]). *Let $\mu \geq 0$ and $\alpha \in \mathscr{K}$. If $V(t) \geq \mu$ implies $\dot{V}(t) \leq -\alpha(V(t))$, then there exists $\beta \in \mathscr{KL}$ (independent of μ) with $\beta(s,0) \geq s$ such that*

$$V(t) \leq \max\{\beta(V(t_0), t - t_0), \mu\} .$$

The following result for the system of Eq. 6.1 is from [182] which is a Razumikhin-type theorem for input-to-state stability of functional differential equations.

Theorem 6.1 ([182, Theorem 2]). *Suppose there exist a continuous function $V : [-t_d, \infty) \times \mathbb{R}^n \to \mathbb{R}_{\geq 0}$, α_1, $\alpha_2 \in \mathscr{K}_\infty$, $\alpha_3 \in \mathscr{K}$, γ_x, $\gamma_w \in \mathscr{G}$ and nonnegative real numbers $\delta < \Delta$ such that*

1. *$\alpha_1(|x|) \leq V(t,x) \leq \alpha_2(|x|)$;*
2. *$|x(t)| \geq \max\{\gamma_x(\|x_d(t)\|), \gamma_w(\|w_d(t)\|)\} \Rightarrow \dot{V}(t, x(t)) \leq -\alpha_3(|x(t)|)$;*
3. *$\alpha_1^{-1} \circ \alpha_2 \circ \gamma_x(s) < s$ for $\delta < s < \Delta$.*

Let $\beta \in \mathscr{KL}$ be as in the conclusion of Lemma 6.1 when $\alpha = \alpha_3 \circ \alpha_2^{-1}$. Then, the origin of the system of Eq. 6.1 is uniformly ISS with gain $\tilde{\gamma}_w := \alpha_1^{-1} \circ \alpha_2 \circ \gamma_w$, offset δ, and restriction (Δ_x, Δ_w) such that $\max\{\alpha_1^{-1}(\beta(\alpha_2(s_1), 0)), \tilde{\gamma}_w(s_2)\} < \Delta$ when $s_1 < \Delta_x$, $s_2 < \Delta_w$.

6.2.2 Class of Nonlinear Time-Delay Systems

The class of nonlinear time-delay systems considered in this chapter are described by a system of differential difference equations (DDEs), which are also commonly referred to as delay differential equations, and have the following form:

$$\dot{x}(t) = f(x(t), x(t - d_1), u(t - d_2)) \tag{6.3}$$

where $x(t) \in \mathbb{R}^n$ is the state, $u(t) \in \mathbb{U} \subset \mathbb{R}^m$ is the bounded control input, $d_1 \geq 0$ and $d_2 \geq 0$ are the state and input delays, respectively, and f is a locally Lipschitz vector function of its arguments with $f(0,0,0) = 0$. The set that bounds the available control action is given by $\mathbb{U} := \{u \in \mathbb{R}^m : |u_i| \leq u_{\max,i},\ i = 1,\ \ldots,\ m\}$. The initial time is taken to be zero ($t_0 = 0$), the initial data is given by the function ϕ_x where $\phi_x \in C([-d_1, 0], \mathbb{R}^n)$, and the initial input function, which is denoted as ϕ_u, is defined over the interval $[-d_2, 0]$, takes values in $\mathbb{U}$ and is therefore, bounded. Moreover, ϕ_u is assumed to be piecewise continuous over its domain. Full state feedback of the system of Eq. 6.3 is assumed.

We will design a controller for the system of Eq. 6.3 on the basis of the ODE model, i.e., Eq. 6.3 with $d_1 = d_2 = 0$. We impose the following stabilizability assumption on the system of Eq. 6.3. For the system of Eq. 6.3 with $d_1 = d_2 = 0$, we assume that there exists a locally Lipschitz control law $h_c : \mathbb{R}^n \to \mathbb{U}$ where $h_c(0) = 0$ such that the origin of the system $\dot{x} = f(x, x, h_c(x))$ is asymptotically stable. This assumption implies that there exists a continuously differentiable function $V : \mathbb{R}^n \to \mathbb{R}_{\geq 0}$ such that the following inequalities hold [100]:

$$\alpha_1(|x|) \leq V(x) \leq \alpha_2(|x|) \tag{6.4a}$$

$$\frac{\partial V}{\partial x}(x) f(x, x, h_c(x)) \leq -\alpha_3(|x|) \tag{6.4b}$$

$$\left| \frac{\partial V}{\partial x}(x) \right| \leq \alpha_4(|x|) \tag{6.4c}$$

for all $x \in D \subset \mathbb{R}^n$ where D is an open neighborhood of the origin and $\alpha_i \in \mathscr{K}$, $i = 1, 2, 3, 4$. In the remainder, we will use the notation $h_c(x)$ when referring to the stabilizing control law.

Remark 6.1. While we restrict our focus to nonlinear systems described by differential difference equations with constant delay, the extension of the results to systems described by more general functional differential equations, bounded time-varying delays, and multiple

state and input delays is conceptually possible.

6.2.3 Controller Emulation Design

Given the stability properties of the control law $h_c(x)$, one may consider designing stability constraints based on the stabilizing control law $h_c(x)$ to be imposed within a model predictive control (MPC) framework. However, MPC is typically implemented in a sample-and-hold fashion; that is, after receiving a state feedback measurement, a control action is computed and applied over a finite-time interval, called the sampling period. The control action for the next sampling period is computed from a new state measurement at the next sampling time.

To design stabilizing constraints based on the control law $h_c(x)$ for MPC, one must first consider the stabilizing properties of the control law $h_c(x)$ when applied to the system of Eq. 6.3 (with time-delays) in a sample-and-hold fashion. When a controller is applied to the continuous-time system of Eq. 6.3 in a sample-and-hold fashion, the resulting closed-loop system is a sampled-data time-delay system and is given by:

$$\begin{aligned} \dot{x}(t) &= f(x(t), x(t-d_1), h_\Delta(x, t-d_2)) \\ h_\Delta(x,t) &= h_c(x(k\Delta)),\ t \in [k\Delta, (k+1)\Delta), \\ & \qquad k = 0,\ 1,\ 2, \ldots \end{aligned} \tag{6.5}$$

where the $\Delta > 0$ is the sampling period and ϕ_x is the initial data. The initial data is assumed to be continuous and defined over the appropriate interval. We assume that the initial input function is determined by $h_\Delta(x, s-d_2)$ for $s \in [0, d_2]$ which implies that the initial data must be defined over a prolonged interval when $\Delta + d_2 > d_1$. Provided the time-delays and sampling rate are sufficiently small and the initial data is restricted to a ball of radius δ_2, i.e., $\phi_x(s) \in B_{\delta_2}$ for all $s \in [-\max\{d_1, \Delta + d_2\}, 0]$, it may be shown that the origin of the closed-

loop system is uniformly ISS which is stated in the proposition below. The result follows the ideas of [183]. Specifically, the system of Eq. 6.5 is treated as a perturbed form of the closed-loop system $\dot{x} = f(x,x,h_c(x))$. By employing Razumikhin-type arguments, we consider solutions to the sampled-data system where the solution at time t may be bounded by the state at time t to show that the origin of the closed-loop system is locally uniformly ISS.

Proposition 6.1. *Consider the sampled-data system of Eq. 6.5. Let* $\tilde{t}_d = \max\{d_1, \Delta + d_2\}$, *then there exists a* t_d^* *such that for all* $\tilde{t}_d \in (0, t_d^*)$, *the origin is uniformly ISS with offset* δ_1 *and restriction* δ_2 *where* $\delta_1 < \delta_2$ *and* $\{x \in \mathbb{R}^n : |x| \leq \delta_2\} \subset D$.

Proof. The sampled-data system of Eq. 6.5 may be written as a time-delay system with time-varying delay to account for sampling:

$$\dot{x}(t) = f(x(t), x(t-d_1), h_c(x(t-\tau(t)))) \tag{6.6}$$

where $\tau(t) = t - \lfloor (t-d_2)/\Delta \rfloor \Delta$ and $\tau(t) \leq (d_2/\Delta + 1)\Delta =: N_d\Delta$ ($N_d := (d_2/\Delta + 1)$). In the sampled-data system with state and input delay setting that we consider, the quantity $t - \tau(t)$ represents the sampling time instance that feedback is received to compute the control action applied to the system at time t. The maximum amount of time in the past that the feedback measurement used to compute the control action applied to the system at the current time (the maximum of $\tau(t)$) is the sampling time, Δ, plus the input delay, d_2.

The system of Eq. 6.6 may be analyzed as a perturbed form of the system without delays and sampling, i.e., the system $\dot{x} = f(x,x,h_c(x))$. In other words, consider the following system:

$$\begin{aligned} \dot{x}(t) &= f(x(t), x(t) + \xi_1(t), h_c(x(t)) + \xi_2(t)) \\ \xi_1(t) &= x(t-d_1) - x(t) \\ \xi_2(t) &= h_c(x(t-\tau(t))) - h_c(x(t)) \end{aligned} \tag{6.7}$$

We define the following: $\xi^T := [\xi_1^T \ \xi_2^T]$ with $\xi(t) \in D \times \mathbb{U} \subset \mathbb{R}^{n+m}$, $t_d := \max\{2d_1, 2N_d\Delta\}$, and

$$g(x,\xi) := f(x, x+\xi_1, h_c(x)+\xi_2) \ .$$

The perturbation term $\xi(t)$ is bounded. From the triangle inequality, we have:

$$|\xi(t)| = \left|[\xi_1^T(t)\ 0^T]^T + [0\ \xi_2^T(t)]^T\right| \leq |\xi_1(t)| + |\xi_2(t)| \ . \tag{6.8}$$

Owing to the fact that f and h_c are locally Lipschitz vector functions, there exists a $\gamma_1^* \in \mathscr{K}$ such that:

$$|\xi_1(t)| = \left| \int_{t-d_1}^{t} f(x(s), x(s-d_1), h_c(x(s-\tau(s)))) \ ds \right| \leq d_1 \gamma_1^*(\|x_d(t)\|) \tag{6.9}$$

where $\|x_d(t)\| = \max_{s\in[-t_d,0]} |x(t+s)|$. Again, by the locally Lipschitz properties assumed for f and h_c, there exist functions L_h, $\gamma_2^* \in \mathscr{K}$ such that:

$$|\xi_2(t)| \leq L_h(\|x_d(t)\|)|x(t-\tau(t)) - x(t)| \leq N_d\Delta L_h(\|x_d(t)\|)\gamma_2^*(\|x_d(t)\|) \ . \tag{6.10}$$

From the inequalities of Eqs. 6.8-6.10, there exists a $\gamma^* \in \mathscr{K}$ such that

$$|\xi(t)| \leq \tilde{t}_d \gamma^*(\|x_d(t)\|) \tag{6.11}$$

where $\tilde{t}_d = \max\{d_1, N_d\Delta\}$.

The time-derivative of V along the state trajectory of Eq. 6.5 is

$$\begin{aligned} \dot{V} &= \frac{\partial V}{\partial x}(x(t)) g(x(t),0) + \frac{\partial V}{\partial x}(x(t)) \left[g(x(t),\xi(t)) - g(x(t),0)\right] \\ &\leq -\alpha_3(|x(t)|) + \alpha_4(|x(t)|) \left|g(x(t),\xi(t)) - g(x(t),0)\right| \end{aligned} \tag{6.12}$$

for all $x(t) \in D$ where the inequality follows from Eq. 6.4b and Eq. 6.4c. Since g is a locally Lipschitz vector function (this follows from the fact that f and h_c are locally Lipschitz), there exists a function $L_\xi \in \mathscr{K}$ such that:

$$\begin{aligned}\dot{V} &\leq -\alpha_3(|x(t)|) + \alpha_4(|x(t)|)L_\xi(|\xi(t)|) \\ &\leq -\alpha_3(|x(t)|) + \alpha_4(|x(t)|)L_\xi(\tilde{t}_d\gamma^*(\|x_d(t)\|))\end{aligned} \tag{6.13}$$

where the second inequality follows from Eq. 6.11. For some pair of strictly positive real numbers δ_1 and δ_2 such that $\delta_1 < \delta_2$ and $\{x \in \mathbb{R}^n : |x| \leq \delta_2\} \subset D$, there exists $t_d^* > 0$ such that $\tilde{t}_d \in (0, t_d^*)$ implies:

$$|x(t)| \geq \alpha_3^{-1}(\alpha_4(\delta_2)L_\xi(\tilde{t}_d\gamma^*(\|x_d(t)\|))/q) \Rightarrow \dot{V} \leq -(1-q)\alpha_3(|x(t)|) \tag{6.14}$$

for some $q \in (0,1)$ and

$$\alpha_1^{-1} \circ \alpha_2 \circ \alpha_3^{-1}\left(\frac{\alpha_4(\delta_2)L_\xi(\tilde{t}_d\gamma^*(s))}{q}\right) < s \tag{6.15}$$

for all $s \in (\delta_1, \delta_2)$. We note that the size of δ_2, which governs the restriction on the initial condition, and $\tilde{t}_d$, which accounts for the magnitude of delays and the sampling period size, are restricted to be sufficiently small so that the arguments of the inverted class $\mathscr{K}$ functions in Eqs. 6.14-6.15 are within the domain of the functions. From Theorem 6.1 (taking $\gamma_x(\cdot) = \alpha_3^{-1}(\alpha_4(\delta_2)L_\xi(\tilde{t}_d\tilde{\gamma}^*(\cdot)/q))$, the origin of the sampled-data time-delay system of Eq. 6.5 is uniformly ISS with offset δ_1 and restriction δ_2 for all $\tilde{t}_d \in (0, t_d^*)$. □

For appropriately chosen offset δ_1 and restriction δ_2, one may find a level set of the Lyapunov (or Lyapunov-Razumikhin) function, Ω_ρ, such that $B_{\delta_1} \subset \Omega_\rho \subseteq B_{\delta_2}$ and for all initial data satisfying $\phi_x(s) \in \Omega_\rho$ for all $s \in [-\tilde{t}_d, 0]$ the closed-loop state trajectory of the

system of Eq. 6.5 under the control law $h_c(x)$ applied in a sample-and-hold fashion will be (uniformly) ultimately bounded in a ball of radius δ_1. Moreover, the closed-loop state is always bounded in Ω_ρ as a consequence of the construction of Ω_ρ and Proposition 6.1. This gives practical stability of the origin of the system of Eq. 6.5. The set Ω_ρ is an estimate of the region of attraction, and is used to design a region constraint in Lyapunov-based EMPC. Thus, Ω_ρ is referred to as the stability region for the remainder.

Remark 6.2. While the system of Eq. 6.3 is autonomous and thus, explicitly referring to the stability properties as uniform may not appear to be needed, the sampled-data system of Eq. 6.5 is a periodically time-varying system and hence, the fact that stability holds uniformly is needed.

6.3 Robustness of LEMPC to Small Time-Delays

In this section, the closed-loop stability of the time-delay system of Eq. 6.3 under LEMPC, formulated with an ordinary differential equation model of the system of Eq. 6.3, is analyzed. The sequence $\{t_k\}_{k\geq 0}$ denotes the sequence of sampling times where $t_k := k\Delta$ and $k \in \mathbb{N}$.

6.3.1 Formulation and Implementation

We assume that the system of Eq. 6.3 is equipped with a stage cost, $l_e : \Omega_\rho \times \mathbb{U} \to \mathbb{R}$, that is a measure of the instantaneous economic cost of Eq. 6.3. The economic stage cost is assumed to be continuous over its domain of definition and to depend on the current state and input, i.e., at time t, the economic stage cost is $l_e(x(t), u(t))$. We will show that applying LEMPC similar to that of Chapter 3, formulated with an ODE model of the system of Eq. 6.3, to the system of Eq. 6.3 will guarantee closed-loop stability (in a sense to be

made precise below) for sufficiently small time-delays. Instead of applying the two-mode LEMPC scheme of Eq. 3.3 directly to the time-delay system of Eq. 6.3, we consider only mode one operation of the LEMPC. Since we only use mode one operation of LEMPC, we drop this distinction and simply refer to this as LEMPC for the remainder of this chapter.

Given that plant-model mismatch affects the accuracy of the prediction of any MPC scheme, a subset of Ω_ρ is used in the design of the LEMPC whereby the LEMPC may dictate a time-varying operating policy. The subset of Ω_ρ, denoted as $\Omega_{\hat{\rho}}$ ($B_{\delta_1} \subset \Omega_{\hat{\rho}} \subset \Omega_\rho$), is designed such that if the current state $x(t_k) \in \Omega_{\hat{\rho}}$ and the predicted state at the next sampling time $z(t_{k+1}) \in \Omega_{\hat{\rho}}$ ($z(t_{k+1})$ denotes the predicted state at the next sampling time), then the actual state at the next sampling time plus the input delay time will be in Ω_ρ. In this case, plant-model mismatch arises from the use of an ODE model to predict the behavior of the time-delay system of Eq. 6.3. For any state in $\Omega_\rho \setminus \Omega_{\hat{\rho}}$, we use the stabilizing control law $h_c(x)$ to force the state back to $\Omega_{\hat{\rho}}$. However, in most practical cases, the amount of time that the stabilizing control law is applied to the system is insignificant relative to the amount of time that the LEMPC is applied for good closed-loop performance. It is important to note that the LEMPC of Eq. 3.3 uses a second mode of operation to force the state to $\Omega_{\hat{\rho}}$, utilizing a contractive Lyapunov-based constraint. Potentially, one could consider using such a contractive constraint within the context of LEMPC for time-delay systems. Nonetheless, the closed-loop stability properties of LEMPC with a contractive constraint for time-delay systems remains an open problem from a theoretical standpoint.

The optimal control problem that defines the LEMPC problem for time-delay systems

is given by the following optimization problem:

$$\min_{v\in S(\Delta)} \quad \int_{t_k}^{t_k+T} l_e(z(\tau),v(\tau))\,d\tau + V_f(z(t_k+T)) \tag{6.16a}$$

$$\text{s.t.} \quad \dot{z}(t) = \bar{f}(z(t),v(t)) \tag{6.16b}$$

$$z(t_k) = x(t_k) \tag{6.16c}$$

$$v(t) \in \mathbb{U},\ \forall\, t \in [t_k, t_k+T) \tag{6.16d}$$

$$z(t) \in \Omega_{\hat{\rho}},\ \forall\, t \in [t_k, t_k+T) \tag{6.16e}$$

where $\bar{f}(z,v) := f(z,z,v)$, $T = N\Delta$ ($N \in \mathbb{N}$) is the prediction horizon, z denotes the predicted state trajectory over the prediction horizon, and v is the piecewise constant input trajectory over the prediction horizon which is the decision variable of the optimal control problem.

The objective function of Eq. 6.16a consists of the economic cost functional with a terminal cost. The design of the terminal cost is beyond the scope of this chapter because it is not needed to prove closed-loop stability (for terminal cost design techniques for EMPC, see, for example, [4, 116]). A model (Eq. 6.16b) of the system of Eq. 6.3 with $d_1 = d_2 = 0$ is used to predict the future behavior of the system under the input trajectory computed by the LEMPC over the prediction horizon. The model is initialized with a state measurement at the current sampling time (Eq. 6.16c). Eq. 6.16d constrains the computed input trajectory to take values within the set of admissible control action values. The constraint of Eq. 6.16e bounds the predicted state trajectory be in $\Omega_{\hat{\rho}}$.

The optimal input trajectory of Eq. 6.16 at sampling time t_k is denoted as $v^*(t|t_k)$ and defined over $t \in [t_k, t_k+T)$. The control action computed at the kth sampling period is $u(t) = v^*(t_k|t_k)$ for $t \in [t_k, t_{k+1})$. At the next sampling time, t_{k+1}, the LEMPC (assuming $x(t_{k+1}) \in \Omega_{\hat{\rho}}$) is reinitialized with an updated state measurement and it computes an optimal input trajectory over a shifted horizon, i.e., LEMPC is applied in a standard receding

horizon fashion. The algorithm below summarizes the implementation of LEMPC:

Algorithm 6.1. Implementation of the LEMPC of Eq. 6.16.

1. At sampling time t_k, the LEMPC receives a state measurement $x(t_k)$.

2. If $x(t_k) \in \Omega_{\hat{\rho}}$, go to Step 2.1. Else, go to Step 2.2.

    2.1 Solve the optimal control problem of Eq. 6.16 to compute the optimal input trajectory $v^*(t|t_k)$ defined for $t \in [t_k, t_k + T)$. Go to Step 3.

    2.2 Compute the control action from the stabilizing control law $v^*(t_k|t_k) = h_c(x(t_k))$ Go to Step 3.

3. Send the control action $v^*(t_k|t_k)$ to the control actuators which will be applied to the system from $t_k + d_2$ to $t_{k+1} + d_2$, i.e., $u(t) = v^*(t_k|t_k)$ for $t \in [t_k, t_{k+1})$. Go to Step 4.

4. Set $k \leftarrow k+1$ and go to Step 1.

The main tuning parameter of LEMPC is $\hat{\rho}$ and does not need to be chosen so that $\Omega_{\hat{\rho}}$ is the largest subset of Ω_ρ such that the state is guaranteed to be in Ω_ρ under LEMPC. The parameter $\hat{\rho}$ governs the set of points (in state-space) where the LEMPC may operate the system in a time-varying fashion to optimize the process economics. It is chosen to manage a potential trade-off between robustness and performance of the closed-loop system. In this case, closed-loop robustness is defined as the ability to maintain the closed-loop state inside an invariant state-space set in the presence of uncertainty. The uncertainty considered here is time-delay that is not included in the process model of the LEMPC. On the other hand, operating over a larger region in state-space may improve closed-loop performance. If there is little plant-model mismatch, i.e., the delay is small, one may take it to be almost the size of ρ because the LEMPC may very accurately predicted the behavior of the process. If there is significant plant-model mismatch, $\hat{\rho}$ will need to be much smaller than ρ. This will be extensively investigated further in the chemical process example of Section 6.3.3.

6.3.2 Closed-loop Stability Analysis

In this subsection, sufficient conditions such that closed-loop stability of the time-delay system of Eq. 6.3 under the LEMPC of Eq. 6.16 in the sense that the state trajectory is bounded in Ω_ρ are derived. We will show that the state will be maintained in Ω_ρ when the control action is computed by LEMPC and if the state is in $\Omega_\rho \setminus \Omega_{\hat{\rho}}$, the state will be converge to $\Omega_{\hat{\rho}}$ in finite-time when the control action is computed by the explicit stabilizing control law.

The following proposition bounds the difference between the state trajectory of the DDE system of Eq. 6.3 and of the ODE system of Eq. 6.3 with $d_1 = d_2 = 0$ over a finite-time interval.

Proposition 6.2. *Consider the following two systems:*

$$\dot{x}(t) = f(x(t), x(t-d_1), u(t-d_2)) \tag{6.17}$$

$$\dot{z}(t) = f(z(t), z(t), v(t)) \tag{6.18}$$

where the initial time is t_0, the initial data of Eq. 6.17 is given by $\eta_x \in C([t_0 - d_1, t_0], \mathbb{R}^n)$ where $\eta_x(\theta) \in \Omega_\rho$ for $\theta \in [t_0 - d_1, t_0]$, $u(t) \in \mathbb{U}$ for all $t \geq t_0 - d_2$, $v(t) \in \mathbb{U}$ for all $t \geq t_0$, and $x(t_0) = z(t_0) \in S$ where S is a compact subset of Ω_ρ. Let $t_1 > 0$ be such that the state trajectories of the systems of Eqs. 6.17-6.18 are bounded in Ω_ρ for all $t \in [t_0, t_0 + t_1]$. There exists $\bar{\alpha} \in \mathscr{K}$ such that

$$|x(t) - z(t)| \leq \bar{\alpha}(t - t_0) \tag{6.19}$$

for all $t \in [t_0, t_0 + t_1]$.

Proof. Owing to the fact that f is locally Lipschitz, there exist positive constants L_{x_1}, L_{x_2},

and L_u such that

$$|f(x,y,u) - f(z,z,v)| \leq L_{x_1}|x-z| + L_{x_2}|y-z| + L_u|u-v| \tag{6.20}$$

for all x, y, $z \in \Omega_\rho$ and u, $v \in \mathbb{U}$. Consider the difference between the state, $x(t)$, of Eq. 6.17 and the state, $z(t)$ of Eq. 6.18, for $t \in [t_0, t_0+t_1]$ where $t_1 > 0$ is such that $x(t)$ and $z(t)$ are bounded in Ω_ρ for all $t \in [t_0, t_0+t_1]$ (the existence of $t_1 > 0$ follows from continuity arguments and the fact that $S \subset \Omega_\rho$ is compact). Let $e(t) := x(t) - z(t)$ which has dynamics $\dot{e}(t) = \dot{x}(t) - \dot{z}(t)$. The error dynamics may be bounded using Eq. 6.20:

$$\begin{aligned}
|\dot{e}(t)| &= |f(x(t), x(t-d_1), u(t-d_2)) - f(z(t), z(t), v(t))| \\
&\leq L_{x_1}|x(t) - z(t)| + L_{x_2}|x(t-d_1) - z(t)| + L_u|u(t-d_2) - v(t)| \\
&\leq L_{x_1}|e(t)| + L_{x_2}|x(t-d_1) - x(t) + x(t) - z(t)| + L_u|u(t-d_2) - v(t)| \\
&\leq (L_{x_1} + L_{x_2})|e(t)| + L_{x_2}|x(t-d_1) - x(t)| + 2L_u|u_{\max}|
\end{aligned} \tag{6.21}$$

for all $t \in [t_0, t_0+t_1]$ where $x(t)$, $x(t-d_1)$, $z(t) \in \Omega_\rho$ and $u(t-d_2)$, $v(t) \in \mathbb{U}$. The last inequality of Eq. 6.21 follows from the triangle inequality and the fact that $u(t-d_2)$ and $v(t)$ are bounded in $\mathbb{U}$. For all $x(s) \in \Omega_\rho$ for $s \in [t-d_1, t]$, we may bound the difference between $x(t-d_1)$ and $x(t)$:

$$|x(t-d_1) - x(t)| \leq d_1 \|x_d(t)\| \leq d_1 \alpha_1^{-1}(\rho) \tag{6.22}$$

where $\|x_d(t)\|$ is a slight abuse of notation and it denotes the max-norm of an element in the space $C([-d_1, 0], \mathbb{R}^n)$, i.e., $\|x_d(t)\| = \max_{\theta \in [-d_1, 0]} |x(t-\theta)|$ where $x_d(t) \in C([-d_1, 0], \mathbb{R}^n)$ and the last inequality follows from Eq. 6.4a. From Eqs. 6.21-6.22, the error dynamics may

be bounded by:

$$|\dot{e}(t)| \leq (L_{x_1} + L_{x_2})|e(t)| + L_{x_2} d_1 \alpha_1^{-1}(\rho) + 2L_u |u_{\max}| \ . \tag{6.23}$$

The error is bounded for all $t \in [t_0, t_0 + t_1]$ which may be shown by integrating the bound of Eq. 6.23 and noting $e(t_0) = 0$ to derive the following bound:

$$|e(t)| \leq \frac{L_{x_2} d_1 \alpha_1^{-1}(\rho) + 2L_u |u_{\max}|}{(L_{x_1} + L_{x_2})} \left[\exp((L_{x_1} + L_{x_2})(t - t_0)) - 1\right] \tag{6.24}$$

for all $t \in [t_0, t_0 + t_1]$. Taking

$$\bar{a}(s) := \frac{L_{x_2} d_1 \alpha_1^{-1}(\rho) + 2L_u |u_{\max}|}{(L_{x_1} + L_{x_2})} \left[\exp((L_{x_1} + L_{x_2})s) - 1\right] \tag{6.25}$$

completes the proof. □

The difference of the Lyapunov function values evaluated at any two points in Ω_ρ may be bounded by a quadratic function because V is continuously differentiable and Ω_ρ is a compact set. This is stated in the following proposition.

Proposition 6.3 (c.f. Proposition 6.3)**.** *For all x_1, $x_2 \in \Omega_\rho$, there exists $\beta > 0$ such that*

$$V(x_1) - V(x_2) \leq f_V(|x_1 - x_2|) \tag{6.26}$$

where the quadratic function $f_V(\cdot)$ is given by

$$f_V(s) := \alpha_4(\alpha_1^{-1}(\rho))s + \beta s^2 \ . \tag{6.27}$$

The following result gives sufficient conditions such that the closed-loop state trajectory of the system Eq. 6.3 under the LEMPC implemented according to Algorithm 6.1 is always

bounded in Ω_ρ.

Theorem 6.2. *Consider the system of Eq. 6.3 under the LEMPC of Eq. 6.16 designed via a control law that satisfies Eq. 6.4 which is implemented according to Algorithm 6.1. Let the initial data $\phi_x \in C([-d_1,0],\mathbb{R}^n)$ be such that $\phi_x(s) \in \Omega_\rho$ for all $s \in [-d_1,0]$ and the initial input ϕ_u be such that the state over the interval $[0,d_2]$ is bounded in Ω_ρ for $t \in [0,d_2]$ in the sense that $x(t) \in \Omega_\rho$ for all $t \in [0,d_2]$. Let $\tilde{t}_d \in (0,t_d^*)$ and $\hat{\rho} > 0$ be such that*

$$\hat{\rho} < \rho - f_V(\bar{\alpha}(\Delta + d_2)) \tag{6.28}$$

and $B_{\delta_1} \subseteq \Omega_{\hat{\rho}} \subset \Omega_\rho \subseteq B_{\delta_2}$. If $T \geq \Delta$, then the closed-loop state trajectory of Eq. 6.3 under the LEMPC is bounded in Ω_ρ for all $t \geq 0$.

Proof. To prove the theorem, we need to show the following: (1) the LEMPC is feasible for all $x(t_k) \in \Omega_{\hat{\rho}}$, under the LEMPC, (2) the state is bounded in Ω_ρ under the LEMPC, and (3) the closed-loop state starting from $\Omega_\rho \setminus \Omega_{\hat{\rho}}$ will converge to $\Omega_{\hat{\rho}}$ in a finite number of sampling times without coming out of Ω_ρ. To help the readability of the proof, we divide the proof into three parts corresponding to the three results that we need to show, respectively.

Part 1: Feasibility of the LEMPC is proved provided that the state at the current sampling time is in $\Omega_{\hat{\rho}}$. If $\tilde{t}_d \in (0,t_d^*)$ (where $\tilde{t}_d$ and t_d^* are defined according to Proposition 6.1), the input trajectory computed by the stabilizing control law $h_c(x)$ applied in a sample-and-hold fashion is a feasible solution to the optimal control problem of Eq. 6.16. Specifically, let $\hat{z}(t)$ and $\hat{v}(t)$ denote the solution and input trajectory, respectively, to the system:

$$\begin{aligned} \dot{\hat{z}}(t) &= \bar{f}(\hat{z}(t),\hat{v}(t)) \\ \hat{v}(t) &= h_c(\hat{z}(j\Delta)),\ t \in [t_j,t_{j+1}) \end{aligned} \tag{6.29}$$

for $j = k,\ k+1,\ \ldots,\ k+N-1$ with the initial condition $\hat{z}(t_k) = x(t_k) \in \Omega_{\hat{\rho}}$. Owing to the properties of the stabilizing control law $h_c(x)$, $\hat{v}(t) \in \mathbb{U}$ for all $t \in [t_k, t_k + T)$. Moreover, from Proposition 6.1, the input trajectory $\hat{v}$ is a feasible input trajectory to the optimal control problem of Eq. 6.16. This statement holds since $\Omega_{\hat{\rho}}$ is forward invariant for the sampled-data system of Eq. 6.29 if $B_{\delta_1} \subseteq \Omega_{\hat{\rho}}$ and if the sampling period is sufficiently small such that Proposition 6.1 holds, i.e., the proof of forward invariance of the set $\Omega_{\hat{\rho}}$ for the system of Eq. 6.29 follows that of Proposition 6.1 with $d_1 = d_2 = 0$.

Part 2: We consider boundedness of the state in Ω_ρ under LEMPC. The LEMPC computes an input trajectory such that the predicted state will be maintained in $\Omega_{\hat{\rho}}$ over the prediction horizon. However, the system of Eq. 6.3 does not evolve according to the ODE model of Eq. 6.16b and the control actions applied to the system over the time t_k to $t_k + d_1$ may be computed by either the LEMPC or the stabilizing control law at previous sampling times. Specifically, the predicted state, $z(t)$, over the prediction horizon will be bounded in $\Omega_{\hat{\rho}}$ for all $t \in [t_k, t_k + T)$ under the computed input trajectory which is guaranteed by the constraint of Eq. 6.16e. Owing to the input delay the control action computed at t_k is applied to the system from $t_k + d_2$ to $t_{k+1} + d_2$. We need to show that $x(t) \in \Omega_\rho$ for all $t \in [t_k, t_{k+1} + d_2]$ when $x(t_k) \in \Omega_{\hat{\rho}}$.

Let $\hat{\rho}$ satisfy Eq. 6.28. We proceed by contradiction and assume there exists a time $\tau^* \in [t_k, t_{k+1} + d_2]$ such that $V(x(\tau^*)) > \rho$ (the case that $x(t)$ is not defined for some $\tau \in [t_k, t_{k+1} + d_2]$ is also covered by this assumption). We define the time τ_1 as follows:

$$\tau_1 := \inf\{\tau \in [t_k, t_{k+1} + d_2] : V(x(\tau)) > \rho\} \,. \tag{6.30}$$

A standard continuity argument in conjunction with the fact that $V(x(t_k)) \leq \hat{\rho} < \rho$ shows that $\tau_1 \in (t_k, t_{k+1} + d_2]$, $V(x(t)) \leq \rho$ for all $t \in [t_k, \tau_1]$ with $V(x(\tau_1)) = \rho$, and $V(x(t)) > \rho$

for some $t \in [\tau_1, t_{k+1} + d_2]$. If $\hat{\rho}$ satisfies Eq. 6.28, we have

$$\rho = V(x(\tau_1)) \leq V(z(\tau_1)) + f_V(\bar{\alpha}(\tau_1)) \leq \hat{\rho} + f_V(\bar{\alpha}(\Delta + d_2)) < \rho \tag{6.31}$$

where the first inequality follows from Propositions 6.2-6.3 and the second inequality follows from the fact that $f_V \circ \bar{\alpha} \in \mathscr{K}$ and $\tau_1 \leq \Delta + d_2$. Eq. 6.31 leads to a contradiction. Thus, $x(t_{k+1} + d_1) \in \Omega_\rho$ if Eq. 6.28 is satisfied (regardless of whether the LEMPC or the stabilizing control $h_c(x)$ is used to compute the input trajectory over t_k to $t_k + d_1$).

Part 3: We prove that the state will converge to $\Omega_{\hat{\rho}}$ for any state starting in $\Omega_\rho \setminus \Omega_{\hat{\rho}}$. When the current state $x(t_k) \in \Omega_\rho \setminus \Omega_{\hat{\rho}}$, the control action is computed from the stabilizing control law $h_c(x)$. First, consider $t_k \in [0, d_2]$, by assumption of the initial data and initial input value, the past data from $t_k - d_1$ to t_k is in Ω_ρ. The stabilizing control law will force the state to converge to $\Omega_{\hat{\rho}}$ without coming out of Ω_ρ in finite-time if $\tilde{t}_d \in (0, t_d^*)$. This follows from Proposition 6.1.

Now, let us consider the case that the LEMPC previously computed the control actions for the system. Owing to the plant-model mismatch, the state may come outside of $\Omega_{\hat{\rho}}$. From Part 2, the state will still remain bounded in Ω_ρ if indeed it comes outside of $\Omega_{\hat{\rho}}$. Again, once the stabilizing control law $h_c(x)$ starts to compute control actions for the system to force the state to converge to $\Omega_{\hat{\rho}}$, all the assumptions of Proposition 6.1 are satisfied (assuming $\tilde{t}_d \in (0, t_d^*)$) and thus, the state will be forced back to $\Omega_{\hat{\rho}}$ in finite-time without coming out of Ω_ρ when $x(t_k) \in \Omega_\rho \setminus \Omega_{\hat{\rho}}$ which completes the proof. □

Remark 6.3. Given the generality of the class of nonlinear time-delay systems considered, it is difficult to explicitly characterize the functions used in the analysis. The results and conditions of this section are constructive in the sense that they provide insight into the relationship of system parameters, e.g., nonlinearities and delay size, and design parameters of the control system, e.g., sampling period, choice of stabilizing control law $h_c(x)$, and

region constraint size, $\Omega_{\hat{\rho}}$.

Remark 6.4. In Eq. 6.21 of the proof of Proposition 6.2, we bound $|u(t-d_2)-v(t)|$ by $2|u_{\max}|$ () which may appear overly conservative. Even if $v(t)=u(t)$ for all t, the input trajectories are piecewise continuous. For a given t, the control actions $u(t-d_2)$ (control action implemented at time t) and $u(t)$ (control action computed at time t) could be computed at different sampling times and $u(t)\neq u(t-d_2)$. Within the context of EMPC, it is conceivable that $|u(t-d_2)-u(t)|=2|u_{\max}|$ as is the case when EMPC computes a bang-bang input trajectory. One could consider imposing rate of change constraints within the context of EMPC that limits how much the computed control action may change at each sampling time, i.e., $|u(t_{k+1})-u(t_k)|\leq \delta u$. This may allow one to upper bound $|u(t-d_2)-u(t)|$ by δu. Nonetheless, this may make the EMPC problem infeasible and/or may limit the achievable closed-loop performance when rate of change constraints are imposed in the EMPC problem.

Remark 6.5. Stabilization at a steady-state typically will provide a degree of robustness to plant-model mismatch. In contrast, LEMPC may dictate a time-varying operating strategy. While time-varying operation may lead to better closed-loop economic performance, it may lead to a decrease in the robustness to uncertainty (see the chemical process example of Section 6.3.3 below for a demonstration of this point).

Remark 6.6. The sampling period Δ plays a role in stability and performance. Sufficiently fast sampling is required to maintain closed-loop stability (Proposition 6.1 and Theorem 6.2). Potentially, faster sampling may also improve closed-loop performance because there are more degrees of freedom to optimize over. However, in the example considered below, little performance benefit is achieved through faster sampling. From a practical standpoint, there may also be limitations on the hardware that may limit how fast one may sample.

Table 6.1: Notation and parameter values of the CSTR with recycle.

Density	$\rho_L = 1.0 \times 10^3\,\mathrm{kg\,m^{-3}}$
Heat capacity	$C_p = 4.18\,\mathrm{kJ\,kg^{-1}\,K^{-1}}$
Flow rate	$F = 6.0\,\mathrm{m^3\,h^{-1}}$
Reactor volume	$V_R = 1.0\,\mathrm{m^3}$
Heat of reaction	$\Delta H = -7.8 \times 10^4\,\mathrm{kJ\,kmol^{-1}}$
Activation energy	$E/R = 5.7 \times 10^4/8.314\,\mathrm{K}$
Feed temperature	$T_f = 300.0\,\mathrm{K}$
Reaction rate constant	$k_0 = 1.0 \times 10^9\,\mathrm{m^3\,kmol^{-1}\,h^{-1}}$
Splitting fraction	$\lambda = 0.70$
Concentration of chemical A	C_A
Reactor temperature	T
Heat removal rate from reactor	Q
Feed concentration	C_{Af}

6.3.3 Application to a Chemical Process Example

Consider a well-mixed, non-isothermal continuous stirred-tank reactor (CSTR) where an irreversible, elementary second-order, and exothermic reaction takes place that converts a reactant A to a desired product B ($A \rightarrow B$). A process flow diagram of the CSTR is given in Fig. 6.1. The inlet stream of the reactor with flow rate λF (constant density of the inlet flow stream is assumed), temperature T_f, and reactant concentration C_{Af} feeds the reactor with the reactant A in an inert solvent D. The outlet stream of the reactor is split with a constant splitting fraction λ ($\lambda \in [0,1]$), and the fraction λ of the outlet stream is the product stream. A recycle stream, which contains a fraction of $1-\lambda$ of the reactor outlet, is used to recover unreacted A. A transportation lag, which is modeled as a time-delay with magnitude d_1, is considered in the recycle stream leading to a state delay in the process model. To supply or remove thermal energy to/from the reactor, the CSTR is outfitted with a jacket. The manipulated inputs to the CSTR are the feed concentration of the reactant C_{Af} and the heat rate Q supplied to/removed from the reactor.

To construct a first-principles model of the reactor, constant liquid hold-up, density, and

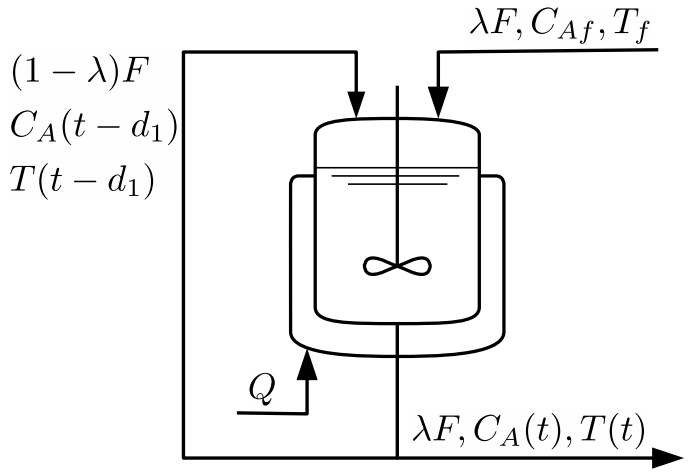

Figure 6.1: Process flow diagram of the CSTR with recycle.

heat capacity are assumed. In addition to the state delay, the control actuators are assumed to operate with dead-time which gives rise to input delay. The input delay is assumed to model, for instance, the actuator dynamics and/or to model the possible computation delay resulting from solving the EMPC optimization problem on-line. The dead-times of the two manipulated inputs are assumed to be the same for simplicity of the presentation and are denoted as d_2. Using a mass balance of the reactant A and energy balance along with standard modeling assumptions, a dynamic model may be constructed of the CSTR with recycle and is given by the following system of DDEs:

$$\dot{C}_A(t) = \frac{(1-\lambda)F}{V_R} C_A(t-d_1) + \frac{\lambda F}{V_R} C_{Af}(t-d_2) - \frac{F}{V_R} C_A(t) - k_0 e^{-E/RT(t)} C_A^2(t) \quad (6.32a)$$

$$\dot{T}(t) = \frac{(1-\lambda)F}{V_R} T(t-d_1) + \frac{\lambda F}{V_R} T_f - \frac{F}{V_R} T(t) - \frac{\Delta H k_0}{\rho_L C_p} e^{-E/RT(t)} C_A^2(t) + \frac{Q(t-d_2)}{V_R \rho_L C_p} \quad (6.32b)$$

where the state variables are the concentration of the reactant C_A in the reactor and the reactor temperature T, i.e., $x^T = [C_A \; T]$. The remaining notation and process parameter values are defined and summarized in Table 6.1. The admissible input values for each input are

bounded in the following sets: $C_{A0} \in [0.5,\ 7.5]$ kmol m^{-3} and $Q \in [-80.0,\ 80.0]$ MJ h^{-1}. The CSTR model of Eq. 6.32 has a steady-state in the operating range of interest: $x_s^T := [C_{As}\ T_s] = [2.96\,\text{kmol m}^{-3}\ 320.0\,\text{K}]$ corresponding to the inputs: $C_{A0s} = 4.0\,\text{kmol m}^{-3}$ and $Q_s = 11.5\,\text{MJ h}^{-1}$. The steady-state x_s is open-loop asymptotically stable.

The control objective is to operate the CSTR around the steady-state to maximize the average production rate of the product B while satisfying two process constraints. The process constraints are: (1) to maintain the closed-loop state within a bounded and well-defined state-space set and (2) the time-averaged amount of reactant A that may be fed to the CSTR must be equal to $\lambda F C_{A0s}$ or mathematically,

$$\frac{1}{t_f}\int_0^{t_f} C_{A0}(t)\,dt = C_{A0s} \tag{6.33}$$

where t_f is the length of operation. To accomplish the control objective while satisfying the process constraints, LEMPC is applied to the CSTR. In the closed-loop simulations of this section, robustness of LEMPC to time-delay is demonstrated. More precisely, we illustrate robustness in the sense that the closed-loop state trajectory of Eq. 6.32 under an LEMPC system formulated with an ODE model of the CSTR will be maintained in a compact state-space set (in $\mathbb{R}^2$) for sufficiently small time-delays.

To design an LEMPC system with the ODE model of the CSTR (Eq. 6.32 with $d_1 = d_2 = 0$), an explicit stabilizing control law is designed and a Lyapunov function for the closed-loop system under the control law is constructed. The explicit stabilizing control law $h_c : \mathbb{R}^2 \to U$ is given component-wise with $h_c^T(x) = [h_{c,1}(x)\ h_{c,2}(x)]$ where $h_{c,1}(x) = C_{A0s}$ to satisfy the input average constraint of Eq. 6.33 and feedback linearization for $h_2(x)$. Specifically, within the range where the input bounds are satisfied, the following nonlinear

control law makes the evolution of T to be described by a linear model:

$$\bar{h}_{c,2}(x) = -V_R \rho_L C_p \left(-\frac{\lambda F}{V_R} T_f + \frac{\lambda F}{V_R} T + \frac{\Delta H k_0}{\rho_L C_p} e^{-E/RT} C_A^2 + K(T - T_s) \right) \tag{6.34}$$

where K is the gain of the control law. To account for the bounds on the admissible input, saturation is accounted for in $h_{c,2}$ which is given by

$$h_2(x) = \begin{cases} Q_{\min} & \text{if } \bar{h}_2(x) < Q_{\min} \\ \bar{h}_2(x) & \text{if } Q_{\min} \leq \bar{h}_2(x) \leq Q_{\max} \\ Q_{\max} & \text{if } \bar{h}_2(x) > Q_{\max} \end{cases} \tag{6.35}$$

where $Q_{\min}$ and $Q_{\max}$ is the minimum and maximum admissible heat rate value. In this example, the gain of the controller is tuned to $K = 2.0$. A quadratic Lyapunov function for the closed-loop system under the stabilizing control law is constructed, which has the form:

$$V(x) = (x - x_s)^T P (x - x_s) \tag{6.36}$$

where

$$P = \begin{bmatrix} 500 & 20 \\ 20 & 1 \end{bmatrix}.$$

With the control law and Lyapunov function, the stability region is estimated to be a level set of the Lyapunov function Ω_ρ with $\rho = 1200$ by taking it to be points in state-space where $\dot{V} < 0$.

The following economic stage cost is used in the LEMPC:

$$l_e(x,u) = -k_0 e^{-E/RT} C_A^2 + q_T (T - T_s)^2 \tag{6.37}$$

where the first term credits the production rate of B and the second term penalizes temperature deviations from the steady-state temperature T_s. The justification for the second term is the stability region of this system is large and operating over a large temperature range may be impractical. Thus, the second term penalizes large deviations of the temperature from the steady-state temperature. In this case, the stage cost parameter is $q_T = 0.05$ which has been tuned on the basis of the delay-free system such that the closed-loop temperature is maintained near the steady-state temperature.

To integrate forward in time the DDEs of Eq. 6.32, the standard Runge-Kutta (4,5) method was used with an absolute tolerance set at 10^{-7}. The remaining parameters of the LEMPC and implementation details of the LEMPC are as followed: the sampling period is $\Delta = 0.01\,\text{h}$, the number of sampling periods in the prediction horizon is $N = 70$, i.e., $T = 0.70\,\text{h}$, and the average constraint must be satisfied over each operating interval of $0.65\,\text{h}$, i.e., the average constraint of Eq. 6.33 must be satisfied every $0.65\,\text{h}$ which guarantees that the average constraint is satisfied over the entire length of operation. For the remainder, the operating period will refer to an interval of length $0.65\,\text{h}$ that the average constraint is imposed. The prediction horizon and operating period length have been chosen so that the asymptotic average closed-loop performance of the CSTR without time-delays leads to better closed-loop performance compared to that of the operation at the steady-state. Orthogonal collocation with three Radau collocation points per sampling period is used to integrate the ODE model within the LEMPC optimal control problem. Ipopt [187] was employed to solve the optimal control problem of the LEMPC at each sampling time. Analytical first-order and second-order derivative information was supplied to the solver. The simulations were completed on a desktop computer with an Intel® Core™ 2 Quad 2.66 GHz processor running an Ubuntu Linux operating system. In the simulations below, the computation time to solve the optimal control problem at each sampling time was less than one percent of the sampling period ($\Delta = 0.01\,\text{h} = 36\,\text{s}$) on average.

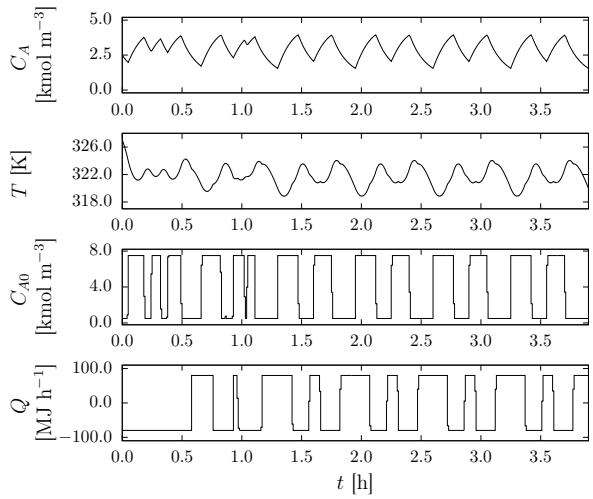

Figure 6.2: The closed-loop trajectories of the CSTR under the LEMPC without time-delays ($d_1 = d_2 = 0$).

In the first set of simulations, the closed-loop stability and performance properties of the CSTR without delays under LEMPC are considered. The level set $\Omega_{\hat{\rho}}$ is such that $\hat{\rho} = 1000$. The closed-loop CSTR under LEMPC without delay is simulated over six operating periods, and the closed-loop trajectories are given in Fig. 6.2. From Fig. 6.2, the LEMPC dictates a cyclical operating policy. Throughout the length of operation, the state trajectory is maintained in Ω_ρ. The asymptotic average production rate of B, i.e., average production rate after the effect of the initial condition becomes insignificant, was $4.820\,\text{kmol}\,\text{m}^{-3}$. As a comparison, the average production rate of B at the steady-state is $4.354\,\text{kmol}\,\text{m}^{-3}$ and the closed-loop (asymptotic) production rate under LEMPC is 10.70 percent better than the steady-state production rate. Moreover, we will use the average closed-loop economic stage cost index (given and explained below) to assess the closed-loop performance of the CSTR with time-delay. The asymptotic average economic stage cost index for this case study is 4.572, while it is 4.354 for operation at the steady-state (performance under LEMPC as assessed through this metric is 5.01 percent better than that at the steady-state).

In the second set of simulations, we consider the effect of the time-delay on perfor-

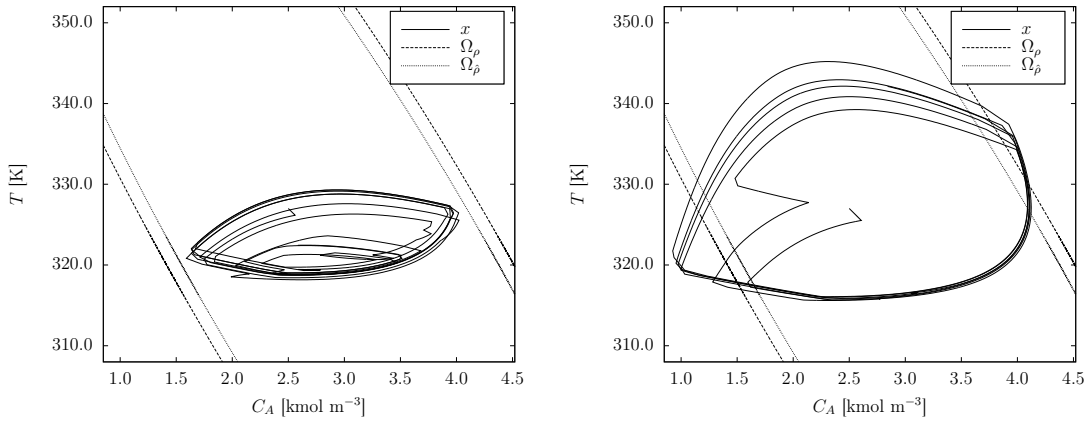

(a) (b)

Figure 6.3: The state-space evolution of the closed-loop CSTR states under LEMPC with (a) $d = 0.05\,\text{h}$ and (b) $d = 0.10\,\text{h}$.

mance and stability. In all cases, the state and input delays are taken to be equal in magnitude and the time-delay is denoted as d ($d = d_1 = d_2$). Fig. 6.3 shows the closed-loop state evolution of the CSTR under the LEMPC for $d = 0.05\,\text{h}$ and $d = 0.10\,\text{h}$, respectively. With the time-delay, the CSTR is still operated in a cyclical manner, but as the time-delay increases, the CSTR operates over a larger region of state-space. The closed-loop state is maintained in Ω_ρ for $d = 0.05\,\text{h}$, but for $d = 0.10\,\text{h}$, the state is not bounded in Ω_ρ over the length of operation. To assess the closed-loop performance, the average economic stage cost performance index is used which is given by:

$$\bar{L}_e = \frac{1}{t_f} \int_0^{t_f} l_e(x(t), u(t-d_2))\, dt\ . \tag{6.38}$$

The average economic stage cost is computed with the closed-loop state and input. The reason for using the metric of Eq. 6.38 as opposed to the average production rate of B to assess the closed-loop performance is as the magnitude of the time-delay increases, the CSTR operates over a larger temperature range (Fig. 6.3). The temperature is greater than

Table 6.2: Closed-loop performance relative to the performance at the steady-state and closed-loop stability properties of the CSTR under LEMPC.

d	$\bar{L}_e$	Diff. (%)	Stability
0	4.668	7.21	Yes
0.01	4.654	6.88	Yes
0.02	4.618	6.07	Yes
0.03	4.518	3.77	Yes
0.04	4.441	1.99	Yes
0.05	4.220	-3.09	Yes
0.06	3.995	-8.26	Yes
0.07	2.763	-36.55	No
0.08	3.002	-31.06	No
0.09	1.801	-58.64	No
0.10	0.565	-87.03	No

The average stage cost index for operation at the steady-state is 4.354. The column "Diff." is the percent difference of the average stage cost index relative to the steady-state stage cost index.

the steady-state temperature on average for the cases with time-delay. Since the production rate scales with temperature, the production rate of B increases with the size of the time-delay. Moreover, the LEMPC does not directly optimize the production rate of B, but rather the stage cost of Eq. 6.37. Thus, we use the metric of Eq. 6.38 to assess the performance because it also accounts for operation over a larger temperature range.

Table 6.2 summaries the closed-loop performance and closed-loop stability properties of the CSTR under LEMPC for several closed-loop simulations each over six operating periods with varying time-delays. Closed-loop stability is defined as the closed-loop state remaining bounded in Ω_ρ over the length of the simulated operation. From Table 6.2, it follows that the closed-loop performance deteriorates as the time-delay increases. Moreover, for time-delays greater than 0.06 h, the closed-loop stability of the CSTR is not maintained. It is important to note that the state trajectory of the closed-loop system under the stabilizing control law remains bounded in Ω_ρ for all the magnitudes of the time-delay used

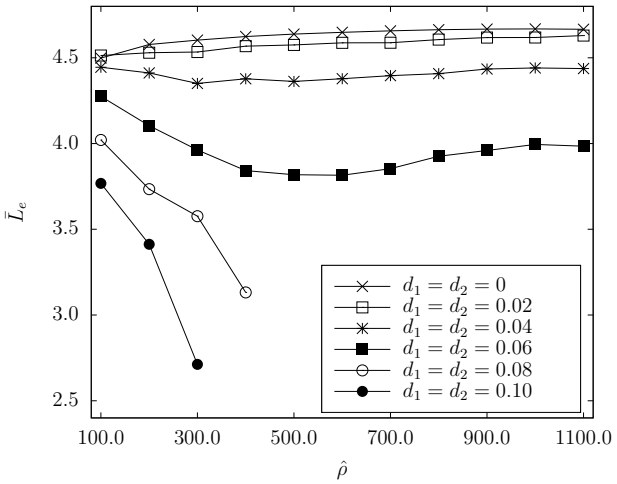

Figure 6.4: A comparison of the closed-loop performance with the tuning parameter $\hat{\rho}$ and magnitude of the time-delay.

in Table 6.2 which suggests that steady-state-type operation, i.e., stabilization at a steady-state, is more robust to time-delays than time-varying-type operation.

The available tuning parameter of LEMPC that may be manipulated to make the closed-loop system more robust to uncertainty is $\hat{\rho}$, i.e., the level set where LEMPC operates. In the last set of simulations, the effect of the size of $\hat{\rho}$ on closed-loop stability and performance is evaluated. Several closed-loop simulations were performed each over six operating periods with varying $\hat{\rho}$ and d. The average economic stage cost indices for these simulations are given in Fig. 6.4. Only the closed-loop simulations that led to a stable operation were included in Fig. 6.4. Fig. 6.4 shows that the closed-loop performance degrades with larger time-delays. For small time-delays, the closed-loop performance is better as the size of $\Omega_{\hat{\rho}}$ increases because the LEMPC may operate the system over a larger state-space set with greater $\hat{\rho}$. For small time-delays, the ODE model may capture enough of the behavior of the system to improve the performance. For larger time-delays, the closed-loop performance is worse than that achieved at the steady-state.

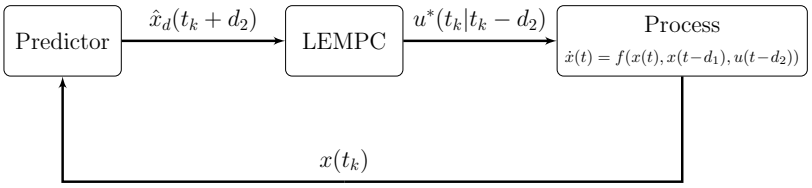

Figure 6.5: Flow diagram of the predictor feedback LEMPC scheme.

6.4 Time-delay Compensation for Improved Closed-loop Performance

Larger time-delay may lead to significant performance degradation when the control system does not explicitly account for the time-delays as demonstrated in the example of the previous section. In this section, a methodological framework for compensating state and input delay within the context of EMPC is presented. A closed-loop predictor is used to compensate the adverse effect of the input delay, and a DDE model is used within the EMPC to predict the behavior of the system of Eq. 6.3. We restrict our attention to nominally operated systems of the form of Eq. 6.3.

6.4.1 Predictor Feedback LEMPC Methodology and Implementation

A block diagram of the predictor feedback LEMPC methodology is shown in Fig. 6.5. At a sampling time t_k, a predictor is used to predict the state at $t_k + d_2$ utilizing the past measurements of the state and the previously computed input trajectory over t_k to $t_k + d_2$ to compensate the effect of the input delay. Then, the LEMPC system is initialized with the predicted state and solves for the optimal control action that will be implemented on the system from $t_k + d_2$ to $t_{k+1} + d_2$. Moreover, instead of using an ODE model within the LEMPC, the DDE model is used to account for the state delay. Thus, the predictor must also generate the initial data used to initialize the DDE model in the LEMPC from

$t_k + d_2 - d_1$ to $t_k + d_2$. The predicted state (initial data) for a given sampling time is denoted as $\hat{x}_d(t_k + d_2) \in C([-d_1, 0], \mathbb{R}^n)$.

Given that we consider nominal operation, the predictor may simply consist of solving the DDEs forward in time which is what we employ in the example below. The predictor is a closed-loop predictor in the sense that the predictor is reinitialized with a new state measurement at each sampling time. The closed-loop nature of the predictor allows for the potential use of the predictor feedback LEMPC on open-loop unstable processes as opposed to open-loop predictors, e.g., the classical Smith predictor, which require the steady-state solution be open-loop asymptotically stable. Other types of time-delay compensators or predictors may potentially be used to possibly increase the robustness of the closed-loop system to plant-model mismatch, e.g., the predictor developed in [82], but we note that most, if not all, of time-delay compensators have been designed for systems with input-delay only. Thus, appropriate modifications may need to be made to these other types of time-delay compensators to account for state delay.

A shifted sampling time sequence is defined as $\{\bar{t}_k\}_{k\geq 0}$ where $\bar{t}_k = k\Delta + d_2$, $k = 0,\ 1,\ \ldots$ which is a time sequence corresponding to when control actions are applied to the system, i.e., the control action computed at t_k is applied to the system from $\bar{t}_k$ to $\bar{t}_{k+1}$. The optimal control problem that defines the predictor feedback LEMPC is:

$$\min_{v\in S(\Delta)} \quad \int_{\bar{t}_k}^{\bar{t}_k+T} l_e(z(\tau), v(\tau))\, d\tau + V_f(z(\bar{t}_k + T)) \tag{6.39a}$$

$$\text{s.t.} \quad \dot{z}(t) = f(z(t), z(t-d_1), v(t)) \tag{6.39b}$$

$$z_d(\bar{t}_k) = \hat{x}_d(\bar{t}_k) \tag{6.39c}$$

$$v(t) \in \mathbb{U},\ \forall\, t \in [\bar{t}_k, \bar{t}_k + T) \tag{6.39d}$$

$$z(t) \in \Omega_{\hat{\rho}},\ \forall\, t \in [\bar{t}_k, \bar{t}_k + T) \tag{6.39e}$$

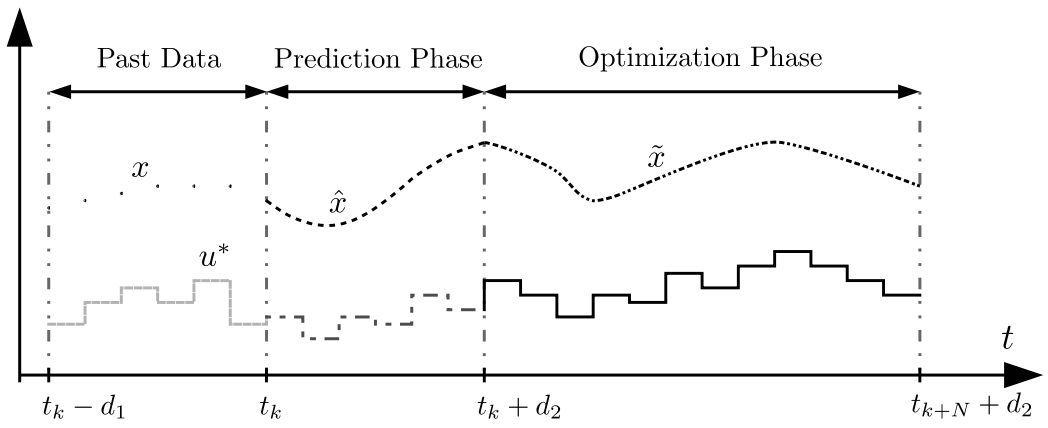

Figure 6.6: An illustration of the phases of the predictor feedback LEMPC scheme.

where $\hat{x}(t_k) = \hat{x}_d(\bar{t}_k)(0)$. The main difference between the predictor feedback LEMPC and the LEMPC of Eq. 6.16 is the DDE model, which is initialized with the initial data computed by the predictor and provides a prediction of the future evolution of the system in the predictor feedback LEMPC. The LEMPC of Eq. 6.16 uses an ODE model and is initialized with a current state measurement.

An illustration of the implementation of the predictor feedback LEMPC methodology is given in Fig. 6.6. At a sampling time t_k, the predictor, i.e., prediction phase, uses past state data and the control actions that will be applied from t_k to $t_k + d_2$ (these control actions are computed at previous sampling times) to predict the state trajectory over t_k to $t_k + d_2$. In the optimization phase, the predictor feedback LEMPC solves for the optimal input trajectory over $t_k + d_2$ to $t_k + d_2 + T$. This implementation is summarized in the following algorithm:

Algorithm 6.2. Implementation of the predictor feedback LEMPC of Eq. 6.39.

1. At sampling time t_k, the predictor receives a state measurement $x(t_k)$. Go to Step 2.

2. The predictor computes the predicted data $\hat{x}_d(\bar{t}_k)$. Go to Step 3.

3. If $\hat{x}(\bar{t}_k) \in \Omega_{\hat{\rho}}$, go to Step 3.1. Else, go to Step 3.2.

3.1 Solve the optimal control problem of Eq. 6.39 to compute the optimal input trajectory $v^*(t|\bar{t}_k - d_2)$ defined for $t \in [\bar{t}_k, \bar{t}_{k+N})$. Go to Step 4.

3.2 Compute the control action from the stabilizing control law $v^*(\bar{t}_k|\bar{t}_k - d_2) = h_c(\hat{x}(\bar{t}_k))$ Go to Step 4.

4. Send the computed control action $v^*(\bar{t}_k|\bar{t}_k - d_2)$, to the control actuators to be applied from $\bar{t}_k$ to $\bar{t}_{k+1}$, i.e., $u(t+d_2) = v^*(t_k + d_2|t_k)$ for $t \in [t_k, t_{k+1})$. Go to Step 5.

5. Set $k \leftarrow k+1$ and go to Step 1.

Remark 6.7. In the design of the LEMPC of Eq. 6.39, we leverage the results of Proposition 6.1 to again design an explicit stabilizing control law and utilize it to characterize a region constraint that is imposed in the LEMPC problem. This design methodology allows for standard control techniques developed for systems described by nonlinear ordinary differential equations be applied to design stabilizing control laws for nonlinear time-delay systems. On the other hand, the results and size of delays that may be handled in the closed-loop systems may be limited owing to the fact that the delays are neglected in the design of the stabilizing control law. However, design of stabilizing control laws for nonlinear time-delay systems is by no means a trivial task. Moreover, a complete and rigorous stability analysis of such a closed-loop system is a challenging and potentially intractable task given the degree of complexity, e.g., state and input delay, sampling, and nonlinearities.

Remark 6.8. It is important to point out that the extension of numerical methods used to obtain solutions of ordinary differential equations (ODEs) to obtaining solutions of differential difference equations (DDEs) is not straightforward [17]. Thus, when selecting the numerical method used to solve the predictor, the practitioner must be aware of potential numerical issues, e.g., "ghost solutions", loss of injectivity, and non-uniqueness of solution.

6.4.2 Application to a Chemical Process Example

The predictor feedback LEMPC methodology is applied to the CSTR example of Eq. 6.32. The LEMPC design and parameters are the same as that used in the previous section (in all simulations below $\hat{\rho} = 1000$). To solve the DDEs of Eq. 6.32 embedded in the LEMPC optimization problem, i.e., the constraint of Eq. 6.39b, orthogonal collocation with three Radau collocation points per sampling period was employed (see, for example, [16, 17] for stability and convergence analysis of collocation methods applied to DDEs). As a qualitative comparison, a single-shooting implementation of the optimal control problem (OCP) of Eq. 6.39 using the explicit Euler method with first-order derivatives approximated through finite-difference and quasi-Newton method with the Broyden-Fletcher-Goldforb-Shanno (BFGS) update method for the second-order derivatives required greater than fifty times more time to solve the optimization problem at each sampling time compared to the implementation with orthogonal collocation. Moreover, the average computation time required to solve the optimal control problem with the collocation implementation was approximately two percent of the sampling period. It is important to point out that while the success of orthogonal collocation used to solve OCPs with ODEs has been well documented [20], fewer cases of employing orthogonal collocation within the context of OCPs formulated with DDE models have reported in the literature especially in context of the EMPC literature.

Several closed-loop simulations were completed of the CSTR under the predictor feedback LEMPC with varying magnitudes of the time-delays. Fig. 6.7 gives the closed-loop trajectories of the CSTR with $d = 0.10\,\text{h}$. In comparison to the CSTR under LEMPC formulated with an ODE model (Fig. 6.3(b)), the predictor feedback LEMPC operates the CSTR over a smaller temperature range (Fig. 6.7). To further emphasize the differences between the evolution of the CSTR under the predictor feedback LEMPC and the LEMPC

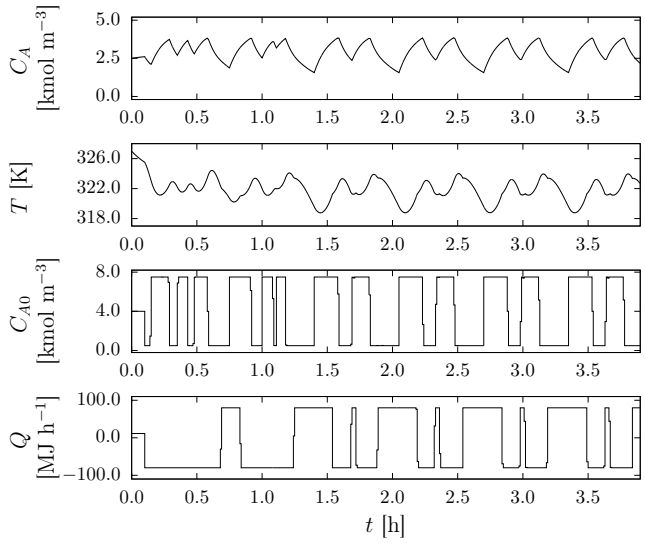

Figure 6.7: The closed-loop trajectories of the CSTR under the LEMPC with time-delay of $d = 0.10\,\text{h}$. The input trajectories shown in the plots correspond to the input values applied to the system at each time.

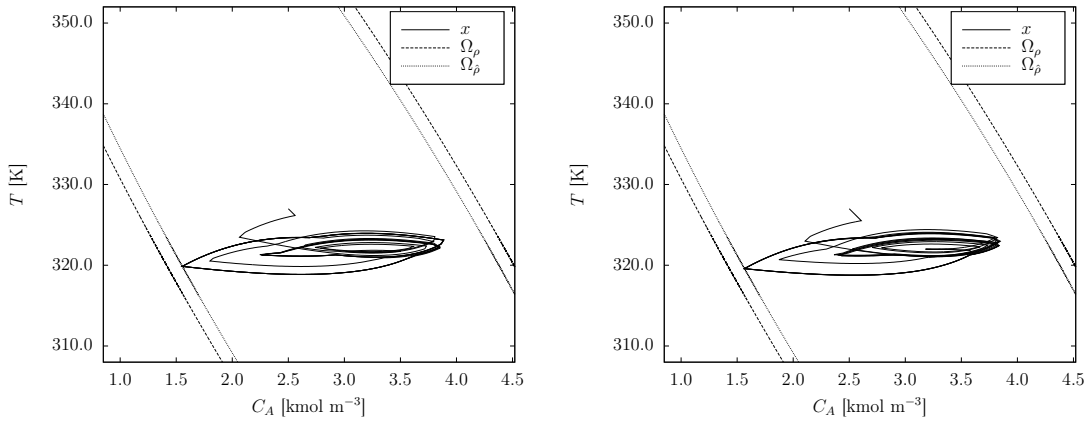

(a) (b)

Figure 6.8: The state-space evolution of the closed-loop CSTR states under LEMPC with (a) $d = 0.05\,\text{h}$ and (b) $d = 0.10\,\text{h}$.

Table 6.3: Closed-loop performance of the CSTR of Eq. 6.32 under the predictor feedback LEMPC relative to the performance at the steady-state.

d	$\bar{L}_e$	Diff. (%)
0	4.668	7.21
0.01	4.675	7.36
0.02	4.682	7.54
0.03	4.690	7.71
0.04	4.697	7.87
0.05	4.703	8.01
0.06	4.710	8.17
0.07	4.705	8.07
0.08	4.722	8.45
0.09	4.728	8.58
0.10	4.733	8.70

The average stage cost index for operation at the steady-state is 4.354. The column "Diff." is the percent difference of the average stage cost index relative to the steady-state stage cost index.

of the previous section, Fig. 6.8 gives the state space evolution of the CSTR with $d = 0.05\,\text{h}$ and $d = 0.10\,\text{h}$, respectively. Comparing the evolution of the two cases shown in Fig. 6.7, fewer differences in the evolution between the two cases are observed compared to the two cases of Fig. 6.3.

The closed-loop performance under the predictor feedback LEMPC is considered with respect to the magnitude of the time-delay. Table 6.3 summarizes the average economic stage cost of Eq. 6.38 of six operating period simulations. Interestingly, the closed-loop performance improves with larger time-delay. The performance improvement is associated with the state delay in the stream recycle (given that the predictor effectively deals with the effect of the input delay on the closed-loop system). In all cases, the closed-loop performance under the predictor feedback LEMPC was at least 7 percent better than that achieved at the steady-state.

6.5 Conclusion

In this chapter, closed-loop stability and performance of systems described by nonlinear DDEs under Lyapunov-based economic model predictive control (LEMPC) was considered. First, conditions such that closed-loop stability for systems with sufficiently small state and input delays under LEMPC, formulated with an ODE model of the system, were derived. A chemical process example demonstrated that indeed closed-loop stability is maintained under LEMPC for sufficiently small time-delays in both the states and the inputs. However, closed-loop performance significantly degraded for larger input delays. This motivated designing a predictor feedback LEMPC methodology. The predictor feedback LEMPC design employs a predictor to compute a prediction of the state after the input delay and an LEMPC scheme, formulated with a DDE model. The predicted state from the predictor is used to initialize the DDE model. The predictor feedback LEMPC was applied to the chemical process example and resulted in better closed-loop stability and performance properties compared to the LEMPC, formulated with an ODE approximation of the nonlinear time-delay system.

Chapter 7

Selection of Control Configurations for Economic Model Predictive Control Systems

7.1 Introduction

Control structure design, i.e., the selection of manipulated, controlled, and measured variables has been the subject of extensive research within the process control community for many years resulting in many methods for input-output loop pairing and control configuration selection, e.g., [131, 177, 113, 173, 186, 154]. For linear systems, an important early result was the relative gain array (RGA) which is commonly used for input-output loop pairing [23], particularly in the context of proportional-integral-derivative (PID) control. Several extensions and variations of the RGA have since been proposed like the extension of the RGA to non-square linear systems, i.e., systems with a different number of inputs than the number of outputs [28] and the various extensions of RGA to nonlinear systems [66, 130]. Two metrics are often used to evaluate conventional control structure

configurations, e.g., control structures consisting of decentralized proportional-integral-derivative control loops: the open-loop and/or closed-loop process economics and controllability analysis [138, 29, 149, 75]. Another potentially important factor in control configuration evaluation may be proper controlled variable (CV) selection. In particular, Skogestad et al.[172] employed and mathematically formalized the concept of *self-optimizing control*, originally proposed by Luyben in 1988 [117], which is a methodology for determining CVs such that when the selected CVs are maintained at their desired set-points, nearly (economically) optimal steady-state operation results with an acceptable loss in the presence of disturbances [172, 12, 43]. Many of the proposed control structure selection methodologies use optimization-based techniques especially mixed-integer optimization problems [149, 75, 102, 163]. One such example is the so-called back-off methodology which consists of solving a mixed-integer optimization program using linearized steady-state process models [75, 102, 151].

Most of the control structure selection methodologies have been developed using linear steady-state or dynamic process models with the assumption that the system is to be operated at steady-state, i.e., the main control objective is to force the system to the desired operating steady-state and maintain operation at this steady-state in the presence of disturbances. Within the context of dynamic operation of nonlinear systems, fewer results and methodologies on control structure selection exist that explicitly consider the process dynamics and nonlinearities. One simple and potentially effective method for evaluating control configurations of multivariable nonlinear systems is to employ a relative degree analysis which may be useful since the relative degree is essentially a measure of the directness of the effect of an input on an output or the physical closeness between an input and an output [35].

In the case of tracking model predictive control (MPC) formulated with a quadratic cost function, i.e., $x^T Q_c x + u^T R_c u$ where Q_c and R_c are positive definite matrices, the weighting

matrices Q_c and R_c are typically tuned such that all the inputs have a direct effect on the cost function. However, for EMPC, not all the possible manipulated inputs must have a direct effect on the economic cost of the EMPC since it is not derived from traditional control objectives. Moreover, since EMPC may dictate a dynamic operating policy, the system may be operated in a larger region of operation, i.e., the effect of nonlinearities in the process may become significant compared to tracking control schemes which force the system to operate in a small neighborhood of the steady-state. Thus, traditional methods that evaluate control structures on the basis of steady-state operation using linear or linearized models may not provide sufficient results within the context of EMPC.

Owing to the aforementioned considerations, a methodology for control configuration selection for EMPC is developed. Treating the economic cost function as the output, a relative degree analysis is completed to determine which inputs have the most direct dynamic effect on the economic cost. The choice of inputs that are controlled by EMPC are the inputs that have a low relative degree with respect to the cost function (typically, one or two). The remaining possible inputs are partitioned to the set of inputs controlled by EMPC and the set of remaining inputs that are not controlled by EMPC on the basis of a sensitivity analysis and a relative degree analysis of any known disturbances. Furthermore, the set of inputs selected for EMPC is ensured to be a stabilizing one. The remaining inputs not controlled by EMPC may be held constant if the control configuration selected has a sufficient degree of robustness or they may be manipulated through other control systems, i.e., outside of EMPC. An evaluation and analysis of the control configuration selection methodology is provided using a chemical process example. The results of this chapter first appeared in [52, 47].

7.1.1 Notation

The notation $L_f h(x)$ denotes the Lie derivative of the scalar field $h(x)$ along the vector field $f(x)$, that is:

$$L_f h(x) = \frac{\partial h(x)}{\partial x} f(x)\,.$$

It is also important to recall the following two types of Lie derivatives:

$$L_g L_f h(x) = \frac{\partial (L_f h)}{\partial x} g(x)\,,$$
$$L_f^k h(x) = L_f \left(L_f^{k-1} h(x) \right) = \frac{\partial (L_f^{k-1} h)}{\partial x} f(x)$$

where $g(x)$ is a vector field.

7.1.2 Class of Nonlinear Systems

The class of input-affine nonlinear systems considered have the following state-space form:

$$\dot{x}(t) = f(x(t)) + \sum_{j=1}^{n_u} g_j(x(t)) u_j(t) + \sum_{i=1}^{n_w} w_i(x(t)) d_i(t) \tag{7.1}$$

where $x \in \mathbb{X} \subset \mathbb{R}^{n_x}$ is the state vector, $u \in \mathbb{U} \subset \mathbb{R}^{n_u}$ is the input vector consisting of all possible manipulated inputs, $\mathbb{U}$ is assumed to be a non-empty compact set, and $d \in \mathbb{W} \subset \mathbb{R}^{n_w}$ is the disturbance vector. The disturbance vectors are bounded in the following sets:

$$\mathbb{W} = \{ d \in \mathbb{R}^{n_w} : |d| \leq w_b \} \tag{7.2}$$

where w_b bounds the norm of the disturbance vector. The vector functions f, g_j for $j = 1, \ldots, n_u$, and w_i for $i = 1, \ldots, n_w$ are sufficiently smooth vector functions on $\mathbb{X}$. The existence of a time-invariant economic cost (scalar) function given by $l_e : \mathbb{X} \times \mathbb{U} \to \mathbb{R}$,

$l_e(x,u) \mapsto l_e(x,u)$, which is a sufficiently smooth function of its arguments, is assumed for the system of Eq. 7.1. For reasons explained below, we assume the economic cost function has the following form:

$$l_e(x,u) = l_{e,x}(x) + l_{e,u}(u)\,. \tag{7.3}$$

This assumption may be relaxed which will be also discussed below. The state vector is assumed to be measured synchronously at sampling times $t_k = t_0 + k\Delta$, $k = 0,1,\ldots$ where t_0 is the initial time and Δ is the sampling period. Within the context of this chapter, any EMPC methods of Chapter 2 may be used.

7.2 Input Selection for Economic Model Predictive Control

In this section, the input selection methodology for EMPC is presented. In the next four subsections, the analysis techniques that are employed in the methodology are described which include: determining the relative degree of the economic cost with respect to the inputs, computing the dynamic sensitivity of the economic cost, computing the steady-state sensitivity of the economic cost, and imposing a stabilizability requirement on the final input selection for EMPC. The last subsection summarizes the input selection methodology.

The next three subsections develop analysis techniques to quantify the sensitivity of the economic cost with respect to inputs. To this end, it is important to point out the differences between EMPC and tracking MPC. Recall, quadratic stage cost functions used in tracking MPC have the form:

$$l_T(x,u) = |x|^2_{Q_c} + |u|^2_{R_c} \tag{7.4}$$

where Q_c and R_c are positive definite weighting matrices and thus, the stage cost function

is sensitive to all the inputs. In other words, the decision variables of a tracking MPC optimization problem have a direct effect on the second quadratic term of the cost function as well as an indirect impact on the first term through the dynamic model. On the other hand, EMPC is formulated with the economic cost function. Since the economic cost function is typically derived from the process economics, it may not be sensitive to all the available inputs.

Several issues may arise when the economic cost is not sensitive to some inputs. First, the optimization problem may be more difficult to solve because, for instance, the optimization problem may be ill-conditioned if an input has little effect, i.e., low sensitivity, on the economic cost function (see, for example, [19] for challenges arising in the context of ill-conditioned optimization problems). Second, the effect of plant-model mismatch may be significant when the economic cost is not as sensitive to an input. For instance, large input changes are needed to influence the cost for inputs with a modeled weak dependence. This makes the optimal solution sensitive to plant-model mismatch (the actual sensitivity of the economic cost with respect to the input may be significantly greater/lower). Third, if an input does not influence the economic cost function much, it may be desirable to decouple this input from the EMPC problem to reduce the computational burden required for solving the optimization problem on-line by either fixing the input to its nominal value or economically optimal steady-state value or by computing its control action through other control systems, e.g., proportional-integral control, or tracking MPC.

7.2.1 Relative Degree of Cost to Inputs

Motivated by the fact that EMPC optimizes the process dynamics with respect to the economic cost which may lead to dynamic operation, one method for carrying out input selection for EMPC is to consider the time evolution of the economic cost along the process

dynamics. Then, select the inputs that have more direct impact on the time evolution of the economic cost. In other words, consider the time derivative of the economic cost function

$$\frac{dl_e}{dt} = \frac{\partial l_{e,x}}{\partial x}\frac{dx}{dt} + \frac{\partial l_{e,u}}{\partial u}\frac{du}{dt} \tag{7.5}$$

where the elements in the term $\partial l_{e,u}/\partial u$ are non-zero for any inputs that explicitly appear in the economic cost. Since the input trajectory is a piecewise constant function, the second term of the right-hand side of Eq. 7.5 is neglected (with this analysis these inputs should be placed on EMPC since they explicitly appear in the economic cost).

The vector field of Eq. 7.1 with $d \equiv 0$ may be substituted into Eq. 7.5 which yields:

$$\frac{\partial l_{e,x}(x)}{\partial x}\left(f(x) + \sum_{j=1}^{n_u} g_j(x)u_j\right) =: L_f l_{e,x} + \sum_{j=1}^{n_u} L_{g_j} l_{e,x}\, u_j(t) \tag{7.6}$$

where $L_f l_{e,x}(x)$ and $L_{g_j} l_{e,x}(x)$ denote the Lie derivatives of $l_{e,x}$ along vector fields $f(x)$ and $g_j(x)$, respectively. If $L_{g_j} l_{e,x}(x) \equiv 0$, the j-th input does not have a direct effect on economic cost (in terms of the first derivative). Due to the coupled nature of the dynamics, the j-th input may still influence the economic cost through higher-order derivatives. Therefore, we define the relative degree or relative order r_j of the economic cost with respect to the j-th input as the smallest positive integer that satisfies:

$$\begin{aligned} &L_{g_j} L_f^{k-1} l_{e,x}(x) \equiv 0,\ k = 1,\ 2,\ \ldots,\ r_j - 1, \\ &L_{g_j} L_f^{r_j-1} l_{e,x}(x) \not\equiv 0 \end{aligned} \tag{7.7}$$

or $r_j = \infty$ if no such integer exists. By convention, the relative degree of the economic cost with respect to any input with $\partial l_{e,u}/\partial u \not\equiv 0$ is zero. Here, the relative degree is similar to standard input-output analysis for nonlinear systems [87, 104, 100] where the economic cost function is treated as an output. It is important to point out that the scalar fields

$l_{e,x}(x), L_f l_{e,x}(x), \ldots, L_f^{r_j-1} l_{e,x}(x)$ are linearly independent [104]. Since $\mathbb{R}^{n_x}$ may only have n_x linearly independent elements, $r_j \leq n_x$ if r_j is finite. Additionally, for disturbances that are explicitly included in the process model, one may be able to compute the relative degree of the economic cost with respect to these disturbances. This may be helpful in the input selection methodology for EMPC (see Section 7.2.5 below).

Since the relative degree is essentially a measure of how fast the input affects the process economics, the relative degree analysis allows for some intuition of how manipulating the j-th input affects the time evolution of the economic cost. This is of particular interest when EMPC dictates a time-varying or dynamic operating policy, i.e., off steady-state operation. Using the relative degree as a basis, a systematic method for selecting the manipulated inputs for which EMPC computes control actions may be developed while explicitly accounting for the dynamics of the system. If the relative degree of the j-th input is large, i.e., the j-th input influences high-order derivatives with respect to each input; perhaps, third-order or higher time derivatives of the economic cost, using EMPC to compute control actions for the j-th input may not be effective with respect to the closed-loop economic performance and/or computationally efficient.

Remark 7.1. It may be possible to consider more general cost functions other than the ones of the assumed form, i.e., $l_e(x,u) = l_{e,x}(x) + l_{e,u}(u)$. In this case, for any inputs where $\partial l_e / \partial u_j$, $j = 1, \ldots, n_u$ is non-zero, i.e., any inputs explicitly appearing in the economic cost function, these inputs have a direct effect on the economic cost. One could still determine the relative degree of the other inputs by taking the inputs appearing in the cost function as fixed parameters to determine the relative degree. It is important to note that one type of cost function that possesses the assumed form is a quadratic cost function. The economic cost functions in the examples considered in this chapter all have the assumed form. Also, the relative degree analysis could be applied to a time-varying cost function, i.e., $l_e(t,x,u) =$

$l_{e,x}(t,x) + l_{e,u}(t,u)$ which is an explicit function of the time when the cost function is a continuous or piecewise continuous function of time by generalizing the definition of Lie derivative to time-varying vector fields.

Connection Between Relative Degree and a Directed Graph

For large-scale process networks, analytical computation of the relative degree may become tedious. However, one may employ the directed graph method for determining the relative degree [99, 35]. This methodology has the advantage that only structural information of the process model is required. In the context of this chapter, the output is considered to be the economic cost. The edges are constructed using the following modified rules based on that of [35] to treat the economic cost as the output:

1. If $\partial f_i(x)/\partial x_k \not\equiv 0$ for $i = 1, \ldots, n_x$ and $k = 1, \ldots, n_x$, then there is an edge from x_k to x_i.

2. If $g_{j,k}(x) \not\equiv 0$ for $k = 1, \ldots, n_x$ and $j = 1, \ldots, n_u$, then there is an edge from u_j to x_k.

3. If $\partial l_e(x,u)/\partial x_i \not\equiv 0$ for $i = 1, \ldots, n_x$, then there is an edge from x_i to l_e.

4. If $\partial l_e(x,u)/\partial u_j \not\equiv 0$ for $j = 1, \ldots, n_u$, then there is an edge from u_j to l_e.

where $f_k(x)$ and $g_{j,k}(x)$ denote the k-th elements of the vector fields $f(x)$ and $g_j(x)$, respectively. If there are known disturbances, the disturbance may be treated as an input in the above directed graph rules.

Utilizing the first main result from [35], a connection between the relative degree as defined in Eq. 7.7 and the directed graph constructed with the rules presented above may be made. Defining the length of the shortest path connecting the j-th input to the economic cost, i.e., the smallest number of edges connecting the j-th input to the economic cost as L_j, the relative degree of the j-th input with respect to the economic cost is $r_j = L_j - 1$. It

is important to point out that this works for many cases. However, there are cases where this does not work like cases where there are potential cancellations (see [35] for more details on this point). This gives a rather intuitive understanding of how the inputs affect the economic cost. Furthermore, it requires only limited structural understanding of the process dynamics, i.e., not detailed process models, during the input selection phase of the control structure design. For instance, consider the following example.

Example 7.1. Consider the following input-affine nonlinear system:

$$\begin{aligned} \dot{x}_1 &= f_1(x_2,x_3) + g_{1,1}(x)u_1 \\ \dot{x}_2 &= f_2(x_1,x_2) \\ \dot{x}_3 &= f_3(x_1,x_3) + g_{2,3}(x)u_2 \end{aligned} \tag{7.8}$$

where the vector fields are $f^T(x) = [f_1(x_2,x_3)\ f_2(x_1,x_2)\ f_3(x_1,x_3)]$, $g_1^T(x) = [g_{1,1}(x)\ 0\ 0]$ and $g_2^T(x) = [0\ 0\ g_{2,3}(x)]$ and the economic cost function has the following form:

$$l_e(x,u) := \hat{l}_{e,x}(x_2) + \hat{l}_{e,u}(u_2) \tag{7.9}$$

The relative degree of the economic cost with respect to u_2 is defined to be 0 since the economic cost is an explicit function of this input. For the input u_1, the Lie derivative of $l_e(x,u)$ along the vector field $g_1(x)$ is

$$L_{g_1} l_e = \frac{\partial l_e}{\partial x} g_1(x) \equiv 0 \tag{7.10}$$

Since the first Lie derivative is zero, higher order Lie derivatives are computed. The next Lie derivative is:

$$L_{g_1} L_f l_e = \frac{\partial}{\partial x_1}\left[\frac{\partial l_e}{\partial x_2} f_2(x_1,x_2)\right] g_{11}(x) \not\equiv 0 \tag{7.11}$$

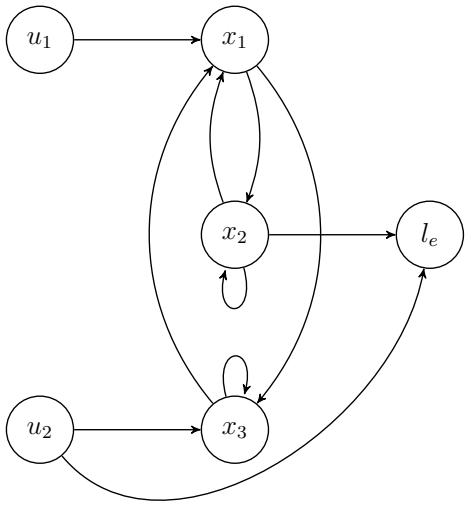

Figure 7.1: Directed graph representing the system of Eq. 7.8.

From this analysis, the relative degree of the economic cost function with respect to the input u_1 is 2.

Applying the construction rules for the nodes and edges, the directed graph for the system of Eq. 7.8 is displayed in Fig. 7.1. From the directed graph, one may easily determine the relative degree. The shortest path between the input u_1 and the economic cost is 3. Therefore, the relative degree of the economic cost with respect to u_1 is 2. Similarly, the shortest path from the input u_2 to the economic cost is 1, so, the relative degree is 0. The relative degrees computed from the directed graph agree with the ones computed analytically.

7.2.2 Dynamic Sensitivity of the Economic Cost

While the relative degree is a readily computable metric that quantifies the directness of the effect of an input on the economic cost, it is unable to capture the magnitude of the interaction between an input and the economic cost [35]. One cannot distinguish the degree

of the sensitivity of the economic cost with respect to inputs of the same relative degree. In linear systems, the steady-state gain on the economic cost with respect to an input is one metric that captures such a sensitivity. However, the steady-state gain is state-dependent for nonlinear systems in general. Therefore, in this subsection, an analysis technique to quantify the dynamic sensitivity of the economic cost with respect to an input is developed.

For dynamic sensitivity analysis, we consider the inputs with the same relative degree. Let $\hat{u} \in \mathbb{R}^{n_r}$ be a vector containing all inputs with relative degree r. The inputs with relative degree not equal to r are taken as constants in this analysis set to their economically optimal value and are incorporated in the $f(x)$ term of the model of Eq. 7.1. To avoid potential scaling differences of inputs which may potentially skew the sensitivity analysis, all inputs contained in the vector $\hat{u}$ are scaled so that $\hat{u}_j \in [-1,1]$ for $j = 1,\ \ldots,\ n_r$. The auxiliary scalar output variable $y(t)$ is defined as the state-dependent part of the economic cost $y(t) = l_{e,x}(x(t))$. Consider a Taylor series expansion of $y(t)$ at a time t^*:

$$y(t) = \sum_{k=0}^{\infty} \frac{(t-t^*)^k}{k!} \frac{d^k y(t^*)}{dt^k} \tag{7.12}$$

The k-th derivative of y for $k = 0,\ 1,\ \ldots,\ r-1$ is:

$$\frac{d^k y(t^*)}{dt^k} = L_f^k l_{e,x}(x(t^*)) \tag{7.13}$$

and the r-th derivative of y is:

$$\frac{d^r y(t^*)}{dt^r} = L_f^r l_{e,x}(x(t^*)) + \sum_{j=1}^{n_r} L_{g_j} L_f^{r-1} l_{e,x}(x(t^*))\hat{u}_j(t^*) \tag{7.14}$$

Thus, the Taylor series expansion may be written as:

$$y(t) = \sum_{k=0}^{r} \frac{(t-t^*)^k}{k!} L_f^k l_{e,x}(x(t^*)) + \frac{(t-t^*)^r}{r!} \sum_{j=1}^{n_r} L_{g_j} L_f^{r-1} l_{e,x}(x(t^*)) \hat{u}_j(t^*) + \sum_{k=r+1}^{\infty} \frac{d^k y(t^*)}{dt^k} \frac{(t-t^*)^k}{k!} \,. \tag{7.15}$$

The high-order ($r+1$ order and higher) derivatives of y are neglected to obtain an approximation of $y(t)$:

$$y(t) \approx \sum_{k=0}^{r} \frac{(t-t^*)^k}{k!} L_f^k l_{e,x}(x(t^*)) + \frac{(t-t^*)^r}{r!} \sum_{j=1}^{n_r} L_{g_j} L_f^{r-1} l_{e,x}(x(t^*)) \hat{u}_j(t^*) \,. \tag{7.16}$$

Consider the difference of the output $\Delta y(t) = y_1(t) - y_2(t)$ with respect to a change

$$\Delta \hat{u}_j(t^*) = \hat{u}_{j,1}(t^*) - \hat{u}_{j,2}(t^*)$$

and all other inputs constant. From Eq. 7.16, the following may be derived:

$$\left. \frac{\Delta y}{\Delta u_j} \right|_{\Delta u_k, k \neq j} = \frac{(t-t^*)^r}{r!} L_{g_j} L_f^{r-1} l_{e,x}(x(t^*)) \tag{7.17}$$

Therefore, the n_r-dimensional vector S_r is defined with elements:

$$S_{r,j} := L_{g_j} L_f^{r-1} l_{e,x}(x(t^*)) \tag{7.18}$$

for $j = 1, \ \ldots, \ n_r$. The vector S_r contains elements that essentially quantify the dynamic sensitivity of inputs with the same relative degree on the economic cost. To use the sensi-

tivities in a comparison, they are normalized with respect to the Euclidean norm:

$$\bar{S}_{r,j} := \frac{S_{r,j}^2}{|S_r|^2} = \frac{S_{r,j}^2}{\left(\sum_{j=1}^{n_r} S_{r,j}^2\right)} \tag{7.19}$$

and $\bar{S}_{r,j} \in [0,1]$. The economic cost is more sensitive to inputs whose corresponding $\bar{S}_{r,j}$ values are close to one compared to inputs with corresponding $\bar{S}_{r,j}$ values close to zero. Thus, the dynamic sensitivity analysis ranks inputs with the same relative degree on the basis of their dynamic sensitivities. Also, $\bar{S}_{r,j}$ may be computed for various points in state-space to capture the dynamic sensitivities, i.e., sensitivity of the economic cost with respect to inputs for states off steady-state.

Example 7.2. Consider a non-isothermal CSTR where an elementary second-order reaction of the form $A \rightarrow B$ occurs. The states of the CSTR are the reactor temperature x_1 and the concentration of A in the reactor which is denoted as x_2, i.e., the state vector is $x^T = [x_1 \; x_2]$. The evolution of the CSTR system is described by the following ordinary differential equations in dimensionless form:

$$\frac{dx_1}{d\tau} = x_{10} - x_1 - \beta_1 e^{-1/x_1} x_2^2 + \beta_2 + \beta_3 u_1 \tag{7.20a}$$

$$\frac{dx_2}{d\tau} = -x_2 - \beta_4 e^{-1/x_1} x_2^2 + \beta_5 + u_2 \tag{7.20b}$$

where the process parameters are $\beta_1 = -1.73 \times 10^5$, $\beta_2 = 1.44 \times 10^{-3}$, $\beta_3 = 1.44 \times 10^{-3}$, $\beta_4 = 5.92 \times 10^6$, and $\beta_5 = 1.14$. The CSTR has two candidate inputs: the heat rate u_1 supplied to the reactor and the inlet concentration of species A to the reactor u_2. Both inputs have been scaled so that $u_j \in [-1,1]$ for $j = 1,\ 2$. The production rate of B corresponds to the dominant factor in the operating profit of the CSTR. Thus, the economic cost function is:

$$l_e(x,u) = e^{-1/x_1} x_2^2 \tag{7.21}$$

The relative degree of the economic cost with respect to both inputs is 1, so the relative degree analysis would not be able to discriminate between the importance of controlling each of the inputs with EMPC. The Lie derivatives of $l_{e,x}(x) = l_e(x,u)$ with respect to the vector fields $g_1(x) = [\beta_3\ 0]^T$ and $g_2(x) = [0\ 1]^T$ are

$$L_{g_1} l_{e,x}(x) = \frac{\beta_3}{x_1^2} e^{-1/x_1} x_2^2, \tag{7.22}$$

$$L_{g_2} l_{e,x}(x) = 2e^{-1/x_1} x_2 . \tag{7.23}$$

From the Lie derivatives, the dynamic sensitivities may be computed. For simplicity of presentation, the Lie derivatives are evaluated at the economically optimal steady-state $x_{1s}^* = 0.08$ and $x_{2s}^* = 0.21$ and the normalized dynamic sensitivity vector for the inputs with relative degree 1 is

$$\bar{S}_1 = [0.0\ 1.0] . \tag{7.24}$$

This analysis suggests that the input u_2 has a more substantial dynamic effect compared to the input u_1. In terms of input selection for EMPC, it would be more desirable in terms of the dynamic sensitivity analysis to control the input u_2 compared to the input u_1. In fact, it has been demonstrated that periodic switching of the inlet concentration achieves greater production rates compared to a constant inlet concentration equal to the time-average inlet concentration of the periodic switching policy (Section 3.3.2). Since the reaction rate is concave with respect to the temperature, the maximum production rate is achieved by supplying the maximum allowable heat rate to the reactor, i.e., little benefit with respect to the economic cost is achieved when the heat rate is controlled by EMPC under nominal operation.

7.2.3 Steady-state Sensitivities of the Economic Cost

From the dynamic sensitivity analysis, the inputs with the same relative degree may be ranked on the basis of the dynamic sensitivity of the economic cost. However, this ranking is made with respect to other inputs with the same relative degree, i.e., the dynamic sensitivity vector $\bar{S}_r$ is normalized with the sensitivity of the other inputs. Therefore, a procedure is needed to identify if the interaction between an input and the economic cost is significant with respect to all the other inputs. To accomplish this, a steady-state sensitivity is employed.

The input vector is scaled so that $u_j \in [-1,1]$ for $j = 1, \ \ldots, \ n_u$ to remove any scaling differences between the inputs. A steady-state of the system of Eq. 7.1, which is denoted as x_s, with its corresponding steady-state input, which is denoted as u_s, satisfies the following algebraic equation:

$$f(x_s) + \sum_{j=1}^{n_u} g_j(x_s) u_{s,j} = 0 \ . \tag{7.25}$$

For a given steady-state input, the corresponding steady-state may be computed, and thus, we may write: $x_s = \bar{f}(u_s)$ where $\bar{f} : \mathbb{U} \to \mathbb{X}$ maps a given steady-state input to a corresponding steady-state. With $x_s = \bar{f}(u_s)$, the state dependence on the steady-state economic cost may be removed: $l_e(x_s, u_s) = l_e(\bar{f}(u_s), u_s) \equiv \bar{l}_e(u_s)$. The steady-state sensitivity on the economic cost to the j-th input is determined numerically by:

$$\begin{aligned} \frac{\partial \bar{l}_e}{\partial u_{s,j}} \approx \frac{1}{2\delta} \big[& (\bar{l}_e(u_{s,1}, \ldots, u_{s,j-1}, u_{s,j} + \delta, u_{s,j+1}, \ldots, u_{s,n_u}) \\ & - \bar{l}_e(u_{s,1}, \ldots, u_{s,j-1}, u_{s,j} - \delta, u_{s,j+1}, \ldots, u_{s,n_u}) \big] \end{aligned} \tag{7.26}$$

where $\delta > 0$ is a small perturbation term. Similar to the dynamic sensitivity analysis, the

steady-state sensitivity is normalized with respect to the other inputs:

$$\hat{S}_j = \left(\frac{\partial \bar{l}_e}{\partial u_{s,j}}\right)^2 \Bigg/ \left|\frac{\partial \bar{l}_e}{\partial u_s}\right|^2 = \left(\frac{\partial \bar{l}_e}{\partial u_{s,j}}\right)^2 \left(\sum_{j=1}^{n_u} \left(\frac{\partial \bar{l}_e}{\partial u_{s,j}}\right)^2\right)^{-1} \tag{7.27}$$

where $\hat{S}_j$ will be approximately one for any inputs with a large steady-state sensitivity on the economic cost and will be approximately zero for any inputs with a small steady-state sensitivity on the economic cost.

7.2.4 Stabilizability of Control Configurations

The aforementioned analysis techniques identify the inputs that influence the economic cost function, but they do not explicitly consider control considerations like controllability and stabilizability. Before a final input selection for EMPC may be made, a verification of such control considerations must be completed. Below, one stabilizability assumption is given which is verifiable for nonlinear systems of the form of Eq. 7.1. If this assumption is satisfied, a specific formulation of EMPC may be applied to the closed-loop system of Eq. 7.1 and the closed-loop system will have guaranteed stability properties. Other EMPC formulations that require other types of controllability/stabilizability assumptions, e.g., weak controllability, could be used instead of the assumption and the EMPC formulation provided below.

Lyapunov-based EMPC

Without loss of generality, the origin of the system of Eq. 7.1 is assumed to be the steady-state of the unforced system, i.e., $f(0) = 0$ with $u \equiv 0$ and $d \equiv 0$. The following assumption is placed on the system of Eq. 7.1 which is essentially a stabilizability assumption for nonlinear systems.

Assumption 7.1 (Existence of a Lyapunov-based Controller)**.** *There exists a Lyapunov-based controller $u = k(x) \in \mathbb{U}$ that renders the origin of the nominal closed-loop system of Eq. 7.1 under $k(x)$ asymptotically stable. This implies that there exists a continuously differentiable Lyapunov function $V(x)$ [115, 100] such that the following holds:*

$$\alpha_1(|x|) \leq V(x) \leq \alpha_2(|x|) \tag{7.28a}$$

$$\frac{\partial V(x)}{\partial x}\left(f(x) + \sum_{j=0}^{n_u} g_j(x)k(x)\right) \leq -\alpha_3(|x|) \tag{7.28b}$$

$$\left|\frac{\partial V(x)}{\partial x}\right| \leq \alpha_4(|x|) \tag{7.28c}$$

for $x \in D$ where D is an open neighborhood of the origin where the functions $\alpha_i : [0,a) \rightarrow [0,\infty)$, $i = 1,\ 2,\ 3,\ 4$ are class $\mathcal{K}$ functions.

It is important to point out that in Assumption 7.1 the controller $k(x)$ is implemented in a continuous fashion. However, when the controller $k(x)$ is implemented in a sample-and-hold fashion with a sufficiently small sampling period, the origin of the closed-loop system is rendered practically stable. The stability region under the Lyapunov-based controller is defined as $\Omega_\rho \subset D$ and $\Omega_\rho \subseteq \mathbb{X}$ which is a level set of $V(x)$ where the time-derivative of the Lyapunov function is negative.

Taking advantage of the explicit Lyapunov-based controller and its corresponding stability region Ω_ρ, the Lyapunov-based economic model predictive control (LEMPC) scheme

is characterized by the following optimization problem:

$$\min_{u\in S(\Delta)} \quad \int_{t_k}^{t_{k+N}} l_e(\tilde{x}(\tau),u(\tau))\,d\tau \tag{7.29a}$$

$$\text{s.t.} \quad \dot{\tilde{x}}(t) = f(\tilde{x}(t)) + \sum_{j=0}^{n_u} g_j(\tilde{x}(t))u_j(t) \tag{7.29b}$$

$$\tilde{x}(t_k) = x(t_k) \tag{7.29c}$$

$$u(t) \in \mathbb{U},\ \forall\, t \in [t_k, t_{k+N}) \tag{7.29d}$$

$$V(\tilde{x}(t)) \leq \rho_e,\ \forall\, t \in [t_k, t_{k+N})$$

$$\text{if } V(x(t_k)) \leq \rho_e \tag{7.29e}$$

$$\frac{\partial V(x(t_k))}{\partial x}\left(f(x(t_k)) + \sum_{j=0}^{n_u} g_j(x(t_k))u_j(t_k)\right)$$

$$\leq \frac{\partial V(x(t_k))}{\partial x}\left(f(x(t_k)) + \sum_{j=0}^{n_u} g_j(x(t_k))k_j(x(t_k))\right),$$

$$\text{if } V(x(t_k)) > \rho_e \tag{7.29f}$$

where the LEMPC is a two-mode control strategy with the two modes defined by the Lyapunov-based constraints of Eqs. 7.29e-7.29f.

The design procedure of LEMPC is as follows: (1) an explicit stabilizing controller $k(x)$ is designed for the system of Eq. 7.1, (2) a Lyapunov function is derived for the closed-loop system under the controller $k(x)$, and (3) the stability region Ω_ρ of the closed-loop system is estimated by taking it to be the (largest) level set of the Lyapunov function such that the time-derivative of the Lyapunov function along the closed-loop state trajectory is negative. For more details on LEMPC, please refer to Chapter 3.

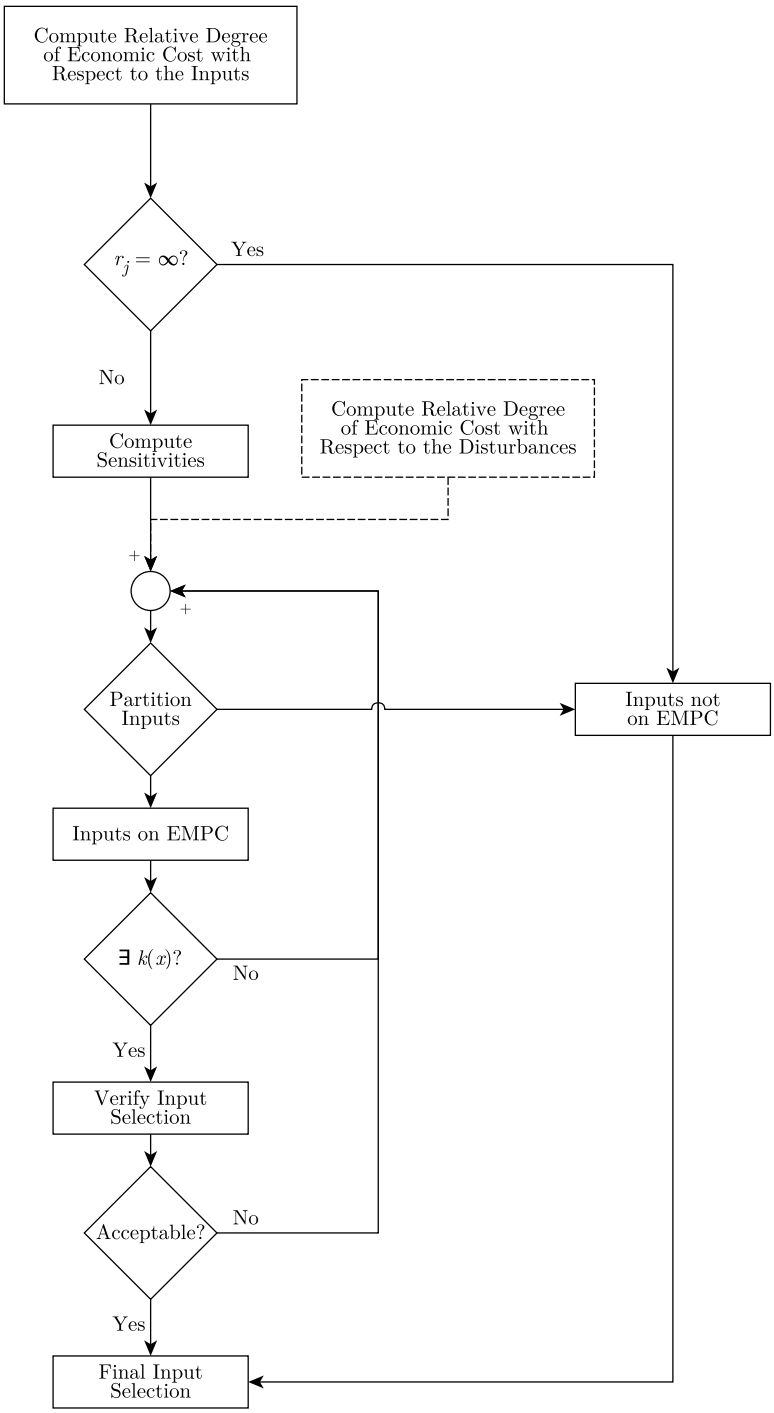

Figure 7.2: A flowchart of the input selection for EMPC methodology. Solid lines are used to represent necessary steps and dashed lines are used to represent optional steps.

7.2.5 Input Selection Methodology

The description of the input selection methodology is given in this subsection which is summarized by the flow chart of Fig. 7.2. All the possible manipulated inputs to the system of Eq. 7.1 are candidate manipulated inputs whose control action may be computed by EMPC. For the remainder of this section, an input on EMPC will refer to an input whose control action is computed by EMPC and an input not on EMPC will refer to an input that is fixed or whose control action is computed through another controller. For the latter case, explicit design of an integrated EMPC with another controller to compute control actions for the inputs not on EMPC is beyond the scope of this chapter and thus, only the case where the inputs not on EMPC are fixed to a constant value will be considered in the example presented in Section 7.3.

The input selection methodology for EMPC is as follows (Fig. 7.2): the relative degree of the economic cost with respect to each candidate input is computed. Any input with an infinite overall relative degree should not be placed on EMPC as these inputs have no influence on the process economics. These inputs may be set to any arbitrary value without adversely affecting the closed-loop economic performance. For the remaining inputs, the inputs with a low relative degree should be on EMPC. Typically, inputs with relative degree 2 or less should be placed on EMPC unless identified otherwise through the sensitivity analysis. When the economic cost function is associated with the outlet product stream of a process network, e.g., the economic cost is the amount of desired product leaving the process, it may be necessary to include more inputs with relative degree greater than 2 owing to closed-loop performance, stability and robustness considerations.

Several factors may influence the decision on which of the remaining inputs, i.e., inputs with relative degree three or higher, should be on EMPC and to confirm that inputs with relative degree two or lower should be on EMPC. First, the dynamic sensitivities are

computed for inputs of the same relative degree which creates a ranking of inputs with the same relative degree on the basis of the dynamic sensitivity of the economic cost. Second, the steady-state sensitivities are computed. If $\bar{S}_{r,j}$ and $\hat{S}_j$ are close to one, the input should be placed on EMPC since it has both a dynamic and a steady-state impact on the economic cost. If $\bar{S}_{r,j}$ and $\hat{S}_j$ are close to zero, the input should not be placed on EMPC since the economic cost is not sensitive with respect to this input. For inputs with $\bar{S}_{r,j}$ close to one and $\hat{S}_j$ close to zero or vice versa, the decision to control these inputs with EMPC should be made on the basis of the remaining two criteria, i.e., relative degree of the economic cost with respect to the disturbances and the stabilizability requirement. It may be desirable from a disturbance rejection standpoint to pick additional inputs that have a smaller relative degree with respect to the cost than the known disturbances. Inputs with $\bar{S}_{r,j}$ close to one and with a low relative degree compared to the disturbances may be chosen to be placed on EMPC. The dynamic sensitivity $\bar{S}_{r,j}$ is used because it quantifies the dynamic sensitivity and EMPC dictates a dynamic operating policy in general to optimize the process economics.

All the aforementioned factors contribute in partitioning the set of inputs controlled by EMPC and the set of inputs not controlled by EMPC. One must try to find a stabilizing Lyapunov-based controller $k(x)$ with the inputs that will be placed on EMPC. This is a verification step to ensure the selected inputs are able to achieve the stabilizability requirement. If no such controller exists, i.e., it is difficult to find such a controller, then the inputs are repartitioned to include more inputs that will be on EMPC. For this step, the additional inputs to be placed on EMPC should be inputs with the lowest relative degree and highest sensitivity. Once a stabilizing controller is constructed for a certain set of inputs that will be on EMPC, an LEMPC may be formulated for the system and a final verification step is completed. In the final verification step, extensive closed-loop simulations are completed to ensure that the LEMPC scheme has desirable closed-loop properties, e.g., performance, stability, and robustness.

It may be beneficial to use more available inputs as manipulated inputs in the final EMPC control configuration than what is determined from the input selection methodology to increase the overall robustness of the control structure to the effects of disturbances and uncertainty. Two strategies to include more manipulated inputs are: (1) to modify the economic cost, i.e., add quadratic terms, so that these inputs have a more direct effect on the cost function used in the EMPC or (2) to use another controller to compute control actions for the added manipulated inputs instead of setting them to a fixed value, e.g., proportional-integral control may be used to compute the control actions for these inputs. In fact, the former strategy has already been utilized in many EMPC case studies [86, 6, 50].

Remark 7.2. If there is some flexibility in the choice of economic cost and the sources of the significant disturbances are known, i.e., how the disturbance enters into the process model of Eq. 7.1 is known, one may determine the relative degree of the candidate economic cost functions with respect to the disturbances. The economic cost that should be used is the one where the disturbances have a high relative degree compared to the selected manipulated inputs, i.e., the disturbances will have a weaker dynamic effect on the economic cost.

Remark 7.3. The potential limitations of the methodology for control structure selection for EMPC are: (1) there is no guarantee that there will be a discrete dichotomy between the relative degree of the economic cost and the sensitivities of economic cost with respect to the inputs. For instance, the relative degree analysis may not result in two distinct sets of inputs: one containing the inputs with a low relative degree and another containing the inputs with high relative degree and similarly for the sensitivity analysis. This may make picking the EMPC inputs solely on the basis of these tools difficult. Since the methodology provides tools to identify which inputs to control with EMPC, (2) the final control structure configuration decision is ultimately left to the control engineer (as is the case in many control configuration selection methodologies). Therefore, there is no guarantee that the

Table 7.1: Process parameters of the reactor-reactor process.

Notation	Value	Description
T_{10}	300.0 K	CSTR-1 Inlet Temp.
T_{20}	300.0 K	CSTR-2 Inlet Temp.
F_{10}	$5.0\,\mathrm{m^3\,h^{-1}}$	CSTR-1 Inlet Flow Rate
F_{20}	$5.0\,\mathrm{m^3\,h^{-1}}$	CSTR-2 Inlet Flow Rate
V_1	$1.5\,\mathrm{m^3}$	CSTR-1 Volume
V_2	$1.0\,\mathrm{m^3}$	CSTR-2 Volume
k_0	$3.0 \times 10^4\,\mathrm{m^3\,kmol^{-1}\,h^{-1}}$	Pre-exponential Factor
E	$3.0 \times 10^4\,\mathrm{kJ\,kmol^{-1}}$	Activation Energy
ΔH	$-5.0 \times 10^3\,\mathrm{kJ\,kmol^{-1}}$	Heat of Reaction
C_p	$0.231\,\mathrm{kJ\,kg^{-1}\,K^{-1}}$	Heat Capacity
R	$8.314\,\mathrm{kJ\,kmol^{-1}\,K^{-1}}$	Gas Constant
ρ_L	$1000\,\mathrm{kg\,m^{-3}}$	Density

optimal input selection will be selected. However, given the possible uncertainty involved with input selection, it may not be possible to determine the optimal input selection. Lastly, (3) closed-loop simulations may be particularly important to select the final input selection from many candidate control configurations. For large-scale systems with many candidate inputs, many simulations may need to be completed to make the final input selection decision given the combinatorial nature of the number of possible control configurations.

7.3 EMPC Input Selection for a Chemical Process Example

In this section, the input selection methodology for EMPC is applied to a chemical process example. Various closed-loop simulation results and analyses are provided to demonstrate the method. The specific example has been chosen since it is manageable to consider all possible combinations of input pairs, while being of sufficient complexity to demonstrate the input selection methodology.

Consider a chemical process example consisting of two continuous stirred tank reactors

(CSTRs) in series. In each of the reactors a second-order, exothermic reaction of the form $A \rightarrow B$ occurs where A is the reactant material and B is the desired product. Each of the two reactors are fed with fresh reactant material with concentration C_{Aj0} and flow rate F_{j0}, $j = 1,\ 2$ where $j = 1$ denotes the first CSTR and $j = 2$ denotes the second CSTR. To provide heat to the reactor contents, each of the reactors has a heating jacket. The contents of each of the CSTRs have a uniform temperature T_j, concentration of the reactant C_{Aj}, and concentration of the product C_{Bj} for $j = 1,\ 2$. Under standard modeling assumptions, the following set of differential equations describing the evolution of the reactor state variables may be derived from first principles modeling techniques:

$$\frac{dT_1}{dt} = \frac{F_{10}}{V_1}(T_{10} - T_1) - \frac{\Delta H k_0}{\rho C_p} e^{-E/RT_1} C_{A1}^2 + \frac{Q_1}{\rho C_p V_1} \tag{7.30a}$$

$$\frac{dC_{A1}}{dt} = \frac{F_{10}}{V_1}(C_{A10} - C_{A1}) - k_0 e^{-E/RT_1} C_{A1}^2 \tag{7.30b}$$

$$\frac{dC_{B1}}{dt} = -\frac{F_{10}}{V_1} C_{B1} + k_0 e^{-E/RT_1} C_{A1}^2 \tag{7.30c}$$

$$\frac{dT_2}{dt} = \frac{F_{20}}{V_2} T_{20} + \frac{F_{10}}{V_2} T_1 - \frac{(F_{10} + F_{20})}{V_2} T_2 - \frac{\Delta H k_0}{\rho C_p} e^{-E/RT_2} C_{A2}^2 + \frac{Q_2}{\rho C_p V_2} \tag{7.30d}$$

$$\frac{dC_{A2}}{dt} = \frac{F_{20}}{V_2} C_{A20} + \frac{F_{10}}{V_2} C_{A1} - \frac{(F_{10} + F_{20})}{V_2} C_{A2} - k_0 e^{-E/RT_2} C_{A2}^2 \tag{7.30e}$$

$$\frac{dC_{B2}}{dt} = \frac{F_{10}}{V_2} C_{B1} - \frac{(F_{10} + F_{20})}{V_2} C_{B2} + k_0 e^{-E/RT_2} C_{A2}^2 \tag{7.30f}$$

where the process parameters are given in Table 7.1. The possible inputs to the process are the heat rates supplied to the reactors Q_1 and Q_2 and the inlet concentrations of the reactant material C_{A10} and C_{A20}. The available control action is bounded in the following set: $Q_j \in [0.0,\ 100.0]\,\mathrm{MJ\,h^{-1}}$, $j = 1,\ 2$ and $C_{Aj0} \in [0.5,\ 7.5]\,\mathrm{kmol\,m^{-3}}$, $j = 1,\ 2$.

The operating profit of the process is considered to be proportional to the product molar

flow rate out of the second reactor. Therefore, the economic cost is:

$$l_e(x,u) = (F_{10} + F_{20})C_{B2} \tag{7.31}$$

where $F_{10} + F_{20}$ is the outlet volumetric flow rate of the second CSTR and C_{B2} is the concentration of the product in the second CSTR. An economics-based constraint is imposed which limits the amount of reactant that may be fed to each reactor:

$$\frac{1}{t_f}\int_0^{t_f} F_{j0}C_{Aj0}\,dt = \dot{M}_{Aj0,\text{avg}} \tag{7.32}$$

for $j = 1, 2$ where $\dot{M}_{Aj0,\text{avg}} = 20\,\text{kmol}\,\text{h}^{-1}$. The average constraint of Eq. 7.32 is enforced over operating windows of length 0.55 h which has been determined through simulations as the operating window length that leads to improved asymptotic performance of the closed-loop system under EMPC compared to steady-state operation (refer to Section 3.3.2 for the details for implementing the average constraint over a finite-length operating window). The economically optimal steady-state with respect to the cost of Eq. 7.31 and the constraint of Eq. 7.32 corresponds to the economically optimal steady-state input of $Q_1^* = Q_2^* = 100\,\text{MJ}\,\text{h}^{-1}$ and $C_{A10}^* = C_{A20}^* = 4.0\,\text{kmol}\,\text{m}^{-3}$ and is open-loop (locally) asymptotically stable.

Remark 7.4. The fact that the economically optimal steady-state is open-loop asymptotically stable implies that there exists a control Lyapunov function (CLF), i.e., there exists a smooth positive-definite function $V(x)$ that satisfies $L_f V < 0$ for all states in some neighborhood of the origin when $L_{g_i} V \equiv 0$ for all $i = 1, \ldots, n_u$, see, for example, [33] for more discussion of this point. Furthermore, there exists a stabilizing controller which satisfies the conditions of Eq. 7.28a-7.28c. Thus, an explicit characterization of the stabilizing controller for each of the simulated control structure configurations is not given. Also, it is

important to point out the EMPC is able to maintain operation in a bounded region around the economically optimal steady-state (verified by extensive simulations). Although the optimal steady-state is open-loop asymptotically stable, the main objective of applying feedback control is to maintain robustness of the operation and to optimize the process economics in a manner that cannot be achieved through open-loop operation.

The purpose of applying EMPC to the process is to maximize the economic cost function of Eq. 7.31 through dynamic (off steady-state) operation of the process. First, we demonstrate that dynamic operation of the process with the cost function of Eq. 2.5a and constraint of Eq. 7.32 is better than operation at the economically optimal steady-state. In this set of simulations, control actions for all possible inputs are computed by EMPC. We apply the EMPC with the following formulation to the process:

$$\begin{aligned}
\max_{u\in S(\Delta)} \quad & \int_{t_k}^{t_{k+N}} l_e(\tilde{x}(\tau),u(\tau))\,d\tau \\
\text{s.t.} \quad & \dot{\tilde{x}}(t) = f(\tilde{x}(t)) + \sum_{j=1}^{4} g_j(\tilde{x}(t))u_j(t) \\
& \tilde{x}(t_k) = x(t_k) \\
& u(t) \in \mathbb{U},\ \forall\, t \in [t_k, t_{k+N}) \\
& \frac{1}{\tau_M}\int_0^{\tau_M} F_{j0}C_{Aj0}\,dt = \dot{M}_{Aj0,\text{avg}},\ j=1,2
\end{aligned} \tag{7.33}$$

where the dynamic model is that of Eq. 7.30, the prediction horizon is $N = 5$, the sampling period is $\Delta = 0.05\,\text{h}$ and the number of sampling periods in the operating window that the average constraint is enforced is $M = 11$, i.e., $\tau_M = 0.55\,\text{h}$. To numerically integrate the dynamic model, explicit Euler method is employed with an integration time step of $1.0\times10^{-3}\,\text{h}$. Ipopt [187] was used to solve the nonlinear optimization problem of Eq. 7.33. All simulations below were completed on a desktop PC with an Intel Core® 2 Duo™ processor running an Ubuntu operating system.

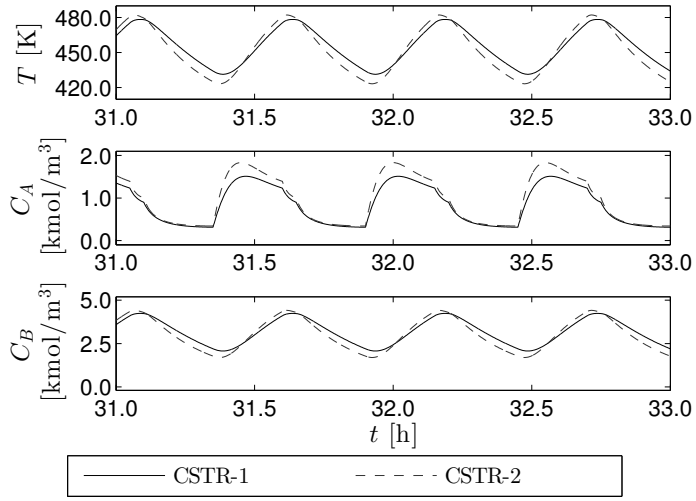

Figure 7.3: The closed-loop state trajectories under the EMPC of Eq. 7.33.

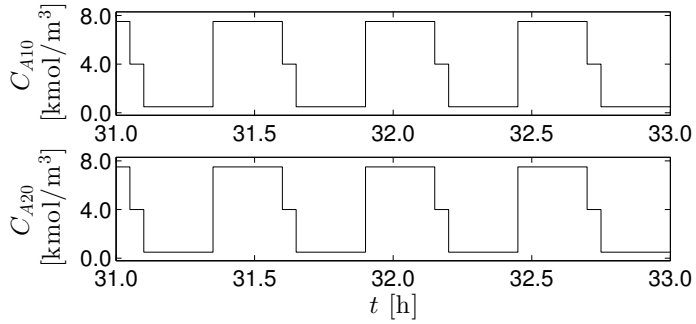

Figure 7.4: The manipulated input trajectories under the EMPC of Eq. 7.33.
The input trajectories $Q_1(t)$ and $Q_2(t)$ are not shown because they are constant profiles with $Q_i(t) = 100\,\mathrm{MJ\,h^{-1}}$, $i = 1,2$ for all $t \geq 0$ over the entire 33.0 hour length of operation.

The EMPC of Eq. 7.33 is applied to the chemical process of Eq. 7.30. The chemical process is initialized at a transient initial condition, i.e., off steady-state initial condition, and a length of operation of 33.0 h was simulated. The closed-loop state and input trajectories over the time period 31.0 h to 33.0 h are shown in Figs. 7.3-7.4 to illustrate the asymptotic operating behavior of the process under EMPC. The EMPC dictates a dynamic operation policy (Figs. 7.3-7.4) through continuous manipulation of the inlet reactant concentration. However, for the heat rate inputs, the EMPC computes a constant input profile which corresponds to 100 MJ h^{-1}, i.e., the maximum allowable heat rate. The reason for this behavior is that the reaction rate is maximized at large temperature and thus, the molar flow rate of the desired product leaving the process is the largest when the maximum amount of heat is provided to the reactors. To show that the operating policy is economically better than steady-state operation, the average economic cost is defined as:

$$\bar{J}_e = \frac{1}{t_f} \int_0^{t_f} l_e(x(t), u(t))\, dt\,. \tag{7.34}$$

For the process of Eq. 7.30 under EMPC, the asymptotic performance, i.e., the average economic cost after a sufficiently long operating time such that the effect of the initial condition becomes negligible, is 29.98. The economically optimal steady-state has an (average) economic cost of 28.21. Thus, asymptotic operation under EMPC is 6.27% better than steady-state operation.

Since there is a benefit in terms of the economic cost to operate the chemical process of Eq. 7.30 under EMPC, input selection for EMPC is considered. First, the input selection methodology (Fig. 7.2) is applied to the chemical process example. Subsequently, closed-loop simulation results are provided to confirm this is the proper choice of input selection for EMPC. Two sets of simulations are considered. In the first set of simulations, all the possible 16 combinations of input selections for EMPC are simulated under nominal

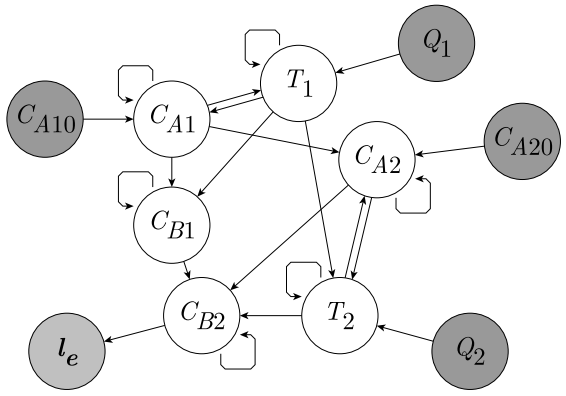

Figure 7.5: A directed graph constructed for the chemical process example for the economic cost function of Eq. 7.31 to compute the relative degree of various input variables using the methodology of [35]. The candidate manipulated inputs are dark gray and the economic cost is light gray.

operation. In the second set, operation with process noise is considered.

Applying the input selection methodology for EMPC (Fig. 7.2), the relative degree of the economic cost with respect to each input is computed with the directed graph method of [35] (Fig. 7.5). Based on this analysis, the inputs Q_1 and C_{A10} have a relative degree of 3, while the inputs Q_2 and C_{A20} have a relative degree of 2. No inputs have an infinite relative degree. The normalized dynamic and steady-state sensitivities are computed. All the inputs are scaled such that $u_j \in [-1,1]$, $j = 1,\ 2,\ 3,\ 4$ and the following notation is adopted for the inputs: $u_1 = (Q_1 - Q_{\text{shift}})/Q_{ref}$, $u_2 = (Q_2 - Q_{\text{shift}})/Q_{ref}$, $u_3 = (C_{A10} - C_{\text{shift}})/C_{ref}$, and $u_4 = (C_{A20} - C_{\text{shift}})/C_{ref}$ where Q_{ref} and C_{ref} are scaling factors, Q_{shift} and C_{shift} are shifting constants, and the vector fields $g_1(x)$, $g_2(x)$, $g_3(x)$, and $g_4(x)$ are the vector fields corresponding to the inputs u_1, u_2, u_3, and u_4, respectively from the dynamic model of Eq. 7.30.

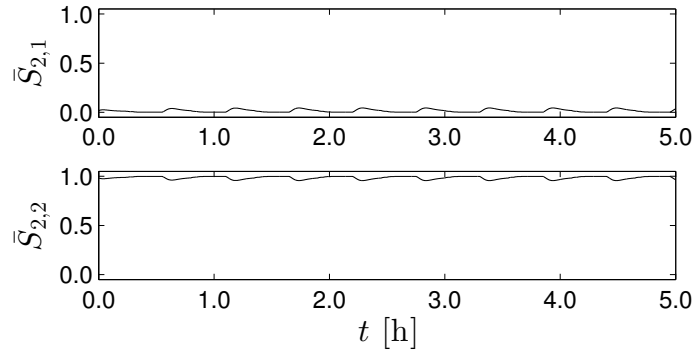

Figure 7.6: The dynamic sensitivities for inputs with relative degree 2 which are computed with the closed-loop state trajectory under the EMPC with all inputs on EMPC.

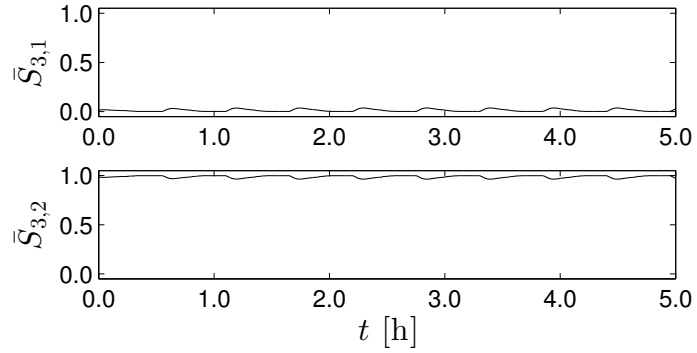

Figure 7.7: The dynamic sensitivities for inputs with relative degree 3 which are computed with the closed-loop state trajectory under the EMPC with all inputs on EMPC.

The dynamic sensitivities of Eq. 7.19 for the inputs with relative degree of 2 are:

$$S_{2,1} = L_{g_2} L_f l_{e,x}(x) = \frac{Q_{ref} k_0 E (F_{10} + F_{20})}{\rho C_p V_2 R T_2^2} e^{-E/RT_2} C_{A2}^2 \ , \tag{7.35}$$

$$S_{2,2} = L_{g_4} L_f l_{e,x}(x) = \frac{2 F_{20} C_{ref} k_0 (F_{10} + F_{20})}{V_2} e^{-E/RT_2} C_{A2} \ . \tag{7.36}$$

for u_2 and u_4, respectively. The dynamic sensitivities are computed from the closed-loop state trajectory under the EMPC with control actions computed by EMPC for all inputs and are shown in Fig. 7.6. The average normalized dynamic sensitivities over the length of operation are $\bar{S}_{2,1} = 0.02$ and $\bar{S}_{2,2} = 0.98$. From this analysis, the input u_4 has a much greater dynamic sensitivity on the economic cost than u_2. A similar analysis is completed for inputs with relative degree of 3 and their dynamic sensitivities are given by:

$$S_{3,1} = L_{g_1} L_f^2 l_{e,x}(x) = \frac{Q_{ref} F_{10} k_0 E (F_{10} + F_{20})}{\rho C_p V_1 V_2 R} \left(\frac{1}{T_1^2} e^{-E/RT_1} C_{A1}^2 + \frac{1}{T_2^2} e^{-E/RT_2} C_{A2}^2 \right) \tag{7.37}$$

$$S_{3,2} = L_{g_3} L_f^2 l_{e,x}(x) = \frac{2 F_{10}^2 C_{ref} k_0 F_3}{V_1 V_2} \left(e^{-E/RT_1} C_{A1} + e^{-E/RT_2} C_{A2} \right) \tag{7.38}$$

for u_1 and u_3, respectively and are shown in Fig. 7.7. The average normalized dynamic sensitivities are $\bar{S}_{3,1} = 0.01$ and $\bar{S}_{3,2} = 0.99$. A similar relationship is observed, that is, the inlet concentration input u_3 has a greater dynamic sensitivity than the heat rate input u_1.

The dynamic sensitivity analysis identified that the inlet concentration inputs have a more substantial dynamic sensitivity compared to the heat rate inputs (comparing inputs with the same relative degree). Using steady-state sensitivity, all inputs are compared to see if these effects are significant across the set of all the possible inputs. For simplicity, the steady-state sensitivities (Eq. 7.27) are computed with the economically optimal steady-

state and are given by:

$$\begin{aligned} \hat{S}_1 &= 0.01 \\ \hat{S}_2 &= 0.01 \\ \hat{S}_3 &= 0.56 \\ \hat{S}_4 &= 0.43 \end{aligned} \tag{7.39}$$

for the inputs u_1, u_2, u_3, and u_4, respectively. Based on both sensitivity analyses, the inlet concentration inputs should be placed on EMPC. Based on the relative degree analysis, Q_2 may also be placed on EMPC. However, the sensitivity analysis revealed that the economic cost is not sensitive to this input.

All 16 possible input selection combinations for EMPC are simulated. If the control action is not computed by EMPC, then it is fixed to its economically optimal steady-state value. The case where no inputs are placed on EMPC is also considered. The resulting EMPC schemes were applied to the process under nominal operation. The average economic cost for each of these cases depended only on whether C_{A10} and C_{A20} were on EMPC. If none of inlet concentrations were on EMPC, the average economic cost was $\bar{J}_e = 28.22$; if C_{A10} was manipulated by EMPC and C_{A20} was fixed, the cost was $\bar{J}_e = 28.54$; if C_{A10} was fixed and C_{A20} was manipulated by EMPC, the cost was $\bar{J}_e = 29.57$; and if both C_{A10} and C_{A20} were on EMPC, the cost was $\bar{J}_e = 30.13$. The reason the economic cost function is not influenced by the heat rates is the computed heat rate trajectories by EMPC are constant trajectories; that is, the constant trajectory when the heat rate was fixed to its economically optimal value is the same as the computed heat rate trajectory of EMPC.

From the average economic cost results, the inlet concentration C_{A20} has more of an impact on the average cost than the inlet concentration C_{A10} (the case that C_{A20} is on EMPC and C_{A10} is not on EMPC the performance is 1.1% better than the case that C_{A10} is on EMPC and C_{A20} is not on EMPC). This agrees with the relative degree of the economic cost function with respect to C_{A10} and C_{A20} which are 3 and 2, respectively. The average

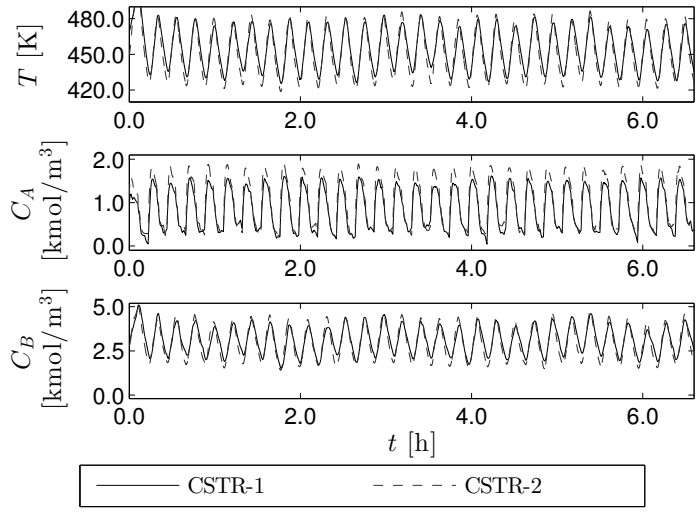

Figure 7.8: The closed-loop state trajectories of the chemical process under EMPC with added process noise.

computation time required to solve the EMPC problem, a key metric considered in the last set of simulations, was also considered for each of the 16 simulations considered here. It was found that the computation time was mainly a function of the number of inputs whose control action was computed by EMPC, i.e., the computation time scaled with the number of decision variables, and the computation time of each EMPC with the same number of inputs were all comparable. The average computation time required to solve the EMPC with the inputs C_{A10} and C_{A20} was 36.4 ms, while, that of the EMPC with all inputs was 163.6 ms.

In the last set of simulations, process operation in the presence of process noise was considered. The process noise was modeled as bounded Gaussian noise. The process noise added to the temperature differential equations was $w_T \sim \mathcal{N}(0, 15^2)$ and was bounded by $w_{b,T} = 40.0$, i.e., $|w_T(t)| \leq w_{b,T}$; the process noise added to the concentration differential equations was $w_C \sim \mathcal{N}(0, 2^2)$ with a bound of $w_{b,C} = 5.0$. The process noise was realized by generating a new random number and adding it to the right-hand side of the process

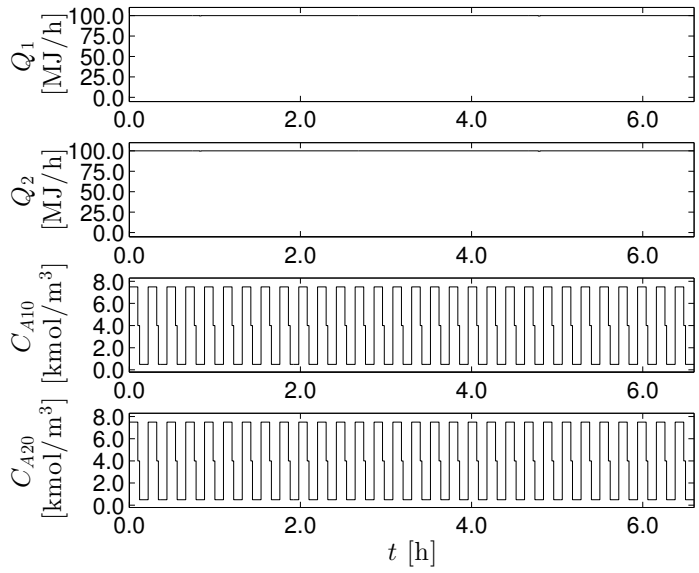

Figure 7.9: The manipulated input trajectories of the chemical process under EMPC with added process noise.

model of Eq. 7.30 over the sampling period. Four cases were considered: (1) all the inputs were controlled by EMPC, (2) the inputs having relative degree 2 (C_{A20} and Q_2) were controlled by EMPC, (3) the inputs having relative degree 3 (C_{A10} and Q_1) were controlled by EMPC, and (4) the inputs C_{A10} and C_{A20} were controlled by EMPC. For each of the four cases the process was initialized with the same initial condition and simulated for 16.5 h length of operation with the same realization of the process noise. The closed-loop trajectories are given in Figs. 7.8-7.9 for the case where control actions for all inputs are computed by EMPC.

The average economic costs over the simulation for these cases were: (1) $\bar{J}_e = 29.87$, (2) $\bar{J}_e = 29.21$ (a decrease of 2.2% over all inputs on EMPC), (3) $\bar{J}_e = 28.26$ (a decrease of 5.4% over all inputs on EMPC) and (4) $\bar{J}_e = 29.87$, respectively for each case. Furthermore, the average computation time required to solve the EMPC for each case was (1) 4041 ms, (2) 239 ms, (3) 584 ms, and (4) 718 ms, respectively. The computation time reduction going from all four inputs to two inputs was an order of magnitude since the number of decision

variables in the optimization problem is a dominant factor in the computational burden of solving the optimization problem. Also, case (4) has two average constraints imposed in the optimization problem compared to cases (2) and (3) which only have one average constraint. It is important to emphasize that the same program and computer processing power were used in all cases. Thus, the comparison of the computation time is consistent. The average computation time was computed for a simulation with 320 sampling periods, i.e., the EMPC was solved 320 times. The computation time required to solve the EMPC that computes control actions for C_{A20} and Q_2 is less than the computation time of EMPC that computes control actions for C_{A10} and Q_1 (the reduction in computation time is approximately a factor of two) which suggests that the computational burden is associated with how direct is the dynamic effect of the input on the economic cost.

This example is relatively small and thus, it may be computationally viable to compute control actions for the full set of manipulated inputs with EMPC. In the final input selection, the inputs C_{A10} and C_{A20} are controlled by EMPC. The inlet concentrations are the inputs that are continuously manipulated by the EMPC which leads to dynamic operation of the process that is economically better compared to steady-state operation. The input C_{A20} has more of an impact on the closed-loop performance compared to the input C_{A10}. Even though the relative degree of the economic cost with respect to Q_2 is 2, it is not included on EMPC because practically no benefit is realized with this input on EMPC which the sensitivity analysis showed.

7.4 Conclusions

In this chapter, control configuration selection for economic model predictive control was considered. A methodology to identify the manipulated inputs from the set of all possible manipulated inputs for which EMPC should compute control actions was developed on the

basis of the process economics. Since EMPC will typically enforce a dynamic operating policy, the relative degree and the sensitivities of the economic cost function with respect to an input were used to explicitly account for the nonlinear process dynamics and choose the manipulated inputs assigned to EMPC. The set of inputs selected for EMPC is guaranteed to be a stabilizing one. The overall methodology was demonstrated with a chemical process example.

Chapter 8

Conclusions

This dissertation presented approaches to economic model predictive control (EMPC) of nonlinear process systems. The approaches were formulated to address several key theoretical considerations of EMPC including recursive feasibility, closed-loop stability, closed-loop performance, and computational efficiency. Many of the developed EMPC schemes took advantage of Lyapunov-based control techniques. The effectiveness and performance of the developed EMPC approaches were illustrated via applications to chemical process examples.

In Chapter 3, various LEMPC designs were developed, which are capable of optimizing closed-loop performance with respect to general economic considerations for nonlinear systems. Numerous issues arising in the context of chemical process control were considered including closed-loop stability, robustness, closed-loop performance, and explicitly time-varying economic cost functions. The formulations of the LEMPC schemes were provided as well as rigorous theoretical treatments of the schemes were carried out. Closed-loop stability, in the sense of boundedness of the closed-loop state, under the LEMPC designs was proven. Additionally, when desirable, the LEMPC designs may be used to enforce convergence of the closed-loop state to steady-state. Under a specific terminal con-

straint design, the closed-loop system under the resulting LEMPC scheme was shown to achieve at least as good closed-loop performance as that achieved under an explicit stabilizing controller. Demonstrations of the effectiveness of the LEMPC schemes on chemical process examples were also provided. Moreover, the closed-loop properties of these examples under the LEMPC schemes were compared with respect to existing approaches to optimization and control. In all cases considered, the closed-loop economic performance under the LEMPC designs was better relative to the conventional approaches.

In Chapter 4, several computationally-efficient two-layer frameworks for integrating dynamic economic optimization and control of nonlinear systems were presented. In the upper layer, EMPC is used to compute economically optimal time-varying operating trajectories. Explicit control-oriented constraints were employed in the upper layer EMPC. In the lower layer, an MPC scheme is used to force the system to track the optimal time-varying trajectory computed by the upper layer EMPC. The properties, i.e., stability, performance, and robustness, of closed-loop systems under the two-layer EMPC methods were rigorously analyzed. The two-layer EMPC methods were applied to chemical process examples to demonstrate the closed-loop properties. In all the examples considered, closed-loop stability was achieved, the closed-loop economic performance under the two-layer EMPC framework was better than that achieved under conventional approaches to optimization and control, and the total on-line computational time was better with the two-layer EMPC methods compared to that under one-layer EMPC methods.

In Chapter 5, a strategy for implementing Lyapunov-based economic model predictive control (LEMPC) in real-time with computation delay was developed. The implementation strategy uses a triggering condition to precompute an input trajectory from LEMPC over a finite-time horizon. At each sampling period, if a certain stability (triggering) condition is satisfied, then the precomputed control action by LEMPC is applied to the closed-loop system. If the stability condition is violated, then a backup explicit stabilizing controller

is used to compute the control action for the sampling period. In this fashion, the LEMPC is used when possible to optimize the economics of the process. Conditions such that the closed-loop state under the real-time LEMPC is always bounded in a compact set were derived. The real-time LEMPC scheme was applied to a chemical process network and demonstrated that it may maintain closed-loop stability in the presence of significant computation delay and process noise while also, improving the closed-loop economic performance compared to the economic performance at the economically optimal steady-state.

In Chapter 6, closed-loop stability and performance of systems described by nonlinear DDEs under Lyapunov-based economic model predictive control (LEMPC) was considered. First, conditions such that closed-loop stability for systems with sufficiently small state and input delays under LEMPC, formulated with an ODE model of the system, were derived. A chemical process example demonstrated that indeed closed-loop stability is maintained under LEMPC for sufficiently small time-delays in both the states and the inputs. However, closed-loop performance significantly degraded for larger input delays. This motivated designing a predictor feedback LEMPC methodology. The predictor feedback LEMPC design employs a predictor to compute a prediction of the state after the input delay and an LEMPC scheme, formulated with a DDE model. The predicted state from the predictor is used to initialize the DDE model. The predictor feedback LEMPC was applied to the chemical process example and resulted in better closed-loop stability and performance properties compared to the LEMPC, formulated with an ODE approximation of the nonlinear time-delay system.

In Chapter 7, control configuration selection for economic model predictive control was considered. A methodology to identify the manipulated inputs from the set of all possible manipulated inputs for which EMPC should compute control actions was developed on the basis of the process economics. Since EMPC will typically enforce a dynamic operating policy, the relative degree and the sensitivities of the economic cost function with respect to

an input were used to explicitly account for the nonlinear process dynamics and choose the manipulated inputs assigned to EMPC. The set of inputs selected for EMPC is guaranteed to be a stabilizing one. The overall methodology was demonstrated with a chemical process example.

In summary, EMPC is a viable option to integrate dynamic economic optimization and control of nonlinear systems, and this dissertation has developed several such EMPC methods that may contribute in enabling the vision of Smart Manufacturing.

Bibliography

[1] A. Alessandretti, A.P. Aguiar, and C.N. Jones. An economic model predictive control scheme with terminal penalty for continuous-time systems. In *Proceedings of the 53rd IEEE Conference on Decision and Control*, pages 2728–2733, Los Angeles, CA, 2014.

[2] F. Alfani and J. J. Carberry. An exploratory kinetic study of ethylene oxidation over an unmoderated supported silver catalyst. *La Chimica e L'Industria*, 52:1192–1196, 1970.

[3] F. Allgöwer and A. Zheng, editors. *Nonlinear Model Predictive Control*, volume 26 of *Progress in Systems and Control Theorey*. Birkäuser Basel, Washington D.C., 2000.

[4] R. Amrit, J. B. Rawlings, and D. Angeli. Economic optimization using model predictive control with a terminal cost. *Annual Reviews in Control*, 35:178–186, 2011.

[5] R. Amrit, J. B. Rawlings, and L. T. Biegler. Optimizing process economics online using model predictive control. *Computers & Chemical Engineering*, 58:334–343, 2013.

[6] D. Angeli, R. Amrit, and J. B. Rawlings. On average performance and stability of economic model predictive control. *IEEE Transactions on Automatic Control*, 57:1615–1626, 2012.

[7] C. Antoniades and P. D. Christofides. Feedback control of nonlinear differential difference equation systems. *Chemical Engineering Science*, 54:5677–5709, 1999.

[8] C. Antoniades and P. D. Christofides. Robust control of nonlinear time-delay systems. *International Journal of Applied Mathematics and Computer Science*, 9:811–837, 1999.

[9] T. Backx, O. Bosgra, and W. Marquardt. Integration of model predictive control and optimization of processes: Enabling technology for market driven process operation. In *Proceedings of the IFAC Symposium on Advanced Control of Chemical Processes*, pages 249–260, Pisa, Italy, 2000.

[10] J. E. Bailey. Periodic operation of chemical reactors: a review. *Chemical Engineering Communications*, 1:111–124, 1973.

[11] J. E. Bailey and F. J. M. Horn. Comparison between two sufficient conditions for improvement of an optimal steady-state process by periodic operation. *Journal of Optimization Theory and Applications*, 7:378–384, 1971.

[12] M. Baldea, A. Araujo, S. Skogestad, and P. Daoutidis. Dynamic considerations in the synthesis of self-optimizing control structures. *AIChE Journal*, 54:1830–1841, 2008.

[13] M. Baldea and C. R. Touretzky. Nonlinear model predictive control of energy-integrated process systems. *Systems & Control Letters*, 62:723–731, 2013.

[14] Y. Barshad and E. Gulari. A dynamic study of CO oxidation on supported platinum. *AIChE Journal*, 31:649–658, 1985.

[15] F. A. Bayer, M. A. Müller, and F. Allgöwer. Tube-based robust economic model predictive control. *Journal of Process Control*, 24:1237–1246, 2014.

[16] A. Bellen. One-step collocation for delay differential equations. *Journal of Computational and Applied Mathematics*, 10:275–283, 1984.

[17] A. Bellen and M. Zennaro. *Numerical Methods for Delay Differential Equations*. Oxford University Press, New York, 2003.

[18] R. E. Bellman. *Dynamic Programming*. Princeton University Press, Princeton, N. J., 1957.

[19] D. P. Bertsekas. *Nonlinear Programming*. Athena Scientific, Belmont, MA, 2nd edition, 1999.

[20] L. T. Biegler. *Nonlinear Programming: Concepts, Algorithms, and Applications to Chemical Processes*. SIAM, Philadelphia, PA, 2010.

[21] L. T. Biegler, X. Yang, and G. A. G. Fischer. Advances in sensitivity-based nonlinear model predictive control and dynamic real-time optimization. *Journal of Process Control*, 30:104–116, 2015.

[22] S. Bittanti, G. Fronza, and G. Guardabassi. Periodic control: A frequency domain approach. *IEEE Transactions on Automatic Control*, 18:33–38, 1973.

[23] E. Bristol. On a new measure of interaction for multivariable process control. *IEEE Transactions on Automatic Control*, 11:133–134, 1966.

[24] H. Budman, M. Kzyonsek, and P. Silveston. Control of a nonadiabatic packed bed reactor under periodic flow reversal. *The Canadian Journal of Chemical Engineering*, 74:751–759, 1996.

[25] H. Budman and P. L. Silveston. Control of periodically operated reactors. *Chemical Engineering Science*, 63:4942–4954, 2008.

[26] C. I. Byrnes and W. Lin. Losslessness, feedback equivalence, and the global stabilization of discrete-time nonlinear systems. *IEEE Transactions on Automatic Control*, 39:83–98, 1994.

[27] E. F. Camacho and C. B. Alba. *Model predictive control*. Springer, 2nd edition, 2013.

[28] Y. Cao. *Control Structure Selection for Chemical Processes Using Input-Output Controllability Analysis*. PhD thesis, University of Exeter, 1996.

[29] Y. Cao, D. Biss, and J. D. Perkins. Assessment of input-output controllability in the presence of control constraints. *Computers & Chemical Engineering*, 20:337–346, 1996.

[30] B. Castillo-Toledo, S. Di Gennaro, and G. S. Castro. Stability analisys for a class of sampled nonlinear systems with time-delay. In *Proceedings of the 49th IEEE Conference on Decision and Control*, pages 1575–1580, Altanta, GA, 2010.

[31] W.-H. Chen, D. J. Ballance, and J. O'Reilly. Model predictive control of nonlinear systems: computational burden and stability. *IEE Proceedings - Control Theory and Applications*, 147:387–394, 2000.

[32] X. Chen, M. Heidarinejad, J. Liu, and P. D. Christofides. Distributed economic MPC: Application to a nonlinear chemical process network. *Journal of Process Control*, 22:689–699, 2012.

[33] P. D. Christofides and N. H. El-Farra. *Control of Nonlinear and Hybrid Process Systems: Designs for Uncertainty, Constraints and Time-Delays*. Springer-Verlag, Berlin, Germany, 2005.

[34] P. D. Christofides, J. Liu, and D. Muñoz de la Peña. *Networked and Distributed Predictive Control: Methods and Nonlinear Process Network Applications*. Advances in Industrial Control Series. Springer-Verlag, London, England, 2011.

[35] P. Daoutidis and C. Kravaris. Structural evaluation of control configurations for multivariable nonlinear processes. *Chemical Engineering Science*, 47:1091–1107, 1992.

[36] M. L. Darby, M. Nikolaou, J. Jones, and D. Nicholson. RTO: An overview and assessment of current practice. *Journal of Process Control*, 21:874–884, 2011.

[37] S. Dashkovskiy and L. Naujok. Input-to-state stability for model predictive control of single systems and networks with time-delays. In *Proceedings of the 51st IEEE Conference on Decision and Control*, pages 2599–2604, Maui, Hawaii, 2012.

[38] J. Davis, T. Edgar, J. Porter, J. Bernaden, and M. Sarli. Smart manufacturing, manufacturing intelligence and demand-dynamic performance. *Computers & Chemical Engineering*, 47:145–156, 2012.

[39] M. Diehl, R. Amrit, and J. B. Rawlings. A Lyapunov function for economic optimizing model predictive control. *IEEE Transactions on Automatic Control*, 56:703–707, 2011.

[40] M. Diehl, H. Bock, and J. Schlöder. A real-time iteration scheme for nonlinear optimization in optimal feedback control. *SIAM Journal on Control and Optimization*, 43:1714–1736, 2005.

[41] M. Diehl, H. J. Ferreau, and N. Haverbeke. Efficient numerical methods for nonlinear MPC and moving horizon estimation. In L. Magni, D. M. Raimondo, and F. Allgöwer, editors, *Nonlinear Model Predictive Control*, volume 384 of *Lecture Notes in Control and Information Sciences*, pages 391–417. Springer-Verlag Berlin Heidelberg, 2009.

[42] J. M. Douglas. Periodic reactor operation. *Industrial & Engineering Chemistry Process Design and Development*, 6:43–48, 1967.

[43] J. J. Downs and S. Skogestad. An industrial and academic perspective on plantwide control. *Annual Reviews in Control*, 35:99–110, 2011.

[44] P. A. A. Driessen, R. M. Hermans, and P. P. J. van den Bosch. Distributed economic model predictive control of networks in competitive environments. In *Proceedings of the 51st IEEE Conference on Decision and Control*, pages 266–271, Maui, HI, 2012.

[45] S. Dubljević and N. Kazantzis. A new Lyapunov design approach for nonlinear systems based on Zubov's method. *Automatica*, 38:1999–2007, 2002.

[46] M. Ellis and P. D. Christofides. Unifying dynamic economic optimization and model predictive control for optimal process operation. In *Proceedings of the American Control Conference*, pages 3135–3140, Washington, D.C., 2013.

[47] M. Ellis and P. D. Christofides. Control configuration selection for economic model predictive control. In *Proceedings of the 53rd IEEE Conference on Decision and Control*, pages 789–796, 2014.

[48] M. Ellis and P. D. Christofides. Economic model predictive control with time-varying objective function for nonlinear process systems. *AIChE Journal*, 60:507–519, 2014.

[49] M. Ellis and P. D. Christofides. Integrating dynamic economic optimization and model predictive control for optimal operation of nonlinear process systems. *Control Engineering Practice*, 22:242–251, 2014.

[50] M. Ellis and P. D. Christofides. On finite-time and infinite-time cost improvement of economic model predictive control for nonlinear systems. *Automatica*, 50:2561–2569, 2014.

[51] M. Ellis and P. D. Christofides. Optimal time-varying operation of nonlinear process systems with economic model predictive control. *Industrial & Engineering Chemistry Research*, 53:4991–5001, 2014.

[52] M. Ellis and P. D. Christofides. Selection of control configurations for economic model predictive control systems. *AIChE Journal*, 60:3230–3242, 2014.

[53] M. Ellis and P. D. Christofides. Handling computational delay in economic model predictive control of nonlinear process systems. In *Proceedings of the American Control Conference*, pages 2962–2967, Chicago, IL, 2015.

[54] M. Ellis and P. D. Christofides. Real-time economic model predictive control of nonlinear process systems. *AIChE Journal*, 61:555–571, 2015.

[55] M. Ellis and P. D. Christofides. Economic model predictive control: Elucidation of the role of constraints. In *Proceedings of 5th IFAC Conference on Nonlinear Model Predictive Control*, Seville, Spain, in press.

[56] M. Ellis and P. D. Christofides. Economic model predictive control of nonlinear time-delay systems: Closed-loop stability and delay compensation. *AIChE Journal*, in press, DOI: 10.1002/aic.14964.

[57] M. Ellis, H. Durand, and P. D. Christofides. A tutorial review of economic model predictive control methods. *Journal of Process Control*, 24:1156–1178, 2014.

[58] M. Ellis, M. Heidarinejad, and P. D. Christofides. Economic model predictive control of nonlinear singularly perturbed systems. *Journal of Process Control*, 23:743–754, 2013.

[59] M. Ellis, I. Karafyllis, and P. D. Christofides. Stabilization of nonlinear sampled-data systems and economic model predictive control application. In *Proceedings of the American Control Conference*, pages 5594–5601, Portland, OR, 2014.

[60] M. Ellis, J. Zhang, J. Liu, and P. D. Christofides. Robust moving horizon estimation based output feedback economic model predictive control. *Systems & Control Letters*, 68:101–109, 2014.

[61] S. Engell. Feedback control for optimal process operation. *Journal of Process Control*, 17:203–219, 2007.

[62] L. Fagiano and A. R. Teel. Generalized terminal state constraint for model predictive control. *Automatica*, 49:2622–2631, 2013.

[63] A. Ferramosca, J. B. Rawlings, D. Limon, and E. F. Camacho. Economic MPC for a changing economic criterion. In *Proceedings of the 49th IEEE Conference on Decision and Control*, pages 6131–6136, Atlanta, GA, 2010.

[64] R. Findeisen and F. Allgöwer. Computational delay in nonlinear model predictive control. In *Proceedings of the IFAC International Symposium of Advanced Control of Chemical Processes*, pages 427–432, Hong Kong, 2004.

[65] N. Ganesh and L. T. Biegler. A reduced Hessian strategy for sensitivity analysis of optimal flowsheets. *AIChE Journal*, 33:282–296, 1987.

[66] S. T. Glad. Extensions of the RGA concept to nonlinear systems. In *Proceedings of the 5th European Control Conference*, Karlsruhe, Germany, 1999.

[67] A. Gopalakrishnan and L. T. Biegler. Economic nonlinear model predictive control for periodic optimal operation of gas pipeline networks. *Computers & Chemical Engineering*, 52:90–99, 2013.

[68] L. Grüne. Economic receding horizon control without terminal constraints. *Automatica*, 49:725–734, 2013.

[69] L. Grüne and J. Pannek. *Nonlinear Model Predictive Control: Theory and Algorithms*. Communications and Control Engineering. Springer London, London, England, 2011.

[70] L. Grüne and M. Stieler. Asymptotic stability and transient optimality of economic MPC without terminal conditions. *Journal of Process Control*, 24:1187–1196, 2014.

[71] K. Gu and S.-I. Niculescu. Survey on recent results in the stability and control of time-delay systems. *Journal of Dynamic Systems, Measurement, and Control*, 125:158–165, 2003.

[72] G. Guardabassi, A. Locatelli, and S. Rinaldi. Status of periodic optimization of dynamical systems. *Journal of Optimization Theory and Applications*, 14:1–20, 1974.

[73] W. Hahn. *Stability of Motion*. Springer-Verlag, New York, 1967.

[74] J. K. Hale and S. M. Verduyn Lunel. *Introduction to Functional Differential Equations*. Springer-Verlag, New York, 1993.

[75] J. A. Heath, I. K. Kookos, and J. D. Perkins. Process control structure selection based on economics. *AIChE Journal*, 46:1998–2016, 2000.

[76] M. Heidarinejad, J. Liu, and P. D. Christofides. Economic model predictive control of nonlinear process systems using Lyapunov techniques. *AIChE Journal*, 58:855–870, 2012.

[77] M. Heidarinejad, J. Liu, and P. D. Christofides. State-estimation-based economic model predictive control of nonlinear systems. *Systems & Control Letters*, 61:926–935, 2012.

[78] M. Heidarinejad, J. Liu, and P. D. Christofides. Algorithms for improved fixed-time performance of Lyapunov-based economic model predictive control of nonlinear systems. *Journal of Process Control*, 23:404–414, 2013.

[79] M. Heidarinejad, J. Liu, and P. D. Christofides. Economic model predictive control of switched nonlinear systems. *Systems & Control Letters*, 62:77–84, 2013.

[80] A. Helbig, O. Abel, and W. Marquardt. Structural concepts for optimization based control of transient processes. In F. Allgöwer and A. Zheng, editors, *Nonlinear Model Predictive Control*, volume 26 of *Progress in Systems and Control Theory*, pages 295–311. Birkhäuser Basel, 2000.

[81] M. A. Henson. Nonlinear model predictive control: current status and future directions. *Computers & Chemical Engineering*, 23:187–202, 1998.

[82] M. A. Henson and D. E. Seborg. Time delay compensation for nonlinear processes. *Industrial & Engineering Chemistry Research*, 33:1493–1500, 1994.

[83] T. G. Hovgaard, S. Boyd, L. F. S. Larsen, and J. B. Jørgensen. Nonconvex model predictive control for commercial refrigeration. *International Journal of Control*, 86:1349–1366, 2013.

[84] L. Hu, Y. Cao, C. Cheng, and H. Shao. Sampled-data control for time-delay systems. *Journal of the Franklin Institute*, 339:231–238, 2002.

[85] R. Huang, L. T. Biegler, and E. Harinath. Robust stability of economically oriented infinite horizon NMPC that include cyclic processes. *Journal of Process Control*, 22:51–59, 2012.

[86] R. Huang, E. Harinath, and L. T. Biegler. Lyapunov stability of economically oriented NMPC for cyclic processes. *Journal of Process Control*, 21:501–509, 2011.

[87] A. Isidori. *Nonlinear Control Systems*. Springer-Verlag, New York, 2nd edition, 1989.

[88] A. Isidori. *Nonlinear Control Systems: An Introduction*. Springer-Verlag, New York, NY, 3rd edition, 1995.

[89] M. Jankovic. Control Lyapunov-Razumikhin functions and robust stabilization of time delay systems. *IEEE Transactions on Automatic Control*, 46:1048–1060, 2001.

[90] M. Jankovic. Control of nonlinear systems with time delay. In *Proceedings of the 42nd IEEE Conference on Decision and Control*, volume 5, pages 4545–4550, 2003.

[91] J. Jäschke, X. Yang, and L. T. Biegler. Fast economic model predictive control based on NLP-sensitivities. *Journal of Process Control*, 24:1260–1272, 2014.

[92] J. V. Kadam and W. Marquardt. Integration of economical optimization and control for intentionally transient process operation. In R. Findeisen, F. Allgöwer, and L. T. Biegler, editors, *Assessment and Future Directions of Nonlinear Model Predictive Control*, volume 358 of *Lecture Notes in Control and Information Sciences*, pages 419–434. Springer Berlin Heidelberg, 2007.

[93] J. V. Kadam, W. Marquardt, M. Schlegel, T. Backx, O. H. Bosgra, P.-J. Brouwer, G. Dünnebier, D. van Hessem, A. Tiagounov, and S. de Wolf. Towards integrated dynamic real-time optimization and control of industrial processes. In *Proceedings of the 4th International Conference of the Foundations of Computer-Aided Process Operations*, pages 593–596, Coral Springs, Florida, 2003.

[94] J. V. Kadam, M. Schlegel, W. Marquardt, R. L. Tousain, D. H. van Hessem, J. van den Berg, and O. H. Bosgra. A two-level strategy of integrated dynamic optimization and control of industrial processes–a case study. In J. Grievink and J. van Schijndel, editors, *Proceedings of the European Symposium on Computer Aided Process Engineering-12*, volume 10 of *Computer Aided Chemical Engineering*, pages 511–516, The Hague, The Netherlands, 2002.

[95] R. E. Kalman. Contributions to the theory of optimal control. *Boletin de la Sociedad Matematica Mexicana*, 5:102–119, 1960.

[96] I. Karafyllis. Stabilization by means of approximate predictors for systems with delayed input. *SIAM Journal on Control and Optimization*, 49:1100–1123, 2011.

[97] I. Karafyllis and L. Grüne. Feedback stabilization methods for the numerical solution of ordinary differential equations. *Discrete and Continuous Dynamical Systems*, 16:283–317, 2011.

[98] I. Karafyllis and M. Krstic. Nonlinear stabilization under sampled and delayed measurements, and with inputs subject to delay and zero-order hold. *IEEE Transactions on Automatic Control*, 57:1141–1154, 2012.

[99] A. Kasinski and J. Levine. A fast graph theoretic algorithm for the feedback decoupling problem of nonlinear systems. In P.A. Fuhrmann, editor, *Mathematical Theory of Networks and Systems*, volume 58 of *Lecture Notes in Control and Information Sciences*, pages 550–562. Springer Berlin Heidelberg, 1984.

[100] H. K. Khalil. *Nonlinear Systems*. Prentice Hall, Upper Saddle River, NJ, third edition, 2002.

[101] P. Kokotović and M. Arcak. Constructive nonlinear control: a historical perspective. *Automatica*, 37:637–662, 2001.

[102] I. K. Kookos and J. D. Perkins. An algorithmic method for the selection of multivariable process control structures. *Journal of Process Control*, 12:85–99, 2002.

[103] N. N. Krasovskii. *Stability of Motion*. Stanford University Press, Stanford, 1963.

[104] C. Kravaris and J. C. Kantor. Geometric methods for nonlinear process control. 1. Background. *Industrial & Engineering Chemistry Research*, 29:2295–2310, 1990.

[105] C. Kravaris and J. C. Kantor. Geometric methods for nonlinear process control. 2. controller synthesis. *Industrial & Engineering Chemistry Research*, 29:2310–2323, 1990.

[106] C. Kravaris and R. A. Wright. Deadtime compensation for nonlinear processes. *AIChE Journal*, 35:1535–1542, 1989.

[107] M. Krstic. Input delay compensation for forward complete and strict-feedforward nonlinear systems. *IEEE Transactions on Automatic Control*, 55:287–303, 2010.

[108] D. S. Laila, D. Nešić, and A. Astolfi. Sampled-data control of nonlinear systems. In A. Loría, F. Lamnabhi-Lagarrigue, and E. Panteley, editors, *Advanced Topics in Control Systems Theory*, volume 328 of *Lecture Notes in Control and Information Science*, pages 91–137. Springer London, 2006.

[109] L. Lao, M. Ellis, and P. D. Christofides. Smart manufacturing: Handling preventive actuator maintenance and economics using model predictive control. *AIChE Journal*, 60:2179–2196, 2014.

[110] C. K. Lee and J. E. Bailey. Modification of consecutive-competitive reaction selectivity by periodic operation. *Industrial & Engineering Chemistry Process Design and Development*, 19:160–166, 1980.

[111] J. Lee and D. Angeli. Cooperative distributed model predictive control for linear plants subject to convex economic objectives. In *Proceedings of the 50th IEEE Conference on Decision and Control and European Control Conference*, pages 3434–3439, Orlando, FL, 2011.

[112] J. Lee and D. Angeli. Distributed cooperative nonlinear economic MPC. In *Proceedings of the 20th International Symposium on Mathematical Theory of Networks and Systems*, Melbourne, Australia, 2012.

[113] J. H. Lee, R. D. Braatz, M. Morari, and A. Packard. Screening tools for robust control structure selection. *Automatica*, 31:229–235, 1995.

[114] J. H. Lee, S. Natarajan, and K. S. Lee. A model-based predictive control approach to repetitive control of continuous processes with periodic operations. *Journal of Process Control*, 11:195–207, 2001.

[115] Y. Lin, E. Sontag, and Y. Wang. A smooth converse Lyapunov theorem for robust stability. *SIAM Journal on Control and Optimization*, 34:124–160, 1996.

[116] S. Liu, J. Zhang, and J. Liu. Economic MPC with terminal cost and application to an oilsand primary separation vessel. *Chemical Engineering Science*, in press, DOI: 10.1016/j.ces.2015.01.041.

[117] W. L. Luyben. The concept of "eigenstructure" in process control. *Industrial & Engineering Chemistry Research*, 27:206–208, 1988.

[118] L. Magni, D. M. Raimondo, and F. Allgöwer. *Nonlinear Model Prediction Control: Towards New Challenging Applications*, volume 384 of *Lecture Notes in Control and Information Sciences*. Springer-Verlag Berlin Heidelberg, 2009.

[119] R. Mahboobi Esfanjani and S. K. Y. Nikravesh. Stabilising predictive control of non-linear time-delay systems using control Lyapunov-Krasovskii functionals. *IET Control Theory Applications*, 3:1395–1400, 2009.

[120] E. Mancusi, P. Altimari, L. Russo, and S. Crescitelli. Multiplicities of temperature wave trains in periodically forced networks of catalytic reactors for reversible exothermic reactions. *Chemical Engineering Journal*, 171:655–668, 2011.

[121] T. E. Marlin and A. N. Hrymak. Real-time operations optimization of continuous processes. In *Proceedings of the Fifth International Conference on Chemical Process Control*, pages 156–164, Tahoe City, CA, 1996.

[122] W. Marquardt. Nonlinear model reduction for optimization based control of transient chemical processes. In *Proceedings of the Sixth International Conference on Chemical Process Control*, pages 12–42, Tucson, AZ, 2001.

[123] J. L. Massera. Contributions to stability theory. *Annals of Mathematics*, 64:182–206, 1956.

[124] D. Q. Mayne, J. B. Rawlings, C. V. Rao, and P. O. M. Scokaert. Constrained model predictive control: Stability and optimality. *Automatica*, 36:789–814, 2000.

[125] D.Q. Mayne and H. Michalska. Receding horizon control of nonlinear systems. *IEEE Transactions on Automatic Control*, 35:814–824, 1990.

[126] D. I. Mendoza-Serrano and D. J. Chmielewski. HVAC control using infinite-horizon economic MPC. In *Proceedings of the 51st IEEE Conference on Decision and Control*, pages 6963–6968, Maui, Hawaii, 2012.

[127] D. I. Mendoza-Serrano and D. J. Chmielewski. Demand response for chemical manufacturing using economic MPC. In *Proceedings of the American Control Conference*, pages 6655–6660, Washington, D.C., 2013.

[128] P. Mhaskar, N. H. El-Farra, and P. D. Christofides. Predictive control of switched nonlinear systems with scheduled mode transitions. *IEEE Transactions on Automatic Control*, 50:1670–1680, 2005.

[129] P. Mhaskar, N. H. El-Farra, and P. D. Christofides. Stabilization of nonlinear systems with state and control constraints using Lyapunov-based predictive control. *Systems & Control Letters*, 55:650–659, 2006.

[130] B. Moaveni and A. Khaki-Sedigh. Input-output pairing for nonlinear multivariable systems. *Journal of Applied Sciences*, 7:3492–3498, 2007.

[131] M. Morari, Y. Arkun, and G. Stephanopoulos. Studies in the synthesis of control structures for chemical processes: Part I: Formulation of the problem. Process decomposition and the classification of the control tasks. Analysis of the optimizing control structures. *AIChE Journal*, 26:220–232, 1980.

[132] M. Morari and J. H. Lee. Model predictive control: past, present and future. *Computers & Chemical Engineering*, 23:667–682, 1999.

[133] D. Muñoz de la Peña and P. D. Christofides. Lyapunov-based model predictive control of nonlinear systems subject to data losses. *IEEE Transactions on Automatic Control*, 53:2076–2089, 2008.

[134] M. A. Müller and F. Allgöwer. Robustness of steady-state optimality in economic model predictive control. In *Proceedings of the 51st IEEE Conference on Decision and Control*, pages 1011–1016, Maui, Hawaii, 2012.

[135] M. A. Müller, D. Angeli, and F. Allgöwer. Economic model predictive control with self-tuning terminal cost. *European Journal of Control*, 19:408–416, 2013.

[136] M. A. Müller, D. Angeli, and F. Allgöwer. On convergence of averagely constrained economic MPC and necessity of dissipativity for optimal steady-state operation. In *Proceedings of the American Control Conference*, pages 3147–3152, Washington, D.C., 2013.

[137] M. A. Müller, D. Angeli, and F. Allgöwer. Transient average constraints in economic model predictive control. *Automatica*, 50:2943–2950, 2014.

[138] L. T. Narraway, J. D. Perkins, and G. W. Barton. Interaction between process design and process control: economic analysis of process dynamics. *Journal of Process Control*, 1:243–250, 1991.

[139] S. Natarajan and J. H. Lee. Repetitive model predictive control applied to a simulated moving bed chromatography system. *Computers & Chemical Engineering*, 24:1127–1133, 2000.

[140] D. Nešić and A. R. Teel. Sampled-data control of nonlinear systems: An overview of recent results. In S. O. R. Moheimani, editor, *Perspectives in Robust Control*, volume 268 of *Lecture Notes in Control and Information Sciences*, pages 221–239. Springer London, 2001.

[141] D. Nešić, A. R. Teel, and D. Carnevale. Explicit computation of the sampling period in emulation of controllers for nonlinear sampled-data systems. *IEEE Transactions on Automatic Control*, 54:619–624, 2009.

[142] J. E. Normey-Rico and E. F. Camacho. *Control of Dead-time Processes*. Advanced Textbooks in Control and Signal Processing. Springer-Verlag London, London, 2007.

[143] B. P. Omell and D. J. Chmielewski. IGCC power plant dispatch using infinite-horizon economic model predictive control. *Industrial & Engineering Chemistry Research*, 52:3151–3164, 2013.

[144] F. Özgülşen, R. A. Adomaitis, and A. Çinar. A numerical method for determining optimal parameter values in forced periodic operation. *Chemical Engineering Science*, 47:605–613, 1992.

[145] F. Özgülşen and A. Çinar. Forced periodic operation of tubular reactors. *Chemical Engineering Science*, 49:3409–3419, 1994.

[146] F. Özgülşen, S. J. Kendra, and A. Çinar. Nonlinear predictive control of periodically forced chemical reactors. *AIChE Journal*, 39:589–598, 1993.

[147] A. Papachristodoulou and S. Prajna. On the construction of Lyapunov functions using the sum of squares decomposition. In *Proceedings of the 41st IEEE Conference on Decision and Control*, pages 3482–3487, Las Vegas, NV, 2002.

[148] P. Pepe. Input-to-state stabilization of stabilizable, time-delay, control-affine, nonlinear systems. *IEEE Transactions on Automatic Control*, 54:1688–1693, 2009.

[149] J. D. Perkins and S. P. K. Walsh. Optimization as a tool for design/control integration. *Computers & Chemical Engineering*, 20:315–323, 1996.

[150] L. S. Pontryagin, V. G. Boltyanskii, R. V. Gamkrelidze, and E. F. Mishchenko. *Mathematical Theory of Optimal Processes*. Fizmatgiz, Moscow, 1961.

[151] A. Psaltis, I. K. Kookos, and C. Kravaris. Plant-wide control structure selection methodology based on economics. *Computers & Chemical Engineering*, 52:240–248, 2013.

[152] S. J. Qin and T. A. Badgwell. A survey of industrial model predictive control technology. *Control Engineering Practice*, 11:733–764, 2003.

[153] T. Raff, C. Angrick, R. Findeisen, J.-S. Kim, and F. Allgöwer. Model predictive control for nonlinear time-delay systems. In *Proceedings of the 7th IFAC Symposium on Nonlinear Systems*, pages 60–65, Pretoria, South Africa, 2007.

[154] G. P. Rangaiah and V. Kariwala, editors. *Plantwide Control: Recent Developments and Applications*. John Wiley & Sons, Ltd, Chichester, England, 2012.

[155] J. B. Rawlings. Tutorial overview of model predictive control. *IEEE Control Systems Magazine*, 20:38–52, 2000.

[156] J. B. Rawlings and R. Amrit. Optimizing process economic performance using model predictive control. In L. Magni, D. M. Raimondo, and F. Allgöwer, editors, *Nonlinear Model Predictive Control*, volume 384 of *Lecture Notes in Control and Information Sciences*, pages 119–138. Springer Berlin Heidelberg, 2009.

[157] J. B. Rawlings, D. Angeli, and C. N. Bates. Fundamentals of economic model predictive control. In *Proceedings of the 51st IEEE Conference on Decision and Control*, pages 3851–3861, Maui, Hawaii, 2012.

[158] J. B. Rawlings, D. Bonné, J. B. Jørgensen, A. N. Venkat, and S. B. Jørgensen. Unreachable setpoints in model predictive control. *IEEE Transactions on Automatic Control*, 53:2209–2215, 2008.

[159] J. B. Rawlings and D. Q. Mayne. *Model Predictive Control: Theory and Design*. Nob Hill Publishing, Madison, WI, 2009.

[160] M. Reble, R. Mahboobi Esfanjani, S. K. Y. Nikravesh, and F. Allgöwer. Model predictive control of constrained non-linear time-delay systems. *IMA Journal of Mathematical Control and Information*, 28:183–201, 2011.

[161] J.-P. Richard. Time-delay systems: an overview of some recent advances and open problems. *Automatica*, 39:1667–1694, 2003.

[162] E. Ronco, T. Arsan, and P. J. Gawthrop. Open-loop intermittent feedback control: practical continuous-time GPC. *IEE Proceedings - Control Theory and Applications*, 146:426–434, 1999.

[163] V. Sakizlis, J. D. Perkins, and E. N. Pistikopoulos. Recent advances in optimization-based simultaneous process and control design. *Computers & Chemical Engineering*, 28:2069–2086, 2004.

[164] P. O. M. Scokaert, D. Q. Mayne, and J. B. Rawlings. Suboptimal model predictive control (feasibility implies stability). *IEEE Transactions on Automatic Control*, 44:648–654, 1999.

[165] D. E. Seborg, T. F. Edgar, D. A. Mellichamp, and F. J. Doyle. *Process dynamics and control*. Wiley, New York, NY, 3rd edition, 2010.

[166] X. Shu, K. Rigopoulos, and A. Çinar. Vibrational control of an exothermic CSTR: Productivity improvement by multiple input oscillations. *IEEE Transactions on Automatic Control*, 34:193–196, 1989.

[167] J. J. Siirola and T. F. Edgar. Process energy systems: Control, economic, and sustainability objectives. *Computers & Chemical Engineering*, 47:134–144, 2012.

[168] P. L. Silveston. Periodic operation of chemical reactors – A review of the experimental literature. *Sādhanā*, 10:217–246, 1987.

[169] P. L. Silveston and R. R. Hudgins, editors. *Periodic Operation of Reactors*. Elsevier, Oxford, England, 2013.

[170] P. L. Silveston, R. R. Hudgins, and A. Renken. Periodic operation of catalytic reactors – Introduction and overview. *Catalysis Today*, 25:91–112, 1995.

[171] D. Sinčić and J. E. Bailey. Analytical optimization and sensitivity analysis of forced periodic chemical processes. *Chemical Engineering Science*, 35:1153–1161, 1980.

[172] S. Skogestad. Self-optimizing control: The missing link between steady-state optimization and control. *Computers & Chemical Engineering*, 24:569–575, 2000.

[173] S. Skogestad and I. Postlethwaite. *Multivariable Feedback Control: Analysis and Design*. John Wiley & Sons, New York, NY, 1996.

[174] O. J. M. Smith. Closer control of loops with dead time. *Chemical Engineering Progress*, 53:217–219, 1957.

[175] E. D. Sontag. A 'universal' construction of Artstein's theorem on nonlinear stabilization. *Systems & Control Letters*, 13:117–123, 1989.

[176] E. D Sontag. *Mathematical Control Theory: Deterministic Finite Dimensional Systems*, volume 6. Springer, 1998.

[177] G. Stephanopoulos. Synthesis of control systems for chemical plants: A challenge for creativity. *Computers & Chemical Engineering*, 7:331–365, 1983.

[178] G. Stephanopoulos. *Chemical Process Control: An Introduction to Theory and Practice*. Prentice Hall, Englewood Cliffs, NJ, 1984.

[179] L. E. Sterman and B. E. Ydstie. The steady-state process with periodic perturbations. *Chemical Engineering Science*, 45:721–736, 1990.

[180] L. E. Sterman and B. E. Ydstie. Periodic forcing of the CSTR: An application of the generalized π-criterion. *AIChE Journal*, 37:986–996, 1991.

[181] P. Tabuada. Event-triggered real-time scheduling of stabilizing control tasks. *IEEE Transactions on Automatic Control*, 52:1680–1685, 2007.

[182] A. R. Teel. Connections between Razumikhin-type theorems and the ISS nonlinear small gain theorem. *IEEE Transactions on Automatic Control*, 43:960–964, 1998.

[183] A. R. Teel, D. Nešić, and P. V. Kokotovic. A note on input-to-state stability of sampled-data nonlinear systems. In *Proceedings of the 37th IEEE Conference on Decision and Control*, volume 3, pages 2473–2478, 1998.

[184] A. R. Teel and L. Praly. Results on converse Lyapunov functions from class-KL estimates. In *Proceedings of the 38th IEEE Conference on Decision and Control*, volume 3, pages 2545–2550, Phoenix, AZ, 1999.

[185] T. Tosukhowong, J. M. Lee, J. H. Lee, and J. Lu. An introduction to a dynamic plant-wide optimization strategy for an integrated plant. *Computers & Chemical Engineering*, 29:199–208, 2004.

[186] M. van de Wal and B. de Jager. A review of methods for input/output selection. *Automatica*, 37:487–510, 2001.

[187] A. Wächter and L. T. Biegler. On the implementation of an interior-point filter line-search algorithm for large-scale nonlinear programming. *Mathematical Programming*, 106:25–57, 2006.

[188] N. Watanabe, H. Kurimoto, M. Matsubara, and K. Onogi. Periodic control of continuous stirred tank reactors–II: Cases of a nonisothermal single reactor. *Chemical Engineering Science*, 37:745–752, 1982.

[189] N. Watanabe, K. Onogi, and M. Matsubara. Periodic control of continuous stirred tank reactors–I: The Pi criterion and its applications to isothermal cases. *Chemical Engineering Science*, 36:809–818, 1981.

[190] J. C. Willems. Dissipative dynamical systems part I: General theory. *Archive for Rational Mechanics and Analysis*, 45:321–351, 1972.

[191] I. J. Wolf, D. A. Muñoz, and W. Marquardt. Consistent hierarchical economic NMPC for a class of hybrid systems using neighboring-extremal updates. *Journal of Process Control*, 24:389–398, 2014.

[192] L. Würth, R. Hannemann, and W. Marquardt. Neighboring-extremal updates for nonlinear model-predictive control and dynamic real-time optimization. *Journal of Process Control*, 19:1277–1288, 2009.

[193] L. Würth, R. Hannemann, and W. Marquardt. A two-layer architecture for economically optimal process control and operation. *Journal of Process Control*, 21:311–321, 2011.

[194] L. Würth and W. Marquardt. Infinite-horizon continuous-time NMPC via time transformation. *IEEE Transactions on Automatic Control*, 59:2543–2548, 2014.

[195] L. Würth, J. B. Rawlings, and W. Marquardt. Economic dynamic real-time optimization and nonlinear model-predictive control on the infinite horizon. In *Proceedings of the 7th IFAC International Symposium on Advanced Control of Chemical Processes*, pages 219–224, Istanbul, Turkey, 2007.

[196] L. Würth, I. J. Wolf, and W. Marquardt. On the numerical solution of discounted economic NMPC on infinite horizons. In *Proceedings of the 10th IFAC International Symposium on Dynamics and Control of Process Systems*, pages 209–214, Bombay, Mumbai, India, 2013.

[197] B. Xu and Y. Liu. An improved Razumikhin-type theorem and its applications. *IEEE Transactions on Automatic Control*, 39:839–841, 1994.

[198] X. Yang and L. T. Biegler. Advanced-multi-step nonlinear model predictive control. *Journal of Process Control*, 23:1116–1128, 2013.

[199] M. Zanon, S. Gros, and M. Diehl. A Lyapunov function for periodic economic optimizing model predictive control. In *Proceedings of the 52nd IEEE Conference on Decision and Control*, pages 5107–5112, Florence, Italy, 2013.

[200] V. M. Zavala and L. T. Biegler. The advanced-step NMPC controller: Optimality, stability and robustness. *Automatica*, 45:86–93, 2009.

[201] J. Zhang, S. Liu, and J. Liu. Economic model predictive control with triggered evaluations: State and output feedback. *Journal of Process Control*, 24:1197–1206, 2014.

[202] X. Zhu, W. Hong, and S. Wang. Implementation of advanced control for a heat-integrated distillation column system. In *Proceedings of the 30th Conference of IEEE Industrial Electronics Society*, pages 2006–2011, Busan, Korea, 2004.